

**EXPERIMENTAL INVESTIGATIONS OF SHEAR CONNECTIONS WITH SELF-
TAPPING-SCREWS FOR CROSS-LAMINATED-TIMBER PANELS**

by

Afrin Hossain

B.Sc. Bangladesh University of Engineering and Technology

M.A.Sc. The University of British Columbia, 2013

A THESIS SUBMITTED IN PARTIAL FULFILLMENT OF
THE REQUIREMENTS FOR THE DEGREE OF

Doctor of Philosophy

in

THE FACULTY OF GRADUATE AND POSTDOCTORAL STUDIES

(Forestry)

THE UNIVERSITY OF BRITISH COLUMBIA

(Vancouver)

December 2019

© Afrin Hossain, 2019

The following individuals certify that they have read, and recommend to the Faculty of Graduate and Postdoctoral Studies for acceptance, a thesis entitled:

Experimental investigations of shear connections with self-tapping-screws for cross-laminated-timber panels

submitted Afrin Hossain in partial fulfilment of the requirements for
the degree of Doctor of Philosophy
in Forestry

Examining Committee:

Thomas Tannert
Supervisor

Gregory Smith
Supervisory Committee Member

Gary S Schajer
University Examiner

Ricardo Foschi
University Examiner

Abstract

Advances in the areas of engineered wood products, such as Cross-laminated Timber (CLT), and wood connection solutions such as Self-tapping Screws (STS), as well as supporting legislation have created new possibilities for the structural application of timber in mid-rise construction. CLT structures and their connections need to be designed for appropriate capacity, stiffness, and if applied in seismic zones – ductility; however, current North American design standards contain no provisions for STS in CLT.

The research developed in this dissertation first examined the withdrawal resistance of STS in CLT for different screw diameters, effective screw embedment lengths, and angles of the screw axis relative to the wood grain. The work demonstrated that the existing product approval equation which was developed for Glulam can be used to predict the withdrawal resistance of STS in CLT.

Subsequently, the performance of CLT-STS joints was investigated under monotonic and reversed cyclic tests. Different conventional joint types were tested, namely surface spline with STS loaded in shear and half-lap with STS loaded in either shear or withdrawal. The research further investigated novel CLT joints combining STS loaded in withdrawal with STS loaded in shear, and butt joints with double inclination of STS.

The joint performance was evaluated in terms of capacity, stiffness, yield strength, and ductility, and it was shown that joints with STS in shear exhibited high ductility but low stiffness, whereas joints with STS in withdrawal were found to be stiff but less ductile. Combining the shear and withdrawal action of STS led to joints exhibiting high stiffness and ductility.

Varying number of screws in one joint allowed evaluating group effect of STS for joint capacity, stiffness, and ductility, under both monotonic and cyclic loading. E.g. for joint capacity, group effect can be expressed as $n_{\text{eff}} = 0.9 \cdot n$ for all joints under static loading, where n , and n_{eff} are actual and effective number of screws respectively. For cyclic loading, more pronounced group-effect was observed that can be expressed as $n_{\text{eff}} = n^{0.9}$. The data and analyses presented in this dissertation will provide guidance to structural engineers and builders for designing CLT-STS shear connections.

Lay Summary

Self-tapping Screw (STS) is one of the popular connectors for Cross-laminated Timber (CLT) structures, yet current North American design standards contain no provisions for STS in CLT. The research presented in this dissertation investigated the performance of STS-CLT shear joints. In addition to conventional joint types, two novel joint types are presented and were tested under monotonic loading and cyclic loading which simulates the impact of an earthquake. The strength and stiffness as well as the so-called group effect of these joints (a measure of whether 10 screws are 10 times stronger than 1 screw) were evaluated. The data and analyses presented in this dissertation will provide guidance to structural engineers and builders for designing shear connections with STS in CLT.

Preface

I, Afrin Hossain, am the principal investigator of this research project under the supervision of Dr. Thomas Tannert. Findings from this dissertation were previously published in journals [I-IV] and conference proceedings [V-XIII]. I am co-author of publication [II] and the primary author of all other publications. My co-authors (Dr. Thomas Tannert, Dr. Marjan Popovski, Ilana Danzig, Max Closen, and Ruthwik Lakshman Chepuri) have provided technical input during the processes of conducting the experimental test, analyzing the results, and summarizing the findings.

- [I] **Hossain, A.**, Popovski, M., Tannert, T. 2019. "Group Effect of Self-Tapping-Screws in Cross-Laminated-Timber Shear Connections". *Journal of Structural Engineering*, 145(8).
- [II] Loss, C., **Hossain, A.**, Tannert, T. 2018. "Simple Cross-Laminated-Timber Shear Connections with Spatially Arranged Screws". *Engineering Structures*, 173, 340–356.
- [III] **Hossain, A.**, Popovski, M., Tannert, T. 2018. "Cross-Laminated-Timber Connections Assembled with a Combination of Screws in Withdrawal and Screws in Shear". *Engineering Structures*, 168, 1–11.
- [IV] **Hossain, A.**, Danzig, I., Tannert, T. 2016. "High Performance Cross-Laminated-Timber Shear Connection with Self-Tapping-Screw Assemblies". *Journal of Structural Engineering*, 142(11).
- [V] **Hossain, A.**, Popovski, M., Tannert, T. "Group Effect of Self-Tapping-Screws in Cross-Laminated-Timber Shear Connections". *5th International Network on Timber Engineering Research (INTER) Meeting. August 13-16, 2018. Tallinn, Estonia.*
- [VI] **Hossain, A.**, Popovski, M., Tannert, T. "Group Effect of Self-Tapping-Screws in Cross-Laminated-Timber Shear Connections" *World Conference on Timber Engineering (WCTE2018). August 20-23, 2018. Seoul, South Korea.*

- [VII] **Hossain, A.**, Tannert, T. "Shear Connections with Self-Tapping-Screws for Cross-Laminated-Timber Panels". *China-Canada Symposium on Structural and Earthquake Engineering. August 20-24, 2017. Vancouver, Canada.*
- [VIII] **Hossain, A.**, Popovski, M., Tannert, T. "Static and Cyclic Performance of Shear Connections with Self-Tapping-Screws for Cross-Laminated-Timber Panels". *16th World Conference on Earthquake Engineering (16WCEE). January 9-13, 2017. Santiago, Chile.*
- [IX] **Hossain, A.**, Popovski, M., Tannert, T. "Shear Connections with Self-Tapping-Screws for Cross-Laminated-Timber". *World Conference on Timber Engineering (WCTE2016). August 22-25, 2016. Vienna, Austria.*
- [X] **Hossain, A.**, Tannert, T. "Shear Connections with Self-Tapping-Screws for Cross-Laminated-Timber Panels". *The 1st International Conference on Advances in Civil Infrastructure and Construction Materials (CICM 2015). December 14-15, 2015. Dhaka, Bangladesh*
- [XI] **Hossain, A.**, Tannert, T. "Shear Connections with Self-Tapping-Screws for Cross-Laminated-Timber Panels". *The 5th Tongji-UBC Symposium on Earthquake Engineering, May 4-8, 2015. Shanghai, China.*
- [XII] **Hossain, A.**, Closen, M., Tannert, T. "Shear Connections with Self-Tapping-Screws for Cross-Laminated-Timber". *Structural Engineers Association of California (SEAOC). September 9-12, 2015. Bellevue, WA.*
- [XIII] **Hossain, A.**, Lakshman, R., Tannert, T. "Performance of Shear Connections with Self-Tapping-Screws for Cross-Laminated-Timber Panels". *ASCE Structures Congress. April 23-25, 2015. Portland, Oregon.*

Table of Contents

Abstract	iii
Lay Summary.....	v
Preface	vi
Table of Contents.....	viii
List of Tables	xiv
List of Figures	xvi
List of Symbols	xxiii
List of Abbreviations	xxviii
Acknowledgements.....	xxx

Chapter 1: Introduction 1

1.1 Background	1
1.2 Cross-laminated-timber.....	1
1.3 Self-tapping screws	2
1.4 Cross-laminated-timber shear connections	3
1.5 Research Need	3
1.6 Objectives	4
1.7 Scope and limitations	5
1.8 Thesis outline	5

Chapter 2: Literature Review.....	7
2.1 Background	7
2.2 Cross-Laminated-Timber	8
2.2.1 General information	8
2.2.2 Advantages of CLT	9
2.2.3 CLT product standardization	10
2.2.4 CLT applications.....	10
2.3 CLT connections	11
2.3.1 Panel-to-panel connections (Detail A).....	12
2.3.2 Other connections	15
2.4 Self-Tapping-Screws.....	16
2.4.1 General information	16
2.4.2 Spacing, end, and edge distances for screws	17
2.4.3 Capacity of laterally loaded screws (pure shear)	18
2.4.4 Capacity of axially loaded screws (pure tension or compression).....	19
2.4.5 Capacity of axially-laterally loaded inclined screws (shear-tension/compression) ..	22
2.4.6 Stiffness of laterally loaded screws (pure shear)	25
2.4.7 Stiffness of axially loaded screws (pure tension)	26
2.4.8 Stiffness axially-laterally loaded inclined screws (shear-tension).....	26
2.5 Group effect for screws.....	28

2.6	State-of-the-art of CLT-STS applications.....	32
2.7	Summary of literature review	35
Chapter 3: Withdrawal Testing of STS in Canadian CLT.....		36
3.1	Overview.....	36
3.2	Materials	36
3.3	Specimen description.....	38
3.3.1	Series 1 (8mm_8d_90°)	40
3.3.2	Series 2 (8mm_12d_90°)	40
3.3.3	Series 3 (8mm_8d_45°)	41
3.3.4	Series 4 (8mm_12d_45°)	41
3.3.5	Series 5 (10 mm_8d_90°)	41
3.3.6	Series 6 (10 mm_12d_90°)	42
3.3.7	Series 7 (10 mm_8d_45°)	42
3.3.8	Series 8 (10 mm_12d_45°)	43
3.4	Design values and estimated resistance	43
3.5	Test methods	44
3.6	Analyses.....	46
3.7	Results.....	47
3.8	Discussion.....	49
3.8.1	Load-deformation behavior	49

3.8.2	Effect of screw diameter	50
3.8.3	Effect of screw embedment length	50
3.8.4	Effect of screw insertion angle	51
3.8.5	Failure modes.....	51
3.8.6	Comparison of test results vs. design values	52
3.9	Summary of withdrawal tests.....	55
Chapter 4: CLT-STs Shear Connections Tests		56
4.1	Materials	56
4.2	Joint types	57
4.1	Experimental test program.....	61
4.1.1	Overview.....	61
4.1.2	One and two STS connections	63
4.1.3	Multiple STS connections.....	64
4.1.4	Specimen preparation.....	72
4.2	Test methods	72
4.2.1	Mini sized specimens (Mi-1, Mi-2) under monotonic loading	72
4.2.2	Mini sized specimens (Mi-1, Mi-2) under cyclic loading.....	74
4.2.3	Small sized specimen with two shear planes (S-2SP) under monotonic loading	75
4.2.4	Small sized specimen with one shear plane (S-1SP) under monotonic loading	76
4.2.5	Small sized specimen with one shear plane under cyclic loading	77

4.2.6	Medium and large sized specimen under monotonic loading.....	78
4.2.7	Medium and large sized specimen under cyclic loading	80
4.2.8	Analyses procedures	82
4.3	Results.....	84
4.3.1	Overview.....	84
4.3.2	One and two STS connections (Mi-1 and Mi-2).....	88
4.3.3	Small sized specimens with two shear planes (S-2SP).....	93
4.3.4	Small sized specimens with one shear plane (S-1SP).....	95
4.3.5	Medium (M) and large (L) sized specimens (2SP).....	102
4.4	Discussion	108
4.4.1	Load-deformation behavior monotonic tests	108
4.4.2	Load-deformation behavior cyclic tests.....	110
4.4.3	Joints with STS in shear.....	113
4.4.4	Joints with STS in withdrawal	116
4.4.5	Joints with STS in shear and withdrawal.....	118
4.4.6	Comparison between tests using specimens using one two and shear planes	120
4.4.7	Failure modes and capacities	122
4.4.8	Comparison of screw actions	131
4.4.9	Comparison of different loading protocols	132
4.4.10	Impact of friction	137

4.4.11	Group effect	139
Chapter 5: Conclusion		143
5.1	Summary	143
5.2	Withdrawal tests.....	144
5.3	CLT-STs shear connections	145
5.3.1	Overview	145
5.3.2	Different screw layouts	146
5.3.3	Group effect	146
5.4	Future research.....	147
5.4.1	Experimental testing	147
5.4.2	Numerical modelling	148
5.4.3	Extension to structural system level	148
Bibliography		150
Appendix A Detailed test results of withdrawal testing		163
Appendix B Spacing of CLT-STs test series		175
Appendix C Detailed test results of mini-sized specimens (Mi-1 & Mi-2)		177
Appendix D Detailed test results of small sized specimens (S-2SP, and S-1SP).....		205
Appendix E Detailed test results of medium sized specimens (M-2SP)		258
Appendix F Detailed test results of large sized specimens (L-2SP)		268

List of Tables

Table 2.1: Different considerations of group-effect factor ¹	31
Table 3.1: Minimum spacing, end, and edge distance of in CLT	38
Table 3.2: Withdrawal test series.....	39
Table 3.3: Withdrawal test results	47
Table 3.4: Comparison to design values	48
Table 4.1 Test series overview for surface spline joints with STS in shear	66
Table 4.2 Test series overview for lap joints with STS in shear.....	68
Table 4.3 Test series overview for lap joints with STS in withdrawal	69
Table 4.4 Test series overview for lap joints with STS in shear and withdrawal.....	70
Table 4.5 Test series overview for butt joints with STS in shear	71
Table 4.6 Test series overview for butt joints with STS in withdrawal.....	71
Table 4.7: Results summary for surface spline joints with STS in shear	84
Table 4.8: Results summary for lap joints with STS in shear.....	85
Table 4.9: Results summary for lap joints with STS in withdrawal	86
Table 4.10: Results summary for lap joints with STS in shear and STS in withdrawal	86

Table 4.11: Results summary for butt joints with STS in shear	87
Table 4.12: Results summary for butt joints with STS in withdrawal.....	87
Table 4.13: Results summary for one and two STS connections (Mi-1 and Mi-2).....	88
Table 4.14: Results summary for small sized specimen S-2SP under monotonic loading.....	93
Table 4.15: Results summary for 3ply joints with STS in shear (S-1SP).....	95
Table 4.16: Results summary for 3ply joints with STS in withdrawal (S-1SP)	95
Table 4.17: Results summary for 3ply joints with STS in shear and withdrawal (S-1SP)	96
Table 4.18: Results summary (M-2SP) under quasi-static monotonic and cyclic loading)	102
Table 4.19: Results summary (L-2SP) under quasi-static monotonic and cyclic loading).....	102
Table 4.20: 1SP-2SP comparison (3-ply)	121
Table 4.21: 1SP-2SP comparison (5-ply)	121

List of Figures

Figure 2.1: CLT: a) 3 and 5-ply CLT, and b) CLT panel layout illustration.....	9
Figure 2.2: Typical CLT building showing various connections between floor and wall panels	12
Figure 2.3: Typical CLT panel-to-panel connections: a) single surface spline, and b) half-lapped joints (Source: My-Ti-Con Timber Connectors Inc.)	13
Figure 2.4: Conventional CLT panel-to-panel connections: a) Internal spline, b) single surface spline, c) double surface spline and d) half-lapped joints.....	14
Figure 2.5: STS: a) partially threaded, and b) fully threaded	17
Figure 2.6: Capacity of STS: a) loaded in shear and b) loaded in withdrawal	23
Figure 2.7: STS stiffness: a) laterally loaded, and b) laterally and axially loaded	27
Figure 2.8: Reduction in strength for n_{eff} according to different design standards.....	30
Figure 3.1: STS ASSY® VG CSK	37
Figure 3.2: Definition of spacing of STS in CLT: a) wide face, and b) edge (ETA-11/0190, 2013)	38
Figure 3.3: Typical test specimen: a) plan view, and b) elevation view.....	39
Figure 3.4: Spacing, edge, and end distances (CCMC 13677-R, 2012)	39
Figure 3.5: Series 1 layout: side section (left) and cross section (right).....	40

Figure 3.6: Series 2 layout: side section (left) and cross section (right)	40
Figure 3.7: Series 3 layout: side section (left) and cross section (right)	41
Figure 3.8: Series 4 layout: side section (left) and cross section (right)	41
Figure 3.9: Series 5 layout: side section (left) and cross section (right)	42
Figure 3.10: Series 6 layout: side section (left) and cross section (right)	42
Figure 3.11: Series 7 layout: side section (left) and cross section (right)	43
Figure 3.12: Series 8 layout: side section (left) and cross section (right)	43
Figure 3.13: Test Setup for a) Withdrawal at 90°, b) 45°, and c) detail	45
Figure 3.14: Average load displacement curves: a) 8mm STS, and b) 10 mm STS	48
Figure 3.15: Typical failure modes: a) screw withdrawal and splitting of wood with STS installed in 90°, and b) screw withdrawal and layer separation with STS installed in 45°	51
Figure 3.16: Comparison of withdrawal resistance of ASSY® STS in CLT vs. design values (Glulam values are from Abukari et al., (2013)): a) 8mm_90°, b) 8mm_45°, c) 10 mm_90°, and d) 10 mm_45°	53
Figure 3.17: Factor of safety associated with ASSY® STS under Withdrawal in CLT: a) 8 mm_90°, b) 8 mm_45°, c) 10 mm_90°, and d) 10 mm_45°	54

Figure 4.1: STS from left: , VG CSK FT 8 x 220 mm, VG CYL FT 8 x 180 mm, Ecofast PT 8 x 160 mm, VG CSK FT 8 x140 mm, Ecofast PT 8 x 100 mm, Ecofast PT 8 x 90 mm, Ecofast PT 8 x 80 mm	57
Figure 4.2: Joint specimen layout : a) spline joint with STS in shear, b) lap joint with STS in shear, c) lap joint with STS in withdrawal, d) butt joint with STS in shear, e) butt joint with STS in withdrawal.....	60
Figure 4.3: Lap joint with STS in shear and STS in withdrawal a) WSSW, b) SWWS, and c) SWSWS	61
Figure 4.4: Experimental test program of CLT-STS shear connections.....	62
Figure 4.5: Test specimen layout: a) small specimens with one shear plane, and b) specimens with two shear planes (not to scale) (all measurements are in mm)	63
Figure 4.6: Test specimen with plastic membrane to eliminate friction between panels	66
Figure 4.7: Test setup for Mini sized specimens under monotonic loading	73
Figure 4.8: Loading protocols: a) EN-26891 (1991) for monotonic tests; and b) CUREE for cyclic tests	74
Figure 4.9: Test setup for Mini sized specimens under cyclic loading.....	75
Figure 4.10: Test setup for small sized specimen with two shear planes under monotonic loading	76

Figure 4.11: Test setup for small sized specimen with one shear plane under monotonic loading	77
Figure 4.12: Test setup for small sized specimen with one shear plane under cyclic loading	78
Figure 4.13: Test setup for medium sized specimen under monotonic loading	79
Figure 4.14: Test setup for large sized specimen under monotonic loading	79
Figure 4.15: Test setup for medium sized specimen under cyclic loading	81
Figure 4.16: Test setup for large sized specimen under cyclic loading	81
Figure 4.17: Development of EEEP curves: a) Envelope curve, b) Interpolated curve, c) EEEP curve.....	83
Figure 4.18: Average load displacement curves from monotonic tests: a) Mi-1, and b) Mi-2.....	89
Figure 4.19: Load displacement curves from cyclic tests on Mi-1 joints: a) Spline_Shear, b) Lap_Shear, and c) Butt_Shear	91
Figure 4.20: Load displacement curves from cyclic tests on (Mi-2) joints: a) Spline_Shear, b) Lap_Shear, c) Butt_Shear, d) Lap-Withdr., and e) Butt-Withdr	92
Figure 4.21: Average load displacement curves from quasi-static monotonic tests on S-2SP): a) 3-ply CLT, and b) 5-ply CLT.....	94
Figure 4.22: Average load displacement curves from quasi-static monotonic tests (S-1SP): a) 3-ply CLT-4STS , and b) 3-ply CLT-8STS	97

Figure 4.23: Average load displacement curves from quasi-static monotonic tests on specimens exhibiting (S-1SP): a) 5-ply CLT-4STS, and b) 5-ply-8STS per shear plane	98
Figure 4.24: Load displacement curves from cyclic tests on S-1SP joints: a) Spline_Shear, b) Lap_Shear, c) Butt_Shear, d) Lap-Withdr., e) Butt-Withdr., f) Lap_WSSW, and g) Lap_SWSWS	101
Figure 4.25: Average load displacement curves from quasi-static tests: a) (M-2SP), and b) (L-2SP)	103
Figure 4.26: Load displacement curves from cyclic tests on M joints: a) Lap_Shear, b) Butt_Shear, c) Lap-Withdr., d) Butt-Withdr., and f) Lap_WSSW	105
Figure 4.27: Load displacement curves from cyclic tests on L specimens: a) Lap_Shear, b) Butt_Shear, c) Lap-Withdr., and d) Lap_WSSW	107
Figure 4.28: Comparison of results from different specimen sizes under monotonic loading; a) capacity, b) ductility, and c) stiffness	110
Figure 4.29: Comparison of results from different specimen sizes under cyclic loading; a) capacity, b) ductility, and c) stiffness	113
Figure 4.30: Load displacement in 3-ply CLT: a) Spline_Shear, b) Lap_Shear, and c) Butt_Shear	116
Figure 4.31: Load displacement in 5-ply CLT: a) Spline_Shear, and b) Lap_Shear	116
Figure 4.32: Load displacement in 3-ply CLT: a) Lap-Withdr. and Butt-Withdr.	118

Figure 4.33: Load displacement in 5-ply CLT: Lap_Withdr.....	118
Figure 4.34: Lap joints with STS in shear and STS in withdrawal in a) 3-ply, and b) 5-ply	119
Figure 4.35 Comparison between specimens with 1 or 2 shear planes a) pure shear in 2SP, and b) bending effect in 1SP	121
Figure 4.36: Failure modes in spline joints: a) pure shear, b) bending, c) gap opening, d) STS yielding, e) screw head sinking, f) screw heading snapping through plywood, and g) separation of CLT panels.....	123
Figure 4.37: Failure modes in spline joints from cyclic tests: a) pure shear, b) separation of CLT panel and plywood, c) plastic hinge at 45° of STS and plywood crushing, and d) STS breaking	124
Figure 4.38: Failure modes in lap joints from monotonic tests: a) large displacement of assemblies with STS loaded in shear, b) small displacements of assemblies with STS loaded in withdrawal, c) screw yielding, d) STS loaded in shear, e) STS loaded in withdrawal, and f) assemblies with STS loaded in shear and STS loaded in withdrawal	126
Figure 4.39: Failure modes in lap joints from cyclic tests: a) STS breaking, b) STS head push-out, c) assembly out-of-plane rotation, d) separation of CLT panel, e) STS yielding, and f) STS embedment.....	128
Figure 4.40: Failure modes in butt joints from monotonic and cyclic tests; a) panel rotation around plastic hinge, b) STS loaded in shear, c) separation of CLT panel, d) STS breaking, e) pure shear	

with rotation, f) no screw breaking or wood crushing, g) wood crushing, and h) STS loaded in withdrawal..... 130

Figure 4.41: Comparison between quasi-static monotonic and cyclic loading: a) Spline_Shear; b) Lap_Shear; c) Butt_Shear; d) Lap-Withdr; e) Butt-Withdr; and f Lap_Shear&Withdr..... 134

Figure 4.42: Comparison between positive and negative envelopes in cyclic loading: a) Spline_Shear; b) Lap_Shear; c) Butt_Shear; d) Lap-Withdr; e) Butt-Withdr; and f Lap_Shear&Withdr..... 136

Figure 4.43: Test series that included friction and non-friction (3-ply_1SP): a) Spline_Shear, b) Lap_Shear, c) Lap-Withdr., d)Butt-Withdr, and e) Lap_Shear&Withdr 138

Figure 4.44: Group-effect on: capacity a) monotonic, and b) cyclic loading; stiffness c) monotonic, and d) cyclic loading; ductility e) monotonic, and f) cyclic loading 142

List of Symbols

A_m	: Gross cross-sectional area of main member
A_s	: Gross cross-sectional area of side member
α	: Angle between the screw axis and the grain direction
b	: Material adjustment factor
β	: Angle between STS axis to the edge of the CLT panels
γ	: Load-slip modulus for a connection
d	: Fastener diameter / outer thread diameter of the screw
d_{core}	: Thread root diameter
d_{ef}	: Effective screw diameter
$d_{\text{F,max}}$: Displacement at capacity
d_h	: Screw head diameter
d_n	: Thread root diameter
$d_{\text{F,Y}}$: Displacement at yield load
δ	: Density adjustment factor
E_m	: Modulus of elasticity of main member

E_s	: Modulus of elasticity of side member
ε	: Factor for stiffness
f_{ax}	: Withdrawal strength perpendicular to the grain
f_h	: Pull-through parameter
$f_{h,\theta}$: Embedment strength at an angle to the wood grain
$f_{h,i,k}$: Characteristic embedding strength of timber element i
F_{max}	: Capacity (ultimate resistance)
$F_{max,mean}$: Mean capacity
$F_{max,5th\%}$: Fifth percentile capacity
F_N	: Load-carrying capacity of a multiple fastener connection
F_S	: Load carrying capacity of a single fastener
F_Y	: Yield load
Φ	: Resistance factor / performance factor
G	: Wood density (or specific gravity)
J_E	: End grain factor for lag screws
J_{PL}	: Factor for reduced penetration
k	: Stiffness

k_{ax}	: Axial stiffness
K_D	: Load duration factor
k_{lat}	: Lateral stiffness
k_s	: Shear component of stiffness
K_{SF}	: Service condition factor
$k_{s,pair}$: Stiffness of crossed STS pair loaded laterally
k_{sw}	: Stiffness with screws in shear and withdrawal
K_T	: Wood treatment factor
k_w	: Withdrawal component of stiffness
$k_{w,pair}$: Stiffness of pair of crossed axially-laterally loaded STS, one acting in tension-shear and the other in compression-shear
$k_{ }$: Stiffness of screws loaded in parallel
k_{\perp}	: Stiffness of screws loaded in perpendicular
k_{90}	: Stiffness for the range of the load-displacement curves between 10% and 90% of screw resistance
l_{ef}	: length of threaded shank penetration into main member / effective screw embedment length
L_t	: Depth of penetration of the threaded portion of the fastener
λ	: Slenderness ratio for timber to timber connections

λ_y	: Slenderness ratio for timber to timber connections
M_y	: Yield moment of screws
$M_{y,Rk}$: Characteristic fastener yield moment
μ	: Friction coefficient
μ	: Ductility
n	: Number of fasteners in a row
n_{eff}	: Effective number of screws
$n_{eff,s}$: Effective number of STS in shear
$n_{eff,w}$: Effective number of STS in withdrawal
n_{STS}	: Number of STS
$P_{r,pt}$: Head pull-through resistance of SWG ASSY [®] screws
s	: Center to center spacing between adjacent fasteners in a row
t	: Timber thickness
t_i	: Embedded fastener length in timber element i
$P_{r,ax}$: Screw withdrawal capacity
$P_{r,lat}$: Factored lateral strength resistance
$P_{r,s}$: Capacity for shear screws

$P_{r,w}$: Capacity for withdrawal screws
$P_{rw,\alpha}$: Factored withdrawal resistance of screws inserted in an angle, α
$P_{rw,\alpha,\text{fact}}$: Factored withdrawal resistance of screws inserted in an angle, α
$P_{rw,\alpha,\text{unfact,mean}}$: Unfactored mean withdrawal resistance of screws inserted in an angle, α
$P_{rw,\alpha,\text{unfact,5th\%}}$: Unfactored 5 th percentile withdrawal resistance of screws inserted with α
$p_{rw,\perp}$: Characteristic withdrawal strength perp. to the grain
p_u	: Lateral strength resistance for parallel-to-grain loading
ρ	: Mean oven-dry relative density
ρ_k	: Characteristic density of wood
ρ_m	: Mean density of the material
r_{PT}	: Characteristic pull-through strength
y_w	: Withdrawal resistance per millimeter of threaded shank penetration

List of Abbreviations

ASTM	: American Society of Testing and Materials
BCBC	: Building Code of British Columbia
BS	: Butt Shear joint
BW	: Butt Withdrawal joint
CLT	: Cross-laminated Timber
CSA-O86	: Canadian Standard Association: Engineering design in wood
CSA	: Canadian Standard Association
EC	: Eurocode
EEEP	: Equivalent Energy Elastic Plastic
ETA	: European Technical Approval of connectors
EWPs	: Engineered Wood Products
FT	: Fully Threaded
IBC	: International Building Code
L-2SP	: Large sized specimen with two Shear Planes
LS	: Lap Shear joint
LSL	: Laminated Strand Lumber
LVL	: Laminated veneer Lumber
LW	: Lap Withdrawal joint

M-2SP	: Medium sized specimen with two Shear Planes
Mi-1	: Mini sized specimen with one STS
Mi-2	: Mini sized specimen with two STS
NBCC	: National Building Code of Canada
NDS	: National Design Specification
OBC	: Ontario Building Code
PT	: Partially Threaded
SCL	: Structural Composite Lumber
S-1SP	: Small sized specimen with one Shear Plane
S-2SP	: Small sized specimen with two Shear Plane
SP	: Shear Plane
SPF	: Spruce-Pine Fir lumber
SS	: Surface Spline joint
STS	: Self-tapping Screw
SWSWS	: Screw pattern: Shear-Withdrawal-Shear-Withdrawal-Shear
SWWS	: Screw pattern: Shear-Withdrawal-Withdrawal-Shear
WSSW	: Screw pattern: Withdrawal-Shear-Shear-Withdrawal

Acknowledgements

First and foremost, I would like to thank my supervisor Dr. Thomas Tannert for his patience, guidance, and encouragements throughout my PhD research. It has been an honor to be his student. He has taught me how to select important problems, think critically and independently about the problem, and how to design experiments to proof my hypotheses and validate my ideas. He also gave me freedom to pursue other interests and encouraged me to collaborate with researchers from industry and academia. Under his supervision and encouragement, I have achieved not only Canada-wide but worldwide exposure in research thorough attending conferences and tradeshow, received several awards, and leadership training. I really appreciate all his contributions of dedicated time, prompt feedback, and great ideas. Mostly I am grateful to him for being supportive not only academically, but also emotionally and morally. I also have learned a lot by taking his graduate level courses and subsequently serving as a teaching assistant for his courses.

Next, I like to express my gratitude to my committee member Dr. Marjan Popovski from FPInnovations. His guidance and encouragement always made me feel there is light at the end of the tunnel. I appreciate all his contributions of time and ideas. I am grateful to him for understanding my excitement and frustrations and guide me accordingly to keep a balance in work and life. I am also indebted to my thesis committee members Prof. Gregory Smith, and Prof. Stavros Avramidis for their valuable comments and constructive suggestions to improve my thesis.

I also like to thank Max Closen, from 'MyTiCon Timber Connectors Inc.' for sponsoring the screws for this research, teaching me connection design from scratch and giving me various networking opportunities through tradeshow and webinars representing 'MyTiCon' to improve my research with feedbacks from researchers across Canada and United States.

This research could not be possible without financial support from Mitacs Canada through an Accelerate program with 'MyTiCon Timber Connectors Inc.', Schlumberger Foundation Faculty for the Future Fellowship, and Graduate Global Leadership Fellowship from UBC.

The help of the students from Dr. Tannert's research team, and the technicians at the UBC Centre for Advanced Wood Processing and Structures Research Laboratory: Ruthwik (for small scale test with two shear planes); Mariana, Paulo, Filipe, and Thomas (for small scale test with one shear plane), Mariana and Eytan (for withdrawal test), Dr. Johannes Schneider (mid and full scale test), Adam, Felix, Lawrence, Joern, and Vincent (for cutting CLT panels), George (for lab testing) is greatly appreciated. I would also like to thank to my colleagues Xiaoyue, Hongmin, Hercend, Kuldeep, and Shahnewaz for their encouragement and support for the success of this project.

I would like to thank to my Landlord, Professor John R Scheffer for taking the time to proofread my thesis.

My special thanks go to all my friends from Bangladeshi community at Vancouver for making my graduate life so enjoyable and supporting me during my ups and downs Thanks to my friend, Minar for her moral support during my five years of graduation life in Vancouver.

Finally, I would like to thank my parents and sister for their unconditional love, sacrifices, and unwavering support for my educational pursuits.

Dedicated to my Parents & Sister

আবু, আম্মু, ও আপুকে

Chapter 1: Introduction

1.1 Background

High strength-to-weight ratio, smaller carbon footprint, and the ease of assembly has allowed wood and engineered wood products (EWPs) to be widely used in residential applications. However, in non-residential construction in North America, these products are still underutilized. Legislation, such as the "Wood First Act" (Bill 9 -2009), passed in 2009 in British Columbia aimed to promote a culture of building with wood by requiring to consider its use as a principal material in any provincially funded building. Subsequently, several Canadian provinces implemented code changes that allowed wood to be used in six-storey light-frame buildings.

These legislative changes, along with novel materials such as Cross-laminated Timber (CLT) (Brandner et al., 2016), novel connectors such as Self-tapping Screws (STS) (Dietsch and Brandner, 2015), and technical documents for wood construction (Karacabeyli and Lum, 2014; Smith and Frangi, 2014) have created new possibilities for use of wood in mid-rise residential and non-residential construction. Pushing the boundaries of wood construction, a number of landmark buildings have been completed such as the world's tallest timber-hybrid building, the UBC Brock Commons, (18 stories and 53m tall) (Moudgil and Tannert, 2017).

1.2 Cross-laminated-timber

CLT is a plate-type structural engineered wood product, composed of multiple layers of dimensional lumber, which are glued together orthogonal to the next (Brandner et al., 2016). CLT offers a renewable alternative as construction material to concrete and steel and can be used for

floor, wall, and roof elements or for the entire building (Blass and Fellmoser, 2004; Vessby et al., 2009). Originally developed in Europe, Canadian and US handbooks (Gagnon and Pirvu, 2011; Karacabeyli and Douglas, 2013) contributed to the increasing use of CLT in North America where fabrication is regulated by the product standard ANSI/APA PRG 320 (PRG-320, 2018). The 2015 International Building Code (IBC, 2015) added a section on CLT complying with ANSI/APA PRG-320 (2012). CLT has been recognised as a state-wide alternative method for seismic design in Oregon with reference to the IBC (2015), and ASCE 7 (2016). Provisions for the design of CLT elements and connections were included in the 2015 National Design Specification for Wood Construction (NDS) (NDS, 2015) and the 2016 supplement to the 2014 edition of CSA-O86, the Canadian Standard for Engineering Design in Wood (CSA O86, 2016).

1.3 Self-tapping screws

STS belong to the group of dowel-type fasteners that includes bolts, dowels, and lag screws, and are considered state-of-the-art in connector technology for timber structures (Dietsch and Brandner, 2015). They are made of hardened steel to achieve a high yield moment, tensile, and torsional strength as well as high withdrawal resistance. STS are manufactured with diameters of up to 14mm and lengths up to 1500 mm, making them highly suitable to connect large wood sections and transfer high loads. The thread also provides a continuous mechanical connection along the embedded length, which helps to eliminate splitting (Blass and Bejtka, 2004). Pre-drilling is not required for STS which makes them faster and more cost efficient to install compared to lag screws. Installing STS at an angle (most often 45°) to the interface also increases the stiffness of the connections they form (Dietsch and Brandner, 2015).

1.4 Cross-laminated-timber shear connections

CLT panel-to-panel connections need to be designed for in-plane shear forces. Being rigid in nature, CLT panels need to be assembled with ductile connections in wall assemblies that are part of the seismic force resisting system to dissipate energy under seismic loading. CLT wall assemblies demonstrated adequate energy dissipation under cyclic loading when connected with ductile dowel-type fasteners (e.g. Gavric et al., 2015b). In practical applications of these panel-to-panel shear connections, different joint types are commonly used such as internal spline, single or double surface spline, or half-lap joints (Brandner et al., 2016), often with a large number of fasteners installed in one row. Alternatively, STS can be installed at an angle to the plane allowing for simple butt joints and avoiding any machining.

1.5 Research Need

Previous research on STS, as reviewed in detail in chapter 2, has focused on the influence of screw and connection parameters along with models that describe their performance. The withdrawal resistance of the STS can be predicted by equations provided by product approvals or the generic design equations for screws in Eurocode 5 (EC5) (EN 1995-1-1, 2008). Multiple proprietary STS products are available to designers and builders, one of them (SWG ASSY® screws) with both Canadian (CCMC 13677-R, 2018) and US product approvals (ESR-3178, 2018). However, the Canadian product approval for STS (CCMC 13677-R, 2018) is limited to visually graded lumber, glued-laminated timber and structural composite lumber produced from Canadian wood species, CLT was not included in that approval.

The current North American timber design standards NDS (NDS, 2015) and CSA-O86 (CSA O86, 2016) do not yet provide any design guidance for STS; therefore, engineers rely on the manufacturer's technical reports or apply the standards' (conservative) lag screw provisions. Furthermore, clause 11.9 of CSA O86 (2014) provides seismic design considerations for CLT structures based on the capacity-based design approach; however, designers lack the information of strength, stiffness, and ductility of STS CLT shear walls connections. This research will address these existing knowledge gaps.

1.6 Objectives

The objectives of the experimental research presented in this dissertation are to:

- 1) Investigate the withdrawal resistance of STS in Canadian CLT and compare the obtained test results with the design values obtained using Canadian product approval (CCMC 13677-R, 2018) equations for these screws;
- 2) Analyze the performance of different conventional joint types (surface spline, half-lap, and butt) and different screw actions (shear, withdrawal) in terms of strength, stiffness, and ductility under quasi-static monotonic and reversed cyclic loading;
- 3) Develop design guidance for two novel connection layouts: i) butt joints with screws installed in double angles acting in withdrawal and ii) lap joint with a combination of screws acting in shear and screws in withdrawal;

- 4) Develop empirical equations for the group effect of STS for strength, stiffness, and ductility under monotonic and reversed cyclic loading and propose design guidance on this topic to future revisions of CSA-O86;

1.7 Scope and limitations

The research presented in this dissertation is limited to experimental investigations at the component level. Full structures were not investigated, neither experimentally nor numerically. The presented results, however, provide input data for the development of numerical models to STS in shear connections and their application at the structural system level. All tests were conducted under short-term loading and room temperature only. Long-term creep effects as well as durability and fire resistance of the connections were outside the scope of this research. The group effect investigations were limited to studying the number of STS in one row. Multiple parallel rows were not studied. Furthermore, all tests were limited to CLT and STS provided by one manufacturer each, Structurlam Products and MyTiCon Timber Connectors Inc., respectively. The CLT was produced of Canadian softwood lumber, (S-P-F – Spruce-Pine-Fir) with layups of 3-ply and 5-ply, and the screws were only 8mm in diameter.

1.8 Thesis outline

Chapter 2 provides a literature review of the research on CLT, its application, STS, capacity and stiffness of STS, group effect of STS, and CLT-STS shear connections. Chapter 3 presents experimental investigations of withdrawal tests on STS in CLT to evaluate the applicability of the product approval equations. Chapter 4 studies the mechanical performance of different CLT-STS shear connections under quasi-static monotonic and cyclic loading in mini, small, medium, and

full-sized specimens. This chapter also proposes group effect for CLT-STs shear connections. Chapter 5 summarizes the findings from this work with recommendations for future research.

Chapter 2: Literature Review

2.1 Background

The forest industry is a key driver of the economy in British Columbia (BC) and a significant contributor for producing jobs, wealth, and government revenue at a national scale. According to Natural Resources Canada (NRCan, 2017), the forest industry of Canada gives direct employment to 209,940 people, and generates \$24.6 billion revenue from goods manufactured. To strengthen the sector, wood was promoted to be used as primary building material for all new provincially funded buildings by the Government of BC issuing a Wood First Act in 2009 (Bill 9, 2009). Wood frame construction of mid-rise buildings, up to six storeys are permitted by the provincial building codes of British Columbia and Ontario (BCBC, 2009; OBC, 2014). On March 13, 2019, the premier of B.C., John Horgan, announced changing the BC building code to allow wood structures of 12 storeys. It is expected that the National Building Code of Canada (NBCC, 2015) will allow for taller wood buildings in the future.

Mass timber construction has been successfully used in multi-storey buildings because of light weight, smaller carbon footprint, as well as ease of prefabrication and assembly. One of the drivers on the technical side is the market introduction of CLT. While Europe has entered into a second-generation of CLT manufacturing and application, the North American CLT market has witnessed a recent growth. The number of projects initiated each year in North America, from fewer than 20 in 2014 to well over 200 by the end of 2018. Approximately 50% of those projects have used CLT as their primary building material (BECK, 2018).

2.2 Cross-Laminated-Timber

2.2.1 General information

CLT is plate-type engineered wood composite element which can be used as structural slab or wall in timber or hybrid structures (Frangi, et al. 2009). It was first developed some 20 years ago in Austria and Germany. Ever since CLT panels for lateral load resisting system has been gaining popularity not only in residential buildings but also in industrial and office buildings especially in Europe. European experience showed that this product could be competitive in mid-rise and high-rise buildings. CLT is a viable structural product that can contribute to a potential shift towards sustainable densification of urban and suburban areas in North America. Canadian and US versions of CLT handbooks (Gagnon and Pirvu, 2011; Karacabeyli and Douglas, 2013) contributed to this development. CLT was included in CSA O86 (2014) in Canada, and NDS (2015) in USA.

CLT is made of multiple layers of wood, with each layer oriented crosswise (90°) to the next (Figure 2.1). CLT is prefabricated gluing at least 3 and up to 11 layers of boards (10-50 mm thick and 60-240 mm wide) using structural adhesive (Brandner et al., 2016). The thickness varies from 60 mm to 400 mm depending on the application (Joebstl et al., 2008). To facilitate transportation each layer is usually up to 18m long and the typical widths are up to 3m (5m in special cases).

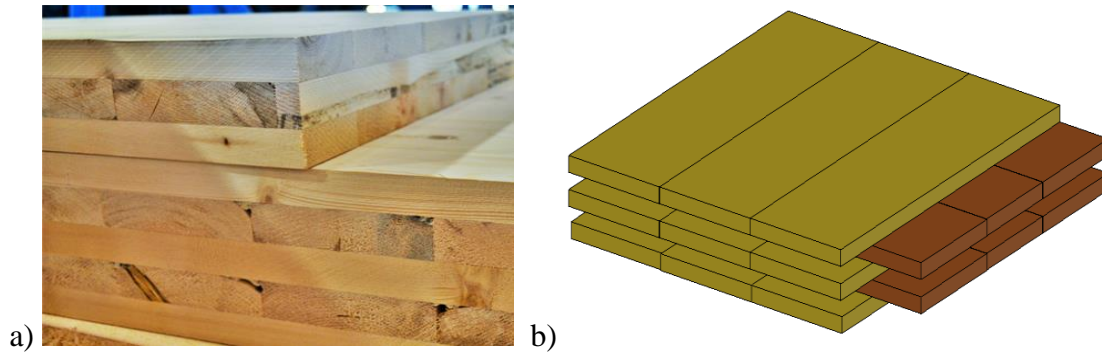


Figure 2.1: CLT: a) 3 and 5-ply CLT, and b) CLT panel layout illustration

2.2.2 Advantages of CLT

As other engineered wood products, CLT has a smaller carbon footprint than concrete or steel and its manufacturing does not require as much energy resulting in lower greenhouse gas emissions (Evans, 2015).. CLT is prefabricated with pre-cut openings for doors, windows, stairs, service channels, and ducts. Manufacturers can ship the panels to the construction site with pre-installed lifting straps to facilitate quick and efficient lifting by crane with easy handling and fewer skilled workers on site (Epp, 2015). Then those panels are joined with simple and rapid connections.

Improved dimensional stability for the cross lamination in all directions, high in-plane and out-of-plane strength and stiffness in both directions make CLT to be used for an entire building or any combination of wall, floor/ceiling and roof applications. The reinforcement effect (applying screws in the perpendicular to the grain) increases splitting resistance in connection systems. CLT can reduce mass, as it is 3 and 6 times lighter than an equivalent steel or concrete building, respectively and as a consequence helps reducing the foundation demands (Epp, 2015; Evans, 2015). Dimensional stability and rigidity make CLT an effective lateral load resisting system with multiple, small connectors showing good ductile behavior and energy dissipation (Evans, 2015).

2.2.3 CLT product standardization

In Europe, CLT achieved Product approval using a proprietary approach through the European Organization for Technical Approvals (ETA), where the grades of lumber to be used, adhesive, manufacturing process and final design value of finished panel are described. In North America, the CLT Handbook (Gagnon and Pirvu, 2011), published by FPInnovations, served as the first CLT related design reference. In 2012, PRG-320 (2012), the first performance-based material standard for CLT in North America was developed through a collaboration lead by the Engineered Wood Association and has been recognized by American National Standards Institute (ANSI). PRG-320 was referenced in the 2015 edition of National Design Specification (NDS 2015) in the US and the 2014 edition of the Canadian Standard for Engineering Design in Wood (CSA O86, 2014). Seven CLT performance grades and the testing methods detailing manufacturing and performance requirements for qualification and quality assurance are described in the standard IBC (2015). Chapter 6 included CLT as heavy timber type IV construction by defining dimensions (6" wall, 4" floors, and 3" roofs). However, the 2021 edition of IBC is going to include provisions for the use of CLT in buildings up to 18 stories in height (BECK, 2018).

2.2.4 CLT applications

Though CLT is already well-established in Europe, generic CLT products were introduced in Canada and the United States in 2010 and design procedures for CLT panels. In 2016, in Canada, Structurlam and Nordic Structures, and in the USA SmartLam, DR Johnson Lumber Co, and the Sterling Lumber Company produced CLT (Pei et al., 2016). As of 2019, there are multiple new manufacturers in the USA including Katerra's new 25,000m² facility in Spokane, Washington, the largest capacity CLT factory in North America (Editors, 2019).

To push the boundary of wood construction and challenge the existing code limitations, a number of CLT landmark buildings have been completed in North America in the last ten years and several more are currently under development. Examples of the application of CLT in Canada are the 5 storey Earth Science Building at UBC Vancouver completed in 2012 which utilizes CLT in the roof (ArchDaily, 2013); the 6 storey (27m) Wood Innovation and Design Center in Prince George completed in 2014 (ArchDaily, 2015b), which uses CLT panels in the elevator/stair core and floor diaphragms; the Fort McMurray Airport completed in 2015 (ArchDaily, 2015a) which uses CLT panels in the roof structure; the Arbora apartment complex in Montreal, Québec completed in 2016, the world's largest CLT building with an area of 55,740 m² (Alter, 2015); the 41 meter tall 12 storey Originie building in Québec City, completed in 2016, which utilizes CLT panels above a concrete ground floor (CCE, 2017); the 18 (53m) storey Brock Commons at UBC Vancouver, completed in 2017, which comprises 16 floors of CLT floor panels (Lau, 2016).

2.3 CLT connections

The structural efficiency of CLT panels used as floor system (acts as diaphragm) or wall system (acts as lateral load resisting system) depends on the connections (see Figure 2.2) between the individual CLT panels. STS are usually recommended by the CLT manufacturers to connect CLT panels (Gagnon and Pirvu, 2011). Traditional dowel-type fasteners: wood screws, nails, lag screws, rivets, bolts, and dowels could also be used; however, their use is rather limited in practice.

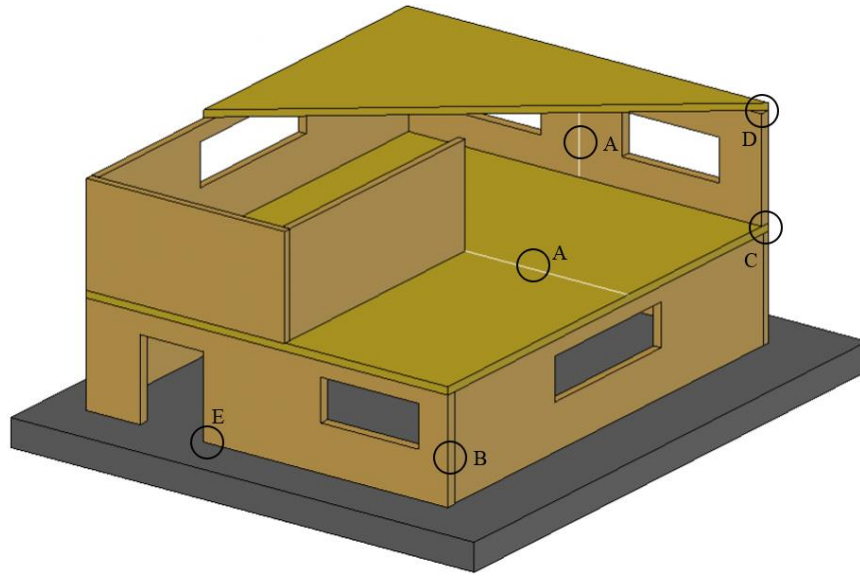
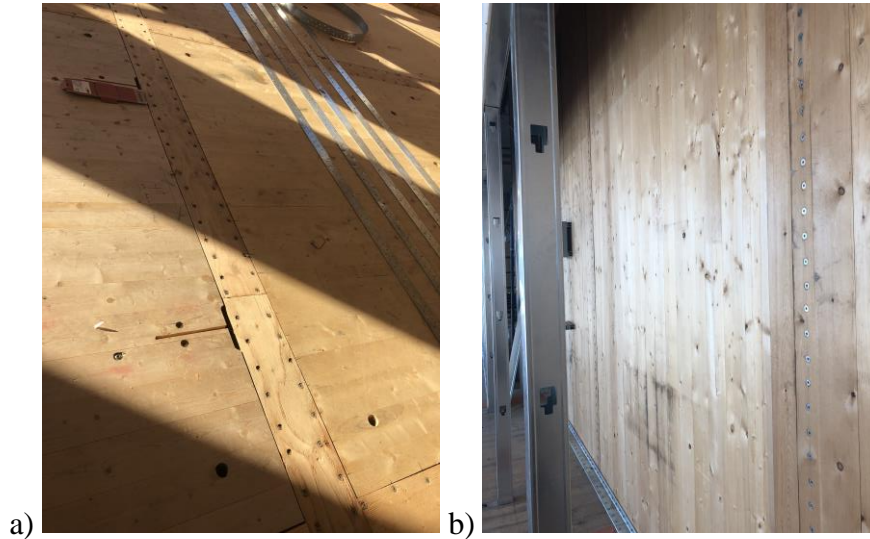


Figure 2.2: Typical CLT building showing various connections between floor and wall panels

2.3.1 Panel-to-panel connections (Detail A)

Panel-to-panel shear connections, which are the focus of this research, are usually made to connect individual CLT panels within wall or floor assemblies along their longitudinal edges (Figure 2.2).

Figure 2.3 shows typical CLT panel-to-panel connections.



***Figure 2.3: Typical CLT panel-to-panel connections: a) single surface spline, and b) half-lapped joints
(Source: My-Ti-Con Timber Connectors Inc.)***

When panel-to-panel connection is made within wall assemblies then the connection must be designed to resist in-plane shear and out-of-plane bending. When this connection is made within floor assemblies then the connection must be designed to transfer in-plane diaphragm forces and maintain the integrity of the diaphragms and the overall lateral load resisting system. Traditionally four different types of panel-to-panel connections can be made in CLT using STS: internal spline, single surface spline, double surface spline, and half-lapped joints (Figure 2.4).

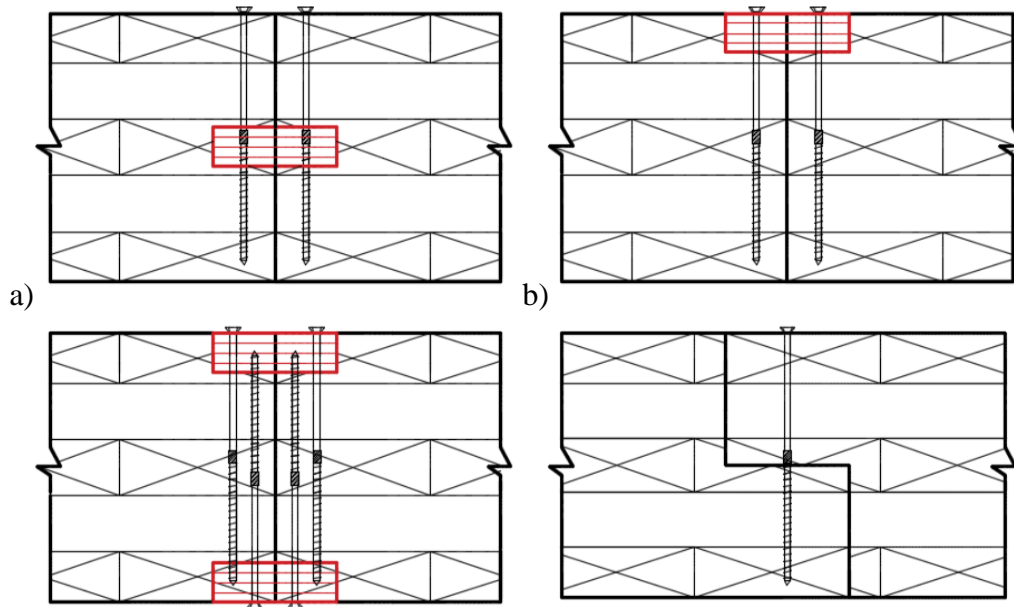


Figure 2.4: Conventional CLT panel-to-panel connections: *a) Internal spline, b) single surface spline, c) double surface spline and d) half-lapped joints*

Internal Spline: Panels need to be profiled in the middle at the plant before using on site. A single wooden spline/strip made of lumber, Plywood, SCL (Structural Composite Lumber), or LVL (Laminated Veneer Lumber) could be used to connect two pieces using STS, wood screws or nails, Figure 2.4 (a). This connection provides double shear; however, accuracy is required in profiling to fit in different pieces together on site. Structural adhesive could also be used along with the mechanical fasteners to connect different pieces together, however, it could make the structural timber reuse difficult. This detail shows better performance regarding resistance to normal and out-of-plane loading.

Single surface spline: Panels need to be profiled at the edges to take a single wooden spline/strip of lumber, or SCL such as LVL or X-ply LVL. STS, wood screws or nails can be used to make this connection Figure 2.4 (b). This is very easy to construct on site. However, due to the single

shear action, this is inferior to the internal spline. Structural adhesive can also be used to connect different parts along with mechanical fasteners.

Double surface spline: To enhance the stiffness and strength, two splines along with two sets of screws are used on top and bottom edges of the panels. Better resistance can be achieved with this detail. More time, machining, and equipment are required for this kind of connection. Structural adhesive could also be used to increase the strength and stiffness, Figure 2.4 (c).

Half-lapped joints: For this connection panels need to be milled as half-lapped joint at the plant. Then the metal fasteners will be inserted from the top. Usually long STSs are used for this detail. This connection is commonly used to connect panel-to-panel in walls and floors, Figure 2.4 (d).

2.3.2 Other connections

Wall-to-wall connections (Detail B) between walls positioned at right angles (Figure 2.2) could be in between interior partition wall to exterior wall or just the exterior corner walls. STS can be used directly in 90° or in angle at the narrow face of the wall to connect it with another wall. Wooden profiles can also be used along with self-tapping-screws. Wall-to-floor connections (Detail C) between floor/roof-to-walls below especially in platform type construction often use STS directly in 90° or in angle from the CLT floor into the narrow face of the wall edge. To connect walls above to floors below, same principle can be applied, where STS needs to be driven at an angle in the wall near the junction with the floor. Depending on the length and angle of STS, it might reach the bottom wall which will further reinforce the connection between the upper and lower walls and the floor. Wall to roof connections (Detail D) between sloped or flat roofs to walls use STS directly in 90° from the roof to the wall or in angle from the wall to the roof for this connection. Finally, in wall to foundation connections (Detail E), STS are traditionally not used.

2.4 Self-Tapping-Screws

2.4.1 General information

Self-tapping screws (STS) are widely recognized as being the state-of-the-art in connector technology for CLT structures (Dietsch and Brandner, 2015). The rigidity and the ductility of CLT will be improved using STS which have high withdrawal capacity compared to dowel-type connections. High withdrawal capacity results in smaller, more efficient connections which require fewer fasteners with reduced project costs (MyTiCon, 2014). In comparison with traditional screws, the STS can be manufactured with a diameter of up to 14mm and a length up to 1500 mm. All STS screws are designed with a self-tapping tip to pre-tap their own core hole along the screw axis. Usually no predrilling is required for STS. This helps onsite installation significantly reducing the prefabrication and installation time along with the labor cost savings. Because of these characteristics, STS have become an efficient option in the market for wood-to-wood and steel-to-wood connections.

The screw is hardened after the rolling of the thread, which makes it stronger in bending. Installation of these screws can be performed at any temperature and full structural capacity of the screw is reached right after the screw installation. Due to its high bending capacity and high withdrawal resistance in compared to traditional screws, STS are very suitable as fasteners for timber to timber connections used both in lateral and axial loads. Bending of screws can be avoided by placing them with an angle of 45° with the interface of the member to be connected instead of placing them perpendicular. By doing that load is then transferred by a truss like system where the screw is in tension (withdrawal) and the contact surface between the members is in compression

(Blass and Bejtka, 2001). When being driven into the wood members, the potential for splitting is reduced because of its small core and large thread wing design.

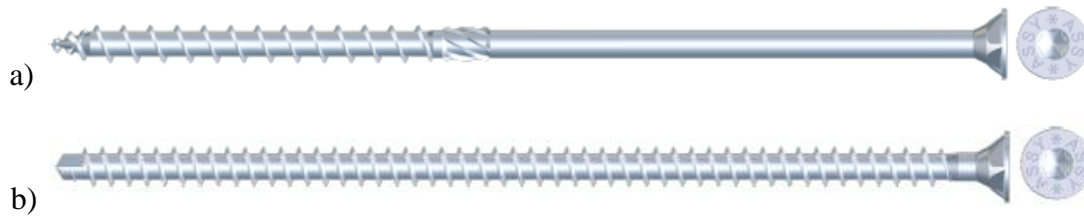


Figure 2.5: STS: a) partially threaded, and b) fully threaded

For STS screws, the outside thread diameter (major diameter) is used to measure the diameter size. Sometimes head diameter or the inner-core diameter (minor diameter) are used by other manufacturers. In order to determine the screw withdrawal capacity outside thread diameter is used whereas shear capacity is determined using the shank diameter. STS are of two types: partially threaded (PT) and fully threaded (FT) (Figure 2.5). Both again have different head types and special characteristics suitable for different connections. PT fasteners' thread extends over part of the screw. The PT screws are designed with a special shank cutter that lies between the threads and the shank of the fastener. These are good for reinforcing wood members in perpendicular to grain tension, perpendicular to grain crushing (compression), and perpendicular to grain shear failure; have high withdrawal capacities which establishes rigid tension connections.

2.4.2 Spacing, end, and edge distances for screws

Requirements for minimum spacing, end, and edge distance as well as the timber thickness need to be met to avoid splitting failure. Most of the failure due to splitting along the wood grain starts in the bolted hole due to the large difference in material strength and stiffness between steel bolts and wood (Yeh et al., 2007; Yeh et al., 2008). The material compatibility near the joints can be

achieved by reducing the diameter of steel fastener by using STS. Most of the STS can be installed having small spacing and edge distance without the risk of splitting the wood. Uibel and Blass (2010) developed a model that determines suitable spacing, end and edge distances for STS along with required timber thickness. For this they conducted 326 conventional screw-in tests following German design code (DIN 1052, 2009) and European design code (EN 1995-1-1, 2008) to estimate the splitting behavior of timber during the screw-in tests considering material, geometry, and fastener-specific influences. Current building code specifies the end distance as a minimum distance not to make splitting or tearing out in lumber or glued laminated timber. However, the end distance of CLT connection needs to be identified because the cross layers of CLT may prevent wood from splitting or tearing-out and allowing for shorter end distance compared to lumber or glued laminated timber (Oh et al., 2018).

2.4.3 Capacity of laterally loaded screws (pure shear)

The factored lateral strength resistance, $P_{r,lat}$, of STS loaded in shear can be calculated using the Johansen's Yield model which described multiple failure modes. The mode with the lowest load-carrying capacity governs the strength of dowel-type joints. Failure modes for two shear planes could be crushing of wood in the side, main or both members, or yielding (formation of one or two plastic hinges) of the fasteners along with crushing of wood. The load-bearing capacity of dowel-type joints is governed by four parameters: the characteristic embedding strength of timber element i $f_{h,i,k}$, the characteristic fastener yield moment $M_{y,Rk}$, the embedded fastener length in timber element i t_i , and the fastener diameter d . CSA O86 (2016) allows estimating the capacity of laterally loaded lag screws; Eq 2.1 is a modified representation:

$$P_{r,lat} = \Phi \cdot P_u \cdot n_{eff} \cdot J_{PL} \quad Eq\ 2.1$$

where Φ is the resistance factor, $P_u = p_u (K_D K_{SF} K_T)$, p_u is the lateral strength resistance for parallel-to-grain loading, K_D the load duration factor, K_{SF} the service condition factor, K_T the wood treatment factor, n_{STS} the number of STS, n_{eff} the group effect for shear screws under static or cyclic loading for capacity, and J_{PL} is the factor for reduced penetration.

2.4.4 Capacity of axially loaded screws (pure tension or compression)

STS have improved thread geometry and are made of hardened steel. These attributes provide these screws with a significantly higher withdrawal capacity and tensile strength than traditional screws (Yeh, al., 2018). Withdrawal resistance of STS depends on the wood density, the penetration depth of STS inside the wood and the angle between the screw axis and the wood grain direction. Screw withdrawal capacity, $P_{r,ax}$ can be predicted using the empirical Eq 2.2:

$$P_{r,ax} = A \cdot d^B \cdot L_t^C \cdot G^D \quad Eq\ 2.2$$

where d is the fastener diameter, L_t the depth of penetration of the threaded portion of the fastener, G the wood density (or specific gravity), and A, B, C, D are regression parameters.

Hansen (2002) determined embedment strength, withdrawal strength, pull-through strength, and bending capacity of individual STS. Influence of different parameters such as moisture content, temperature at "screw-in" and "pull-out", slenderness, embedment of the threaded part, angle between the screw axis and the grain, pre-drilling were considered by Pirnbacher et al. (2009) to develop equations for withdrawal resistance. Most prominent effect was found to be the embedment length. High withdrawal resistance along with high stiffness can be achieved by

installing STS at 45 degrees (Blass et al., 2001; Kevarinmäki, 2002). Furthermore, this angle happens to be economical to fabricate steel plates which incorporate special angle geometry (Krenn and Schickhofer, 2009). Frese and Blass (2009) developed withdrawal resistance equations for soft wood using structural screws considering nominal screw diameter, penetration depth, characteristic density of the soft wood, and angle between the screw axis and the grain. Later Prati-Vincent et al. (2010) conducted test programs on the use of STS in the joist-to-header connections to structural glulam and developed a modified expression to predict the connection resistance for cross screws considering withdrawal, tension, and compression effects. Abukari et al. (2012) performed 1760 experimental tests on the withdrawal resistance of STS installed in Canadian glulam. Ringhofer et al. (2013) developed stochastic models considering the density of the base material and the number of layers penetrated by the screws to predict the withdrawal capacity of self-tapping screws used in the Glue Laminated Timber (GLT) or CLT. Yeh et al. (2013) and Yeh et al. (2018) performed bending and withdrawal resistance tests on different STS types and diameters installed in glulam.

According to CSA O86 (2016), the factored withdrawal resistance, $P_{r,ax}$ for lag screws can be calculated using Eq 2.3:

$$P_{r,ax} = \Phi \cdot Y_w \cdot l_{ef} \cdot n_{STS} \cdot J_E \quad \text{Eq 2.3}$$

where Φ (=0.6) is the resistance factor, $Y_w = y_w (K_D K_{SF} K_T)$, y_w is the basic withdrawal resistance per millimeter of threaded shank penetration ($59 \cdot d^{0.82} \cdot G^{1.77}$), G is the mean relative density of main member, K_D is the load duration factor, K_{SF} the service condition factor, K_T is the wood treatment factor, n_{STS} is the number of STS in the joint, l_{ef} is the length of threaded shank penetration into main member, and J_E is the end grain factor for lag screws.

According to EC5 (EN 1995-1-1, 2008), the factored withdrawal resistance, $P_{r,ax}$ for STS can be calculated using Eq 2.4:

$$P_{r,ax} = \frac{n_{eff} \cdot p_{rw\perp} \cdot d \cdot l_{ef} \cdot k_d}{1.2 \cos^2 \alpha + \sin^2 \alpha} \quad \text{Eq 2.4}$$

where $p_{rw\perp}$ is the characteristic withdrawal strength perp. to the grain ($0.52 \cdot d^{0.5} \cdot l_{ef}^{0.1} \cdot \rho_k^{0.8}$), d is the outer thread diameter, n_{eff} is the effective number of screws, l_{ef} is the length of threaded shank penetration into main member, ρ_k is the characteristic density, α is the angle between the screw axis and the grain direction, with $\alpha \geq 30^\circ$, and k_d is the minimum of $d/8$ and 1.

According to European technical approval for SWG ASSY® screws (ETA-11/0190, 2018), the factored withdrawal resistance, $P_{r,ax}$ for STS can be calculated using Eq 2.5:

$$P_{r,ax} = \frac{f_{ax} \cdot d \cdot l_{ef}}{1.2 \cos^2 \alpha + \sin^2 \alpha} \cdot \left(\frac{\rho_k}{350} \right)^{0.8} \quad \text{Eq 2.5}$$

where f_{ax} is the withdrawal strength perpendicular to the grain, d is the outer thread diameter of the screw, l_{ef} is the penetration length of the threaded part, α is the angle between the screw axis and the grain direction, and ρ_k is the characteristic density of wood.

According to the Canadian product approval for SWG ASSY® screws (CCMC, 2018), the factored withdrawal resistance, $P_{r,ax}$, for the screws can be calculated using Eq 2.6:

$$P_{r,ax} = \Phi \frac{0.8 \cdot \delta \cdot (b \cdot 0.84 \cdot \rho)^2 \cdot d \cdot l_{eff} \cdot 10^{-6}}{\sin^2 \alpha + \frac{4}{3} \cos^2 \alpha} K_D K_{SF} \quad \text{Eq 2.6}$$

where Φ (=0.9) is the performance factor, δ the density adjustment factor, b the material adjustment factor, ρ the mean oven-dry relative density, d the screw outer diameter, K_D the load duration factor, K_{SF} the service condition factor, l_{ef} the effective screw embedment length, and α the angle between grain and screw.

The head pull-through resistance of SWG ASSY® screws, $P_{r,pt}$, can be calculated using Eq 2.7 according to the European technical approval (ETA-11/0190, 2018) and using Eq 2.8 according to the Canadian product approval (CCMC, 2018):

$$P_{r,pt} = f_h \cdot d_h^2 \cdot \left(\frac{\rho_k}{350}\right)^{0.8} \quad \text{Eq 2.7}$$

$$P_{r,pt} = \Phi \cdot (r_{PT} \cdot K_D K_{SF}) \quad \text{Eq 2.8}$$

where d_h is the screw head diameter, f_h the pull-through parameter, Φ the resistance factor, r_{PT} the characteristic pull-through strength; K_D the load duration factor; K_{SF} the service condition factor.

2.4.5 Capacity of axially-laterally loaded inclined screws (shear-tension/compression)

The load-carrying capacity models for laterally loaded STS assume rigid-plastic behavior of the materials associated with yielding of screws and embedding of the wood when subjected to compression. Conversely, capacity models for axially loaded STS assume rigid-brittle behavior of materials accompanied mainly by a shear failure of the wood close to the screw thread. EC5 (EN 1995-1-1, 2008) provides models for STS subjected to lateral or axial loadings and a quadratic interaction equation in the case of screws under combined axial-lateral loading. This equation was initially developed for laterally-axially loaded nails, where strengths models do not account for the

load to grain angle. Therefore, it does not properly fit to STS installed inclined and subjected to combined lateral and axial loadings.

Bejtka and Blass (2002) and Jockwer et al. (2014) proposed empirical equations to assess the load-carrying capacity of inclined screws loaded in axial and lateral directions, accounting for the loading direction angle with respect to the grain. These models, developed for an individual screw, can be used to evaluate the resistance of CLT lap and butt-joints with inclined STS.

A design approach for shear connections with inclined screws for different shank to grain angles α was proposed by Bejtka and Blass (2006). According to the Johansen model based on the failure mode 3 with plastic hinges in the screw, the resistance $P_{r,w}$ of a shear connection with one single inclined screw loaded in axial tension parallel to the grain can be calculated by Eq 2.9 which is portions of the axial and the lateral resistance of the screw ($P_{r,ax}$ and $P_{r,lat}$) in Figure 2.6.

$$P_{r,w} = P_{r,ax}(\mu \cdot \sin\alpha + \cos\alpha) + P_{r,lat}(\sin\alpha - \mu \cdot \cos\alpha) \quad \text{Eq 2.9}$$

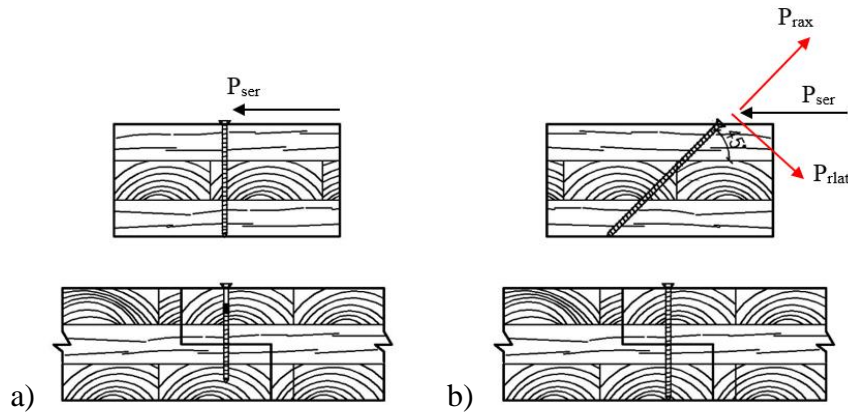


Figure 2.6: Capacity of STS: a) loaded in shear and b) loaded in withdrawal

$P_{r,lat}$ can be calculated using Eq 2.1 according to CSA O86 (2016). EC5 (EN 1995-1-1, 2008) includes Johansen's (Johansen, 1949) modified equations to evaluate the load-carrying capacity of

dowel-type fasteners (like screws) in different failure modes. The EC5 formula includes the rope effect of the connector (accounting for withdrawal resistance for fasteners loaded in shear) and is the recognized analytical method to estimate $P_{r,lat}$. For CLT-STs joints, the fastener slenderness ensures the development of failure mode with plastic hinges formed in the fastener (Jockwer et al., 2014). Based on this work, Eq 2.10 (from the various possible failure modes) can be used to estimate the shear resistance of a single STS:

$$P_{r,lat} = \sqrt{2 \cdot M_y \cdot f_{h,\theta} \cdot d_{ef}} \quad \text{Eq 2.10}$$

where M_y is the yield moment of screws calculated from EC5 (Table 1.2), $f_{h,\theta}$ the embedment strength at an angle θ to the wood grain, and d_{ef} the effective screw diameter taken as 1.1 times the thread root diameter, d_n . To apply Eq 2.10, auxiliary equation Eq 2.11 to evaluate $f_{h,\theta}$ is provided as function of the screw diameter and the wood density. For CLT panels, the angle θ changes along the screw axis to account for the different orientations of the intersected layers. The embedment strength, $f_{h,\theta}$ for self-tapping-screws was determined by Bejtka (2005) in terms of the density ρ of the timber and the load to grain angle α :

$$f_{h,\theta} = \Phi \cdot \frac{0.22 \rho^{1.24} \cdot d^{-0.3}}{2.5 \cos^2 \alpha + \sin^2 \alpha} \quad \text{Eq 2.11}$$

The term $P_{r,ax}$ in Eq 2.9 represents the minimum value of the withdrawal (pure axial) resistance, the tensile resistance and the pull-through resistance of a single screw described in section 2.4.4.

The value for the friction coefficient included in the EC5 (EN 1995-1-1, 2008) in the case of wood-to-wood surfaces is 0.25 and can be assumed 0 when contact surfaces are covered with polymeric

materials that minimize friction, such as Teflon. The capacity for cross screws can be expressed in Eq 2.12 taking into account of the equilibrium conditions without friction between wood elements:

$$P_{r,w,xpair} = P_{r,ax} \cdot \cos\alpha + P_{r,lat} \cdot \sin\alpha \quad \text{Eq 2.12}$$

2.4.6 Stiffness of laterally loaded screws (pure shear)

The design of timber structures for serviceability limit states requires knowledge of the stiffness of the elements and connections. It is common practice to derive the stiffness of connections as a function of the slip modulus of the individual connector. For joints made with dowel-type fasteners, the slip modulus, known as k_s , is provided by EC5 (EN 1995-1-1, 2008) per shear plane with empirical equations expressed in terms of the timber density and the fastener diameter. Specifically, for screws laterally loaded k_s is given by:

$$k_{lat} = k_s = k_{\perp} = \rho_m^{1.5} \cdot d / 23 \quad \text{Eq 2.13}$$

where ρ_m is mean density of the material (determined experimentally), d the effective diameter of the screw, and $d_{eff} = 1.1 \cdot d_{core}$, where d_{core} is the thread root diameter.

The empirical model of Eq 2.13 is based on the regression analysis of a wide number of experimental tests, and assumes the slip moduli as the ratio between the load and displacement of fasteners at 40% of their maximum load, as discussed in Ehlbeck and Larsen (1993). The main drawbacks of Eq 2.13 are that details of its derivation are lacking, and that since it was developed for traditional fasteners, it remains to be proven whether it can be applied to evaluate the slip modulus of modern STS screws which are characterized by higher slenderness and strength.

2.4.7 Stiffness of axially loaded screws (pure tension)

The axial component, k_{ax} or k_{\parallel} could be either tension or compression. However, EC5 (EN 1995-1-1, 2008) does not provide any empirical models to assess the axial slip modulus (axial component) of STS axially loaded, and hence equations proposed by manufacturers included in their technical approval (ETA-11/0190, 2018) is used.

$$k_{ax} = k_{\parallel} = 780 d^{0.2} \cdot l_{ef}^{0.4} \quad \text{Eq 2.14}$$

Eq 2.14 can be applied only in cases where d of the inserted screws exceeds 6 mm and their d is higher than the maximal width of the gaps in the layers of the CLT panels. Besides, screws need to penetrate into the CLT elements for at least four times their d .

Bejtka (2005) determined the axial stiffness of screws experimentally and proposed axial stiffness:

$$k_{ax} = k_{\parallel} = 234(\rho \cdot d)^{0.2} \cdot l_{ef}^{0.4} \quad \text{Eq 2.15}$$

Further, according to the technical approval (DIBt, 2011), axial stiffness is:

$$k_{ax} = k_{\parallel} = 25 \cdot d \cdot l_{ef} \quad \text{Eq 2.16}$$

where, l_{ef} is the effective embedment length of the threaded part of screw in wood element.

2.4.8 Stiffness axially-laterally loaded inclined screws (shear-tension)

When the screws are applied at an angle then the load has two components: one acting parallel (axial component, k_{ax} or k_{\parallel}) and another acting perpendicular to the load (lateral/shear component, k_{lat} or k_s or k_{\perp}) shown in Figure 2.7. Tomasi et al. (2010) developed a model to propose the stiffness

for inclined screws with two different equations. One is per screw where the screw could be in shear-tension or shear-compression or per screw pair where one screw needs to be in shear-tension, and one in shear-compression. In this study as all stiffness values were calculated per screw so the stiffness equation for per screw was chosen to calculate the stiffness for inclined screws:

$$k_w = k_{\perp} \cdot \cos\alpha \cdot (\cos\alpha - \mu \cdot \sin\alpha) + k_{\parallel} \cdot \sin\alpha \cdot (\sin\alpha + \mu \cdot \cos\alpha) \quad \text{Eq 2.17}$$

where k_{\perp} is lateral stiffness component, k_{\parallel} is axial stiffness component, and α angle of screw insertion to the grain. Eq 2.13 can be used for the lateral component k_{\perp} and for the axial component k_{\parallel} , Eq 2.14, Eq 2.15 or Eq 2.16 can be used.

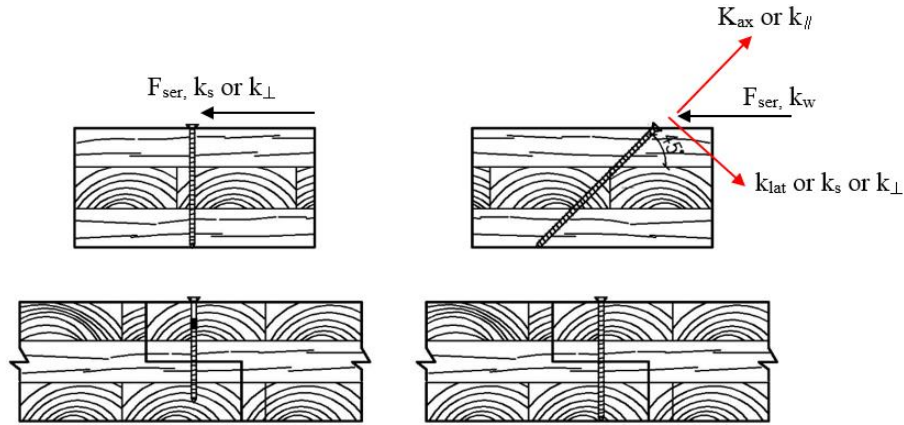


Figure 2.7: STS stiffness: a) laterally loaded, and b) laterally and axially loaded

With respect to the initial stiffness of CLT joints with pairs of crossed STS loaded laterally and assuming a linear elastic stress distribution, the relative elastic stiffness $k_{s,pair}$ is given by Eq 2.18.

$$k_{s,pair} = 2 k_s \quad \text{Eq 2.18}$$

Conversely, for CLT joints with pairs of crossed axially-laterally loaded STS, one acting in tension-shear and the other in compression-shear, the elastic stiffness, $k_{w,pair}$ represents the

combination of their lateral and axial slip moduli as a function of α , screw insertion angle. Tomasi et al. (2010) also proposed a linear model combination of k_s and k_w for shear connections with screws with different shank to grain angles while also taking into account the effect of friction. From this model, assuming that compression component perpendicular to the shear plane is equal and reversed between the screws acting in shear-tension and in shear-compression, $k_{w,pair}$ becomes:

$$k_{w,pair} = k_{\perp} \sin^2 \alpha + k_{\parallel} \cos^2 \alpha \quad \text{Eq 2.19}$$

2.5 Group effect for screws

The phenomenon that the load-carrying capacity of timber connections with multiple mechanical fasteners is smaller than the sum of the single fastener's capacities is called 'group-effect'. This reduction can be described using the concept of an effective number of fasteners (n_{eff}) (Jorissen, 1998) as shown in equation (Eq 2.20):

$$F_N = F_S \cdot n_{eff} \quad \text{Eq 2.20}$$

where F_N is the load-carrying capacity of a multiple fastener connection and F_S is the load carrying capacity of a single fastener.

Until the 1970s, this group-effect was not explicitly considered in timber design. Then, equations to consider the group-effect in bolted connections based on theoretical considerations were proposed (Doyle, 1964; Fahlbusch, 1949; Kunesh and Johnson, 1968), see Table 2.1. Madsen (Madsen, 1992) investigated the group-effect for bolts and indicated the previous practice was not safe. EC5 (EN 1995-1-1, 1994) included an equation to estimate n_{eff} for a connection with more than six bolts in one row parallel to the grain. The load carrying capacity for the extra bolts is

reduced by one third. Other group-effect equations were suggested by Gehri (1996) and Jorissen (1998). Later Jorissen's work was included in EC5 (EN 1995-1-1, 2004). The current EC5 (EN 1995-1-1, 2008) accounts for group-effect for screwed connections loaded parallel to the grain using the relationship $n_{\text{eff}} = n^{0.9}$, however, it does not account for a group-effect in connections loaded perpendicular to the grain.

Before that, the strength of a connection was simply assumed to be the design value of a single fastener multiplied by the number of the fasteners. In the 1986 NDS (1986), tables based on the work by Cramer (1968) provided reduction factors to account for the fact that the fasteners arranged in a serial row do not share load equally. In such arrangements, the outermost fasteners carry the most load while the innermost ones carry the least load. In 1980, Wilkinson (1980) showed that this model is only valid in the linear-elastic range and for loads applied parallel to grain. Since 1997, the NDS (AFPA, 1997) used the Lantos model (Lantos, 1969), in a tabulated form for bolts, lag screws, split rings, and shear plates in a row based on an equation format developed by Zahn (1991).

Since 1984, the Canadian Standard for Engineering Design in Wood CSA O86 (1984) included the modification factor J_G for bolts, lag screws, split rings and shear plates which was based on a ratio of the cross-sections of the timber members. In 1989, CSA086 (1989) added adjustments that accounted for the number of bolts in a row, the loaded end distance, the number of bolt rows, and the bolt slenderness ratio based on new findings (Yasumura et al., 1987; Masse et al., 1989). In 2009, CSA-086 (2009) introduced a mechanics based-model for the capacity of bolted connections that accounts for brittle failure modes and the group-effect modification factor for bolts was taken out. The provisions for lag screws, however, remained unchanged. The group effect expressions implemented into EC5, NDS, and CSA-O86 differ significantly, see Figure 2.8; e.g., the value of

n_{eff} according to EC5 is twice that of CSA-O86 for a larger number of screws in one row. These discrepancies indicate the need and importance for further fundamental research on multiple screw timber connections.

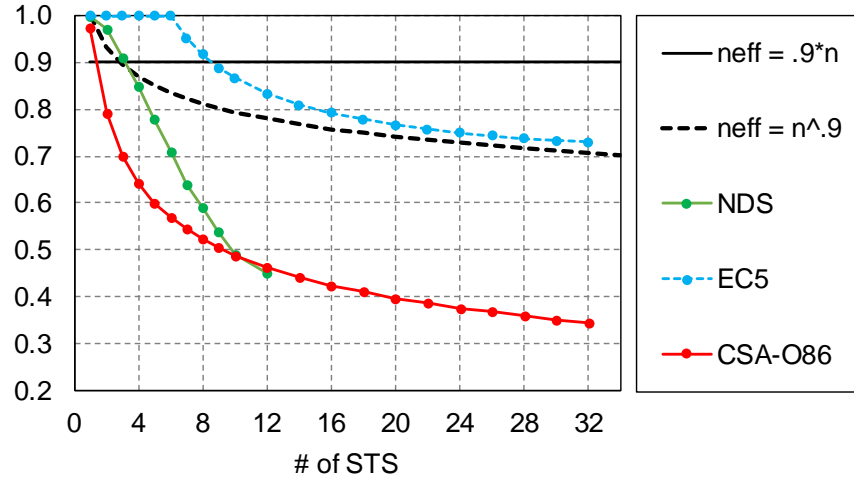


Figure 2.8: Reduction in strength for n_{eff} according to different design standards

With respect to the group-effect in STS, Brandner (2016) investigated the withdrawal capacity of STS groups placed in the narrow face of CLT and conservatively proposed the relationship $n_{\text{eff}} = 0.9 \cdot n$, even though the test results indicated $n_{\text{eff}} > 1$. Krenn and Schickhofer (2009) performed tension tests on glulam joints connected with steel plates as outer members using inclined STS in both single and multiple rows up to a maximum of 8 screws per joint and proposed $n_{\text{eff}} = 0.9 \cdot n$ for the capacity reduction. For serviceability limit states, $n_{\text{eff}} = n^{0.8}$ was suggested to account for the group effect. Krenn and Schickhofer (2009) further showed that the influence of number of fasteners on the joint capacity is variable and inconsistent when comparing ductile and withdrawal failure modes.

Table 2.1: Different considerations of group-effect factor¹

Source	Group-effect factor	Fastener
Fahlbusch, 1949	$n_{\text{eff}} = \frac{4 \cdot n}{n+3}$	Bolts
Doyle, 1964	$n_{\text{eff}} = 0.6-0.90$	Bolts
Kunesh and Johnson, 1968	$n_{\text{eff}} = 0.5-0.95$	Bolts
Lantos, 1969; NDS, 1973	$n_{\text{eff}} = \left[\frac{m(1 - m^{2n})}{n [(1 + R_{EA}m^n)(1 + m) - 1 + m^{2n}]} \right] \left[\frac{1 + R_{EA}}{1 - m} \right]$	Bolts, Lag screws
Yasumura, et al, 1987	$n_{\text{eff}} = 0.5$	Bolts
CSA-086, 1989	$n_{\text{eff}} = 0.33 k_n \left(\frac{t}{d}\right)^{0.5} \left(\frac{a_1}{d}\right)^{0.2} n^{0.7} \leq n$	Bolts
Gehri, 1996	$n_{\text{eff}} = 2 \left(\frac{n}{2}\right)^{0.8\lambda_r}$ where $\lambda_r = \frac{\lambda}{\lambda_y} \leq 1.0$	Bolts
EN 1995, 1994	$n_{\text{eff}} = \frac{6+2 \cdot n}{3} \leq n$	Bolts
Jorissen, 1998; EN 1995-1-1, 2004	$n_{\text{eff}} = \min \left\{ \frac{n}{n^{0.9} \sqrt{\frac{a_1}{13d}}} \right\}$	Bolts
EN 1995, 2008	$n_{\text{eff}} = n^{k_{\text{eff}}}$ where $k_{\text{eff}} = f(\text{spacing, predrilling})$	Nails
	$n_{\text{eff}} = n^{0.9}$	Screws
CSA O86, 2016	$n_{\text{eff}} = \left[\frac{m(1 - m)^{2n}}{n [(1 + R_{EA}m^n)(1 + m) - 1 + m^{2n}]} \right] \left[\frac{1 + R_{EA}}{1 - m} \right]$	Lag screws
	$n_{\text{eff}} = n$	Bolts, Nails
ETA-11/0190, 2018	$n_{\text{eff}} = n$ (loaded laterally)	Screws
	$n_{\text{eff}} = \max\{n^{0.9}; 0.9 * n\}$ (loaded axially)	

¹ where n = number of fasteners in the row, R_{EA} = the lesser of $\frac{E_s A_s}{E_m A_m}$ or $\frac{E_m A_m}{E_s A_s}$, E_m or E_s = modulus of elasticity of main or side member, A_m or A_s = gross cross-sectional area of main or side member, $m = u - \sqrt{u^2 - 1}$, $u = 1 + \gamma \frac{s}{2} \left[\frac{1}{E_m A_m} + \frac{1}{E_s A_s} \right]$, s = center to center spacing between adjacent fasteners in a row, in, γ = load/slip modulus for a connection, lb/in, a_1 = spacing between bolts in the grain direction, d = bolt diameter, λ and λ_y = slenderness ratio for timber to timber connections, where, n = number of bolt rows, t = timber thickness, $k_n = 1$ for $n=1$, $k_n = 0.8$, for $n=2$, and $k_n = 0.6$ for $n=3$

2.6 State-of-the-art of CLT-STS applications

Spline, lap, and butt joints combined with applying screws loaded either laterally and or axially can be used in the CLT-STS wall-to-wall or floor-to-floor connections. These connections have to resist primarily in-plane shear forces. As CLT panels mostly behave as rigid bodies, the desired energy dissipation under seismic loading must be achieved by the connections between panels. CLT assemblies have been shown to provide adequate seismic performance when ductile dowel-type fasteners are used (Sandhass et al., 2009; Joyce et al., 2011; Gavric et al. 2015a).

Sandhass et al. (2009) tested single spline joints under quasi-static monotonic and reversed cyclic shear loading and successfully described their load-carrying capacity with Johansen's model. Vessby et al. (2009) tested internal spline connection, and spline joints with outside fiber boards placed in top and bottom connected using screws and glue and compared the results with solid CLT specimens with no joinery. Internal spline joint was half as stiff and yielded at much lower ultimate load than the glued and screwed fiberboard surface spline. The fiberboard surface spline specimens yielded nearly identical results to the non-jointed solid CLT specimens. Follesa et al. (2010) tested internal spline, single surface spline, and lap joints and found 1.5 times higher capacity and significant differences in stiffness values compared to predictions according to (EN 1995-1-1, 2008). EC5 stiffness formula does not take into account many parameters as the thickness of the wooden elements and the type of steel used for the fasteners which results in very large estimates.

Popovski et al. (2010) conducted an extensive experimental program on CLT wall panels subjected to monotonic and cyclic lateral loads. They tested single panel walls with different aspect ratios, multi-panel walls with step joints and different connections (types of screws), as well as one- and two-storey wall assemblies. They considered various types of fasteners such as annular ring nails,

spiral nails, and screws with different diameters and lengths. Results showed that CLT walls with nails or screws along with steel brackets had adequate seismic performance. Diagonally placed long screws were not recommended to connect walls to floors due to their brittle failure mode. Using step joints in long walls was found to be beneficial due to the reduction in stiffness of the walls which decreased the seismic load input and increased the deformation capability of the walls.

Joyce et al. (2011) tested double spline joints and achieved high ductility with STS loaded in shear and high stiffness with STS acting in withdrawal. Half-lapped and single-spline in edge-to-edge CLT-STs plate connections that perform diaphragm or shear wall functions were tested by Sadeghi and Smith (2014). They found the half-lapped joints are about 50% stronger and stiffer than single-spline joints when acting as plate edge-to-edge in-plane shear connections in CLT slabs.

Gavric et al. (2015b) investigated CLT panel-joints using lap and spline joints under monotonic and cyclic loading and concluded that half-lap joints showed superior performance compared to spline joints. Gavric (2013), and Gavric et al. (2011 and 2014) performed cyclic tests focusing on coupled CLT wall panel behavior considering different types of screwed vertical joints (step joint, spline LVL joint) with several different configurations of anchor connectors and hold downs. Gavric et al. (2014; 2015a; 2015b) tested 12 different connections between adjacent CLT wall-to-wall, wall-to-floor, and floor-to-floor panels, both parallel and orthogonal, under monotonic and cyclic loading. The step joint connections were found to have higher stiffness compared to the spline LVL joints, however, in some cases the step joints experienced a brittle failure due to splitting in the inner layer of the panel. Spline joints could resist greater forces at higher displacements.

Partially threaded (PT) or fully threaded (FT) STS are commonly used as fasteners and considerable benefits are observed in the case of crossed inclined screws. In this configuration, the screws are subjected either to a combined shear-compression or shear-tension stress state. The resistance mechanism can be idealized as a truss system in which the screws are the truss diagonals, surrounded and stabilized in the cross-section transversal directions by the wood. Lam (2011) tested three different types of layout of butt joints and found that STS loaded in withdrawal performed considerably better than STS loaded in shear.

Richardson (2015) tested three small-scale CLT connection configurations using non-proprietary fasteners. Three different connections (LVL surface spline with lag screws, half-lap joint with lag screws, and butt joint with a steel plate fastened with nails) were tested in both monotonic and cyclic tests. The surface spline and half-lap connections often failed in a catastrophic manner usually due to splitting of the spline and fastener failure. Experimental capacities were generally 14% lower than predicted by the yield models for the surface spline and steel plate butt joints. The half-lap connection resulted in 21% higher experimental capacities than predicted.

Jockwer et al. (2014) experimentally determined the capacity and stiffness of joints with screws loaded axially varying different shank to grain angles, i.e. 90° , 60° , and 45° . They found axially loaded fully threaded STS showed highest load-carrying capacity and stiffness. The capacity and the stiffness become lower with the screw loaded more laterally. Choosing an appropriate angle between screw shank and grain direction can result in achieving high capacity and stiffness.

The feasibility of an innovative STS assembly with a double inclination of fasteners in butt-joints was demonstrated with high stiffness and ductility under quasi-static monotonic loading and moderate ductility under reversed cyclic loading (Zhang et al., 2015, 2016). Sullivan et al. (2018)

found half-lap connections with a unique combination of angled and vertical screws performed exceptionally well with both high, linear elastic initial stiffness and ductile, post-peak behavior.

2.7 Summary of literature review

Manufacturing of CLT in North America is driven by a rising demand for construction and building applications, due to its cost-effectiveness and sustainability. Multiple proprietary STS products are available to designers and builders, one of them (SWG ASSY® screws) with both Canadian (CCMC 13677-R, 2018) and US product approvals (ESR-3178, 2018). The Canadian product approval for STS (CCMC 13677-R, 2018), however, is limited to visually graded lumber, glued-laminated timber and structural composite lumber produced from Canadian wood species, and CLT was not included in that approval.

In the US, design provisions for CLT were added to the 2015 edition of the (NDS, 2015), including details on edge spacing requirements for dowel type connectors. The 2015 International Building Code (IBC, 2015) added a section on CLT complying with ANSI/APA PRG-320 (2012). CLT has been recognised as a state-wide alternative method for seismic design in Oregon with reference to the IBC (2015), NDS (2018), and ASCE 7 (2016). In Canada, comprehensive CLT provisions for the design of members, connections with bolts and lateral load resisting systems were introduced in the 2016 supplement to the 2014 version of CSA 086 (2014). However, no guidance for the use of STS is given. Sub-section 11.9.2 of CSA 086 (2014) provides seismic design considerations for CLT structures based on the capacity-based design approach; however, there is not any information on the strength, stiffness, and ductility requirements for CLT shear walls connections. The research presented in this thesis will address some of these existing knowledge gaps.

Chapter 3: Withdrawal Testing of STS in Canadian CLT

3.1 Overview

Experimental investigations of withdrawal tests on ASSY[®] structural STS installed in SPF based CLT were performed. At the time of the work the Canadian product approval for these screws (CCMC 13677-R, (2012)) was limited to visually graded lumber, GLT, and SCL produced from Canadian wood species. The screws, however, had a European Technical Approval for use in CLT (ETA-11/0190, 2013). Therefore, the tested hypothesis was that the withdrawal resistance, $P_{rw,\alpha}$, in CLT produced from Canadian lumber can be calculated using the CCMC 13677-R equations. Withdrawal tests were performed varying screw diameter d , effective screw embedment length l_{ef} , and angle α between the screw axis relative to the grain orientation of the top layer of the CLT panel. In addition to the main metric: withdrawal resistance; labeled F_{max} (with COV and 5th%), yield load, displacement at capacity, displacement at yield load, and ductility were determined and evaluated.

3.2 Materials

CLT panels fabricated according to ANSI/APA PRG-320 (2012) were supplied by Structurlam Products Ltd. 3-ply (thickness 99mm) and 5-ply (thickness 169mm) CLT were used for this test. CLT grade used was V2M1, with 12% (+/-2%) moisture content at time of production and 0.42 specific gravity. Canadian softwood, species group SPF No.1/No. 2, was used in combination with Purbond polyurethane adhesive.

SWG ASSY® VG with CSK head type fully threaded 8mm diameter 140 mm long and 10 mm diameter 220 mm long STS were used (CCMC 13677-R, 2012). This kind of screws have countersunk head style where the screw head is required to be flush with the surface. These are usually recommended for steel-to-wood connections where the screw head is flush finished into the steel plate. The minimum spacing, end, and edge distance requirements of screws in plane and edge surface of CLT according to ETA-11/0190 (2013) are summarized in Table 3.1 and shown in Figure 3.2.



Figure 3.1: STS ASSY® VG CSK

Table 3.1: Minimum spacing, end, and edge distance of in CLT

Series	a_{1-90}	$a_{1,t}$	$a_{1,c}$	a_2	$a_{2,t}$	$a_{2,c}$
Plane surface	4d	6d	6d	2.5d	6d	2.5d
Edge surface	10d	12d	7d	4d	6d	3d

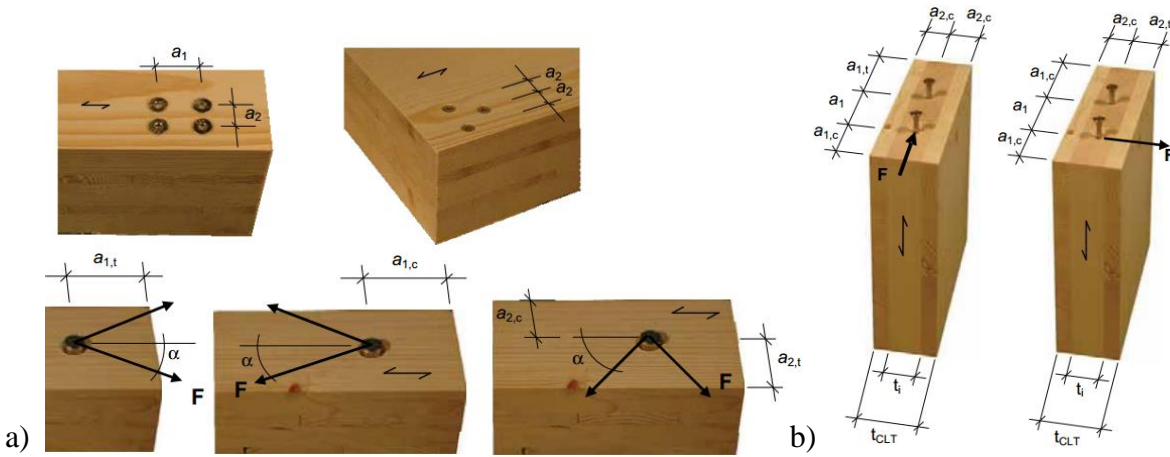


Figure 3.2: Definition of spacing of STS in CLT: a) wide face, and b) edge (ETA-11/0190, 2013)

3.3 Specimen description

One hundred and eighty withdrawal tests were performed varying three parameters: screw diameter d (8mm and 10 mm), effective screw embedment length l_{ef} ($8d$ and $12d$), and angle α between the screw axis relative to the grain orientation of the top layer of the CLT panel (90° and 45°). The spacing, edge, and end distances of screws installed in the specimens are based on the requirements specified in CCMC 13677-R (2012). A typical test specimen is shown in Figure 3.3. The minimum requirements of spacing between screws, between rows, end and edge distances are $10d$, $5d$, $10d$, and $5d$ respectively and are shown in Figure 3.4.

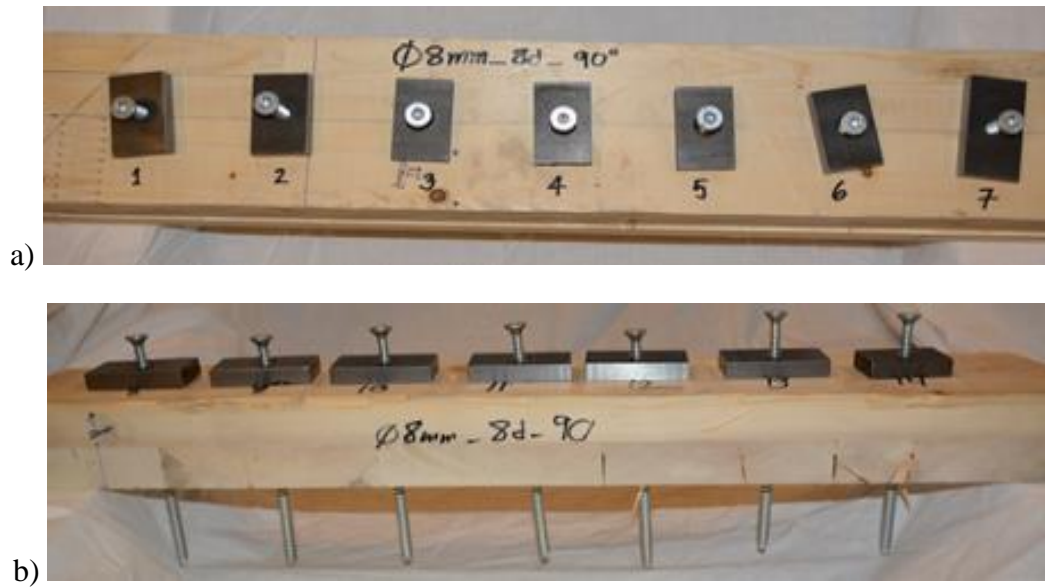


Figure 3.3: Typical test specimen: a) plan view, and b) elevation view

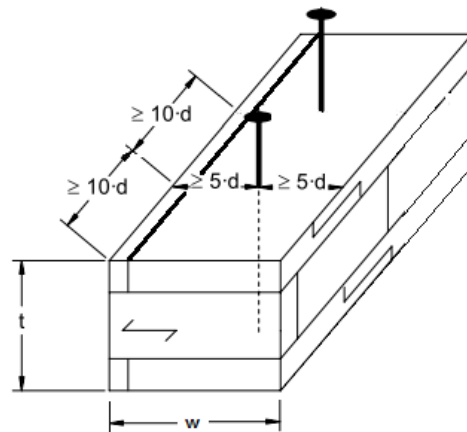


Figure 3.4: Spacing, edge, and end distances (CCMC 13677-R, 2012)

Table 3.2: Withdrawal test series

Series	d [mm]	l_{ef} [mm]	α [°]	n [-]
1	8	64	90	30
2	8	96	90	30
3	8	64	45	30

4	8	96	45	30
5	10	80	90	15
6	10	120	90	15
7	10	80	45	15
8	10	120	45	15

3.3.1 Series 1 (8mm_8d_90°)

In this series, 8mm diameter 140 mm long ASSY® VG CSK head type screw was installed in 90° where the penetration depth was 64mm (8d).

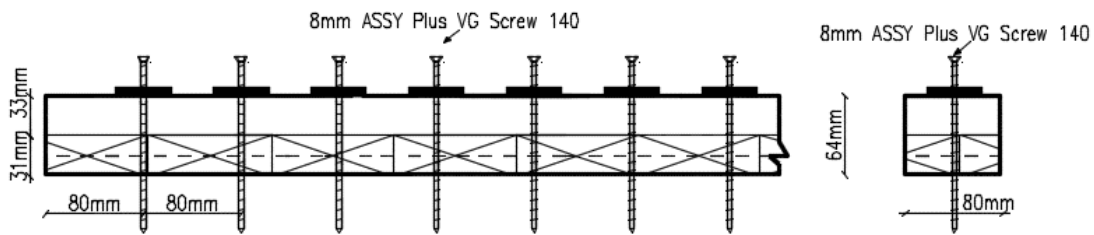


Figure 3.5: Series 1 layout: side section (left) and cross section (right)

3.3.2 Series 2 (8mm_12d_90°)

In this series, 8mm diameter 140 mm long ASSY® VG CSK head type screw was installed in 90° where the penetration depth was 96mm (12d).

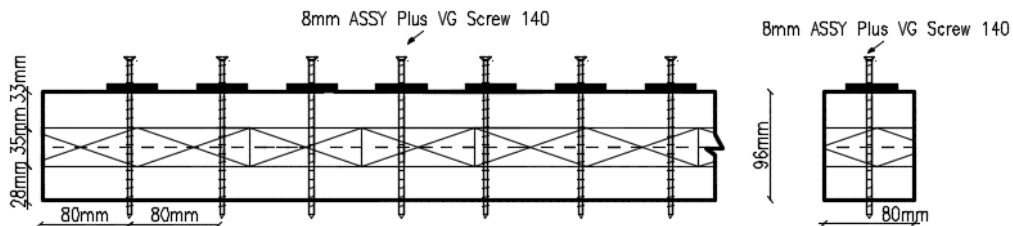


Figure 3.6: Series 2 layout: side section (left) and cross section (right)

3.3.3 Series 3 (8mm_8d_45°)

In this series, CLT was cut in 45°. Then 8mm diameter 140 mm long ASSY® VG CSK head type screw was installed in 90° in that 45° cut CLT specimen, which makes the angle between the screw axis and the CLT grain orientation 45°. Penetration depth for this series was 64mm (8d).

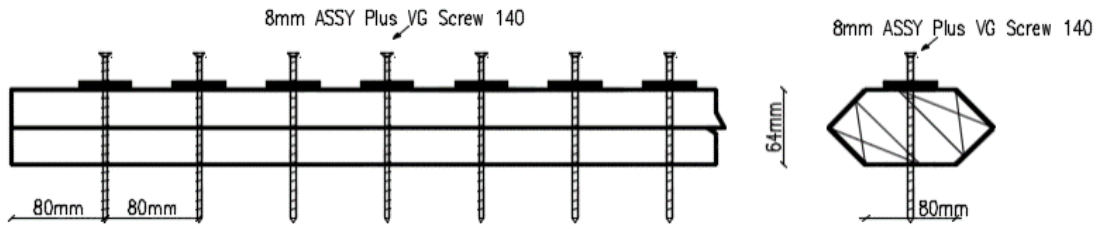


Figure 3.7: Series 3 layout: side section (left) and cross section (right)

3.3.4 Series 4 (8mm_12d_45°)

In this series, CLT was cut in 45°. Then 8mm diameter 140 mm long ASSY® VG CSK head type screw was installed in 90° in that 45° cut CLT specimen, which makes the angle between the screw axis and the CLT grain orientation 45°. Penetration depth for this series was 96mm (12d).

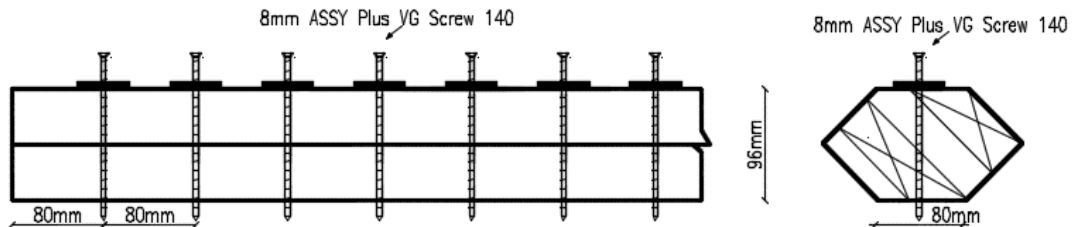


Figure 3.8: Series 4 layout: side section (left) and cross section (right)

3.3.5 Series 5 (10 mm_8d_90°)

In this series, 10 mm diameter 220 mm long ASSY® VG CSK head type screw was installed in 90° where the penetration depth was 80 mm (8d).

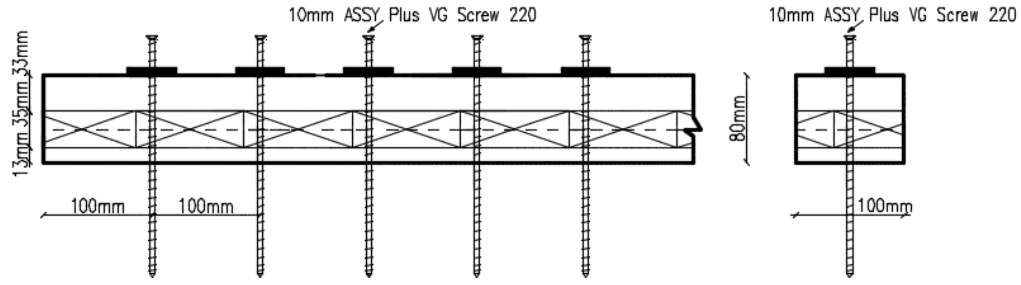


Figure 3.9: Series 5 layout: side section (left) and cross section (right)

3.3.6 Series 6 (10 mm_{12d}_{90°})

In this series, 10 mm diameter 220 mm long ASSY[®] VG CSK head type screw was installed in 90° where the penetration depth was 120 mm (10*d*).

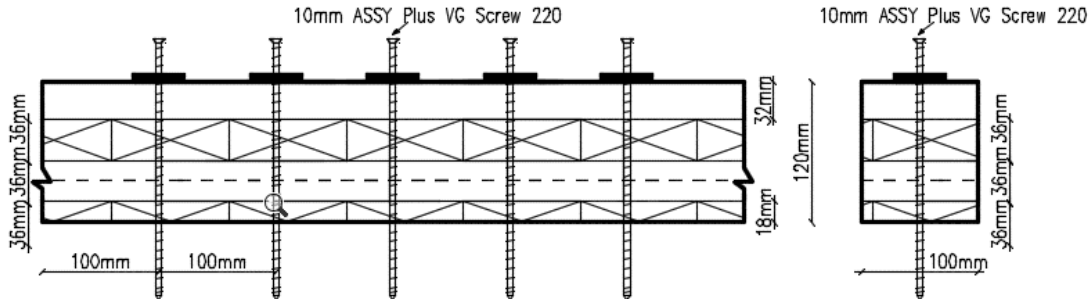


Figure 3.10: Series 6 layout: side section (left) and cross section (right)

3.3.7 Series 7 (10 mm_{8d}_{45°})

In this series, CLT was cut in 45°. Then 10 mm diameter 220 mm long ASSY[®] VG CSK head type screw was installed in 90° in that 45° cut CLT specimen, which makes the angle between the screw axis and the CLT grain orientation layer 45°. Penetration depth for this series was 80 mm (8*d*).

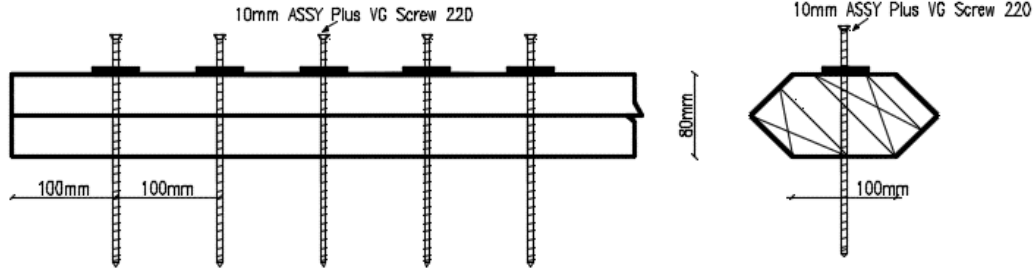


Figure 3.11: Series 7 layout: side section (left) and cross section (right)

3.3.8 Series 8 (10 mm_12d_45°)

In this series, CLT was cut in 45°. Then 10 mm diameter 220 mm long ASSY® VG CSK head type screw was installed in 90° in that 45° cut CLT specimen, which makes the angle between the screw axis and the CLT grain orientation 45°. Penetration depth for this series was 120 mm (12d).

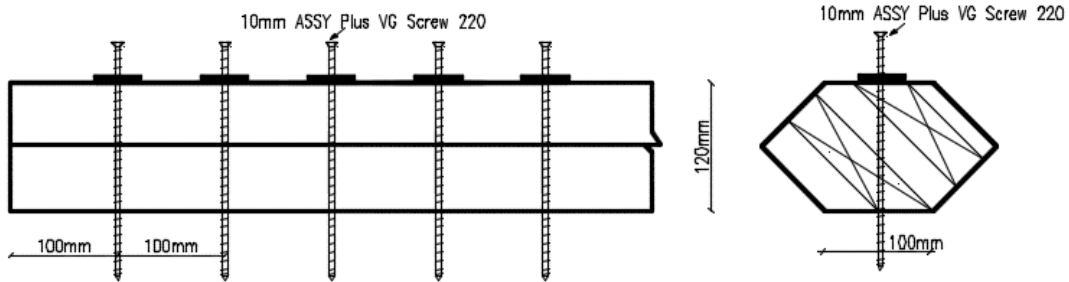


Figure 3.12: Series 8 layout: side section (left) and cross section (right)

3.4 Design values and estimated resistance

The product approval (CCMC 13677-R, 2018) provides design guidance for SWG ASSY® fully threaded STS. For screws loaded in withdrawal, as used in this research, the designer must consider the withdrawal resistance of the screw thread embedment length. The factored withdrawal resistance, $P_{rw,\alpha}$, can be calculated using Eq 3.1:

$$P_{rw,\alpha} = \Phi \cdot \frac{0.8 \cdot \delta \cdot (b \cdot 0.84 \cdot \rho)^2 \cdot d \cdot l_{ef} \cdot 10^{-6}}{\sin^2 \alpha + \frac{4}{3} \cos^2 \alpha} K_D K_{SF} \quad Eq\ 3.1$$

where Φ is the resistance factor, δ the density adjustment factor, b the material adjustment factor, ρ the mean oven-dry relative density, d the screw outer diameter, l_{ef} the effective screw embedment length (thread length minus tip length), α the angle between grain and screw, K_D the load duration factor, and K_{SF} the service condition factor.

Herein, to estimate the average resistance of the screws in tests using CLT manufactured from SPF, the resistance factor is taken as $\Phi = 1.0$, $\delta = 85$ (for $\rho < 440 \text{ kg/m}^3$); $b = 1.0$; $\rho = 420 \text{ kg/m}^3$; $d = 8 \text{ mm}$ and 10 mm , $l_{ef} = 8d$ and $12d$; $\alpha = 90$ and 45° for the top layer of the CLT panel; $K_{SF} = 1.0$ (for dry service conditions), and the load duration adjustment factor as $K_D = 1.25$ ($=1/0.8$).

3.5 Test methods

The test setup consisted of CLT samples fixed to the test table with STS drilled in from the top. The test was performed according to ASTM D1761 -12 (2013). Seven steps were followed:

- 1) The specimens were cut and planed to the required depths equaling the design embedment depth of the screws of $8d$ and $12d$. For ease of testing screws at a 45° orientation to the top layer, instead of installing the screws at 45° , the specimens were cut at 45° and then placed flat on the testing fixture.
- 2) STS were inserted with a steel hook on their neck on top of the CLT. This hook had a hole through which the STS precisely penetrated and was used to properly pull the STS.

- 3) The screws were installed in the CLT member avoiding gaps, checks, or cracks following the spacing requirements.
- 4) The specimens were placed in the loading apparatus such that the screw axis was aligned with the direction of the applied load.
- 5) The specimen was loaded in a Sintech 30/D universal test machine using a displacement controlled tensile load at a constant displacement rate of 3.5 mm/min. The test was stopped when the applied load decreased to about 80% of the peak load. As stiffness and ductility metrics were not of interest, only the actuator displacement was recorded.
- 6) After each single screw withdrawal test, the specimen was then re-positioned such that the next screw was aligned with the direction of the applied load.
- 7) Steps 4-6 were repeated until all screws in one specimen were tested. Then, the specimen was removed from the testing apparatus. Only tests where screw withdrawal was the initial failure mode were accounted for in the subsequent analyses.

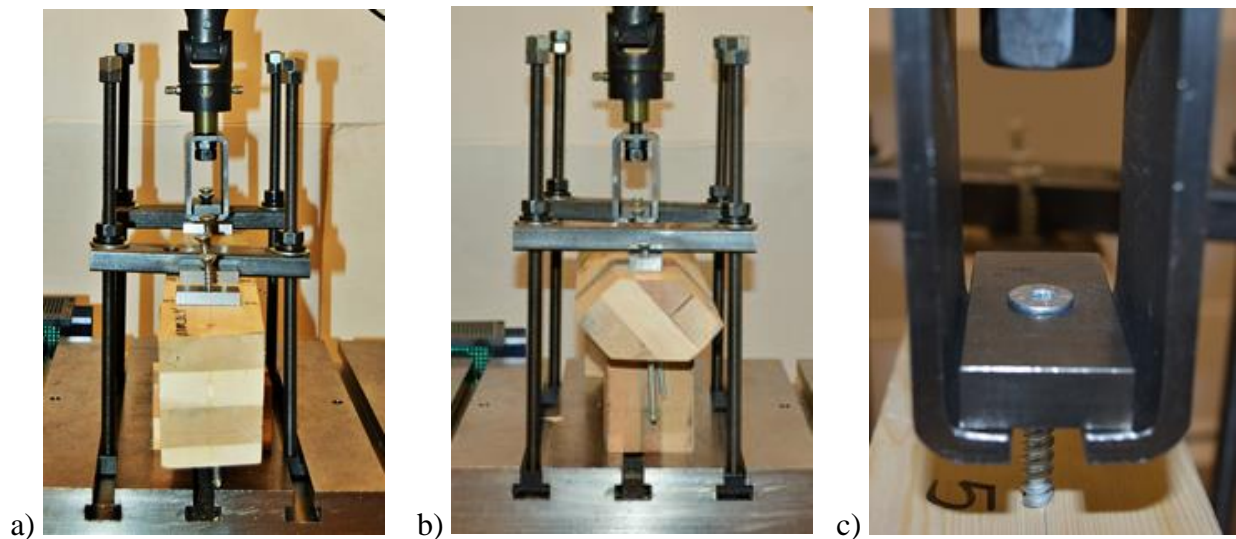


Figure 3.13: Test Setup for a) Withdrawal at 90°, b) 45°, and c) detail

3.6 Analyses

From the tests, the withdrawal resistance labeled F_{\max} with its COV were determined. The 5th percentile values of the F_{\max} were calculated according to Eq 3.2. Herein a normal distribution was assumed with COV = 13.5% based on the actual tests.

$$x_{5\%} = x_{\text{mean}} \cdot \exp \left[- \left(2.645 + \frac{1}{\sqrt{n}} \right) \cdot COV(x) + 0.15 \right] \quad \text{Eq 3.2}$$

In addition, following connection metrics were obtained: i) Yield load; labeled F_Y ; ii) Displacement at capacity; labeled $d_{F,\max}$; iii) Displacement at yield load; labeled $d_{F,Y}$; iv) Stiffness; labeled k ; and v) Ductility; labeled μ . Stiffness was calculated in accordance with EN-26891 (1991) for the range of the load-displacement curves between 10% and 40% of screw withdrawal resistance, labeled as k . As a second metric. To calculate yield strength, displacement corresponding to yield strength, equivalent energy elastic-plastic (EEEP) curves according to ASTM E2126–11 (2014) were developed. Ductility (μ) was calculated taking the ratio between the ultimate displacement, $d_{F,\max}$ at maximum load, F_{\max} and the yield displacement, $d_{F,Y}$ ($d_{F,\max}/d_{F,Y}$). Ductility of the joints were categorized based on the classification by Smith et al. (2006). Smith et al. (2006) proposed a scale based on the ratio between displacement at capacity to displacement at yield: brittle ($\mu \leq 2$), low ductility ($2 \leq \mu \leq 4$), moderate ductility ($4 \leq \mu \leq 6$) and high ductility ($\mu > 6$). While not originally proposed for this purpose, these ductility categories were used herein together with the EEEP method. Finally, for discussion purposes, following ratios between predictions using Eq 3.2 and the experimentally observed results were calculated: vi) $F_{\max,5\%} / P_{\text{rw},\alpha,\text{fact}}$, vii) $F_{\max,5\%} / P_{\text{rw},\alpha,\text{unfact},5\%}$, and viii) $F_{\max,\text{mean}} / P_{\text{rw},\alpha,\text{unfact},\text{mean}}$.

3.7 Results

The recorded load displacement relationships for 8mm and 10 mm STS are shown in Figure 3.14.

In this test campaign, the presented curves are the displacement recordings of the actuator head plotted against the recorded load in the actuator's load cell. Table 3.3 summarizes the results,

Table 3.4 shows a comparison between design values and experimental results.

Table 3.3: Withdrawal test results

Series	d [mm]	l_{ef} [mm]	α [°]	n [-]	F_{max} [kN]	F_Y [kN]	d_{Fmax} [mm]	d_{FY} [mm]	μ [-]	k [kN/mm]
1	8	64	90	30	8.5	7.7	4.0	2.3	1.8	3.7
2	8	96	90	30	15.3	12.7	3.2	2.0	1.7	6.6
3	8	64	45	30	9.7	7.5	3.0	1.9	1.8	4.3
4	8	96	45	30	13.9	11.3	2.8	1.6	1.7	7.0
5	10	80	90	15	13.8	8.5	3.8	1.6	1.5	5.5
6	10	120	90	15	19.7	18.5	4.1	2.7	1.6	7.0
7	10	80	45	15	14.7	13.7	3.7	2.7	1.4	5.4
8	10	120	45	15	19.7	17.4	3.6	2.7	1.5	7.4

Table 3.4: Comparison to design values

Series	F_{\max} [kN]			$P_{rw,\alpha}$ [kN]			Ratio [-]		
	mean	COV	5 th %	factored	5 th %	mean	$F_{\max,5th\%}/P_{\text{factored}}$	$F_{\max,5th\%}/P_{\text{unfact,5th\%}}$	$F_{\max,mean}/P_{\text{unfact,mean}}$
1	8.5	16.4	5.6	3.9	5.4	6.6	1.4	1.0	1.3
2	15.3	12.0	11.7	5.9	8.1	9.9	2.0	1.4	1.5
3	9.7	14.5	6.8	3.3	4.6	5.7	2.0	1.5	1.7
4	13.9	14.5	9.8	5.0	7.0	8.5	1.9	1.4	1.6
5	13.8	9.9	11.3	6.1	8.5	10.3	1.9	1.3	1.3
6	19.7	14.9	13.6	9.1	12.7	15.5	1.5	1.1	1.3
7	14.7	12.8	10.9	5.2	7.3	8.9	2.1	1.5	1.7
8	19.7	13.0	14.5	7.8	10.9	13.3	1.9	1.3	1.5

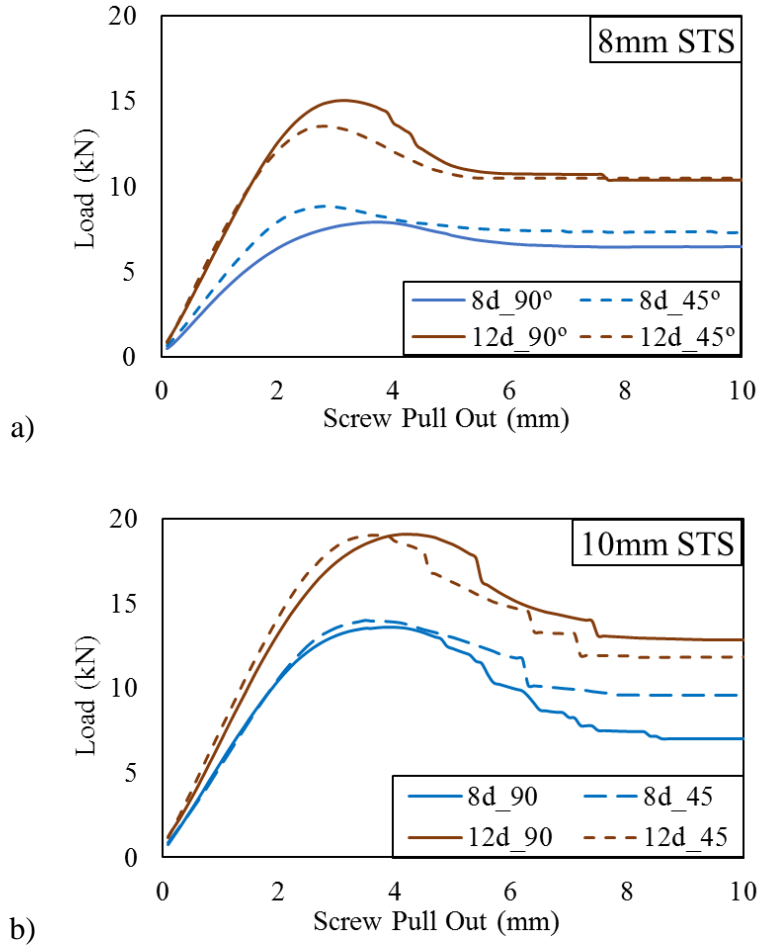


Figure 3.14: Average load displacement curves: a) 8mm STS, and b) 10 mm STS

3.8 Discussion

3.8.1 Load-deformation behavior

It is quite important to recognize that due to the test setup utilized and the fact that displacement measurements were obtained through the actuator displacement, these plots in Figure 3.14 exhibit a much “softer” response than what is the true behavior of self-tapping screws in withdrawal. This is simply because slip will occur within the test apparatus and fixtures that are not intrinsic with the specific behavior of the screws. Yet, even though the actual stiffness values cannot (and should not) be obtained from these plots, several key performance characteristics can be determined which are summarized in Table 3.3. First, the average Peak Loads attained are presented. The variability of resistance within the individual test series was on average 13.5%, see appendix A. Interestingly, for both 8mm and 10 mm fasteners, the average peak load at $12d$ embedment is higher (or equal) at 90° than for STS at 45° . Conversely, at $8d$ embedment, the average peak load is higher for STS at 45° than at 90° . This phenomenon may be attributed to the selected test configuration. Due to the setup screws barely engage the top layer and therefore for $8d$ penetration most of the fastener’s axis runs at 45° to the orientation of the grain. However, for $12d$ penetration, the fastener extends all the way to the third layer and now only about 60% of the embedment length is at 45° to the grain and the remainder is embedded perpendicular to the grain of the third cross layer.

Second, a general idea of the behavior associated with STS in CLT can be obtained. From a serviceability standpoint, it can be seen that the effect of angle of insertion of screws in CLT does not seem to have a significant impact on stiffness. Additionally, it can also be observed that within the linear region the stiffness of fasteners at the same embedment length but inserted at a different angle relative to the grain of the top layer, do not exhibit large variation (CoV on average 7%).

A deeper embedment results in higher stiffness and higher withdrawal strength until the upper boundary, the STS tensile resistance, is reached. The angle of insertion seems to have a small effect on the behavior of STS in withdrawal. As pointed out, this can be attributed to the fact that a variety of screw in angles are apparent when fasteners are driven inclined into CLT. Irrespective of the embedment depth and insertion angle, all the series are consistent with the expected associated rather brittle nature of mechanical fasteners in withdrawal showing low ductility ranging from 1.4-1.8. This low ductility value is classified as brittle according to Smith et al. (2006).

3.8.2 Effect of screw diameter

As expected, resistance was proportional to screw diameter d with 10 mm screws leading to approx. 46% larger resistance than 8mm screws. The expected difference, however, was only 15% larger. Based on the small number of replicates n , no explanation can be offered. The resistance for $8d$ and $12d$ embedment for both the insertion angle was 57% and 35% higher in 10 mm screws compared to 8mm screws. The increment of resistance in the $12d$ embedment was not linear compared to $8d$ embedment. It might be due to the test setup and the cross layer of CLT, where even though the embedment length increased from $8d$ to $12d$, 60% of the screw is in 45° angle and rest is in 90° angle with the grain of the CLT.

3.8.3 Effect of screw embedment length

The withdrawal resistance increased with an increase of penetration depth, however, this increase was not linearly proportional to the screw diameter. With the 1.5 times increase in penetration depth from $8d$ to $12d$ embedment leading to approx. 60% and 40% increase in resistance for 8mm and 10 mm STS respectively. For 8mm screws the increase was 10% higher than the expected, however, for 10 mm STS the increase was 10% lower than the expected increase.

3.8.4 Effect of screw insertion angle

The withdrawal resistance for both 8mm and 10 mm screws at 8d embedment increased 10% at 45° screws compared to the 90° screws. However, the withdrawal resistance for both 8mm and 10 mm screws at 12d embedment decreased 10% at 45° screws compared to the 90° screws. This might be due to the test setup where for 8d embedment most of the fastener's axis runs at 45° to the orientation of the grain leading 10% higher resistance. Conversely, for 12d embedment, the fastener extends all the way to the third layer and now only about 60% of the embedment length is at 45° to the grain and the remainder is embedded perpendicular to the grain of the third cross layer leading to 10% decrease in the resistance.

3.8.5 Failure modes

The initial failure mode for all test specimens was brittle screw withdrawal. For screws in 90°, subsequent splitting of the wood was observed as well (Figure 3.15 left). For screws installed at 45° after screw withdrawal, small sections of the CLT's top layer separated (Figure 3.15 right) indicating that edge distances should be increased in future tests.

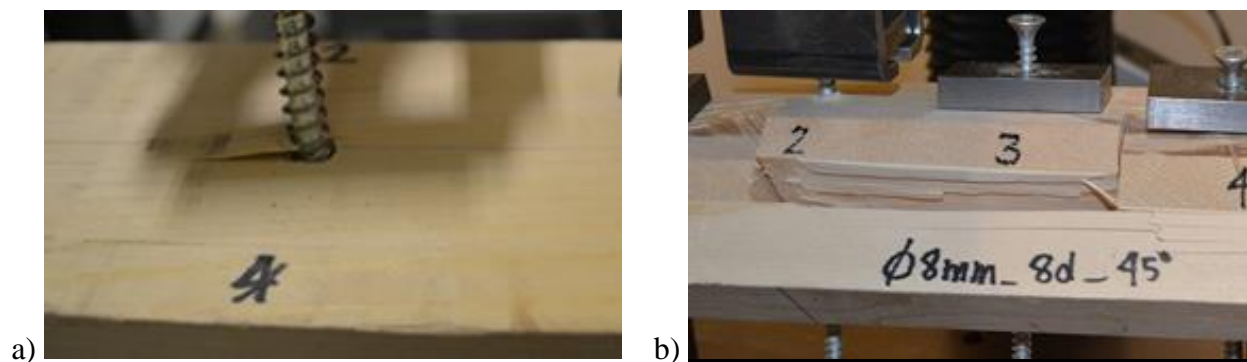


Figure 3.15: Typical failure modes: a) screw withdrawal and splitting of wood with STS installed in 90°, and b) screw withdrawal and layer separation with STS installed in 45°

3.8.6 Comparison of test results vs. design values

Obtained results consistently provided reasonable variance (COV consistently between 13-16%), for the purposes of design and an essential factor of safety was found. The plots in Figure 3.17 depict this phenomenon in an illustrative manner. First, 8mm screws' average peak loads obtained during this test campaign is compared against calculated 5th percentile test values, as well as design values constructed from their respective Canadian approval. The plots demonstrate the inherent margin of safety. Additionally, the withdrawal test results for ASSY fully threaded screws in SPF Glulam are also plotted for only 90° from (Abukari et al., 2012). This simply aims to illustrate the performance differences utilizing the same material species but different material quality i.e. lower and higher density. Similar findings can also be made for 10 mm diameter STS embedded at 90° and 45°. Figure 3.17 provides a visual comparative between the obtained test data for the four different test series in this research campaign and the design value utilized for ASSY® fully threaded screws as per their respective product Code Approval Report valid in Canada. The COV for 8mm and 10 mm diameter screws are 14% and 13% respectively.

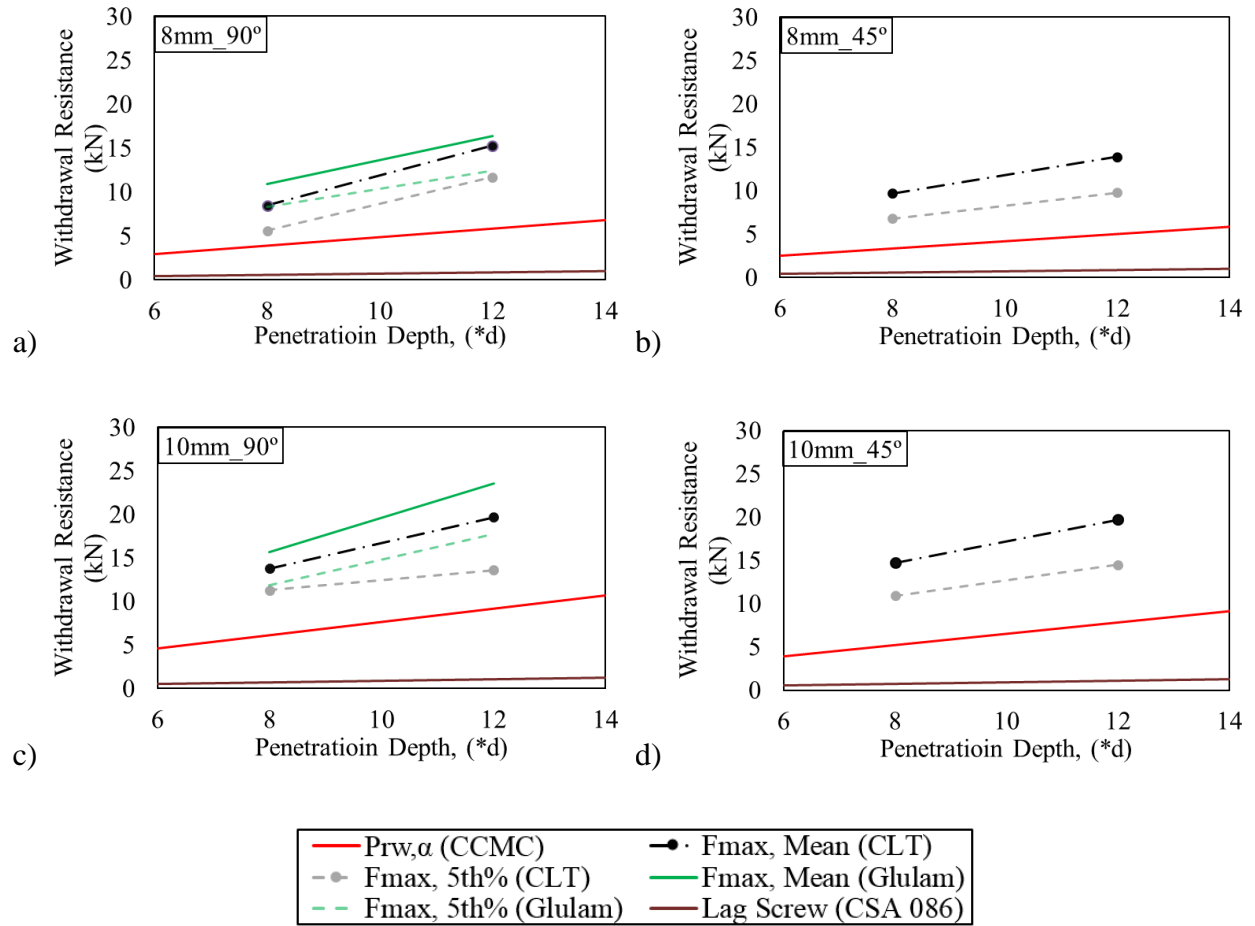


Figure 3.16: Comparison of withdrawal resistance of ASSY® STS in CLT vs. design values (Glulam values are from Abukari et al., (2013)): a) 8mm_90°, b) 8mm_45°, c) 10 mm_90°, and d) 10 mm_45°

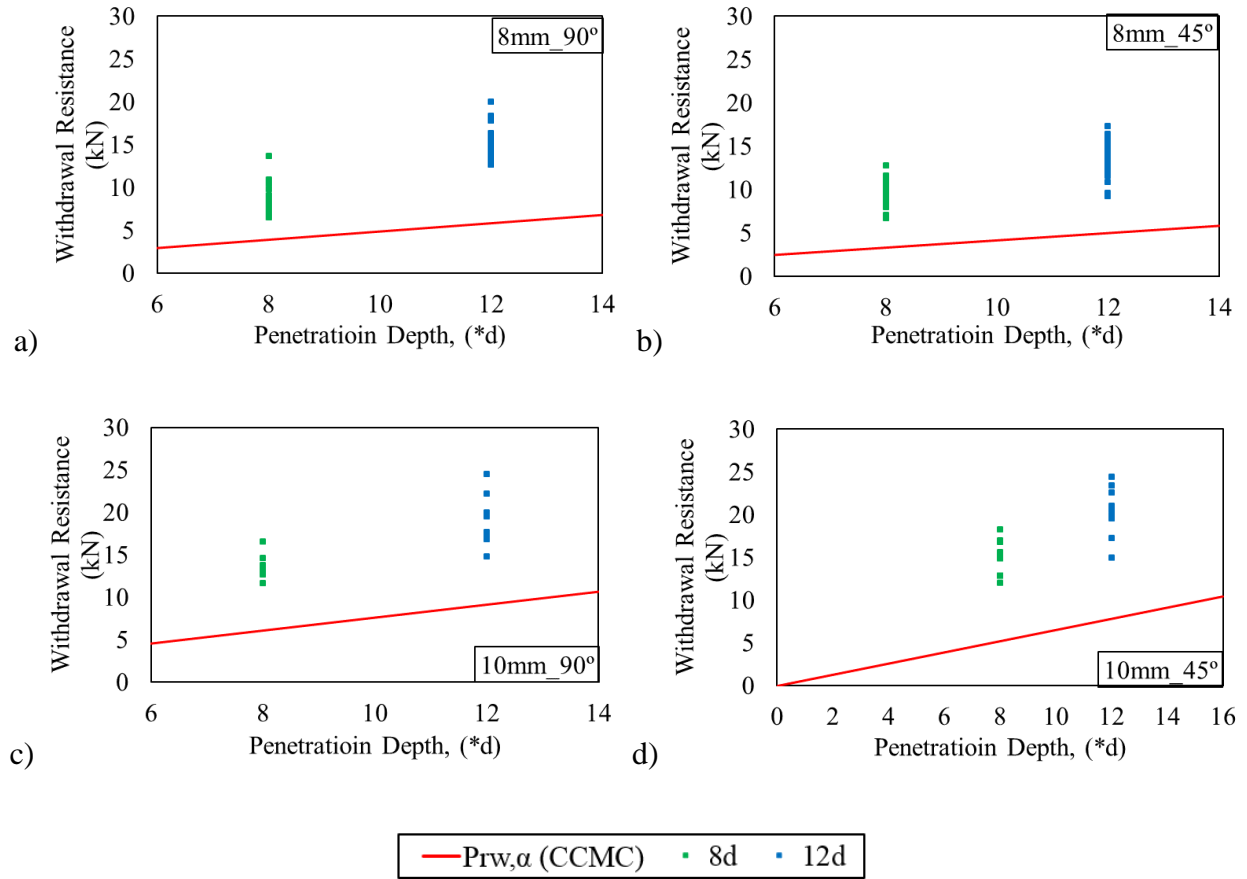


Figure 3.17: Factor of safety associated with ASSY® STS under Withdrawal in CLT: a) 8 mm_90°, b) 8 mm_45°, c) 10 mm_90°, and d) 10 mm_45°

3.9 Summary of withdrawal tests

The main result from the tests is that the hypothesis cannot be rejected: there is no evidence that the CCMC 13677-R 2012 equation cannot be safely applied to predict the withdrawal resistance of STS in CLT made of Canadian softwood lumber. The ratios between the test results and the design values indicate that design values obtained using the approval are conservative in CLT. Further results were extracted:

- Failure in all tests was brittle with ductility ratios of smaller than 2 for all series. The variability of resistance within the individual test series was on average 13.5%.
- Resistance was proportional to screw embedment l_{ef} with $12d$ embedment leading to approx. 50% larger resistance than $8d$ and therefore almost exactly the expected increase.
- Resistance was proportional to screw diameter d with 10 mm screws leading to approx. 46% larger resistance than 8mm screws. The expected difference, however, was only 15%. Based on the small number of replicates n , no explanation can be offered.
- No conclusive relation between screw angle and resistance was found. On average, an inclination of 45^0 to the top CLT layer did not decrease resistance when compared to an inclination of 90^0 to the top CLT layer.

Chapter 4: CLT-STs Shear Connections Tests

4.1 Materials

CLT panels, 3-ply (99 mm or 105 mm) and 5-ply (169 mm or 173 mm), fabricated by Structurlam Products Ltd. according to ANSI/APA PRG-320 (2012) were used. The CLT grade was V2M1, with 12% (+/-2%) moisture content at time of production and 0.42 specific gravity. SPF No.1/No.2 and Purbond polyurethane adhesive were used. For the spline joints in the 3-ply and 5-ply CLT panels, 19 mm and 25 mm plywood sheets (Douglas fir, Veneer Grades A) were used, respectively. A 4 mm thick plastic membrane was used to prepare test specimens where friction between the CLT panels was to be avoided.

Different types and lengths of 8mm diameter SWG ASSY STS were used: partially threaded Ecofast CSK (80 mm, 90 mm, 100 mm, and 160 mm) for shear action and fully threaded VG CSK (140 mm, and 220 mm) or cylindrical head (180 mm) for withdrawal action. Different lengths, see Figure 4.1 were chosen based on the CLT thickness and joint type.



Figure 4.1: STS from left: , VG CSK FT 8 x 220 mm, VG CYL FT 8 x 180 mm, Ecofast PT 8 x 160 mm, VG CSK FT 8 x 140 mm, Ecofast PT 8 x 100 mm, Ecofast PT 8 x 90 mm, Ecofast PT 8 x 80 mm

4.2 Joint types

All CLT assemblies were connected with STS designed for three different joint types with two different screw actions using angle α =angle between STS axis and CLT grain, and β =angle between STS axis to the edge of the CLT panels (Figure 4.5b):

- I) Surface spline joint with STS in shear
- II-a) Lap joint with STS in shear
- II-b) Lap joint with STS in withdrawal
- II-c) Lap joint with STS in shear and STS in withdrawal
- III-a) Butt joint with STS in shear
- III-b) Butt joint with STS in withdrawal

I) Surface spline joint with STS in shear

19 mm (for 3-ply) or 25 mm (for 5-ply) deep and 80 mm (40 mm for mini and small-sized specimens) wide slots were cut into the joining edge of the panels. Plywood sheet of 19 mm (for 3-ply) or 25 mm (for 5-ply) thick and 160 mm (80 mm for mini and small-sized specimens) wide were used as splines. 8 mm diameter 80 mm (for 3-ply) or 100 mm (for 5-ply) long partially threaded ASSY Ecofast STS was placed at 90° (α) to the load for this connection. Spline joints were not tested for mid and full scale tests due to lack of materials (Figure 4.2a).

IIa) Lap joint with STS in shear

The panel laps were 80 mm wide and 50 mm (for 3-ply) or 85 mm (for 5-ply) deep (half the panel thickness). 8mm diameter 90 mm (for 3-ply) or 160 mm (for 5-ply) long partially threaded ASSY Ecofast STS was placed at 90° (α) to the load for this connection (Figure 4.2b).

IIb) Lap joint with STS in withdrawal: The laps were cut identical to those of the lap joints with STS in shear. In this joint, however, the STS were placed at an angle of 45° (α) in two different directions one in tension another one in compression to load the screws in withdrawal. 8 mm diameter 140 mm (for 3-ply) or 220 mm (for 5-ply) long ASSY VG CSK head type fully threaded STS was used for this configuration (Figure 4.2c).

IIc) Lap joint with STS in shear and STS in withdrawal: 90 mm or 160 mm long ASSY Ecofast STS was used in shear action and 140 mm or 220 mm long ASSY VG STS was used in withdrawal action for 3-ply and 5-ply CLT joint configurations, respectively. Three layouts (Figure 4.3) were manufactured and tested:

- WSSW: Half of the total number of STS were placed in shear ($\alpha=90^\circ$) in the middle of the panels and one quarter of the total number of STS were placed in withdrawal ($\alpha=\pm 45^\circ$) towards each end of the panel in opposite directions (Figure 4.3a);
- SWWS: This configuration had the reverse layout of WSSW. Shear screws are placed towards the ends whereas withdrawal screws were placed in the middle (Figure 4.3b);
- SWSWS: In this configuration, STS were placed in alternating orientation changing between shear and withdrawal (Figure 4.3c).

IIa) Butt joint with STS in shear: No machining is required for this joint. Fully threaded STS were installed at an angle of $\alpha=\pm 45^\circ$ to the face of the panels to stitch two panels together. 8 mm diameter 140 mm (for 3-ply) long ASSY VG CSK head type STS were used. This joint was only tested in 3-ply CLT panels (Figure 4.2d).

IIIb) Butt joint with STS in withdrawal: Fully threaded STS were installed at an angle of $\beta=\pm 45^\circ$ to the edge and at an angle of $\alpha=\pm 33^\circ$ to the face of the CLT panels. 8 mm diameter 180 mm long ASSY VG CYL were used. This joint was only tested in 3-ply CLT panels (Figure 4.2e).

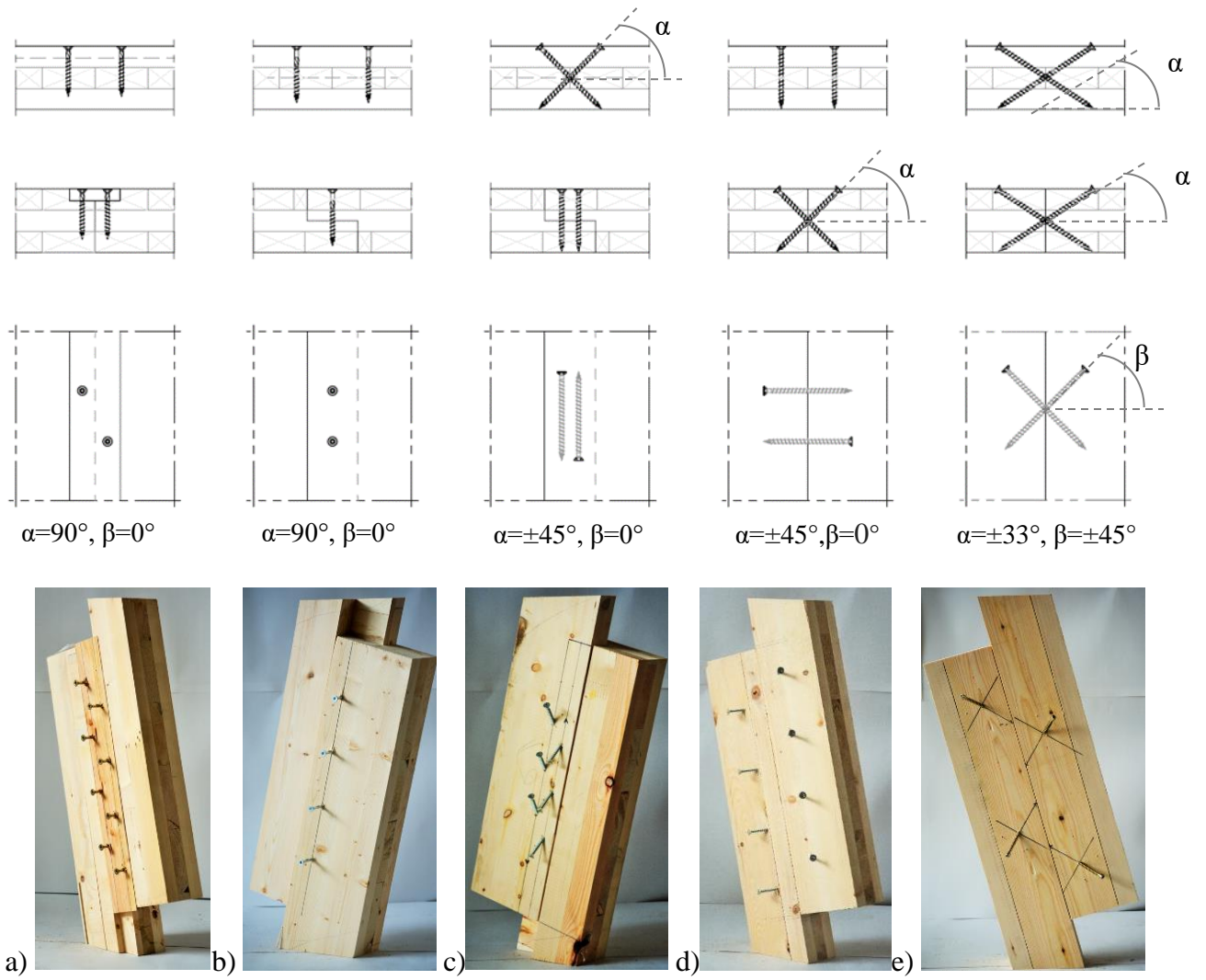


Figure 4.2: Joint specimen layout : a) spline joint with STS in shear, b) lap joint with STS in shear, c) lap joint with STS in withdrawal, d) butt joint with STS in shear, e) butt joint with STS in withdrawal

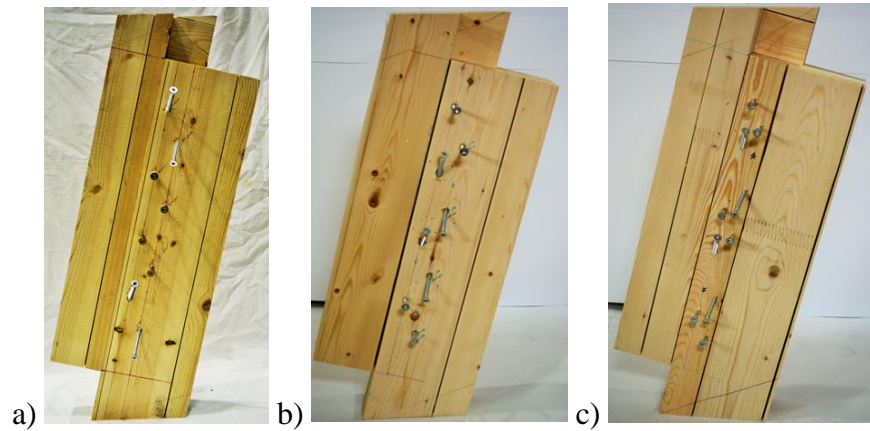


Figure 4.3: Lap joint with STS in shear and STS in withdrawal a) WSSW, b) SWWS, and c) SWSWS

4.1 Experimental test program

4.1.1 Overview

The first part of testing included connections with one STS or two STS (the latter considered as one connector unit) to obtain the reference value, e.g. F_S for strength. For connections, where two STS worked as a pair (one in tension and the other in compression), the reference values for joints were based on two screws. Then multiple screw connections were tested to investigate the group effect comparing the results with the reference values.

The experimental test program is shown in the flowchart of Figure 4.4. Tests were performed in one and two shear planes. In one shear plane (1SP) specimen (Figure 4.5), two pieces of CLT panels were connected, and in two shear planes (2SP), three pieces of CLT panels were connected. The experimental campaign was divided into five parts in mini (150 mm x 200 mm), small (400 mm x 400 mm for 2SP, 145mm x 700 mm for 1SP static, and 300 mm x 1200 mm for 1SP cyclic), medium (400 mm x 1200 mm), and large specimen sizes (800 mm x 1200 mm).

The main parameters of all test series using the six different joint types are summarized in Table 4.1 to Table 4.6. XY-n-z-ply-SP indicates the series name, where X indicates joint types: Spline (S), Lap (L), or Butt (B), Y indicates STS action: Shear (S)/Withdrawal (W), n indicates the number of STS used per shear planes, z indicates loading type: monotonic (m)/cycle (c), ply could be 3 or 5-ply of CLT, and SP (shear plane) could be 1 or 2.

ASTM D1761 (2012) recommends ten replicates for mechanical fasteners in wood. In this study, however, in each test specimen multiple mechanical fasteners are tested; therefore, the number of

replicates was reduced to six, respectively three for some series. A total of 372 shear tests were performed in 84 different series using a total of 1622 STS.

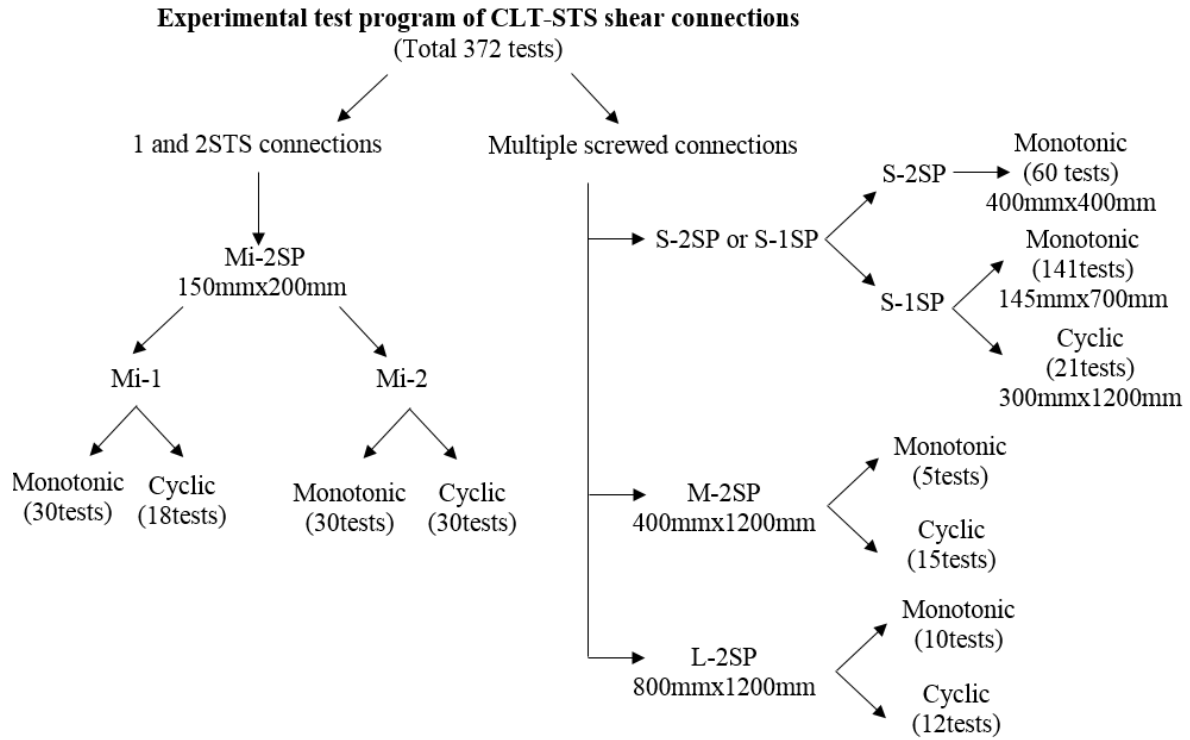


Figure 4.4: Experimental test program of CLT-STS shear connections

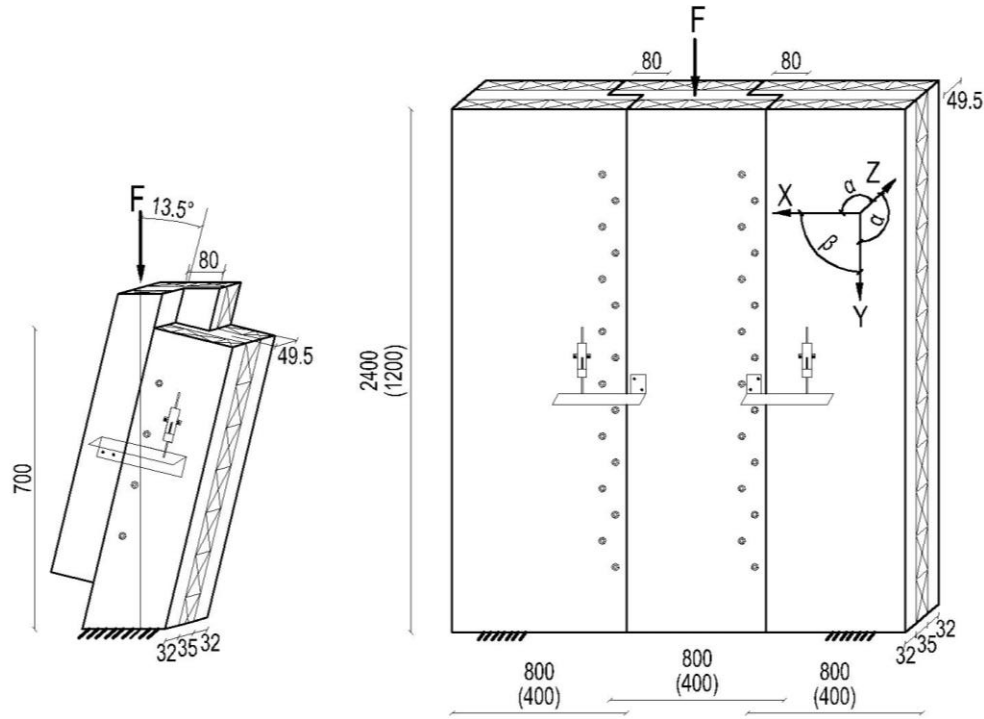


Figure 4.5: Test specimen layout: a) small specimens with one shear plane, and b) specimens with two shear planes (not to scale) (all measurements are in mm)

4.1.2 One and two STS connections

One and two STS connections using mini sized specimens (Mi-1 and Mi-2) were needed to obtain reference values. For static tests, one screw can be used to obtain that reference value. However, for cyclic tests with STS in withdrawal at least two screws are required to resist the load during pulling and pushing. All the tests were performed for mini sized specimen for this connection type with three individual panels connected at two shear planes, each panel being 150 mm wide and 200 mm long (Figure 4.5 b). In the single-STS tests, 48 specimens (30 monotonic in 5 and 18 cyclic in 3 different test series), and in the double screwed connection tests, 60 specimens (30 monotonic in 5 and 30 cyclic in 5 different test series) were tested. Six replicates of each test series were tested under quasi-static monotonic and cyclic loading. Spline joint with STS in shear, lap joint with STS in shear, lap joint in STS in withdrawal, butt joint with STS in shear, and butt joint

with STS in withdrawal were tested. However, for one screw tests, lap and butt joints with STS in withdrawal could not be tested under cyclic loading as to resist the pulling and pushing under cyclic loading at least 2 screws are required. Lap joint with STS in shear and STS in withdrawal could not be tested in this joint and the group effect for this kind was not investigated.

4.1.3 Multiple STS connections

Three different specimen sizes (small with one and two shear planes, medium and large with two shear planes) were fabricated and subsequently tested for multiple screw connection.

- Small sized specimens with one shear plane (S-1SP)
- Small sized specimens with two shear planes (S-2SP)
- Medium sized specimens (M-2SP)
- Large sized specimens (L-2SP)

Small sized specimens with two shear planes (S-2SP):

For small sized two shear planes (S-2SP) three individual panels were connected, each panel being 400 mm long, 400 mm wide, 99 mm or 105 mm (3-ply) / 169 mm (5-ply) thick) as shown in Figure 4.5b. For this specimen size, 3, 4, 5, or 8 STS were installed per row in each shear plane where one, two, or four rows were used based on joints, screw action, and number of CLT plies. Three or six replicates were tested of each test series in total of 13 test series with 60 specimens under quasi-static monotonic loading. This was the first experimental program where butt joints with STS in shear and lap joints with STS in shear and STS in withdrawal were not investigated.

Small sized specimens with one shear plane (S-1SP):

For small sized specimens with one shear plane (S-1SP), two individual panels were connected, each panel being 145 mm (300 mm) wide, 700 mm (1200 mm) long, and 99 mm or 105 mm (3-ply) / 169 mm (5-ply) thick) for quasi-static monotonic (cyclic) tests (Figure 4.5a). 5-ply CLT were only used under quasi-static monotonic loading. For this specimen size, between 2 and 8 STS were installed per row in each shear plane. The number of STS varied based on different joints, screw action, and number of CLT plies. Six (3) replicates of each test series in total of 135 (21) specimens in 26 (7) different series were tested under quasi-static monotonic (cyclic) loading. Within the lap-joints, all three arrangements WSSW, SWWS, and SWSWS were investigated in this part.

The influence of friction was also investigated with the 3-ply CLT panels under quasi-static monotonic loading. One layer of 4mil plastic was attached between the two CLT panels with spray-on adhesive, and then the STS were installed, see Figure 4.6. The membrane prevented friction between the two panels of selected tests series indicated with asterisk in Table 4.1 to Table 4.6.



Figure 4.6: Test specimen with plastic membrane to eliminate friction between panels

Medium sized specimens (M-2SP):

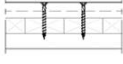
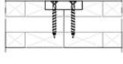
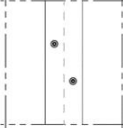
Medium (M) sized specimens were connected with three individual panels at two shear planes, each panel being 1200 mm long and 400 mm wide, as shown in Figure 4.5b. For this size, 16 STS were installed in each shear plane. One replicate of each series was tested under quasi-static monotonic loading in total of 5 specimens and three replicates of each series were tested under reversed cyclic monotonic loading in total of 15 specimens. Spline joints with STS in shear was not tested due to limited CLT panels. Again, only WSSW arrangement in lap joint with STS in shear and STS in withdrawal action was tested as this arrangement showed superior behavior in the small-scale tests compared to SWWS and SWSWS arrangements. However, all other joints were investigated.

Large sized specimens (L-2SP):

Large (L) sized specimens were connected with three individual panels at two shear planes, each panel being 2400 mm long and 800 mm wide, as shown in Figure 4.5b. For this size, 32 STS were installed in each shear plane. One replicate of each series was tested under quasi-static monotonic loading in total of 4 specimens and two replicates of each series were tested under reversed cyclic monotonic loading in total of 8 specimens. Joint similar to the medium sized specimens were tested in large sized specimens too. However, butt joint with STS in withdrawal were not tested as it was previously tested by Danzig et al. (2014) in large-scale.

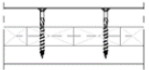
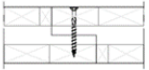
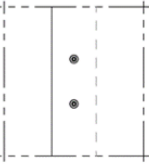
Table 4.1 Test series overview for surface spline joints with STS in shear

Joint & Screw Type	Specimen size	Series Name	Shear planes	STS/ plane	Loading	Repl.
--------------------	---------------	-------------	--------------	------------	---------	-------

Spline_Shear $\alpha=90^\circ$, $\beta=0^\circ$ PT 8X80 mm or 8X100 mm Ecofast CSK   	150x200 (Mi)	SS-2-m-3ply-2SP SS-2-c-3ply-2SP	2	2 2	Monotonic Cyclic	6 6
	150x200 (Mi)	SS-4-m-3ply-2SP SS-4-c-3ply-2SP		4 4	Monotonic Cyclic	6 6
	145x700 (S)	SS-8-m-3ply-1SP	1	8	Monotonic	6
	145x700 (S)	SS-8-m-5ply-1SP	1	8	Monotonic	6
	400x400 (S)	SS-10-m-3ply-2SP	2	10	Monotonic	6
	400x400 (S)	SS-10-m-5ply-2SP	2	10	Monotonic	6
	145x700 (S)	SS-16-m-3ply-1SP	1	16	Monotonic	6
	145x700 (S)	SS-16-m-3ply-1SP*	1	16	Monotonic	3
	300x1200 (S)	SS-16-c-3ply-1SP	1	16	Cyclic	3
	145x700 (S)	SS-16-m-5ply-1SP	1	16	Monotonic	6
	400x400 (S)	SS-20-m-3ply-2SP	2	20	Monotonic	3
	400x400 (S)	SS-20-m-5ply-2SP	2	20	Monotonic	3
	400x400 (S)	SS-32-m-3ply-2SP	2	32	Monotonic	3
	400x400 (S)	SS-32-m-5ply-2SP	2	32	Monotonic	3

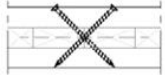
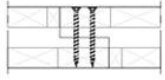
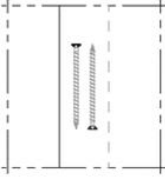
*indicates specimen with friction-eliminating membrane

Table 4.2 Test series overview for lap joints with STS in shear

Joint & Screw Type	Specimen size	Series Name	Shear planes	STS/ plane	Loading	Repl.
Lap_Shear ($\alpha=90^\circ$, $\beta=0^\circ$) PT 8X90 mm or 8X160 mm Ecofast CSK   	150x200 (Mi)	LS-1-m-3ply-2SP LS-1-c-3ply-2SP	2	1 1	Monotonic Cyclic	6 6
	150x200 (Mi)	LS-2-m-3ply-2SP LS-2-c-3ply-2SP		2 2	Monotonic Cyclic	6 6
	145x700 (Mi)	LS-4-m-3ply-1SP	1	4	Monotonic	6
	145x700 (S)	LS-4-m-5ply-1SP	1	4	Monotonic	6
	400x400 (S)	LS-5-m-3ply-2SP	2	5	Monotonic	6
	400x400 (S)	LS-5-m-5ply-2SP	2	5	Monotonic	6
	145x700 (S)	LS-8-m-3ply-1SP	1	8	Monotonic	6
	145x700 (S)	LS-8-m-3ply-1SP*	1	8	Monotonic	3
	300x1200 (S)	LS-8-c-3ply-1SP	1	8	Cyclic	3
	400x400 (S)	LS-8-m-3ply-2SP	2	8	Monotonic	3
	145x700 (S)	LS-8-m-5ply-1SP	1	8	Monotonic	6
	400x400 (S)	LS-8-m-5ply-2SP	2	8	Monotonic	3
	400x1200 (M)	LS-16-m-3ply-2SP	2	16	Monotonic	1
		LS-16-c-3ply-2SP		16	Cyclic	3
	800x2400 (L)	LS-32-m-3ply-2SP	2	32	Monotonic	1
		LS-32-c-3ply-2SP		32	Cyclic	2

*indicates specimen with friction-eliminating membrane

Table 4.3 Test series overview for lap joints with STS in withdrawal

Joint & Screw Type	Specimen size	Series Name	Shear planes	STS/ plane	Loading	Repl.
Lap_Withdr. ($\alpha=\pm 45^\circ$, $\beta=0^\circ$), FT 8X140 mm or 8X220 mm ASSY VG CSK   	150x200 (Mi)	LW-1-m-3ply-2SP	2	1	Monotonic	6
	150x200 (Mi)	LW-2-m-3ply-2SP		2	Monotonic	6
		LW-2-c-3ply-2SP		2	Cyclic	6
	145x700 (S)	LW-4-m-5ply-1SP	1	4	Monotonic	6
	145x700 (S)	LW-6-m-3ply-1SP	1	6	Monotonic	6
	400x400 (S)	LW-6-m-5ply-2SP	2	6	Monotonic	6
	400x400 (S)	LW-8-m-3ply-2SP	2	8	Monotonic	6
	145x700 (S)	LW-10-m-5ply-1SP	1	10	Monotonic	6
	145x700 (S)	LW-12-m-3ply-1SP	1	12	Monotonic	6
	145x700 (S)	LW-12-m-3ply-1SP*	1	12	Monotonic	3
	300x1200 (S)	LW-12-c-3ply-1SP	1	12	Cyclic	3
	400x1200 (M)	LW-16-m-3ply-2SP	2	16	Monotonic	1
		LW-16-c-3ply-2SP		16	Cyclic	3
	800x2400 (L)	LW-32-m-3ply-2SP	2	32	Monotonic	1
		LW-32-c-3ply-2SP		32	Cyclic	2

*indicates specimen with friction-eliminating membrane

Table 4.4 Test series overview for lap joints with STS in shear and withdrawal

Joint & Screw Type	Specimen size	Series Name	Shear planes	STS/ plane	Loading	Repl.
Lap_Shear& Withdr. ($\alpha=90^\circ$, $\beta=0^\circ$), PT 8X90 mm or 8X160 mm ASSY Ecofast CSK+ ($\alpha=\pm 45^\circ$, $\beta=0^\circ$), FT 8X140 mm or 8X220 mm ASSY VG CSK	145x700 (S)	LC-WSSW-8-m-3ply-1SP	1	8	Monotonic	6
	145x700 (S)	LC-WSSW-8-m-3ply-1SP*		8	Monotonic	3
	300x1200 (S)	LC-WSSW-8-c-3ply-1SP		8	Cyclic	3
	145x700 (S)	LC-WSSW-8-m-5ply-1SP		8	Monotonic	6
	145x700 (S)	LC-SWWS-8-m-3ply-1SP		8	Monotonic	6
	145x700 (S)	LC-SWWS-8-m-5ply-1SP		8	Monotonic	6
	145x700 (S)	LC-SWSWS-10-m-3ply-1SP		10	Monotonic	6
	300x1200 (S)	LC-SWSWS-10-c-3ply-1SP		10	Cyclic	3
	145x700 (S)	LC-SWSWS-10-m-5ply-1SP		10	Monotonic	6
	400x1200 (M)	LC-WSSW-16-m-3ply-2SP	2	16	Monotonic	1
		LC-WSSW-16-c-3ply-2SP		16	Cyclic	3
	800x2400 (L)	LC-WSSW-32-m-3ply-2SP	2	32	Monotonic	1
		LC-WSSW-32-c-3ply-2SP		32	Cyclic	2

Table 4.5 Test series overview for butt joints with STS in shear

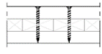
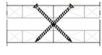

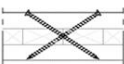
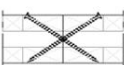
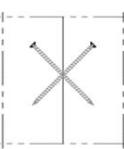
Joint & Screw Type	Specimen size	Series Name	Shear planes	STS/ plane	Loading	Repl.
Butt_Shear $(\alpha=\pm 45^\circ, \beta=0^\circ)$ FT 8X140 mm ASSY VG CSK   	150x200 (Mi)	BS-1-m-3ply-2SP BS-1-c-3ply-2SP	2	1 1	Monotonic Cyclic	6 6
	150x200 (Mi)	BS-2-m-3ply-2SP BS-2-c-3ply-2SP		2 2	Monotonic Cyclic	6 6
	145x700 (S) 300x1200 (S)	BS-8-m-3ply-1SP BS-8-c-3ply-1SP	1	8 8	Monotonic Cyclic	6 3
	400x1200 (M)	BS-16-m-3ply-2SP BS-16-c-3ply-2SP	2	16 16	Monotonic Cyclic	1 3
	800x2400 (L)	BS-32-m-3ply-2SP	2	32	Monotonic	1
		BS-32-c-3ply-2SP		32	Cyclic	2

Table 4.6 Test series overview for butt joints with STS in withdrawal

Joint & Screw Type	Specimen size	Series Name	Shear planes	STS/ plane	Loading	Repl.
Butt_Withdr $(\alpha=\pm 33^\circ, \beta=\pm 45^\circ)$, FT 180 mm ASSY VG CYL   	150x200 (Mi)	BW-1-m-3ply-2SP	2	1	Monotonic	6
	150x200 (Mi)	BW-2-m-3ply-2SP		2	Monotonic	6
		BW-2-c-3ply-2SP		2	Cyclic	6
	145x700 (S)	BW-4-m-3ply-1SP	1	4	Monotonic	6
	145x700 (S)	BW-8-m-3ply-1SP	1	8	Monotonic	6
	145x700 (S)	BW-8-m-3ply-1SP*	1	8	Monotonic	3
	400x400 (S)	BW-8-m-3ply-2SP	2	8	Monotonic	6
	300x1200(S)	BW-8-c-3ply-1SP	1	8	Cyclic	3
	400x1200(M)	BW-16-m-3ply-2SP	2	16	Monotonic	1
		BW-16-c-3ply-2SP		16	Cyclic	3
	800x2400(L)	BW-20-m-3ply-2SP	2	20	Monotonic	6
		BW-20-c-3ply-2SP		20	Cyclic	4

*indicates specimen with friction-eliminating membrane

4.1.4 Specimen preparation

Though pre-drilling is not required for STS, the installation of screws was facilitated by a jig, which allowed lead holes to be drilled at the correct angle and orientation. The pre-drilled holes extended through only one panel using a 4.8 mm diameter drill bit, which guided the STS to the correct orientation in the second panel. This partial pre-drilling of a pilot hole was not expected to have any impact on the connection performance. For those tests series with STS installed at an angle so that they act in withdrawal, all screws were installed from the same CLT panel face but with two different orientations, so that half of the screws were in tension and half in compression.

The STS were spaced using parameters meeting or exceeding the requirements according to the European technical approval (ETA-11/0190, 2018) and Canadian product approval (13677-R, 2013) (see Figure 3.2, Table 3.1, and Appendix B).

4.2 Test methods

4.2.1 Mini sized specimens (Mi-1, Mi-2) under monotonic loading

ASTM D198-13 (2012) was followed for the tests exhibiting two shear planes. The panels were supported by two hollow steel plates (100 x 100 x 200 mm) placed on a 50 x 460 x 620 mm steel plate of the machine frame. The outer two panels were kept in place by two hollow sections (50 x 70 x 380 mm) on the top of the specimen placed 180 mm away from the centerline. The hollow sections were attached to the bottom steel plate of the machine frame using 15 mm diameter B7 threaded rods and grade 8 hex nuts, as shown in Figure 4.7. A hydraulic actuator with a capacity of 250 kN was used to apply the load onto the middle panel by means of one 25 x 50 x 210 mm and two 10 x 60 x 100 mm steel sections. The actuator load and the relative vertical displacements

between the individual panels were recorded at a sampling rate of 10 Hz. The displacements were recorded using two transducers (front left and front right) attached at mid-height of the assembly.

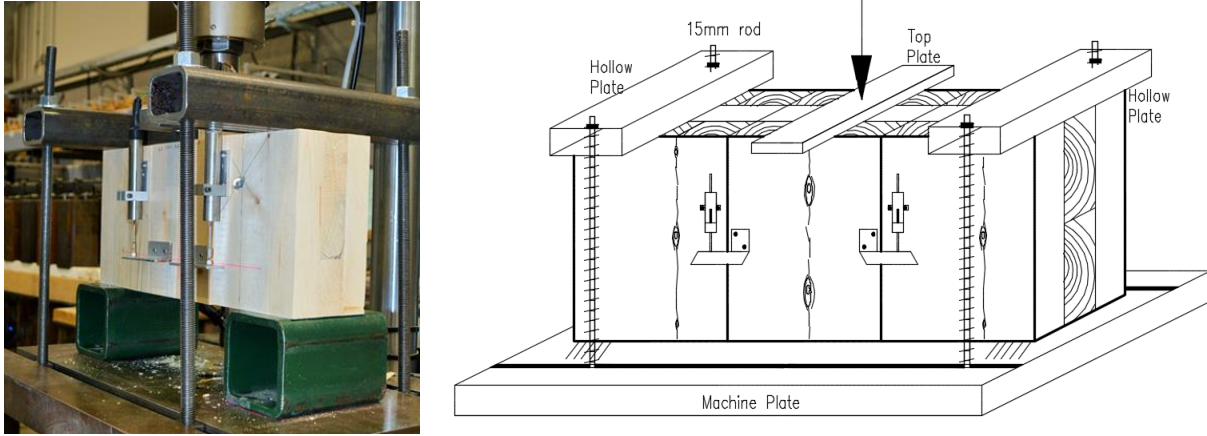


Figure 4.7: Test setup for Mini sized specimens under monotonic loading

The actuator load was applied according to a modified EN-26891 (1991) loading protocol (Figure 4.8a) at a displacement controlled rate of 2.5mm/min for joints with STS in withdrawal and 5mm/min for joints with STS in shear. First, the specimen was loaded up to 40% of estimated capacity, the load was held constant for 30 seconds, then the specimen was unloaded to 10% of estimated capacity and again the load was held for 30 seconds. Finally, the specimen was loaded to failure, i.e. when the load dropped to 80% of the recorded maximum load.

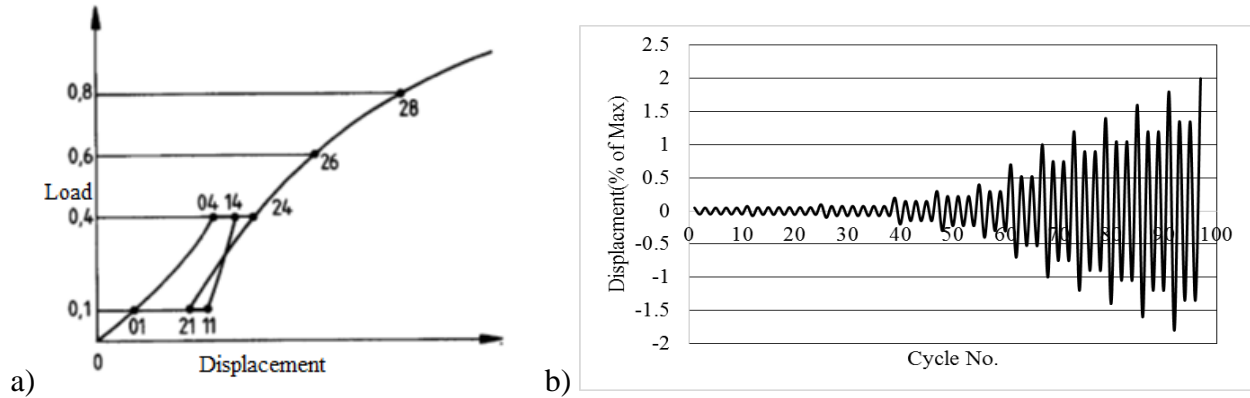


Figure 4.8: Loading protocols: a) EN-26891 (1991) for monotonic tests; and b) CUREE for cyclic tests

4.2.2 Mini sized specimens (Mi-1, Mi-2) under cyclic loading

The set up for cyclic tests was similar to the static tests; however, to prevent out of plane during displacements, the middle panel was braced using 300 mm long 19 mm diameter B7 threaded rod with grade 8 hex nuts and standard washer attached through 25 x 50 x 210 mm steel sections from top and bottom. The top bars in the side panels were braced horizontally using two 400 mm long 20 mm diameter B7 threaded rod and grade 8 hex nuts and standard washer. The steel supports were restrained to the steel machine frame using clamps on both sides. The test setup is shown in Figure 4.9. For the cyclic tests the actuator load was applied according to a CUREE loading protocol (ASTM 2126-09 2009) at a displacement-controlled rate of 2.5 mm/sec (Figure 4.8b).

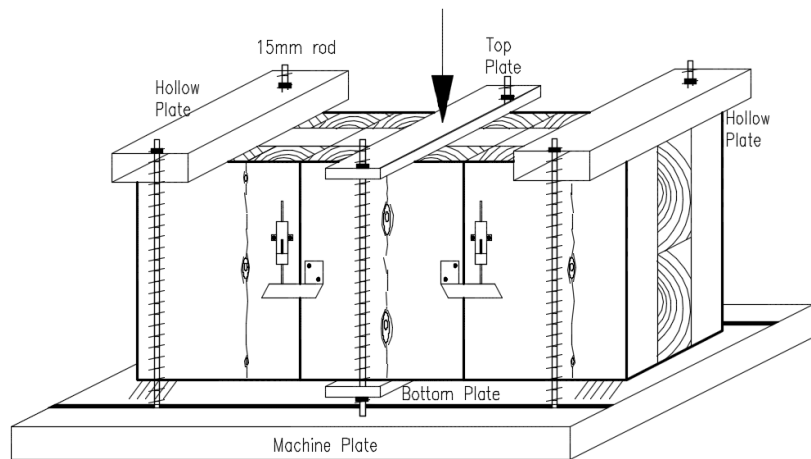


Figure 4.9: Test setup for Mini sized specimens under cyclic loading

4.2.3 Small sized specimen with two shear planes (S-2SP) under monotonic loading

The procedure in accordance with ASTM D198-13 (2012) was followed for the monotonic tests exhibiting two shear planes. The span of the assembly was kept short in an attempt to investigate the shear connection between the individual panels rather than the bending behavior of the assembly. A hydraulic actuator with a capacity of 400 kN was used to apply the load to the middle panel. To avoid crushing of the CLT, two 100 x 100 x 20 mm steel plates were used to distribute the load. The side panels were placed on two steel bearings. The test setup is shown in Figure 4.10.

The actuator load was applied according to a modified EN-26891 (1991) (Figure 4.8a) loading protocol at a displacement controlled rate of 5mm/min. Loading was stopped when the applied load fell below 80% of the peak load or when the maximum actuator displacement of 50 mm was reached. The load and the relative vertical displacements between the individual panels using two transducers attached at mid- height of the assembly were recorded at a sampling rate of 10 Hz.

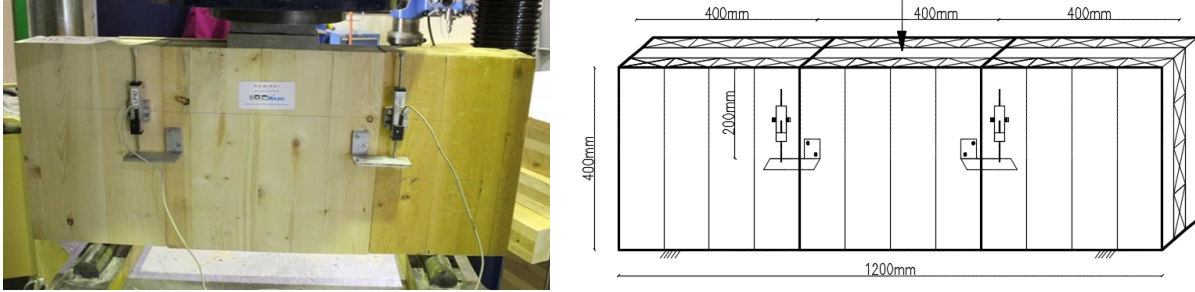


Figure 4.10: Test setup for small sized specimen with two shear planes under monotonic loading

4.2.4 Small sized specimen with one shear plane (S-1SP) under monotonic loading

The test setup followed to test specimens with one shear plane was based on (Brandner et al. (2013)). The specimen was rotated 13.5° , equal to the recommendations in EN 408 (2010) so that the resultant forces of loading and support are aligned. All results presented herein are the load components parallel to the shear planes. A hydraulic actuator with a capacity of 400 kN was used to apply the load to one CLT panel. To avoid crushing, two 100 x 100 x 20 mm steel plates were used to distribute the load. The other CLT panel was placed on steel supports, see Figure 4.11.

The load was applied according to a modified EN-26891 (1991) loading protocol at a load controlled rate of 20 kN/min, see (Figure 4.8a)) in a similar manner to mini sized specimen. The actuator load and the relative vertical displacements between two panels using two transducers of 25 mm for lap and butt joints with STS in withdrawal and 75 mm for spline, lap, and butt joints with STS in shear attached in front and back at the mid height of the assembly were recorded at a sampling rate of 10 Hz. The reported displacements are the averages between the front and the back-side measurements. The out-of-plane rotations (or any relative motion across the splices in the perpendicular direction) were neither measured during testing nor quantified after testing.

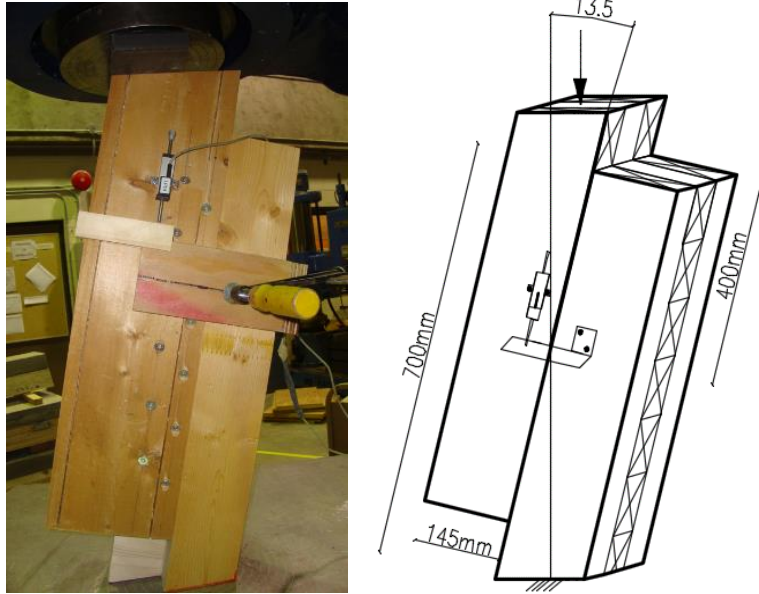


Figure 4.11: Test setup for small sized specimen with one shear plane under monotonic loading

4.2.5 Small sized specimen with one shear plane under cyclic loading

For the cyclic tests, the specimens were put in two like 300 x 370 x 120 fixtures and attached by nine 400 mm long 20 mm diameter Grade 8 bolts (Figure 4.12). The holes in the specimen were made at 13.5° so that the line of action of load makes 13.5° to the center line of the specimen. The actuator load (applied according to CUREE loading protocol) and the relative vertical displacements between two panels using two transducers attached at front and back of the assembly were recorded at a sampling rate of 10 Hz.

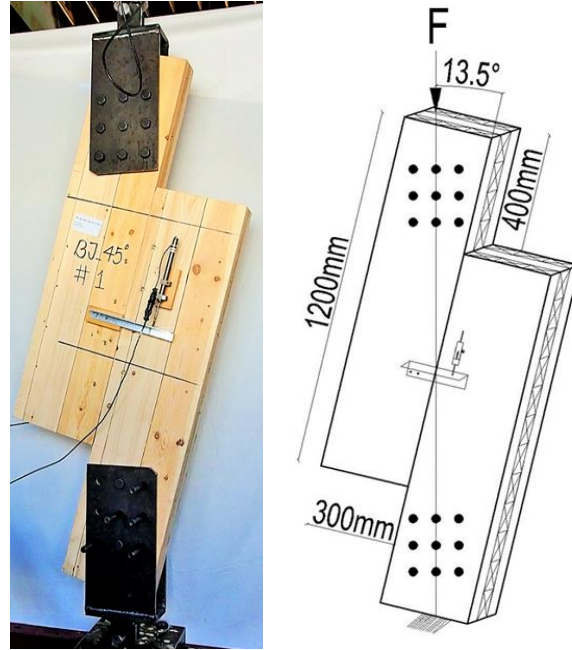


Figure 4.12: Test setup for small sized specimen with one shear plane under cyclic loading

4.2.6 Medium and large sized specimen under monotonic loading

The procedure in accordance with ASTM D198-13 (2012) was followed for the monotonic tests exhibiting two shear planes. The panels for the large sized specimens were supported by steel plates (50 x 500 x 500 mm) on each side. The panels for the medium sized specimens were supported by steel plates on each side (100 x 380 x 750 mm). The outer two panels were kept in place by two hollow sections (75 x 100 mm) on the top of the steel beam placed 685 mm (for large sized specimen) and 150 mm (for medium sized specimen) away from the centerline of the specimen as shown in Figure 4.13 and Figure 4.14 for medium and large sized specimen respectively. The hollow sections were attached with the steel beam using 300 mm long and 25mm diameter B7 threaded rod and grade 8 hex nuts and standard washers. A hydraulic actuator with a capacity of 250 kN was used to apply the load onto the middle panel by means of one 25 x 250 x 250 mm steel section.

The actuator load was applied according to a modified EN-26891 (1991) loading protocol (Figure 4.8a) at a displacement controlled rate of 2.5mm/min for lap and butt joints with STS in withdrawal and 5 mm/min for lap joints with STS in shear and STS in combined action see in a similar manner to mini sized specimen. The actuator load and the relative vertical displacements between the individual panels using four transducers (two front and two back) attached at mid- height of the assembly were recorded at a sampling rate of 10 Hz.

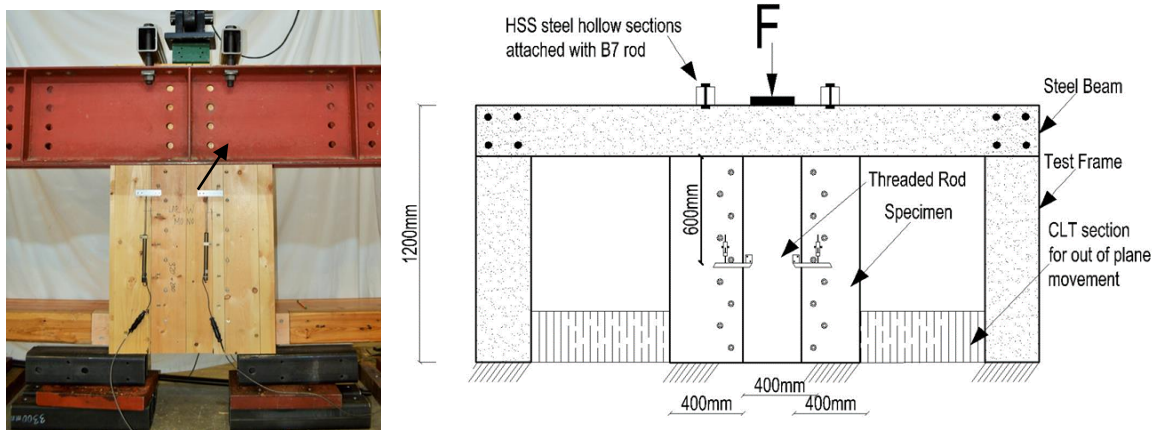


Figure 4.13: Test setup for medium sized specimen under monotonic loading

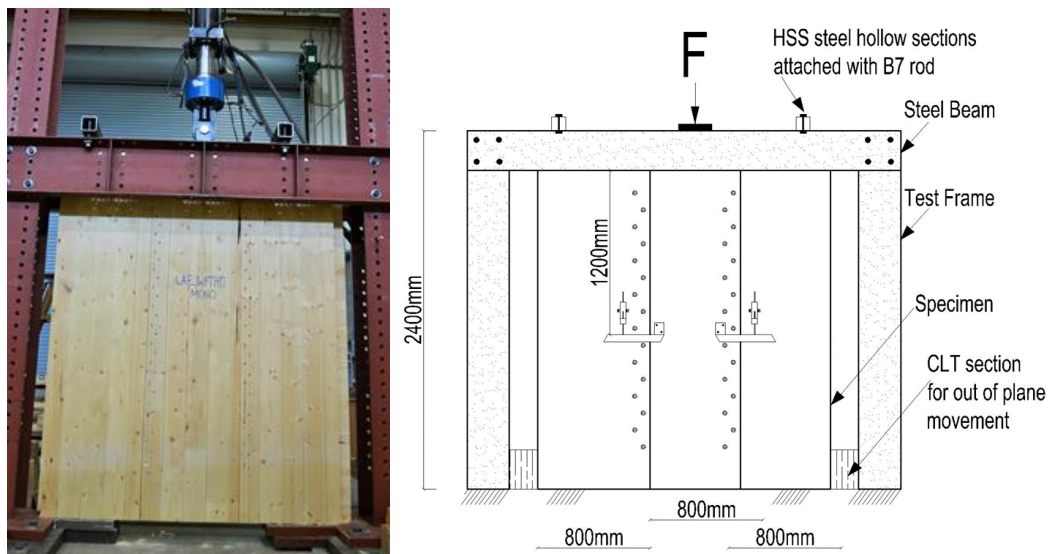


Figure 4.14: Test setup for large sized specimen under monotonic loading

4.2.7 Medium and large sized specimen under cyclic loading

For cyclic tests, for the medium sized specimen, the outer two panels were kept in place by applying four hollow sections (50 x 75 mm) horizontally and two hollow sections (75 x 100 mm) vertically on the top of the steel beam. Two 1500 mm long and 25 mm diameter B7 threaded rods were used to brace the middle panel to facilitate pulling which were attached using steel sections and two hollow steel sections (100 x 100 x 150 mm) from top and bottom (Figure 4.15).

For the large sized specimen, the outer two panels were kept in place by applying four instead of two 520 mm long hollow sections (75 x 100 mm) on the top of the steel beam. The first and second two hollow sections were placed 530 mm and 685 mm away from the centerline of the machine respectively. Four 2400 mm long and 25 mm diameter B7 threaded rod were used to brace the middle panel to facilitate pulling which were attached using two 25 x 250 x 250 mm steel sections from top and bottom (Figure 4.16).

A hydraulic actuator with a capacity of 250 kN was used to apply the load onto the middle panel by means of a steel section (25 x 250 x 250 mm). Further the outer two panels were held in place by a CLT section from the back which was connected using long STS to prevent the outer panels from moving out of plane. The actuator load and the relative vertical displacements between two panels using four transducers attached at front (two) and back (two) of the assembly were recorded at a sampling rate of 10 Hz. The actuator load was applied according to a CUREE loading protocol (ASTM 2126-09, 2009) at a displacement-controlled rate of 2.5 mm/sec (Figure 4.8b)).

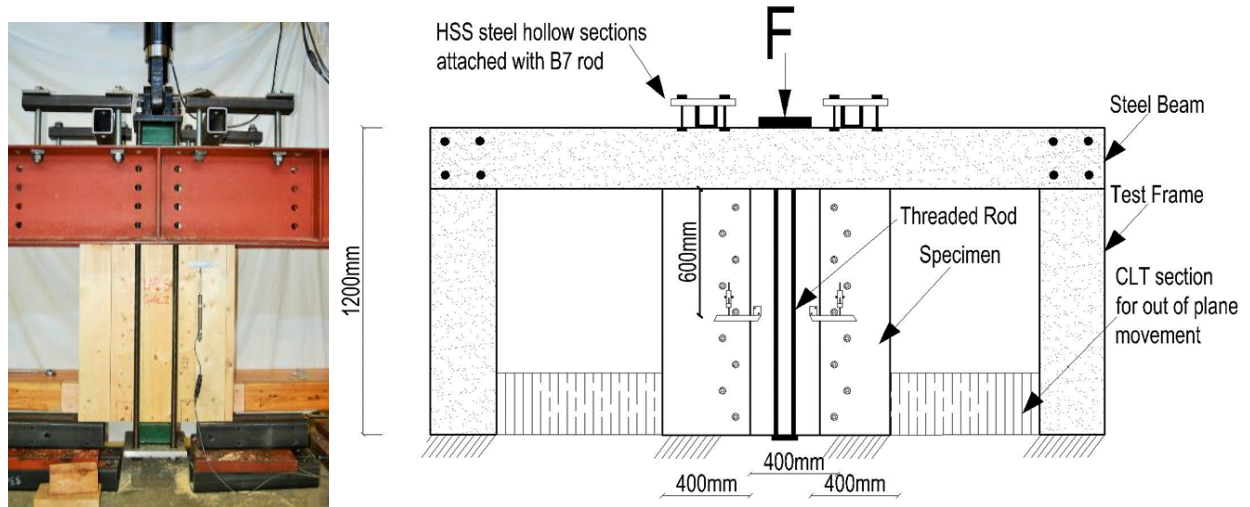


Figure 4.15: Test setup for medium sized specimen under cyclic loading

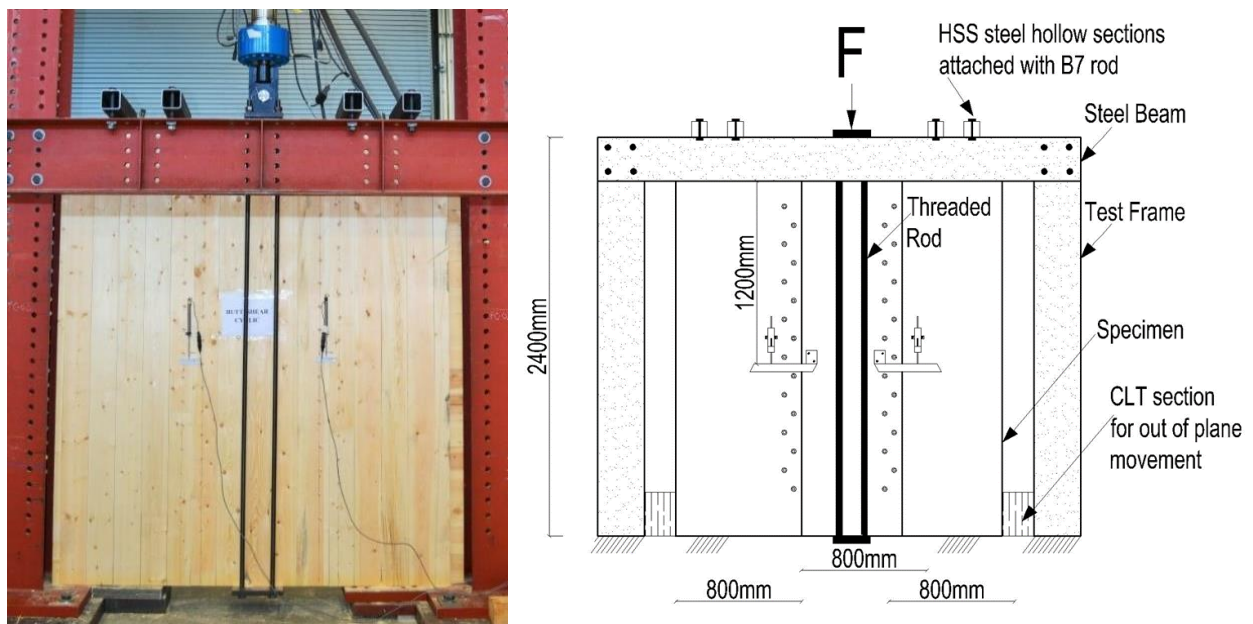


Figure 4.16: Test setup for large sized specimen under cyclic loading

4.2.8 Analyses procedures

From the tests, following connection characteristics were obtained and evaluated:

- i) Capacity (ultimate resistance); labeled F_{\max}
- ii) Yield load; labeled F_Y
- iii) Displacement at capacity; labeled $d_{F,\max}$
- iv) Displacement at yield load; labeled $d_{F,Y}$
- v) Stiffness; labeled k
- vi) Ductility; labeled μ

To calculate yield strength, displacement corresponding to yield strength, equivalent energy elastic-plastic (EEEP) curves according to ASTM 2126-09 (2009) were developed. For the cyclic tests, EEEP curves were developed for both positive and negative loading envelopes for each specimen. At first, envelop curves were developed connecting the load peaks and their corresponding displacements for each cycle (Figure 4.17a). Then, interpolated curves were developed based on these peaks to get more data points for predicting the yield loads and corresponding displacements (Figure 4.17b). Finally, EEEP curves were developed based on the interpolated curve (Figure 4.17c). All curves combined are illustrated in Figure 4.17d.

Stiffness k was calculated in accordance with EN-26891 (1991) for the range of the load-displacement curves between 10% and 40% of the joints capacity. Ductility μ was calculated taking the ratio between the ultimate displacement, $d_{F,\max}$ at maximum load, F_{\max} and the yield displacement, $d_{F,Y}$ ($d_{F,\max}/d_{F,Y}$). Ductility of the joints were categorized based on the system of classification by Smith et al. (2006) using an average ductility ratio (μ): brittle ($\mu \leq 2$), low-ductility ($2 < \mu \leq 4$), moderate-ductility ($4 < \mu \leq 6$), high-ductility ($\mu > 6$).

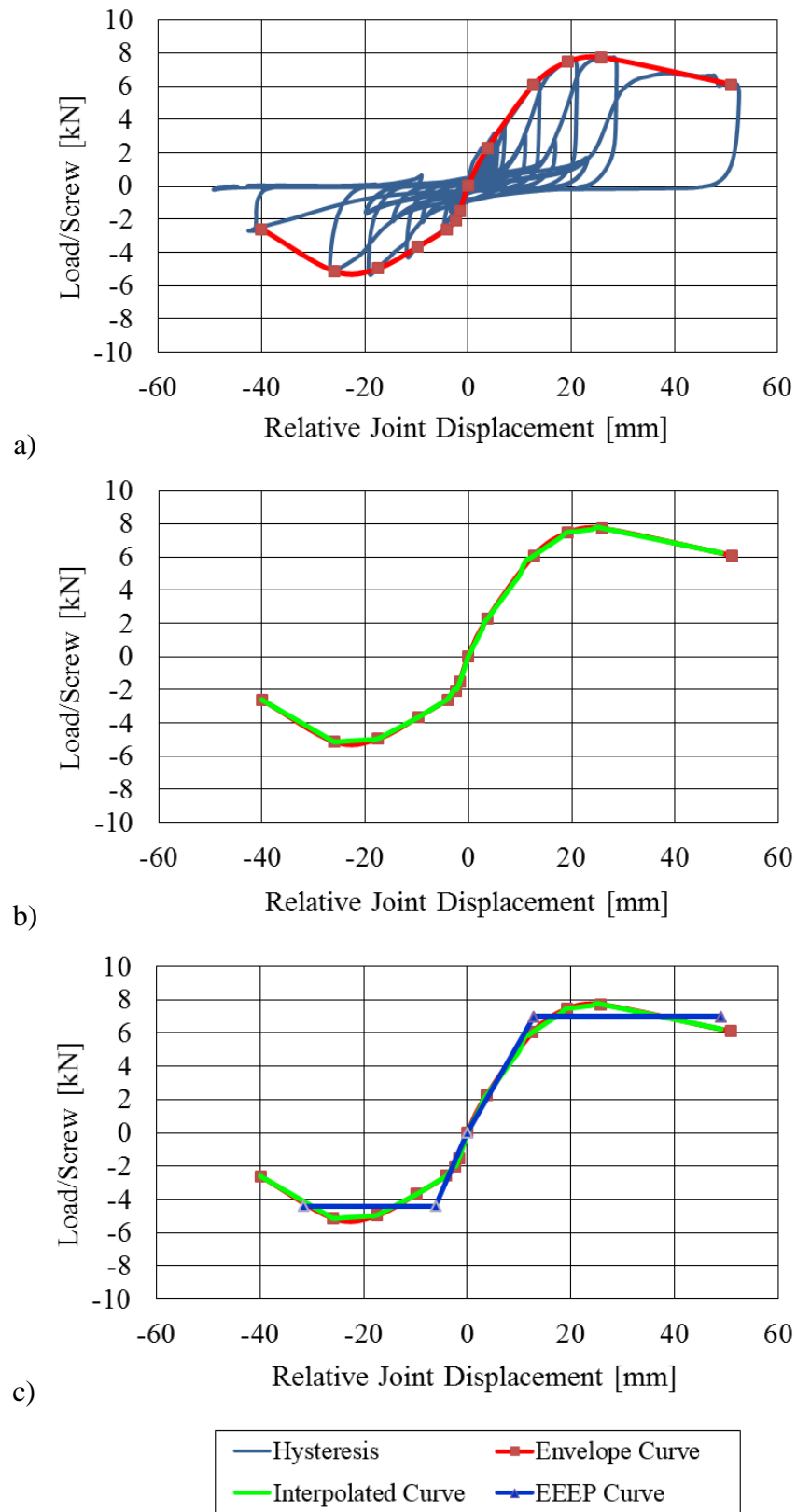


Figure 4.17: Development of EEEP curves: a) Envelope curve, b) Interpolated curve, c) EEEP curve

4.3 Results

4.3.1 Overview

Table 4.7 to Table 4.12 summarize the test results for all six tested joint types. While ductility is given for the assembly, all values for load and stiffness in these graphs and tables are shown as values per individual screw and the displacements are the averages of the two measurements from the back and the front of the specimen. All cyclic values are the averages of positive and negative envelopes. Following this overview, and Figure 4.18 to Figure 4.27 present average load-deformation curves for the loads obtained per screw. Table 4.13 to Table 4.19 summarize the test results based on different specimen sizes tested.

Table 4.7: Results summary for surface spline joints with STS in shear

Series	Repl.	F_{\max}	F_Y	$d_{F,\max}$	$d_{F,Y}$	μ	k
		[kN]	[kN]	[mm]	[mm]	[-]	[kN/mm]
SS-2-m-3ply-2SP	6	6.4	5.4	27.8	3.0	9.8	1.6
SS-2-c-3ply-2SP	6	5.8	4.6	13.5	2.3	6.2	1.9
SS-4-m-3ply-2SP	6	6.2	5.6	23.6	3.0	9.1	1.7
SS-4-c-3ply-2SP	6	6.0	4.7	13.0	2.0	8.5	2.0
SS-8-m-3ply-1SP	6	6.9	4.5	52.8	7.0	7.5	0.5
SS-8-m-5-ply-1SP	6	7.3	4.8	46.0	6.1	7.8	0.7
SS-10-m-3ply-2SP	6	4.0	2.8	41.8	4.7	7.4	0.6
SS-10-m-5ply-2SP	6	6.2	4.1	50.7	8.0	6.4	0.4
SS-16-m-3ply-1SP	6	6.5	4.2	46.8	6.0	8.0	0.5
SS-16-m-3ply-1SP	3	6.4	4.2	52.7	7.0	7.6	0.5
SS-16-c-3ply-1SP	3	4.4	2.9	27.5	5.5	5.3	0.6
SS-16-m-5ply-1SP	6	10.8	7.2	57.5	9.4	6.5	0.5
SS-20-m-3ply-2SP	3	3.4	2.3	23.0	5.2	4.5	0.4
SS-20-m-5ply-2SP	3	4.6	2.9	38.0	9.0	4.3	0.3
SS-32-m-3ply-2SP	3	2.2	1.7	11.7	4.5	2.6	0.6
SS-32-m-5ply-2SP	3	3.0	2.0	17.7	6.0	3.0	0.4

Table 4.8: Results summary for lap joints with STS in shear

Series	Repl.	F_{\max} [kN]	F_Y [kN]	$d_{F,\max}$ [mm]	$d_{F,Y}$ [mm]	μ [-]	k [kN/mm]
LS-1-m-3ply-2SP	6	6.6	5.4	29.0	6.4	4.5	0.7
LS-1-c-3ply-2SP	6	5.8	4.0	22.0	4.2	5.4	1.3
LS-2-m-3ply-2SP	6	6.2	5.1	28.7	4.9	6.3	0.9
LS-2-c-3ply-2SP	6	6.9	4.7	25.3	4.8	5.8	1.1
LS-4-m-3ply-1SP	6	6.4	4.3	24.8	4.7	5.3	0.9
LS-4-m-5ply-1SP	6	10.8	6.8	62.3	13.8	5.1	0.6
LS-5-m-3ply-2SP	6	5.1	3.4	25.2	3.0	11.0	1.2
LS-5-m-5ply-2SP	6	10.7	7.0	46.3	5.6	9.5	1.5
LS-8-m-3ply-1SP	6	6.7	4.3	25.8	4.4	6.6	1.0
LS-8-m-3ply-1SP	3	7.6	5.0	30.0	7.0	4.3	0.9
LS-8-c-3ply-1SP	3	5.1	3.4	22.3	4.1	5.6	0.8
LS-8-m-3ply-2SP	3	5.2	3.5	24.0	4.0	6.0	0.7
LS-8-m-5ply-1SP	6	11.0	6.9	64.3	5.6	12.6	0.8
LS-8-m-5ply-2SP	3	7.4	4.9	49.3	4.1	12.0	1.3
LS-16-m-3ply-2SP	1	7.3	6.0	31.0	6.6	5.1	0.8
LS-16-c-3ply-2SP	4	6.3	5.4	27.8	6.1	5.0	0.8
LS-32-m-3ply-2SP	1	6.9	5.7	32.5	5.3	6.1	0.9
LS-32-c-3ply-2SP	3	5.8	4.2	20.5	5.1	5.1	0.8

Table 4.9: Results summary for lap joints with STS in withdrawal

Series	Repl.	F_{\max} [kN]	F_Y [kN]	$d_{F,\max}$ [mm]	$d_{F,Y}$ [mm]	μ [-]	k [kN/mm]
LW-1-m-3-ply-2SP	6	8.8	7.6	6.5	2.7	2.5	3.1
LW-2-m-3ply-2SP	6	7.0	6.2	2.8	1.4	2.1	4.5
LW-2-c-3ply-2SP	6	9.2	8.3	3.3	1.8	1.9	4.7
LW-4-m-5ply-1SP	6	9.7	9.0	2.6	1.6	1.7	5.6
LW-6-m-3ply-1SP	6	7.6	7.1	2.7	1.8	1.5	4.2
LW-6-m-5ply-2SP	6	10.3	9.7	2.0	1.1	1.8	310.2
LW-8-m-3ply-2SP	6	5.3	4.9	2.3	0.7	3.0	3.8
LW-10-m-5ply-1SP	6	13.0	11.3	4.7	1.9	2.8	7.8
LW-12-m-3ply-1SP	6	7.2	6.3	5.5	2.0	2.9	4.8
LW-12-m-3ply-1SP*	3	6.6	5.5	6.4	1.1	9.6	5.5
LW-12-c-3ply-1SP	3	5.9	5.1	4.4	2.1	2.3	2.7
LW-16-m-3ply-2SP	1	7.2	6.6	2.8	2.0	1.4	3.1
LW-16-c-3ply-2SP	3	6.6	5.3	2.7	1.7	1.8	3.6
LW-32-m-3ply-2SP	1	6.5	6.0	3.6	1.9	1.9	2.8
LW-32-c-3ply-2SP	4	5.2	4.9	1.9	1.4	1.3	3.9

Table 4.10: Results summary for lap joints with STS in shear and STS in withdrawal

Series	Repl.	F_{\max} [kN]	F_Y [kN]	$d_{F,\max}$ [mm]	$d_{F,Y}$ [mm]	μ [-]	k [kN/mm]
LWSSW-8-m-3ply-1SP	6	6.7	5.1	14.7	1.0	17.5	4.1
LWSSW-8-m-3ply-1SP*	3	6.7	5.6	8.7	0.9	9.2	7.1
LWSSW-8-c-3ply-1SP	3	4.3	3.8	7.4	1.3	7.6	3.0
LWSSW-8-m-5ply-1SP	6	8.9	7.9	3.4	0.7	6.2	8.8
LSWWS-8-m-3ply-1SP	6	5.0	4.5	12.6	1.4	9.1	4.0
LSWWS-8-m-5ply-1SP	6	7.3	6.7	11.4	1.2	9.1	4.6
LSWSWS-10-m-3ply-1SP	6	4.9	4.3	24.9	1.8	16.3	16.9
LSWSWS-10-c-3ply-1SP	3	3.9	3.5	12.5	1.7	8.8	2.1
LSWSWS-8-m-5ply-1SP	6	7.3	6.6	24.6	1.2	26.6	4.7
LWSSW-16-m-3ply-2SP	1	5.5	5.0	31.0	1.4	34.4	2.3
LWSSW-16-c-3ply-2SP	4	5.4	4.8	12.3	1.3	14.6	5.2
LWSSW-32-m-3ply-2SP	1	5.0	5.1	15.0	1.5	10.5	3.4
LWSSW-32-c-3ply-2SP	3	4.5	3.3	5.8	0.6	11.9	5.3

Table 4.11: Results summary for butt joints with STS in shear

Series	Repl.	F_{\max} [kN]	F_Y [kN]	$d_{F,\max}$ [mm]	$d_{F,Y}$ [mm]	μ [-]	k [kN/mm]
BS-1-m-3ply-2SP	6	6.9	4.8	36.7	11.2	3.8	0.4
BS-1-c-3ply-2SP	6	6.1	3.9	28.8	9.5	3.4	0.4
BS-2-m-3ply-2SP	6	6.1	5.1	38.5	7.4	6.0	0.7
BS-2-c-3ply-2SP	6	7.1	5.0	25.6	7.7	3.8	0.7
BS-8-m-3ply-1SP	6	6.8	4.3	39.2	7.9	5.0	0.5
BS-8-c-3ply-1SP	3	6.4	3.9	32.3	6.4	5.1	0.6
BS-16-m-3ply-2SP	1	6.7	4.7	42.0	7.9	5.5	0.4
BS-16-c-3ply-2SP	4	6.1	5.3	24.3	4.8	5.5	0.6
BS-32-m-3ply-2SP	1	6.0	4.1	23.0	5.0	4.6	0.5
BS-32-c-3ply-2SP	4	5.2	4.0	16.6	4.5	7.0	1.0

Table 4.12: Results summary for butt joints with STS in withdrawal

Series	Repl.	F_{\max} [kN]	F_Y [kN]	$d_{F,\max}$ [mm]	$d_{F,Y}$ [mm]	μ [-]	k [kN/mm]
BW-1-m-3ply-2SP	6	11.8	9.9	7.3	3.0	3.0	3.3
BW-2-m-3ply-2SP	6	7.7	6.8	3.7	1.5	3.3	5.9
BW-2-c-3ply-2SP	6	9.4	8.4	2.0	1.2	2.4	7.5
BW-4-m-3ply-1SP	6	7.6	6.9	3.8	1.6	2.8	4.5
BW-8-m-3ply-1SP	6	7.8	6.6	6.5	1.2	5.4	5.3
BW-8-m-3ply-1SP*	3	7.3	6.3	7.4	1.5	5.1	4.3
BW-8-m-3ply-2SP	6	6.1	5.7	2.5	0.6	3.7	4.8
BW-8-c-3ply-1SP	3	6.9	6.0	4.7	2.2	2.0	2.6
BW-16-m-3ply-2SP	1	6.9	6.1	6.5	1.3	6.4	3.6
BW-16-c-3ply-2SP	3	6.7	5.6	6.4	1.3	5.3	2.9
BW-20-m-3ply-2SP	6	6.7	5.7	6.7	2.3	3.0	2.4
BW-20-C-3ply-2SP	4	6.2	5.5	6.1	1.9	4.1	3.0

4.3.2 One and two STS connections (Mi-1 and Mi-2)

Table 4.13: Results summary for one and two STS connections (Mi-1 and Mi-2)

Series	Repl.	F_{\max} [kN]	F_Y [kN]	$d_{F,\max}$ [mm]	$d_{F,Y}$ [mm]	μ [-]	k [kN/mm]
SS-2-m-3ply-2SP	6	6.4	5.4	27.8	3.0	9.8	1.6
SS-2-c-3ply-2SP	6	5.8	4.6	13.5	2.3	6.2	1.9
LS-1-m-3ply-2SP	6	6.6	5.4	29.0	6.4	4.5	0.7
LS-1-c-3ply-2SP	6	5.8	4.0	22.0	4.2	5.4	1.3
BS-1-m-3ply-2SP	6	6.9	4.8	36.7	11.2	3.8	0.4
BS-1-c-3ply-2SP	6	6.1	3.9	28.8	9.5	3.4	0.4
LW-1-m-3ply-2SP	6	8.8	7.6	6.5	2.7	2.5	3.1
BW-1-m-3ply-2SP	6	11.8	9.9	7.3	3.0	3.0	3.3
SS-4-m-3ply-2SP	6	6.2	5.6	23.6	3.0	9.1	1.7
SS-4-c-3ply-2SP	6	6.0	4.7	13.0	2.0	8.5	2.0
LS-2-m-3ply-2SP	6	6.2	5.1	28.7	4.9	6.3	0.9
LS-2-c-3ply-2SP	6	6.9	4.7	25.3	4.8	5.8	1.1
BS-2-m-3ply-2SP	6	6.1	5.1	38.5	7.4	6.0	0.7
BS-2-c-3ply-2SP	6	7.1	5.0	25.6	7.7	3.8	0.7
LW-2-m-3ply-2SP	6	7.0	6.2	2.8	1.4	2.1	4.5
LW-2-c-3ply-2SP	6	9.2	8.3	3.3	1.8	1.9	4.7
BW-2-m-3ply-2SP	6	7.7	6.8	3.7	1.5	3.3	5.9
BW-2-c-3ply-2SP	6	9.4	8.4	2.0	1.2	2.4	7.5

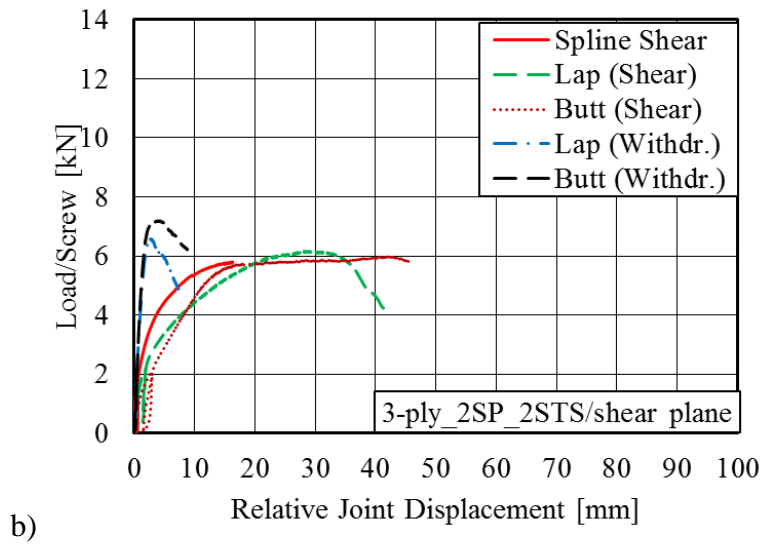
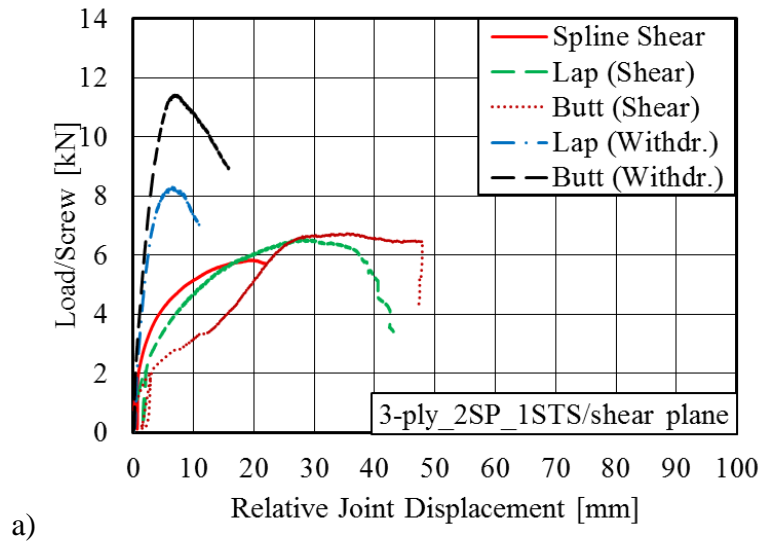


Figure 4.18: Average load displacement curves from monotonic tests: a) Mi-1, and b) Mi-2

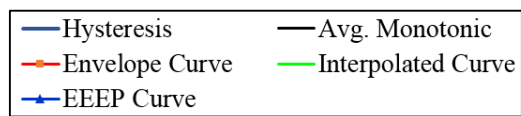
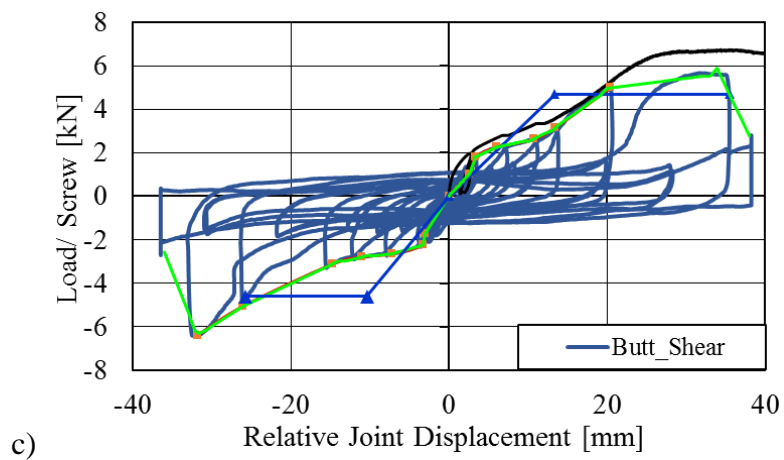
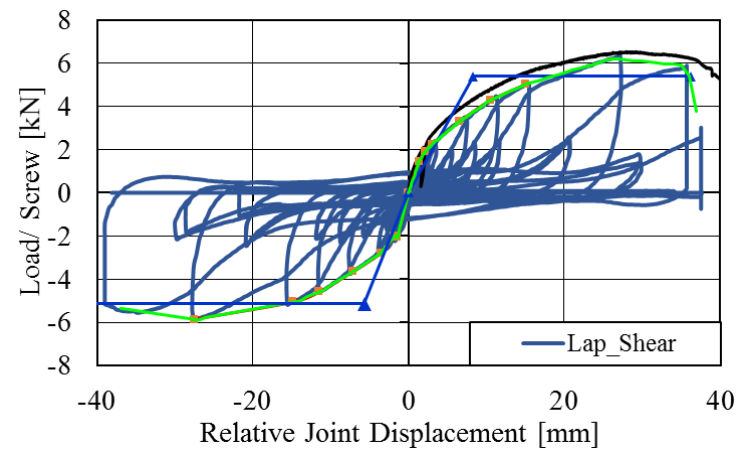
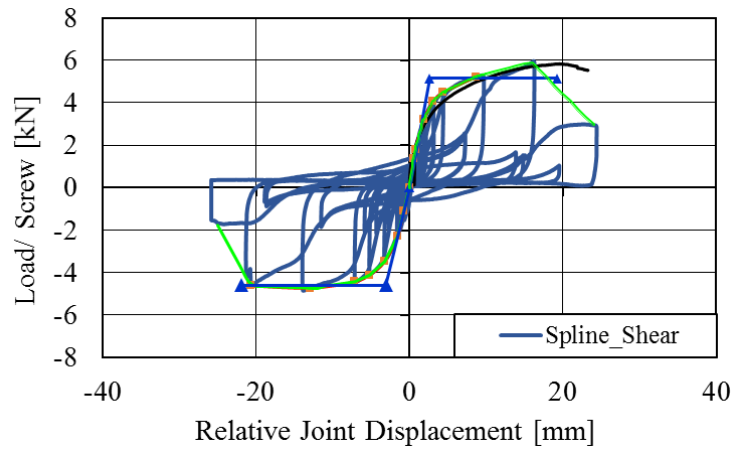
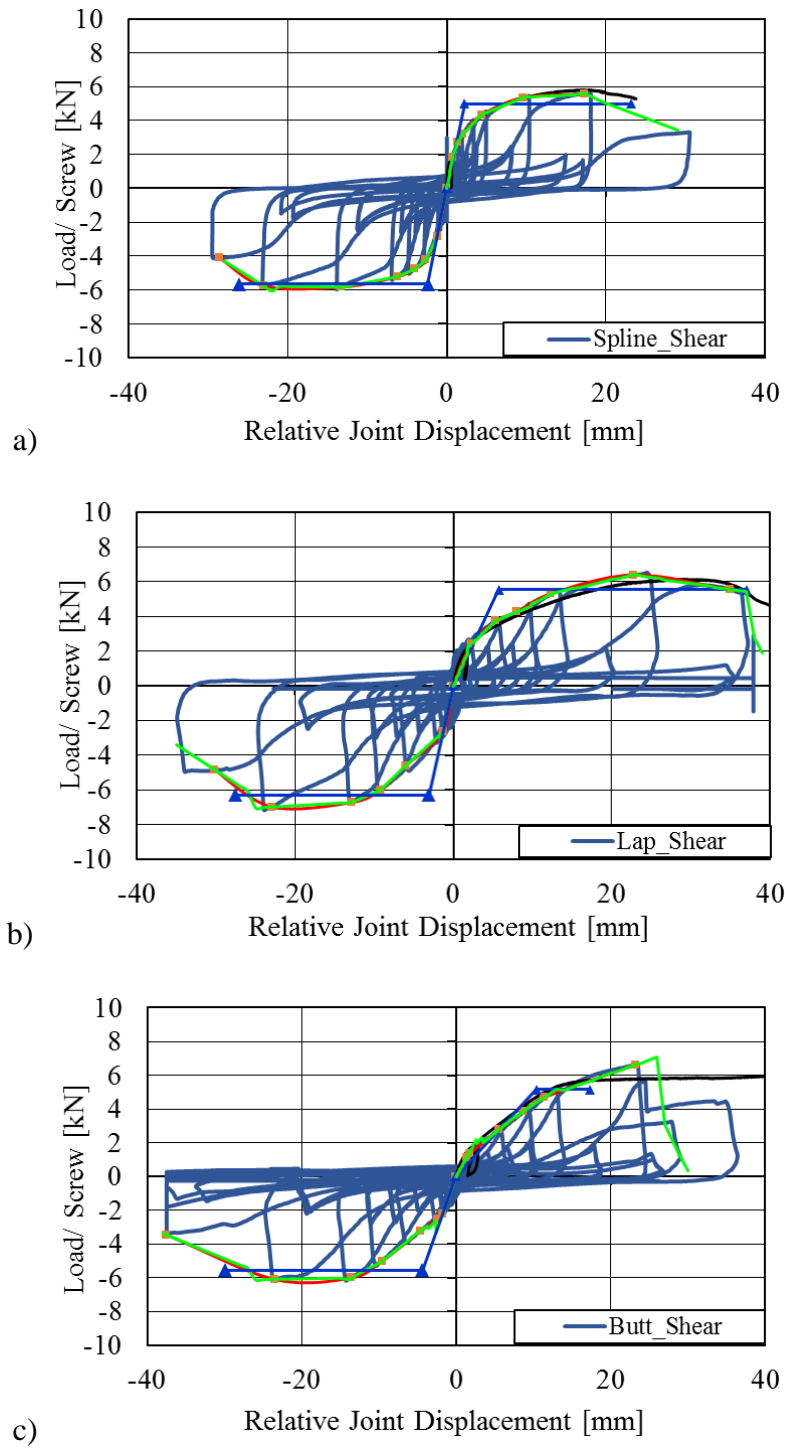
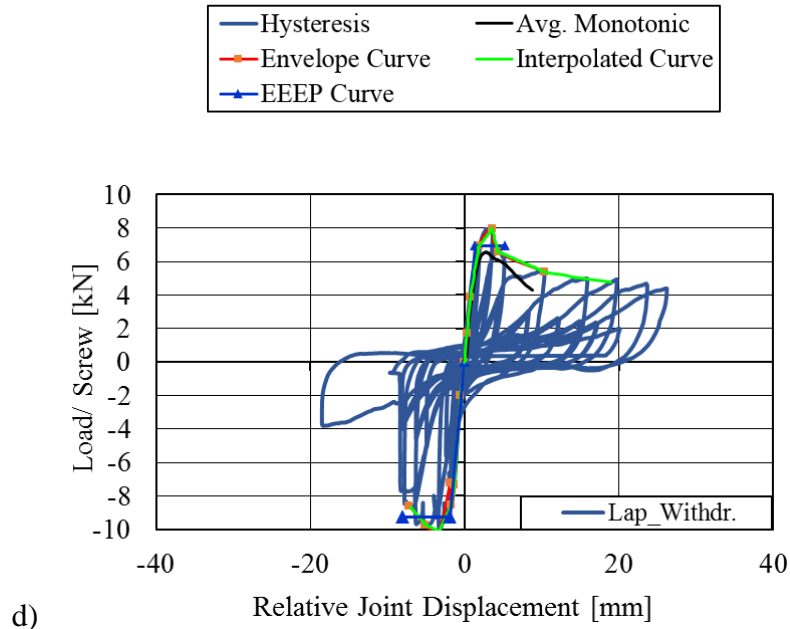
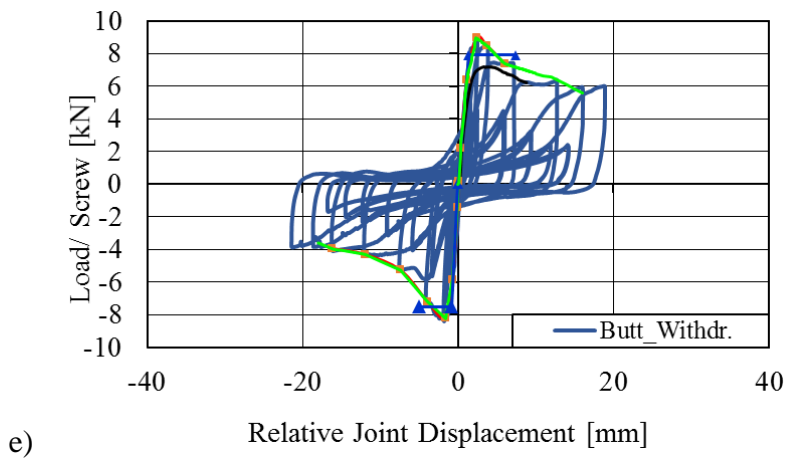


Figure 4.19: Load displacement curves from cyclic tests on Mi-1 joints: a) Spline_Shear, b) Lap_Shear, and c) Butt_Shear





d)



e)

Figure 4.20: Load displacement curves from cyclic tests on (Mi-2) joints: a) Spline_Shear, b) Lap_Shear, c) Butt_Shear, d) Lap_Withdr., and e) Butt_Withdr

4.3.3 Small sized specimens with two shear planes (S-2SP)

Table 4.14: Results summary for small sized specimen S-2SP under monotonic loading

Series	Repl.	F_{\max} [kN]	F_Y [kN]	$d_{F,\max}$ [mm]	$d_{F,Y}$ [mm]	μ [-]	k [kN/mm]
SS-10-m-3ply-2SP	6	4.0	2.8	41.8	4.7	10.1	0.8
SS-20-m-3ply-2SP	3	3.4	2.3	23.0	5.2	4.5	0.4
SS-32-m-3ply-2SP	3	2.2	1.7	11.7	4.5	2.6	0.6
SS-10-m-5ply-2SP	6	6.2	4.1	50.7	8.0	6.4	0.4
SS-20-m-5ply-2SP	3	4.6	2.9	38.0	9.0	4.3	0.3
SS-32-m-5ply-2SP	3	3.0	2.0	17.7	6.0	3.0	0.4
LS-5-m-3ply-2SP	6	5.1	3.4	25.2	3.0	11.0	1.2
LS-8-m-3ply-2SP	3	5.2	3.5	24.0	4.0	6.0	0.7
LS-5-m-5ply-2SP	6	10.7	7.0	46.3	5.6	9.5	1.5
LS-8-m-5ply-2SP	3	7.4	4.9	49.3	4.1	12.0	1.3
LW-8-m-3ply-2SP	6	5.3	4.9	2.3	0.7	3.0	135.9
LW-6-m-5ply-2SP	6	10.3	9.7	2.0	1.1	1.8	310.2
BW-8-m-3ply-2SP	6	6.1	5.7	2.5	0.6	3.7	102.0

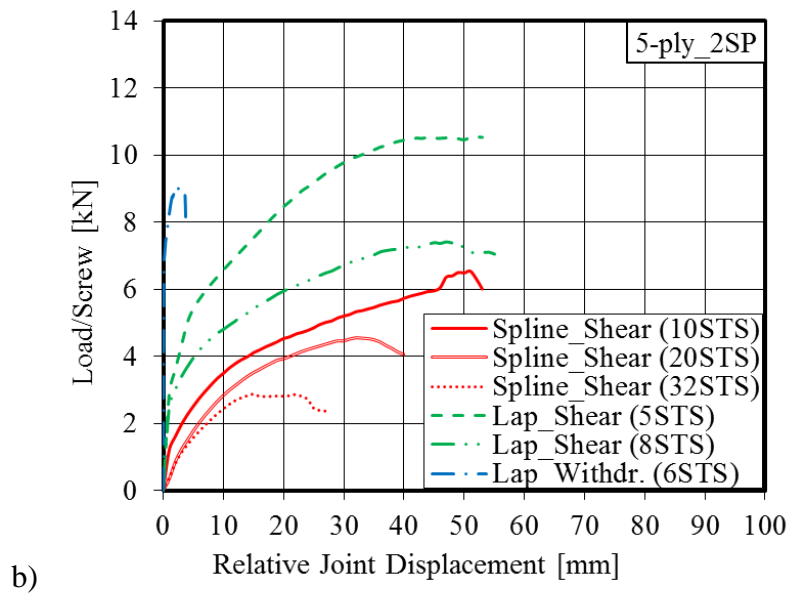
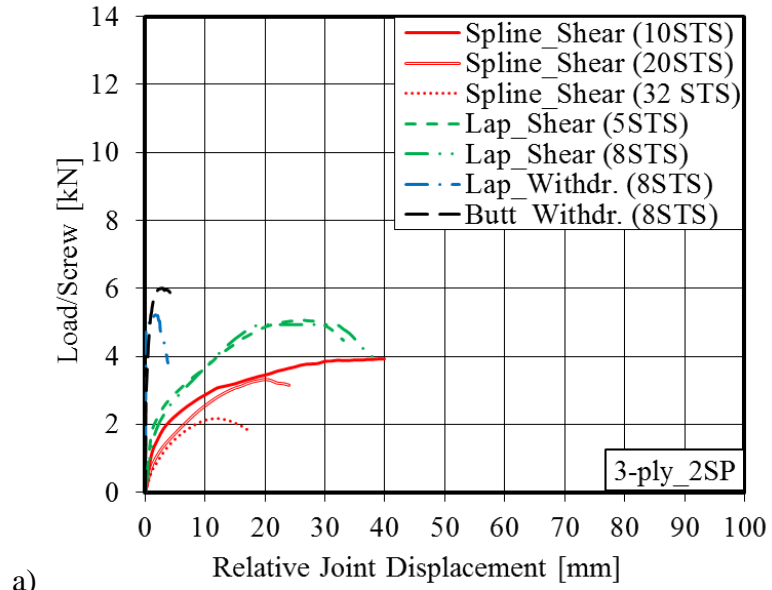


Figure 4.21: Average load displacement curves from quasi-static monotonic tests on S-2SP): a) 3-ply CLT, and b) 5-ply CLT

4.3.4 Small sized specimens with one shear plane (S-1SP)

Table 4.15: Results summary for 3ply joints with STS in shear (S-1SP)

Series	Repl.	F_{\max} [kN]	F_Y [kN]	$d_{F,\max}$ [mm]	$d_{F,Y}$ [mm]	μ [-]	k [kN/mm]
SS-8-m-3ply-1SP	6	6.9	4.5	52.8	7.0	7.5	0.5
SS-16-m-3ply-1SP	6	6.5	4.2	46.8	6.0	8.0	0.5
SS-16-m-NF-3ply-1SP*	3	6.4	4.2	52.7	7.0	7.6	0.5
SS-16-c-3ply-1SP	3	4.4	2.9	27.5	5.5	5.3	0.6
LS-4-m-3ply-1SP	6	6.4	4.3	24.8	4.7	5.3	0.9
LS-8-m-3ply-1SP	6	6.7	4.3	25.8	4.4	6.6	1.0
LS-8-m-3ply-1SP*	3	7.6	5.0	30.0	7.0	4.3	0.9
LS-8-c-3ply-1SP	3	5.1	3.4	22.3	4.1	5.6	0.8
BS-8-m-3ply-1SP	6	6.8	4.3	39.2	7.9	5.0	0.5
BS-8-c-3ply-1SP	3	6.4	3.9	32.3	6.4	5.1	0.6

*indicates specimen with friction-eliminating membrane

Table 4.16: Results summary for 3ply joints with STS in withdrawal (S-1SP)

Series	Repl.	F_{\max} [kN]	F_Y [kN]	$d_{F,\max}$ [mm]	$d_{F,Y}$ [mm]	μ [-]	k [kN/mm]
LS-16-m-3ply-2SP	1	7.3	6.0	31.0	6.6	5.1	0.8
LS-16-c-3ply-2SP	4	6.3	5.4	27.8	6.1	5.0	0.8
BS-16-m-3ply-2SP	1	6.7	4.7	42.0	7.9	5.5	0.4
BS-16-c-3ply-2SP	4	6.1	5.3	24.3	4.8	5.5	0.6
LW-16-m-3ply-2SP	1	7.2	6.6	2.8	2.0	1.4	3.1
LW-16-c-3ply-2SP	3	6.6	5.3	2.7	1.7	1.8	3.6
BW-16-m-3ply-2SP	1	6.9	6.1	6.5	1.3	6.4	3.6
BW-16-c-3ply-2SP	3	6.7	5.6	6.4	1.3	5.3	2.9
LWSSW-16-m-3ply-2SP	1	5.5	5.0	31.0	1.4	34.4	2.3
LWSSW-16-c-3ply-2SP	4	5.4	4.8	12.3	1.3	14.6	5.2

Table 4.17: Results summary for 3ply joints with STS in shear and withdrawal (S-1SP)

Series	Repl.	F_{\max} [kN]	F_Y [kN]	$d_{F,\max}$ [mm]	$d_{F,Y}$ [mm]	μ [-]	k [kN/mm]
LWSSW-8-m-3ply-1SP	6	6.7	5.1	14.7	1.0	17.5	4.1
LWSSW-8-m-3ply-1SP*	3	6.7	5.6	8.7	0.9	9.2	7.1
LWSSW-8-c-3ply-1SP	3	4.3	3.8	7.4	1.3	7.6	3.0
LSWWS-8-m-3ply-1SP	6	5.0	4.5	12.6	1.4	9.1	4.0
LSWSWS-10-m-3ply-1SP	6	4.9	4.3	24.9	1.8	16.3	16.9
LSWSWS-10-c-3ply-1SP	3	3.9	3.5	12.5	1.7	8.8	2.1

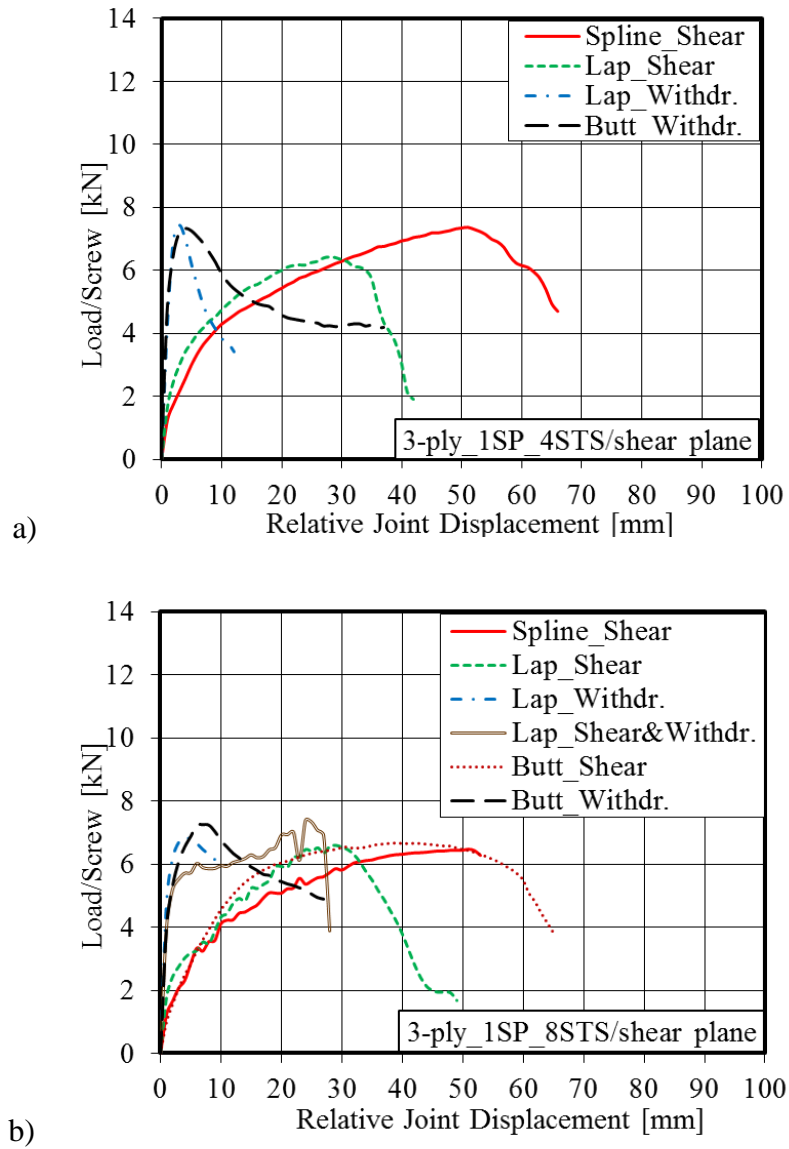


Figure 4.22: Average load displacement curves from quasi-static monotonic tests (S-ISP): a) 3-ply CLT-4STS , and b) 3-ply CLT-8STS

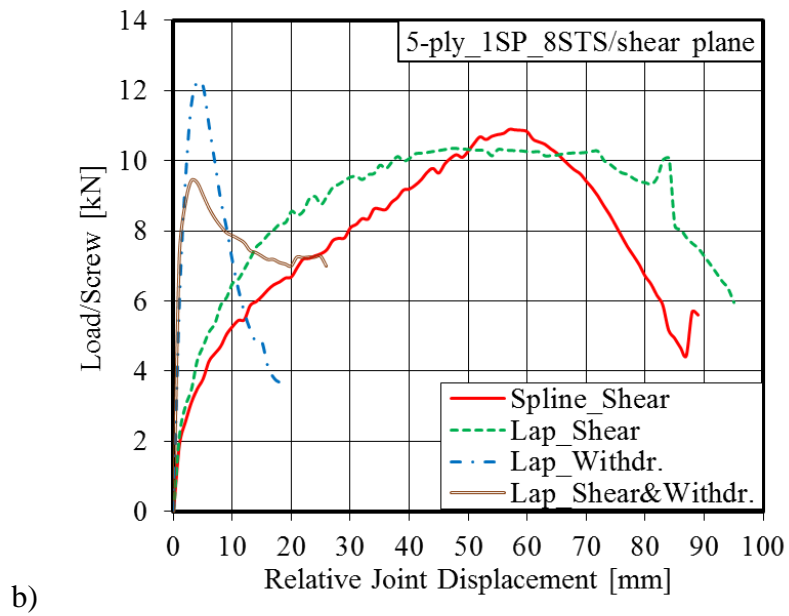
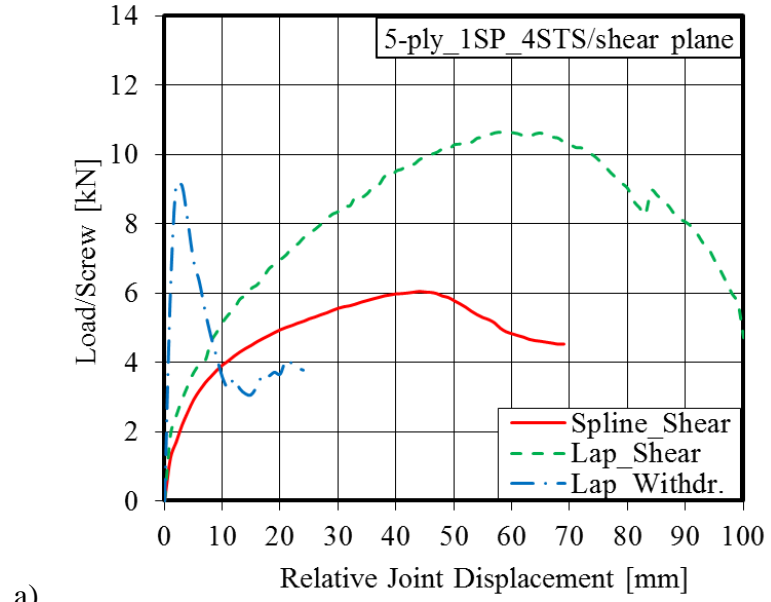
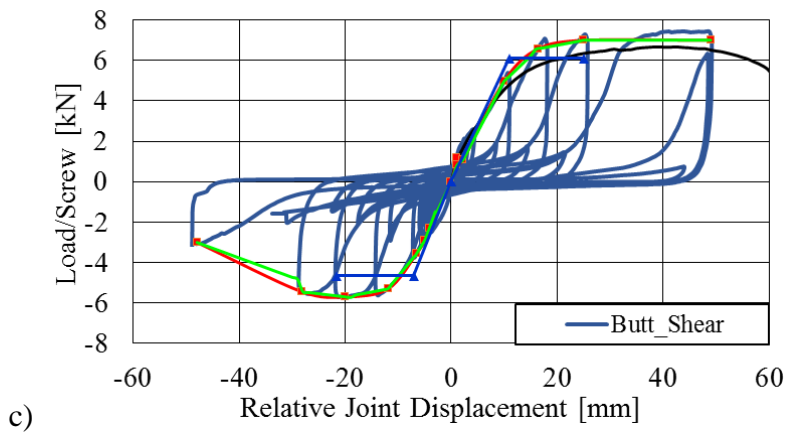
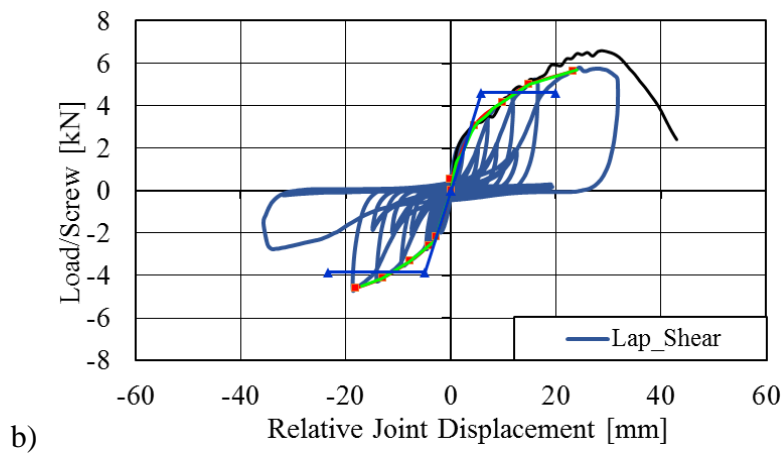
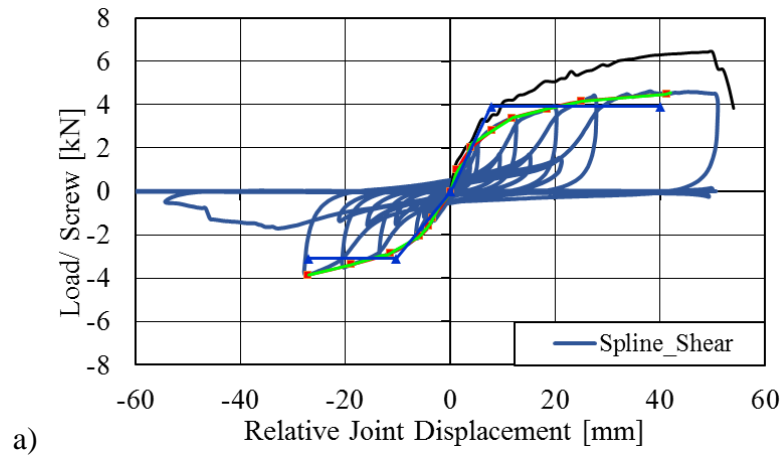
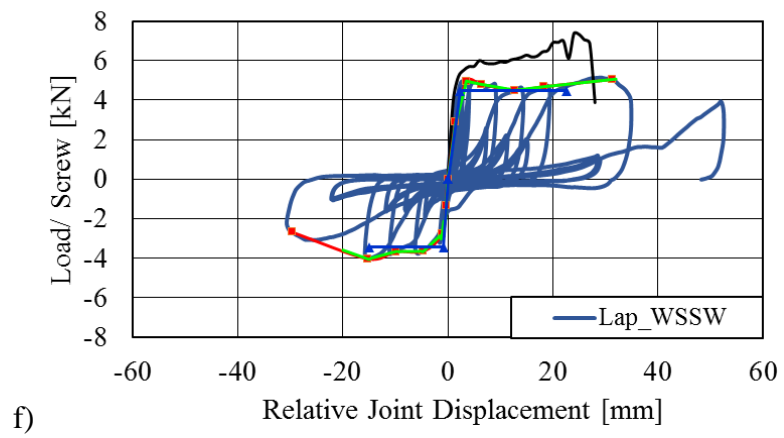
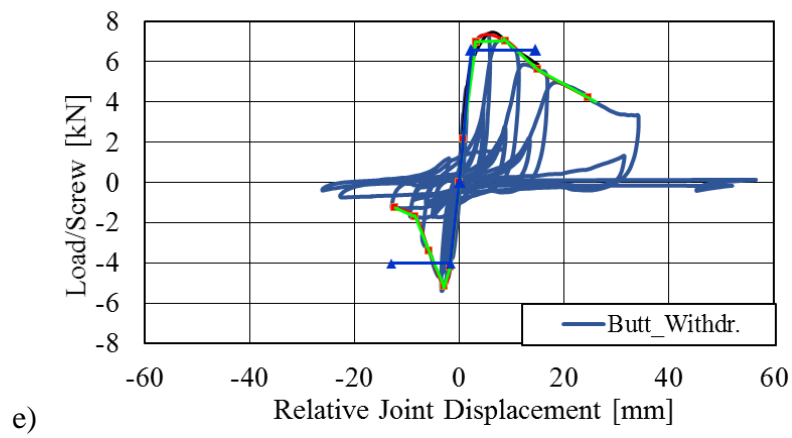
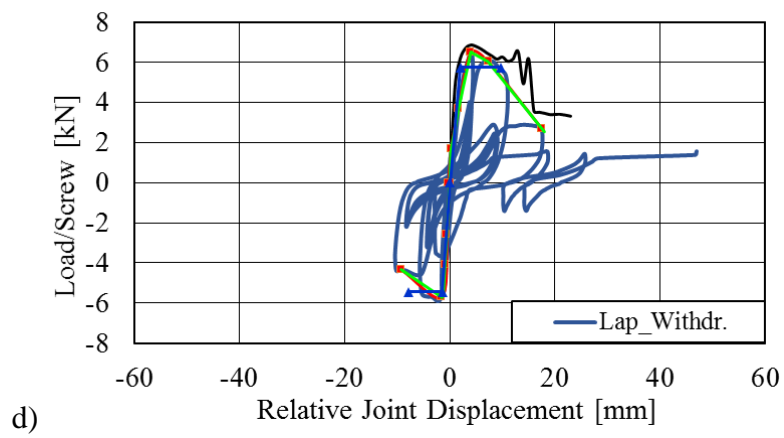


Figure 4.23: Average load displacement curves from quasi-static monotonic tests on specimens exhibiting (S-1SP): a) 5-ply CLT-4STS, and b) 5-ply-8STS per shear plane





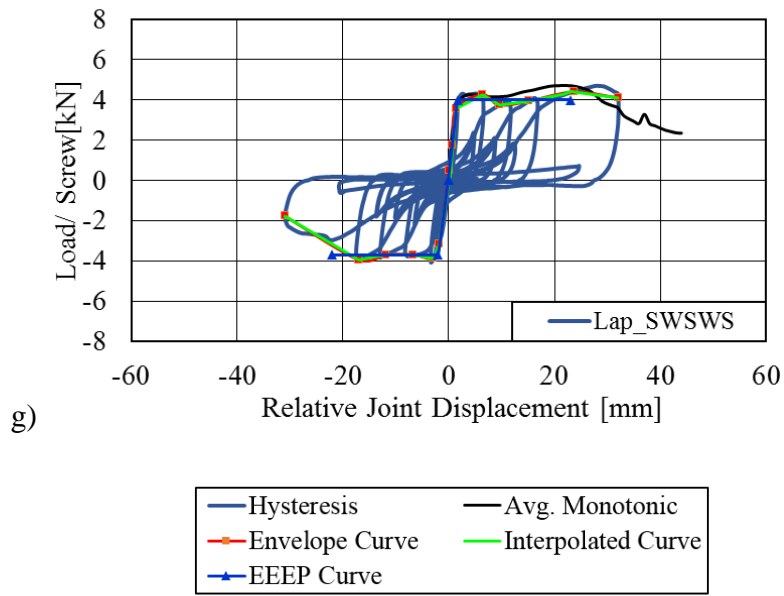


Figure 4.24: Load displacement curves from cyclic tests on S-ISP joints: a) *Spline_Shear*, b) *Lap_Shear*, c) *Butt_Shear*, d) *Lap-Withdr.*, e) *Butt-Withdr.*, f) *Lap_WSSW*, and g) *Lap_SWSWS*

4.3.5 Medium (M) and large (L) sized specimens (2SP)

Table 4.18: Results summary (M-2SP) under quasi-static monotonic and cyclic loading)

Series	Repl.	F_{\max} [kN]	F_Y [kN]	$d_{F,\max}$ [mm]	$d_{F,Y}$ [mm]	μ [-]	k [kN/mm]
LS-16-m-3ply-2SP	1	7.3	6.0	31.0	6.6	5.1	0.8
LS-16-c-3ply-2SP	4	6.3	5.4	27.8	6.1	5.0	0.8
BS-16-m-3ply-2SP	1	6.7	4.7	42.0	7.9	5.5	0.4
BS-16-c-3ply-2SP	4	6.1	5.3	24.3	4.8	5.5	0.6
LW-16-m-3ply-2SP	1	7.2	6.6	2.8	2.0	1.4	3.1
LW-16-c-3ply-2SP	3	6.6	5.3	2.7	1.7	1.8	3.6
BW-16-m-3ply-2SP	1	6.9	6.1	6.5	1.3	6.4	3.6
BW-16-c-3ply-2SP	3	6.7	5.6	6.4	1.3	5.3	2.9
LWSSW-16-m-3ply-2SP	1	5.5	5.0	31.0	1.4	34.4	2.3
LWSSW-16-c-3ply-2SP	4	5.4	4.8	12.3	1.3	14.6	5.2

Table 4.19: Results summary (L-2SP) under quasi-static monotonic and cyclic loading)

Series	Repl.	F_{\max} [kN]	F_Y [kN]	$d_{F,\max}$ [mm]	$d_{F,Y}$ [mm]	μ [-]	k [kN/mm]
LS-32-m-3ply-2SP	1	6.9	5.7	32.5	5.3	6.1	0.9
LS-32-c-3ply-2SP	3	5.8	4.2	20.5	5.1	5.1	0.8
BS-32-m-3ply-2SP	1	6.0	4.1	23.0	5.0	4.6	0.5
BS-32-c-3ply-2SP	4	5.2	4.0	16.6	4.5	7.0	1.0
LW-32-m-3ply-2SP	1	6.5	6.0	3.6	1.9	1.9	2.8
LW-32-c-3ply-2SP	4	5.2	4.9	1.9	1.4	1.3	3.9
BW-20-m-3ply-2SP	6	6.7	5.7	6.7	2.3	3.0	2.4
BW-20-C-3ply-2SP	4	6.2	5.5	6.1	1.9	4.1	3.0
LWSSW-32-m-3ply-2SP	1	5.0	5.1	15.0	1.5	10.5	3.4
LWSSW-32-c-3ply-2SP	3	4.5	3.3	5.8	0.6	11.9	5.3

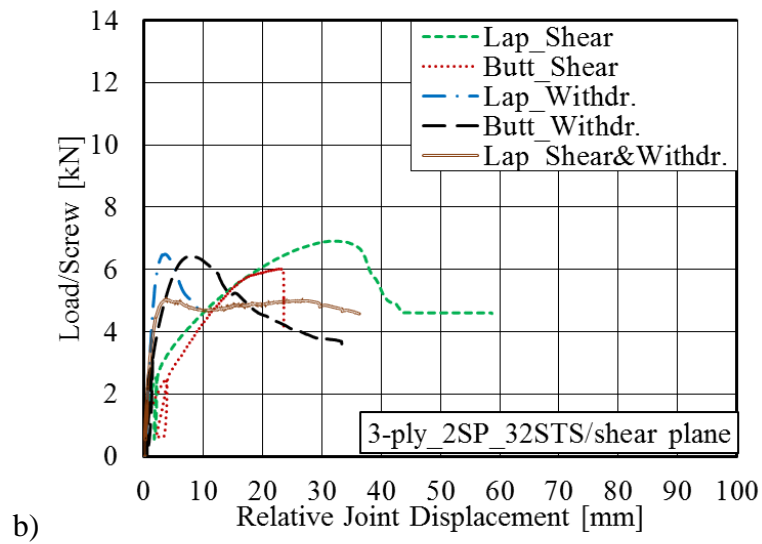
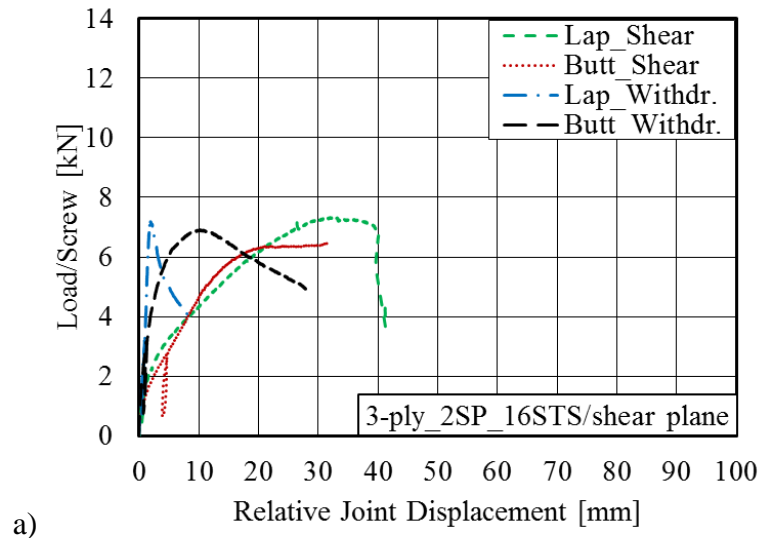
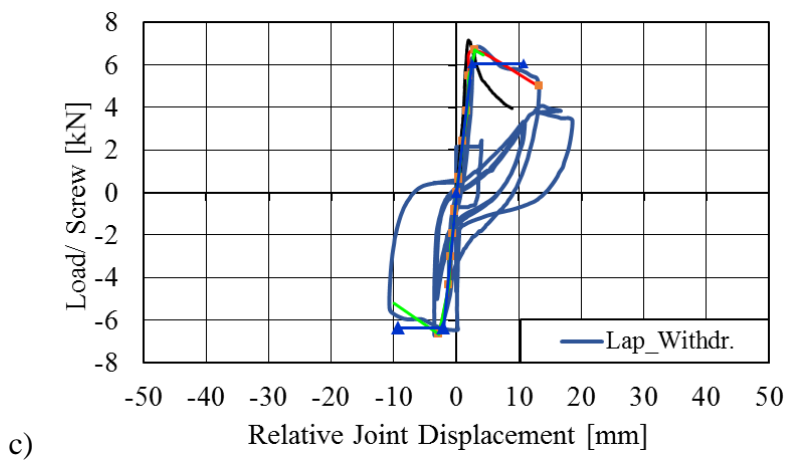
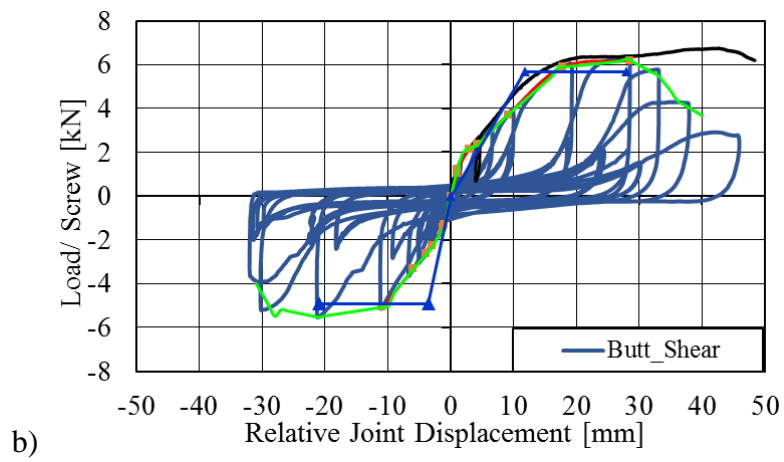
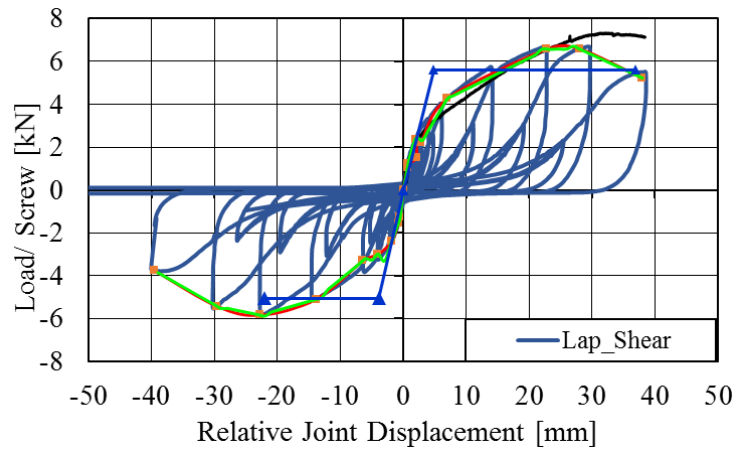


Figure 4.25: Average load displacement curves from quasi-static tests: a) (M-2SP), and b) (L-2SP)



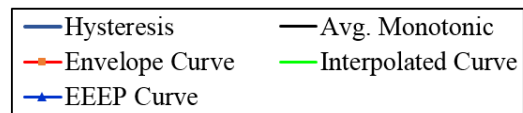
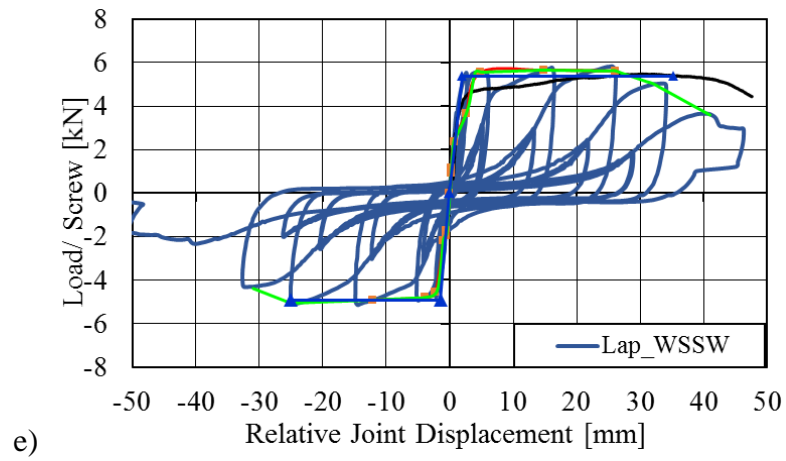
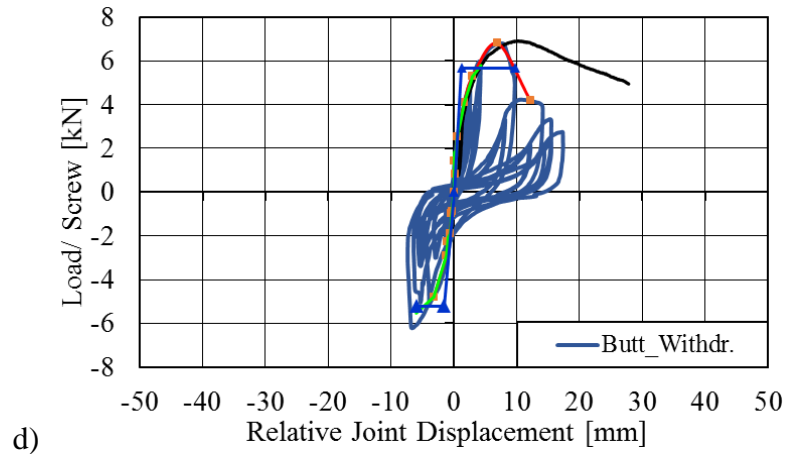
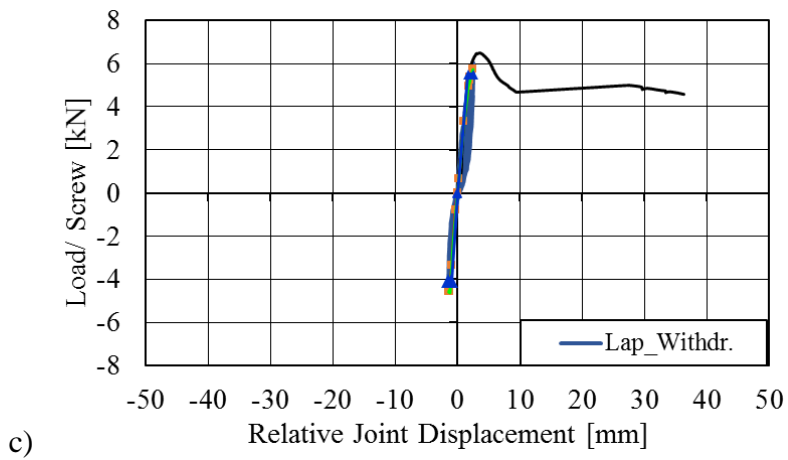
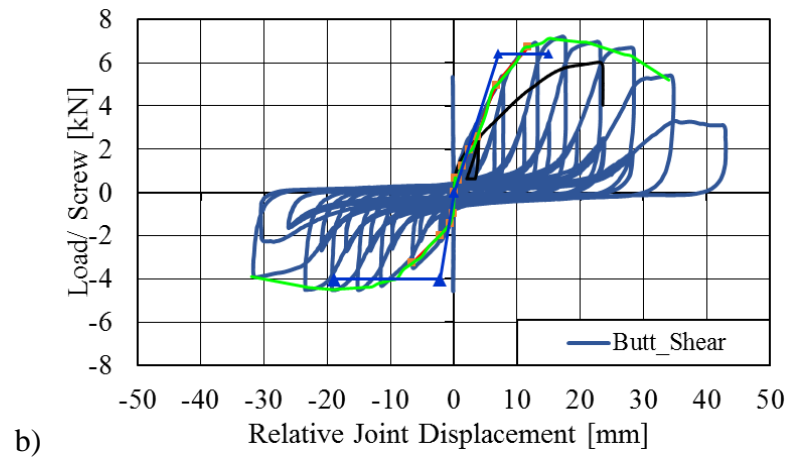
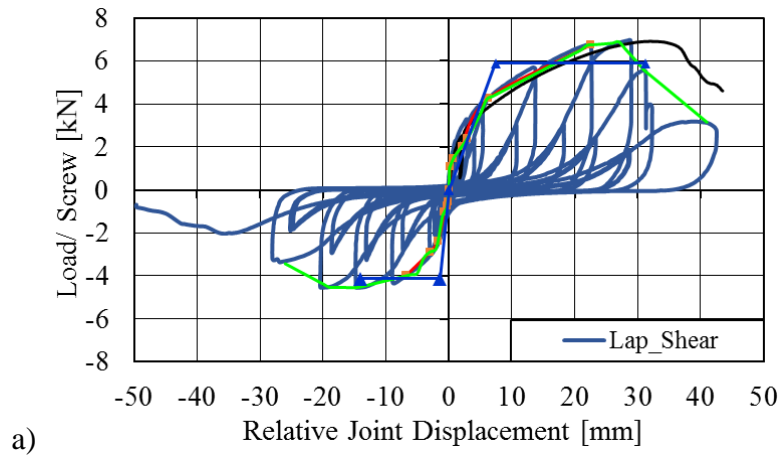


Figure 4.26: Load displacement curves from cyclic tests on M joints: a) Lap_Shear, b) Butt_Shear, c) Lap-Withdr., d) Butt-Withdr., and f) Lap_WSSW



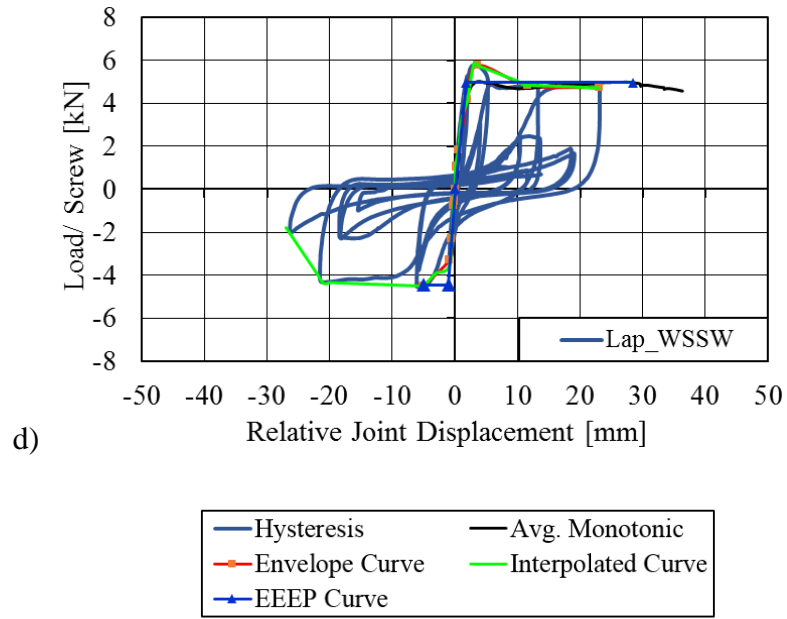


Figure 4.27: Load displacement curves from cyclic tests on *L* specimens: a) *Lap_Shear*, b) *Butt_Shear*, c) *Lap-Withdr.*, and d) *Lap_WSSW*

4.4 Discussion

4.4.1 Load-deformation behavior monotonic tests

Figure 4.18, Figure 4.21, Figure 4.22, Figure 4.23, and Figure 4.25 illustrated the behavior from the different sized specimens under-static monotonic loading. From all these figures irrespective of number of screws (1-32), size (mini- large), and number of CLT plies (3 or 5), it can clearly be observed that ductile joints can be achieved using STS in shear. In contrast, when STS are used in withdrawal, very high stiffness but low ductility ($\mu < 3$) is obtained.

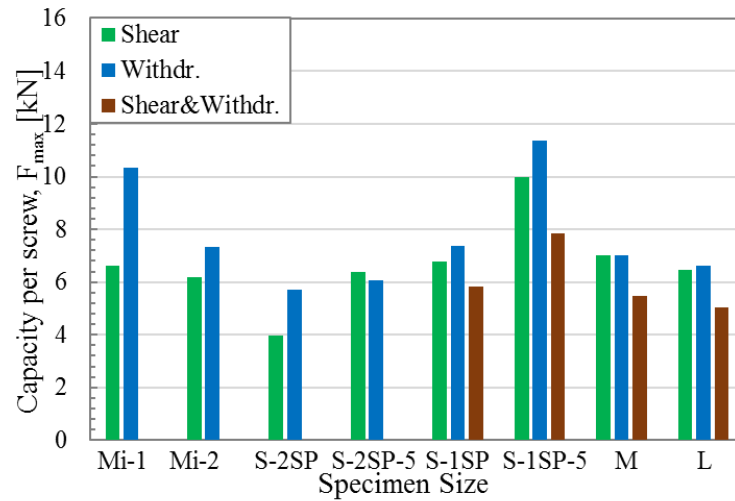
Specimens with STS loaded in shear reach large displacements, and reach their average maximum load of 6.7 kN/screw at a deformation of around 36 mm for all types tested as illustrated in Figure 4.28 (Mi-1: 6.6 kN 31 mm; Mi-2: 6.2 kN, 30 mm; S-2SP: 4 kN, 25 mm; S-2SP-5ply: 6.4 kN, 40 mm; S-1SP: 6.8 kN, 40 mm; S-1SP-5ply: 10 kN, 57 mm; M: 7 kN, 36 mm; and L: 6.5 kN, 28 mm).

Specimens with STS loaded in withdrawal reach an average capacity of 7.7 kN but consistently failed before reaching 10 mm of displacement at a deformation of around 4.2 mm (Mi-1: 10.3 kN, 6.9 mm; Mi-2: 7.3 kN, 3.3 mm; S-2SP: 5.7 kN, 2.4 mm; S-2SP-5ply: 6.1 kN, 2.5 mm; S-1SP: 7.4 kN, 5.4 mm; S-1SP-5ply: 11.4 kN, 3.6 mm; M: 7 kN, 4.7 mm; and L: 6.6 kN, 5.1 mm).

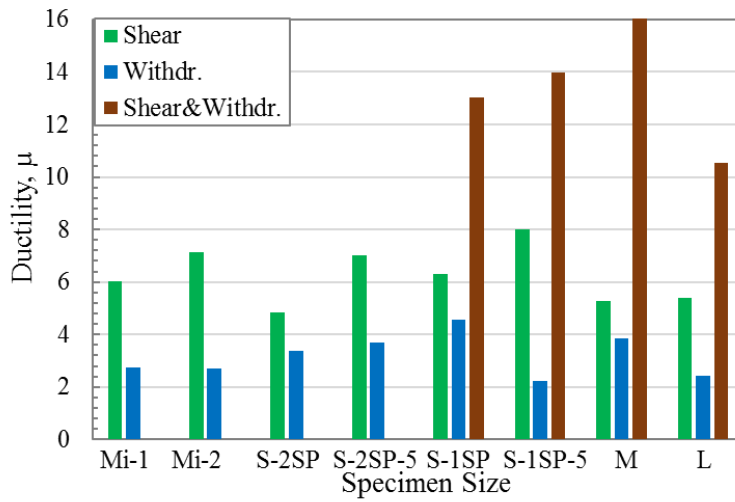
The CLT connections that use both STS loaded in shear and STS loaded in withdrawal combine both favorable performance attributes: high stiffness (4.9 kN/mm) and large ductility (12.5) as well as large deformation capacity of approximately 17 mm.

All assemblies showed almost similar capacity 6.7, 7.7, and 6 kN/screw when STS are applied in shear, withdrawal, and both in shear and withdrawal respectively. However, assemblies with STS

loaded in shear showed low stiffness 0.8 kN/mm compared to the assemblies with STS loaded in withdrawal (4.3 kN/mm) and STS loaded in shear and withdrawal (4.9 kN/mm).



a)



b)

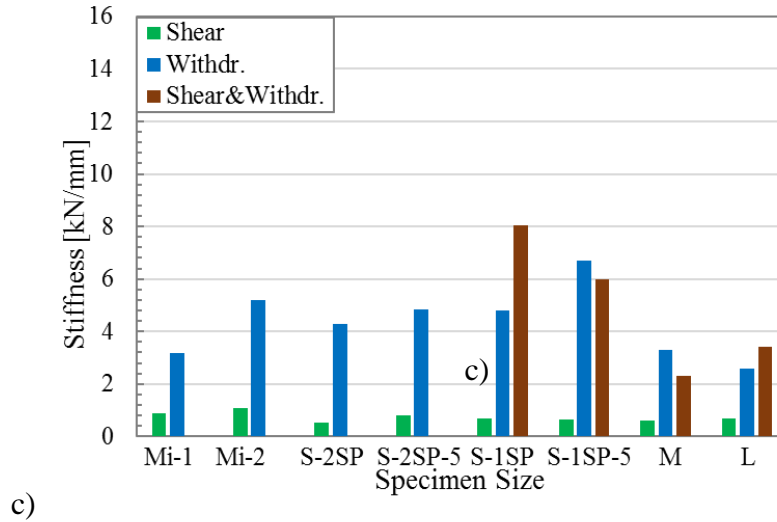


Figure 4.28: Comparison of results from different specimen sizes under monotonic loading; a) capacity, b) ductility, and c) stiffness

4.4.2 Load-deformation behavior cyclic tests

Figure 4.19, Figure 4.20, Figure 4.24, Figure 4.26, and Figure 4.27 illustrate the load-displacement behavior of STS shear connections under reversed cyclic loading for different sized specimens. All individual load deformation curves are shown in the Appendix.

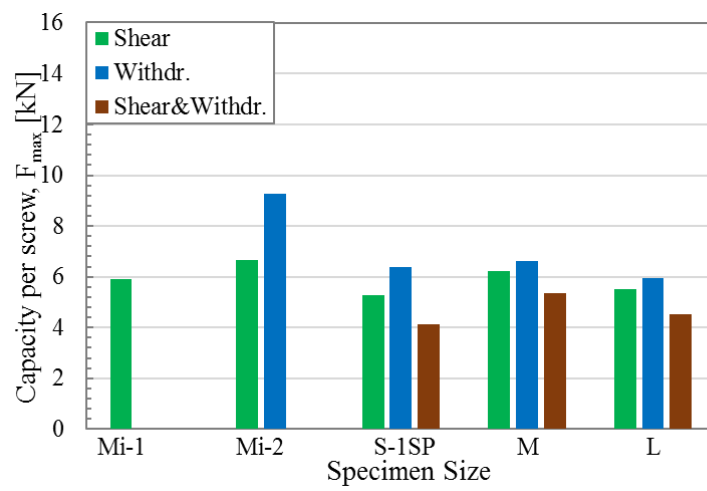
Similar to the monotonic tests, using STS in shear led to ductile connections (5.5) while using STS in withdrawal led to high stiffness (4 kN/mm). As demonstrated from the hysteretic loops, the ductile connections were able to dissipate large amounts of energy. As typical for wood connections with dowel-type fasteners, pronounced pinching behavior was observed.

In contrast, when STS were used in withdrawal, high stiffness (4 kN/mm) but low ductility (2.6) was obtained. Small amounts of energy were dissipated in case of the large-scale specimens, where almost no hysteresis loops were observed. The CLT assemblies that used both STS loaded in shear with STS loaded in withdrawal were able to combine the favorable performance attributes: high

stiffness (4 kN/mm), large ductility (11.6), as well as large deformation capacity of approximately 20 mm.

Figure 4.29a shows mini sized specimens achieved 12% and 33% higher capacity compared to the average joint capacity with STS in shear and STS in withdrawal, group effect section 4.4.11 will further elaborate on this. Small sized specimens with one shear plane had approximately 10% reduced joint capacity compared to the average value for both with STS in shear and STS in withdrawal. A possible explanation is that the down strokes partially withdrew half of the screws, and thus weakened them before they were needed to carry a compression load in the upstrokes which caused the overall capacity (average of positive and negative envelop) reduced.

Figure 4.29b shows all the joints with shear screws achieved moderate to high ductility (average 6), joints with withdrawal screws achieved low to brittle ductility (<2.5), and joints with combined screw stiffness achieved high ductility (average 12) irrespective to the specimen sizes tested. Joints with one shear plane in small sized specimen had 13%, 40%, and 47% less stiffness compared to the average values of all two shear planes connections with STS in shear, withdrawal, and shear with withdrawal. Though this setup showed proper shear, however, it lacked stability for being inclined in nature with just one shear plane. All the mini specimens achieved 50% and 40% higher stiffness compared to the average joint stiffness with screws in shear and withdrawal respectively (Figure 4.29c).



a)

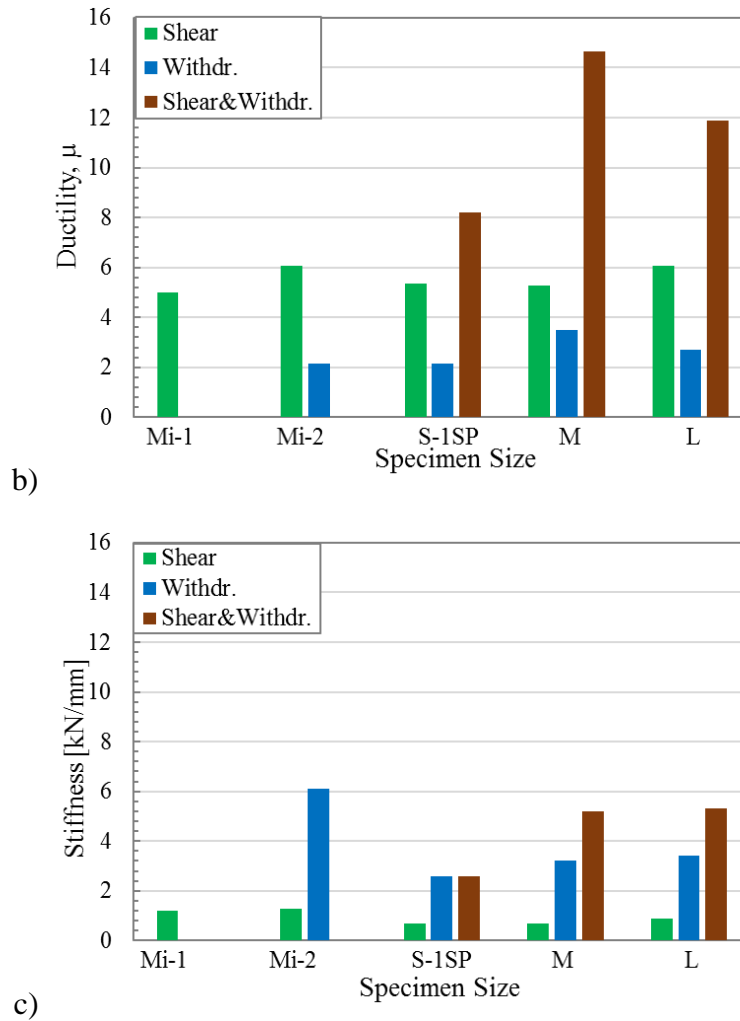


Figure 4.29: Comparison of results from different specimen sizes under cyclic loading; a) capacity, b) ductility, and c) stiffness

4.4.3 Joints with STS in shear

Comparisons between different joints with STS loaded in shear (Spline_Shear, Lap_Shear, and Butt_Shear) are shown in Figure 4.30 and Figure 4.31 for different number of screws per shear plane in different sized specimens for 3-ply and 5-ply respectively. All series in 3-ply (Figure 4.30) achieved comparable capacities 5 kN, 6.3 kN, and 6.5 kN, at displacements of 32 mm, 27 mm and 35 mm for Spline, Lap, and Butt joints respectively. In case of stiffness, Spline and Lap joints were found to be 1.8 times higher (0.9 kN/mm) compared to Butt joints (0.5 kN/mm). In terms of

ductility, Spline, and Lap joints were found to be highly ductile ($\mu > 6$) whereas Butt joints were found to be moderately ductile ($\mu > 4$).

Similar trend was also obtained in 5-ply (Figure 4.31) CLT panels. Comparable capacities (6.4 kN and 6.2 kN) were observed in Spline and Butt joints. However, Lap joints had 1.5 times higher capacity compared to the others. Butt joints had 1.2 and 1.5 times less stiffness compared to spline and lap joints. Both spline and butt joints for 5-ply were found to be moderately ductile with μ ranging between 4-6 however, lap joints showed high ductility ($\mu > 9$).

For both 3-ply and 5-ply connections, butt joints had comparable load-displacement behaviour irrespective of different number of screws, however, for lap 3-ply (5 and 8) and spline 3 and 5-ply (10, 20, and 32) joints graphs varied in terms of capacity, stiffness, and ductility with varying number of screws. It is due to the bending effect in small sized specimen with two shear planes which will be discussed in a subsequent section. Spline joints were only tested in small sized specimen with one and two shear planes. Butt joint with STS in shear was not tested in S-2SP and had all comparable graphs. Lap joint with STS in 5-ply did not seem to be affected due to the bending, it might be the reason of increased number of plies.

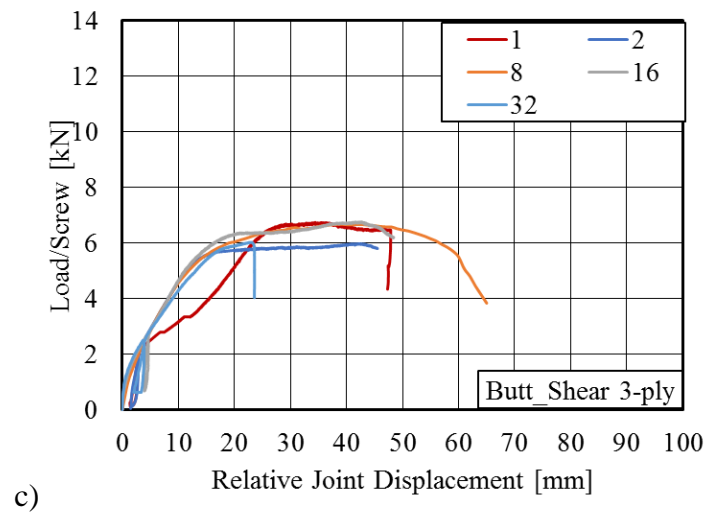
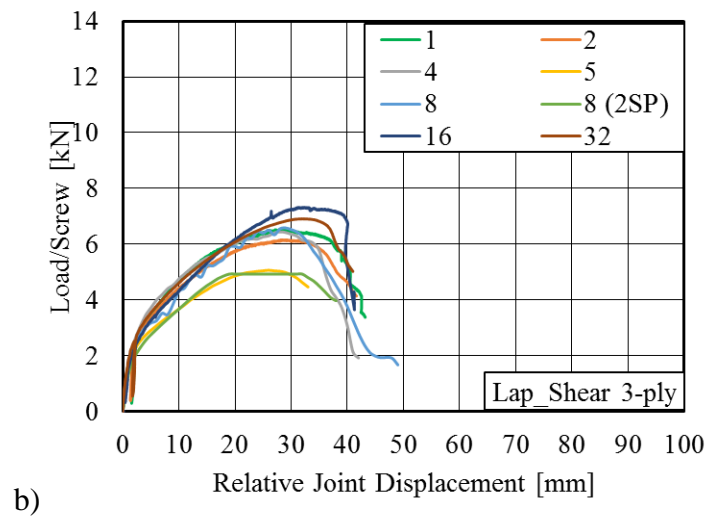
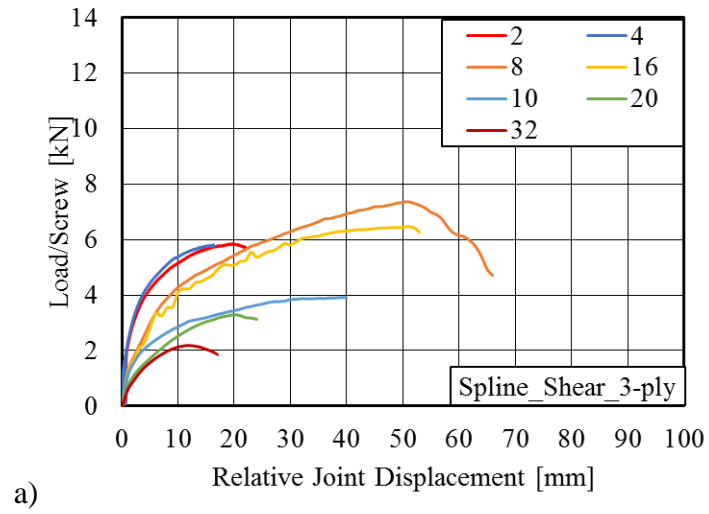


Figure 4.30: Load displacement in 3-ply CLT: a) Spline_Shear, b) Lap_Shear, and c) Butt_Shear

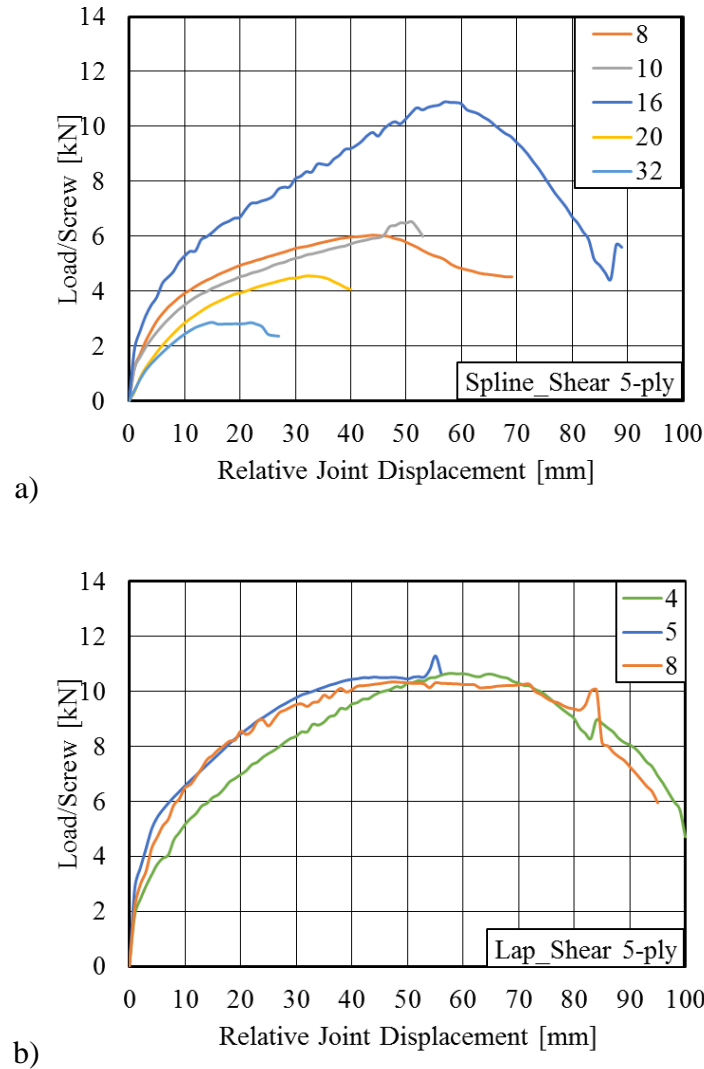


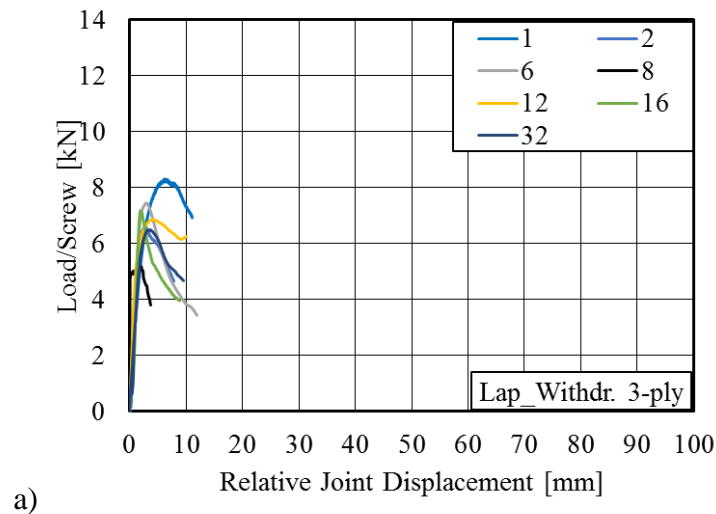
Figure 4.31: Load displacement in 5-ply CLT: a) Spline_Shear, and b) Lap_Shear

4.4.4 Joints with STS in withdrawal

A comparison between test series with STS loaded in withdrawal is shown in Figure 4.32 (3-ply) and Figure 4.33 (5-ply). Lap and butt joints in 3-ply CLT exhibited comparable capacity (7.1 kN and 7.8 kN) at small displacement (4 mm and 5 mm), high stiffness (22 kN/mm and 18 kN/mm), and low ductility (μ 2 and 4) respectively. Joints with 1 STS per shear plane had 1.2-1.5 times

higher capacity as those are the joints where screw was under shear-tension load whereas other joints had screw pair one in shear-tension and the other one in shear-compression. That is the reason this one screw test result was not considered to develop the group effect factor.

All joints tested in small-sized specimen with two shear planes had 1.2 – 1.5 times lower capacity compared to the other joints due to bending effects which will be discussed in later section. Similar results were obtained for 5-ply CLT. No butt joints were tested in 5-ply, so the comparison only applies to lap joints varying the number of screws. Joints with 10 screws showed 1.2 times higher capacity compared to 4 and 6 screws, more tests need to be done in 5-ply CLT to confirm the trend.



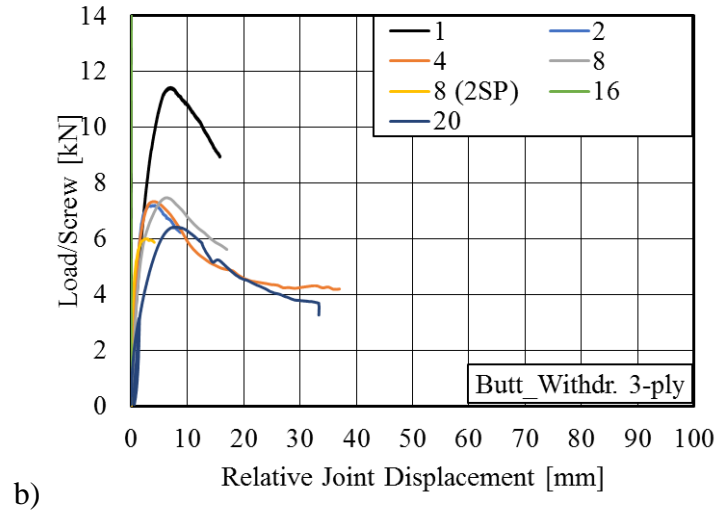


Figure 4.32: Load displacement in 3-ply CLT: a) Lap_Withdr. and Butt_Withdr.

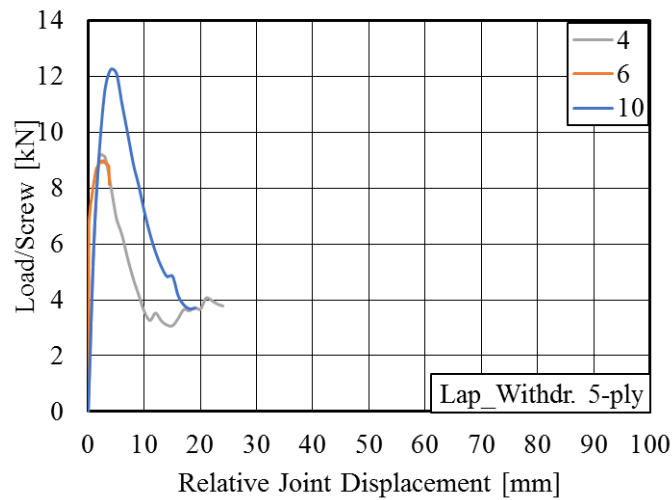


Figure 4.33: Load displacement in 5-ply CLT: Lap_Withdr.

4.4.5 Joints with STS in shear and withdrawal

The comparison between all series that combined with STS loaded in shear with STS loaded in withdrawal is shown in Figure 4.34 for both 3-ply and 5-ply. There different layouts (WSSW, SWWS, and SWSWS) were tested in small sized specimen with one shear plane. All three layouts achieved a unique combination of comparable high stiffness (around 6 kN/mm) and high ductility

(μ 17 and 14). However, WSSW layout showed 1.2 times higher capacity compared to the other layouts both in 3-ply and 5-ply. Using withdrawal screws in the end and shear screws in the middle increased the capacity. As a consequence, only WSSW layout was chosen to be tested in medium and large sized specimen in 3-ply CLT.

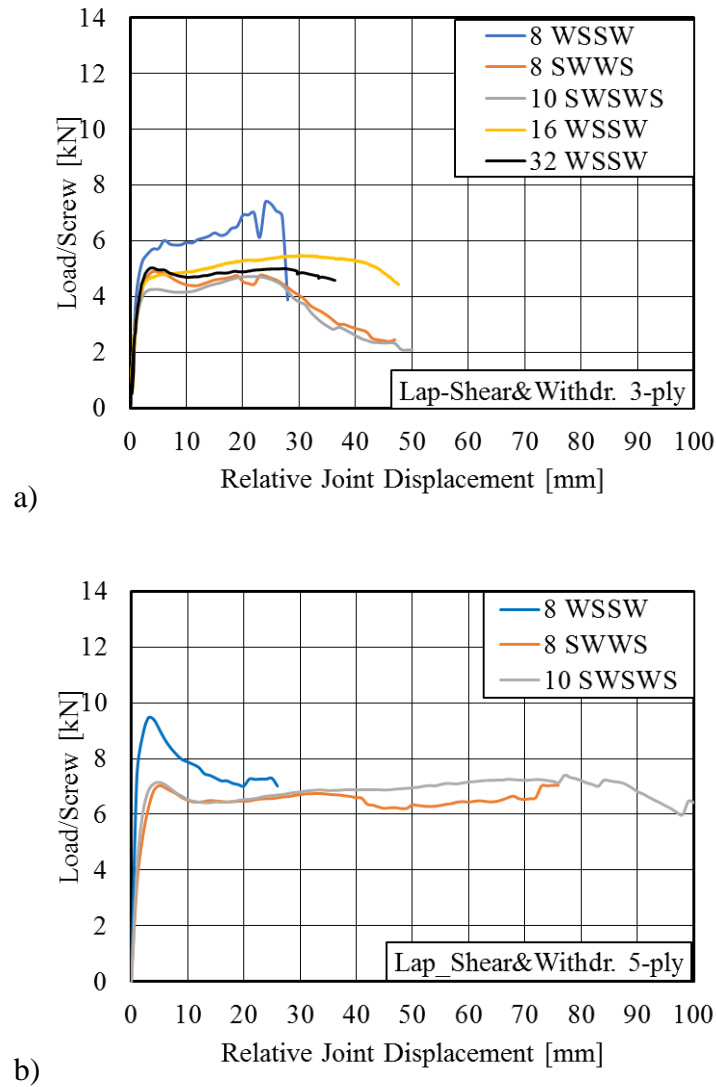


Figure 4.34: Lap joints with STS in shear and STS in withdrawal in a) 3-ply, and b) 5-ply

4.4.6 Comparison between tests using specimens using one two and shear planes

This comparison was only possible in small sized specimens as all other specimen sizes were tested only in two shear planes, so no comparison was made for that. This comparison was made based on the similar spacing, and same number of STS per shear plane. The number of STS in one shear plane (1SP) with similar spacing and rows are higher as because in 1SP connection was made in 600 mm and for 2SP it was in 400 mm height. 3-ply specimens with one shear plane has 30-75% higher capacity, 2-50% higher ductility (except for Lap_Withdr which has 4% less ductility), and 10-40% higher stiffness (except for Spline_Shear which has 20% less stiffness) compared to specimens with two shear planes (Table 4.20).

5ply specimens with one shear plane have 20-50% higher capacity, up to 50% higher ductility, and 55% higher stiffness in Spline joint but 35% less stiffness in lap joints with STS in withdrawal compared to specimens with two shear planes. Stiffness in Lap_Withdr joints in 2SP was high which was not comparable to any other stiffness values for this kind of joint.

The effect of bending in the test assemblies exhibiting two shear planes explained the inferior performance achieved in these test series (Figure 4.35). This bending effect exhibited due to low aspect ratio 1:1 for each panel in 2SP specimen. The opening of the shear plane effectively created another force perpendicular to the joints which reduced the results. The test setup having one shear plane only created a clear load path and resulted in higher capacity, ductility, and stiffness which are a better representation of connection performance. Therefore, only the latter set-up was chosen for the subsequent cyclic tests (Table 4.21).

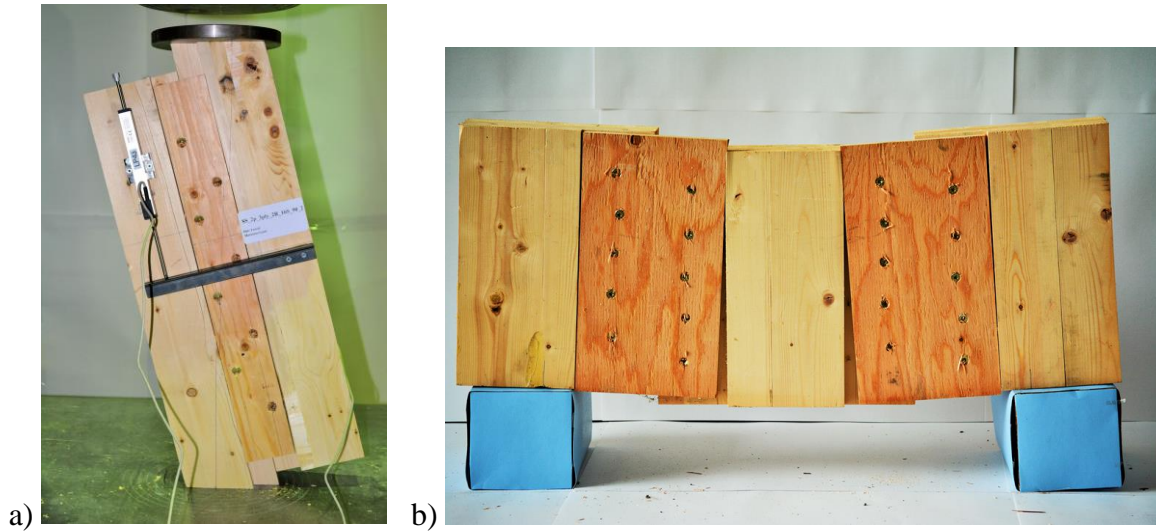


Figure 4.35 Comparison between specimens with 1 or 2 shear planes a) pure shear in 2SP, and b) bending effect in 1SP

Table 4.20: ISP-2SP comparison (3-ply)

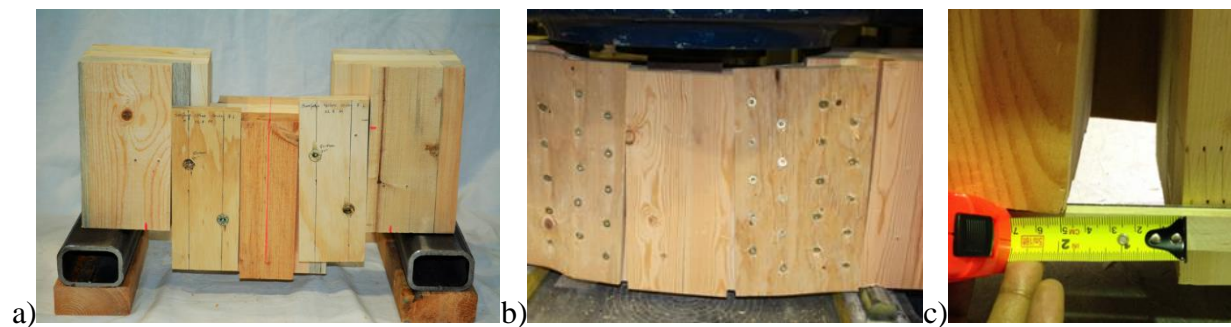
Joints	STS/SP	SP#	F_{max} [kN]	F_Y [kN]	$d_{F,max}$ [mm]	$d_{F,Y}$ [mm]	μ [-]	k [kN/mm]
Spline_Shear	8	1	6.9	4.5	52.8	7.0	7.5	0.5
	10	2	4.0	2.8	41.8	4.7	7.4	0.6
Lap_Shear	8	1	6.7	4.3	25.8	4.4	6.6	1.0
	8	2	5.2	3.5	24.0	4.0	6.0	0.7
Lap_Withdr.	8	2	5.3	4.9	2.3	0.7	3.0	3.8
	12	1	7.2	6.3	5.5	2.0	2.9	4.8
Butt_Withdr.	8	1	7.8	6.6	6.5	1.2	5.4	5.3
	8	2	6.1	5.7	2.5	0.6	3.7	4.8

Table 4.21: ISP-2SP comparison (5-ply)

Joints	STS/SP	SP#	F_{max} [kN]	F_Y [kN]	$d_{F,max}$ [mm]	$d_{F,Y}$ [mm]	μ [-]	k [kN/mm]
Spline_Shear	8	1	7.3	4.8	46.0	6.1	7.8	0.7
	10	2	6.2	4.1	50.7	8.0	6.4	0.4
Lap_Shear	8	1	11.0	6.9	64.3	5.6	12.6	0.8
	8	1	7.4	4.9	49.3	4.1	12.0	1.3
Lap_Withdr.	6	2	10.3	9.7	2.0	1.1	1.8	310.2

4.4.7 Failure modes and capacities

Failure modes are discussed based on joints. In the spline joints, the middle panel of the specimen exhibited large displacements (Figure 4.36a). Though the specimen showed proper shear behaviour, some bending behavior (especially in small sized specimen with two shear planes) along with opening up in the bottom of the specimen was observed after the ultimate load (Figure 4.36b and c). Screw yielding (Figure 4.36d), screw head-pull through inside the plywood (Figure 4.36e and Figure 4.36f) were the major failure mode. To make room for the screw yielding, embedment failure in the plywood took place. Cracking noise and correspondingly many discontinuities in the load-displacement curves were observed. It might be because of small cracks; however, no significant load drop was observed. After the cracking noise screw head snapped through the plywood making some chunk of the spline came off followed by the separation of the CLT panels (Figure 4.36g). No screw breaking was observed.



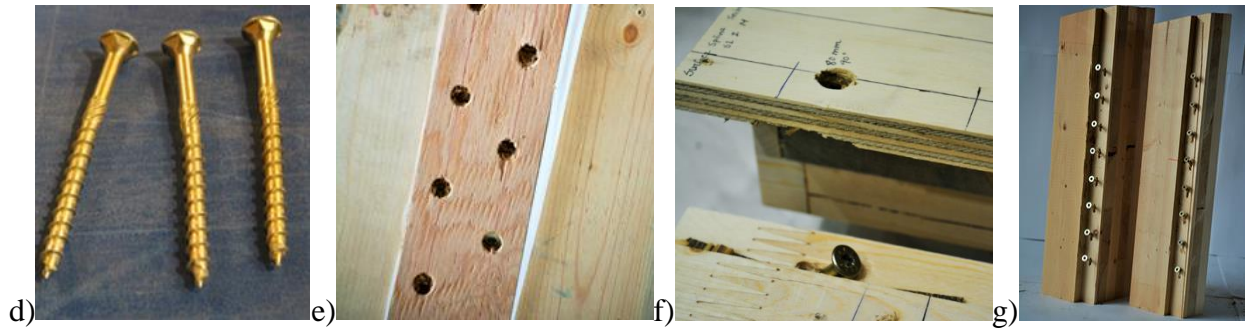


Figure 4.36: Failure modes in spline joints: a) pure shear, b) bending, c) gap opening, d) STS yielding, e) screw head sinking, f) screw heading snapping through plywood, and g) separation of CLT panels

For spline joints with STS loaded in shear, the middle panel of the specimen went through large displacement showing proper shear with a little bit of out of plane during pulling cycles (Figure 4.37a). In this joint initially plastic hinge was formed at 45° demonstrating significant screw yielding and plywood was crushed to make extra room for the distorted screws. (Figure 4.37b). After reaching the ultimate load, with repeated load cycles, 70-100% screws were broken (Figure 4.37c) in the plastic hinge point at the middle of the screw in two parts resulting in two CLT side panels and the plywood separation (Figure 4.37d). In the static tests for spline joints, the screws only yielded and deformed. The failure could be caused by low-cycle steel fatigue.

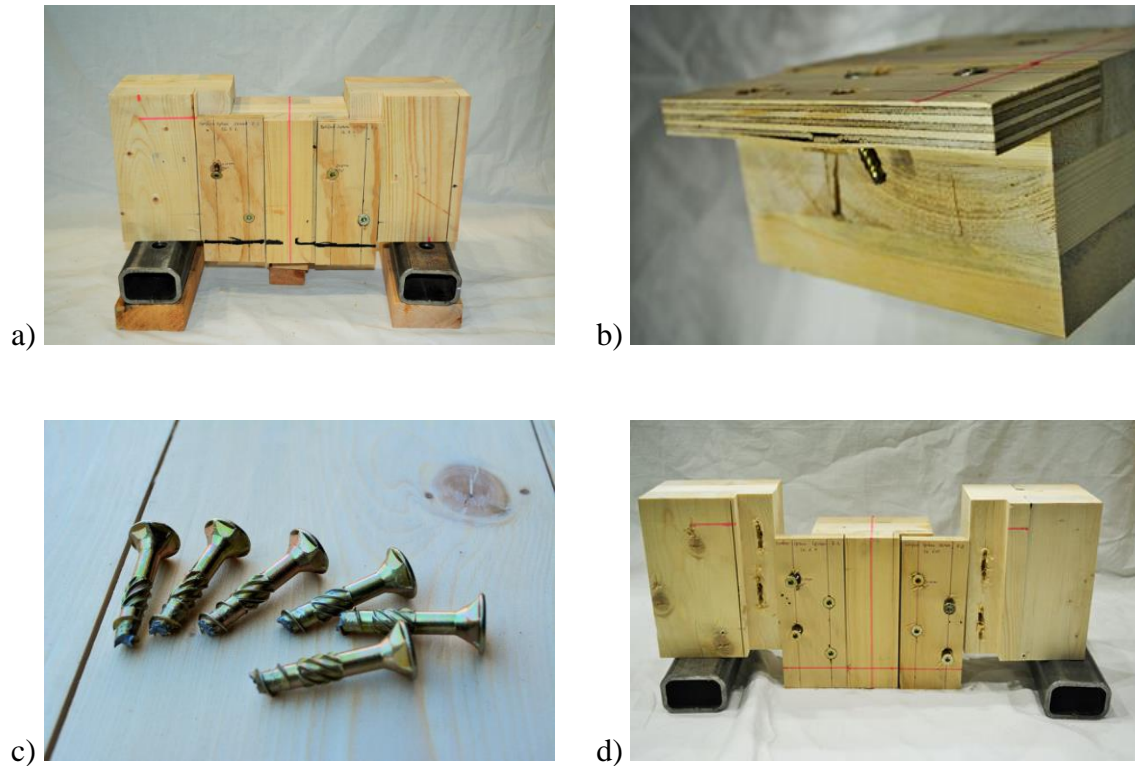


Figure 4.37: Failure modes in spline joints from cyclic tests: a) pure shear, b) separation of CLT panel and plywood, c) plastic hinge at 45° of STS and plywood crushing, and d) STS breaking

Figure 4.38 illustrates the failure modes observed in all three lap joints under monotonic tests. All CLT assemblies where the STS were loaded in shear experienced very large displacements before failure as illustrated in Figure 4.35a. As shown in Figure 4.35c, the failure mode was a combination of wood crushing and screw yielding. No screw withdrawal was seen from the outside of the panel (c.f. Figure 4.38d). No distinct moment of failure was observed during testing and the load-deformation curves (Figure 4.18, Figure 4.21, Figure 4.22, Figure 4.23, and Figure 4.25) show a continuous decrease in stiffness at load levels between 2 kN and 4 kN per screw. The CLT panel itself behaved as a rigid body with no damage outside the connection interface.

The Canadian product approval requires the factored lateral resistance to be calculated in accordance with the CSA O86 (2016) lag screw provisions. For the smaller embedment length of

30 mm (3-ply) and 65 mm (5-ply) in the second CLT panel, and the given CLT and STS material properties, an un-factored unit lateral yielding resistance of 1.9 kN/screw (mode f of the yield model) and 2.9 kN/screw (mode g) was determined. The experimental results indicated that these design provisions are reasonably conservative. Of more interest, however, is that the Johansen Yield equations predicted mode f (crushing of the wood side members) to be the governing failure mode for 3-ply, with mode g (yielding and bending of the screw at the connection interface) only slightly higher with 2.9 kN/screw. These predictions were confirmed by the experiments.

All CLT assemblies where the STS were loaded in withdrawal experienced very small displacements before failure as illustrated in Figure 4.35b. The failure mode was screw withdrawal, with the screws in tension being pulled in and the screws in compression were pushed out of the CLT specimens, as shown in Figure 4.38e. For the STS inserted at an angle of 45° to the grain, the applied load was predominantly carried by the withdrawal resistance; this mechanism leads to much stiffer joints and a distinct and brittle failure with little ductility (c.f. Figure 4.18, Figure 4.21, Figure 4.22, Figure 4.23, and Figure 4.25). Using the Canadian product approval (CCMC 13677-R, 2013) equation a factored withdrawal resistance of 4.5 kN (3-ply) and 6.8 kN (5-ply) was obtained for 60 mm and 90 mm of thread penetration which is reasonably conservative given the average test results and well below the factored tensile resistance (15 kN/20 mm of thread penetration) of the screws. These failure mode predictions were confirmed by the experiments.

For the test series that combined STS that act in shear with STS that act in withdrawal, a more complex failure behavior was observed. The high initial stiffness was supplied to the connection by the screws loaded in withdrawal that were activated immediately. As a first connection failure mode, the STS loaded in withdrawal started to fail at small displacements around 2-3 mm by being pulled in or pushed out of their initial position as shown in Figure 4.38f. The connection assembly,

however, maintained its load-carrying capacity with increasing displacements. Subsequently, the force was carried by the STS loaded in shear which then started to crush the wood and yield at the interface. These ductile failure modes resulted in the connection being able to maintain its load carrying capacity while undergoing large deformations.



Figure 4.38: Failure modes in lap joints from monotonic tests: a) large displacement of assemblies with STS loaded in shear, b) small displacements of assemblies with STS loaded in withdrawal, c) screw yielding, d) STS loaded in shear, e) STS loaded in withdrawal, and f) assemblies with STS loaded in shear and STS loaded in withdrawal

Figure 4.39 illustrates the failure modes observed in the lap joints under reversed cyclic tests. In assemblies with STS loaded in shear, failure was initiated by screw yielding, and the joints experienced large displacement before failing through separation of the CLT panels. At that stage, some screws were completely sheared off due to low-cycle fatigue (Figure 4.39a). For assemblies with STS loaded in withdrawal, head pull in and head push out failures were observed (Figure 4.39b). Since the specimens were not completely restrained in the out-of-plane direction, some out-of-plane displacement was observed (c.f. Figure 4.39c). This displacement was not measured during or after testing.

The failure mode observed in half-lap joints with STS loaded in shear combined with STS loaded in withdrawal was, similarly to the monotonic tests, first withdrawal of the stiff screws placed at 45° and then wood crushing and yielding of the shear screws placed at 90°. Since loading continued with larger displacement amplitude after the load-carrying capacity dropped, the two CLT panels were separated and some screws broke (Figure 4.39d). The STS loaded in shear experienced yielding (Figure 4.39e) and crushed the wood in embedment (Figure 4.39f), and facilitated increased ductility when compared to the test series with screws loaded in withdrawal only.

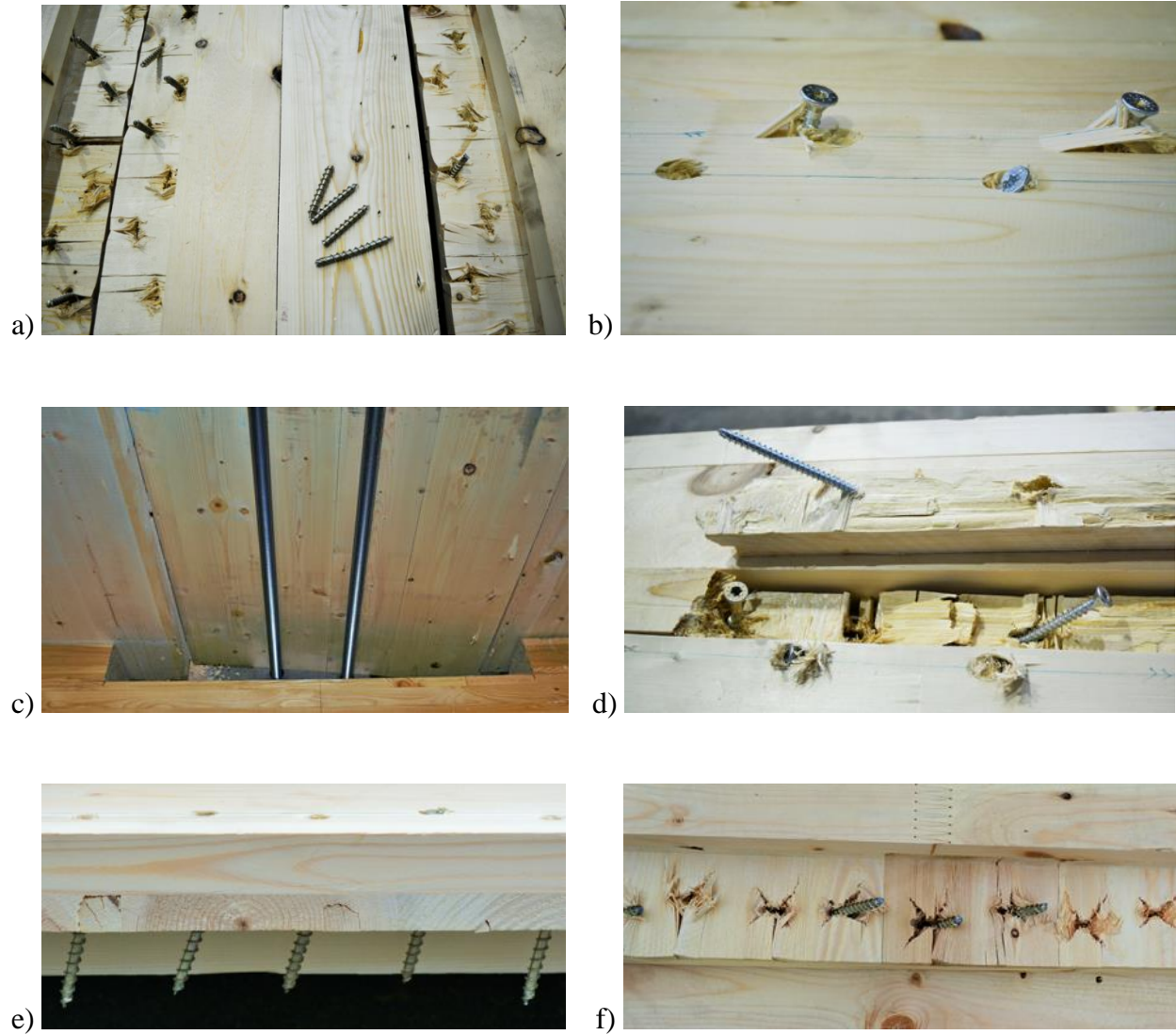


Figure 4.39: Failure modes in lap joints from cyclic tests: a) STS breaking, b) STS head push-out, c) assembly out-of-plane rotation, d) separation of CLT panel, e) STS yielding, and f) STS embedment

The failure mechanism observed in butt joints are illustrated in Figure 4.40. More specifically, Figure 4.40a, c, and d show that butt joints with screws loaded in shear experienced plastic hinges in the screws during monotonic and cyclic tests. Under monotonic tests, it was observed that panels started rotating around the plastic hinge points making the connection experiencing in-plane and out-of-plane rotation for large deformation (slip major of 30 mm) (Figure 4.40a). The connection exhibited ductile behavior, without screw breaking and wood failure and no screw withdrawal was seen from the outside of the panel (c.f. Figure 4.39 b). Under cyclic loading, screws broke in correspondence of formed plastic hinges, which resulted in panel separations accompanied by wood crushing (c.f. Figure 4.40c and d).

Butt joints with screws loaded in withdrawal in monotonic tests, a pure shear of the mid panel with no horizontal displacements and out-of-plane rotation was observed (Figure 4.40e) also for large deformation to the ultimate load. No screw breaking and wood failure was observed during the test (Figure 4.40f). For cyclic tests (Figure 4.40g), the achievement of large deformations was followed by the local crushing of CLT due to screw withdrawal. The failure mode was screw withdrawal, with the screws in tension being pulled in and the screws in compression were pushed out of the CLT specimens, as shown in Figure 4.40h.

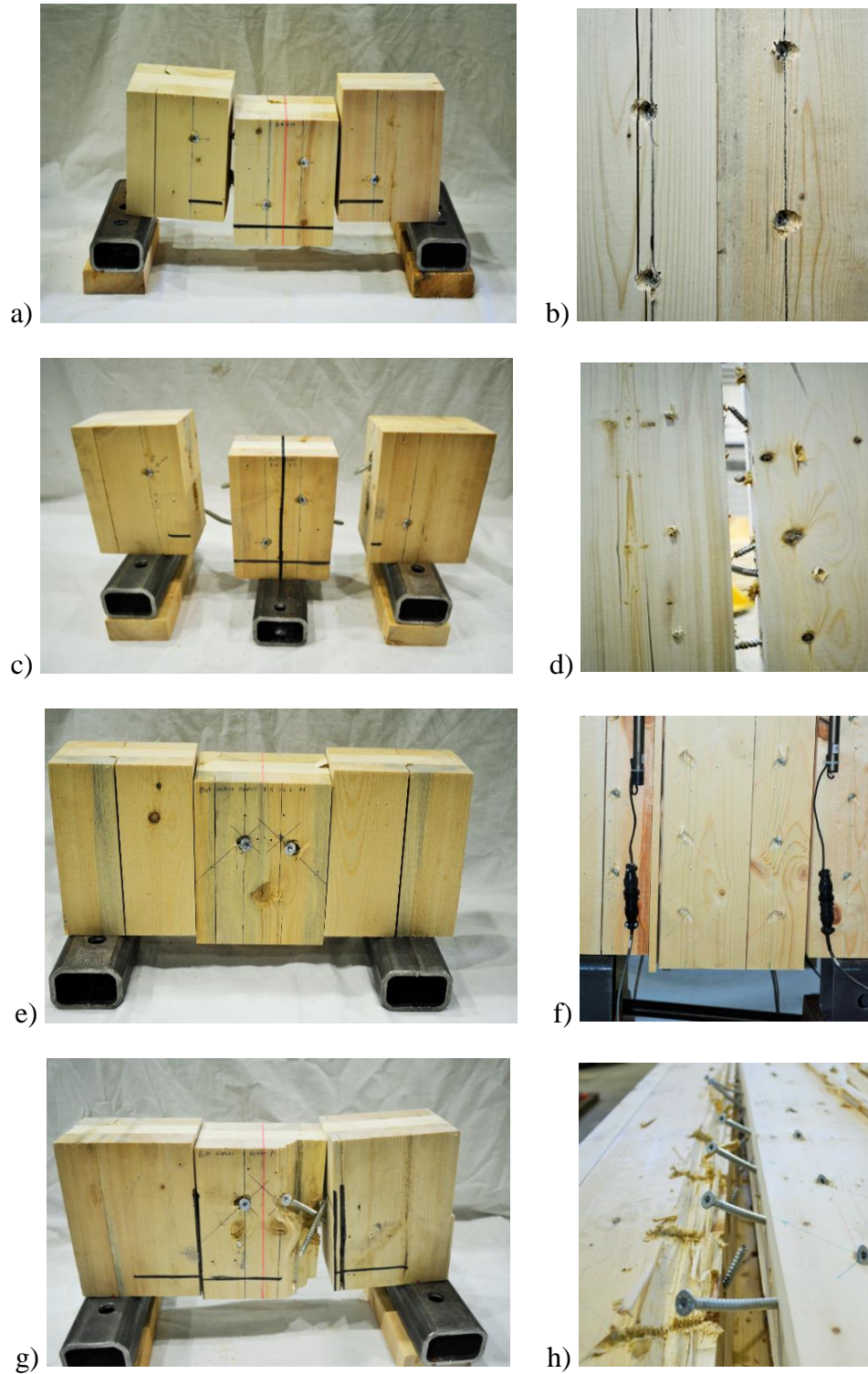


Figure 4.40: Failure modes in butt joints from monotonic and cyclic tests; a) panel rotation around plastic hinge, b) STS loaded in shear, c) separation of CLT panel, d) STS breaking, e) pure shear with rotation, f) no screw breaking or wood crushing, g) wood crushing, and h) STS loaded in withdrawal

4.4.8 Comparison of screw actions

This comparison was made for lap and butt joints with different screw actions: shear, withdrawal, and shear and withdrawal. Table 4.13 to Table 4.19 summarized the main connection properties for lap joints in different sized specimens. Joints with STS loaded in shear exhibited low elastic stiffness ($k < 1$ kN/mm), high ($\mu > 6$ for static) to moderate ($\mu > 4$ for cyclic) ductility and reached very large displacements, $d_u > 30$ mm (> 20 mm for cyclic) before failing. Stiffer connections can be achieved by activating the withdrawal resistance of STS, $k > 6$ kN/mm ($k > 3.5$ kN/mm for cyclic). These connection configurations, however, exhibited low ductility ($\mu < 2.2$) and failed at deformations less than 6 mm. The assemblies containing STS loaded in shear and STS loaded in withdrawal reached similar stiffness values like the assemblies with STS in withdrawal, $k > 6$ kN/mm ($k > 3.5$ kN/mm for cyclic).

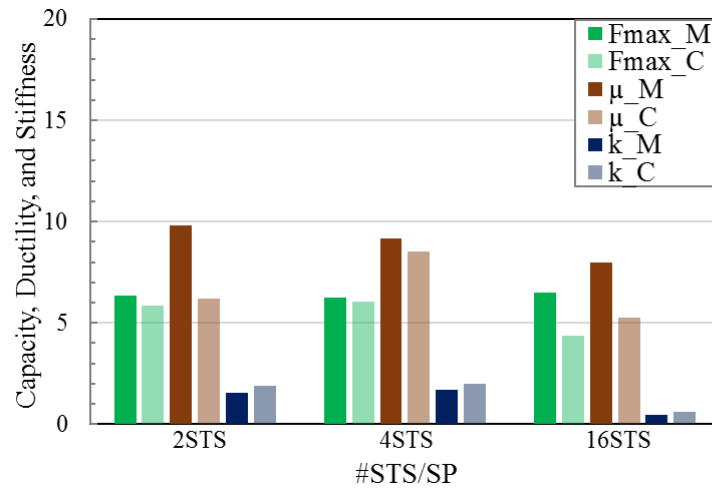
Furthermore, the assemblies containing STS loaded in shear and STS loaded in withdrawal also reached high ductility ($\mu > 10$ for both static and cyclic) and similar large deformations before failing ($d > 20$ mm, 13 mm for 5-ply, and 10 mm for cyclic) like the connections with STS in shear. Therefore, connections with screws loaded in withdrawal or withdrawal and shear were on average 5 times stiffer than connections with screws loaded in shear only. According to the classification as proposed by Smith et al. [45], joints with STS loaded in shear exhibited high ductility, joints with STS loaded in withdrawal can be classified as low ductility, and the assemblies with screws in combined action are high ductile. It is important, however, not to evaluate ductility independent from the deformation capacity. Joints with STS loaded in shear were able to undergo large deformation while joints with STS in withdrawal failed in very small deformation.

In terms of load-carrying capacity and yield load, the differences between the different screw assemblies were less pronounced. Layouts where the screws acted in withdrawal reached on average 7% higher load-carrying capacity and 13% higher yield load than layouts where the screws acted in shear. Layouts combining screws in shear and screws in withdrawal reached on average 13% lower load-carrying capacity and 10% lower yield load than layouts where the screws acted in shear only, demonstrating that both sets of fasteners contribute to the load-carrying mechanism.

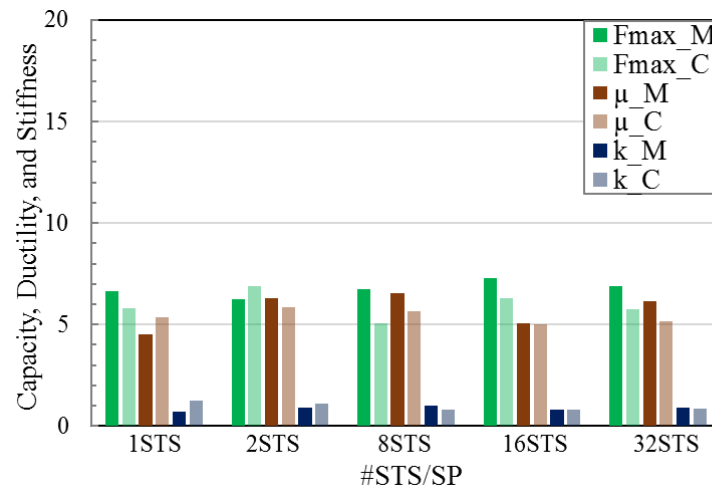
Table 4.13 to Table 4.19 shows the main connection properties for butt joints in different sized specimens. Similar to lap joints all butt joints with STS in shear achieved moderate ductility ($\mu > 4$), however very low stiffness ($k < 0.5$ kN/mm). Stiffer but low ductile connections can be achieved by activating the withdrawal resistance of STS ($k > 6$ kN/mm, $\mu < 4$). The series with STS in withdrawal had on average 10% higher capacity. Butt withdrawal joints are low ductile compared to the brittle lap withdrawal joints.

4.4.9 Comparison of different loading protocols

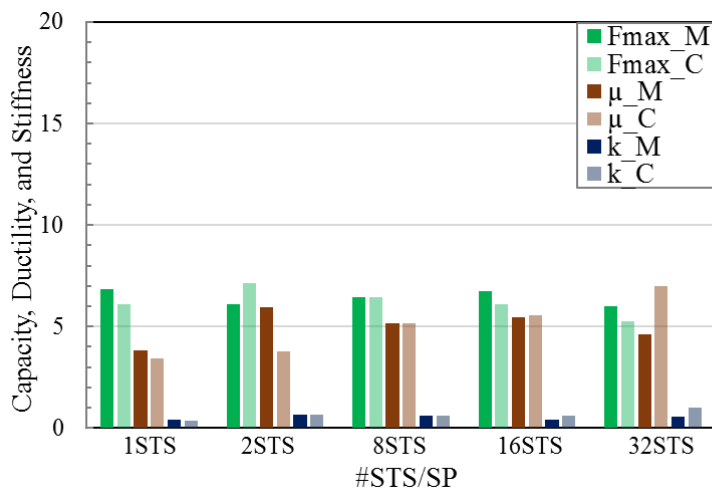
A comparison between monotonic and cyclic tests results for those series with the same screw layout are shown in Figure 4.41. Joints under cyclic loading reached consistently lower load-carrying capacity (on average 10-20%), lower yield load (on average 10-20%), smaller maximum deformation (on average 50%), lower ductility (on average 50%). However, the assemblies tested under cyclic loading were stiffer (on average 25%) with few exceptions for all parameters. The higher stiffness might be the reason of test setup in order to facilitated pulling cycles. The reduction in performance needs to be properly accounted for when designing CLT assemblies for seismic applications. A comparison between positive and negative envelopes in the cyclic curves were also made which are shown in Figure 4.42.



a)



b)



c)

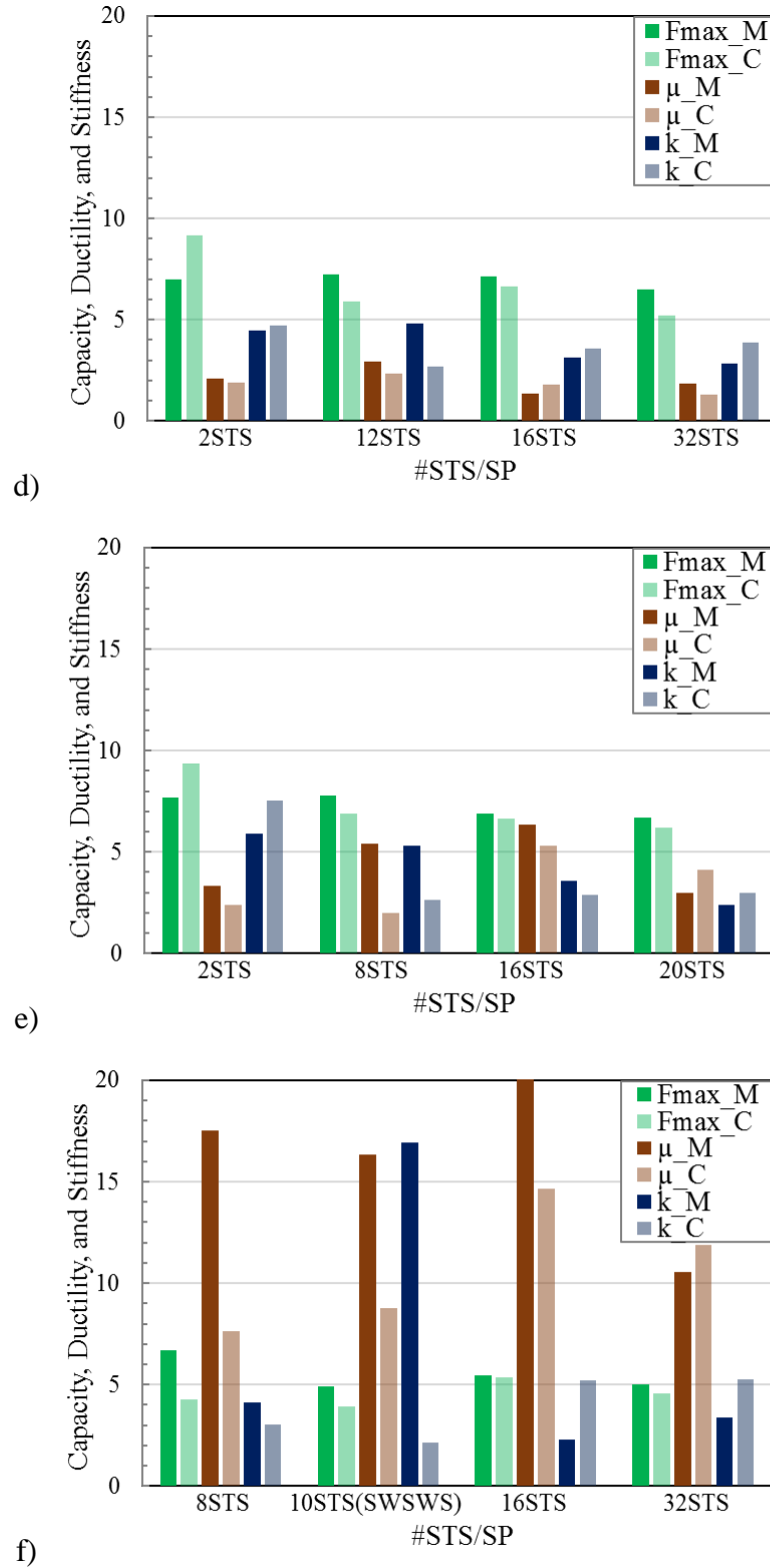
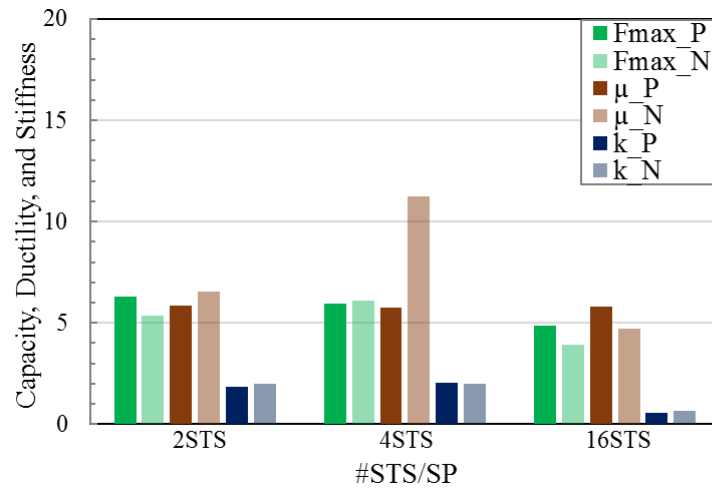
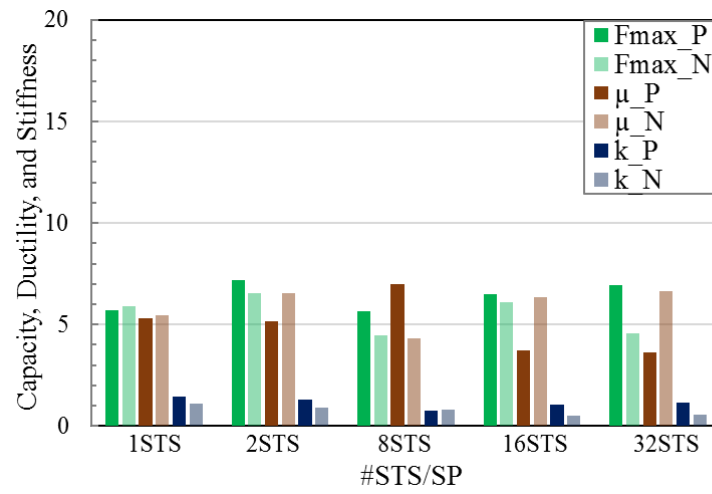


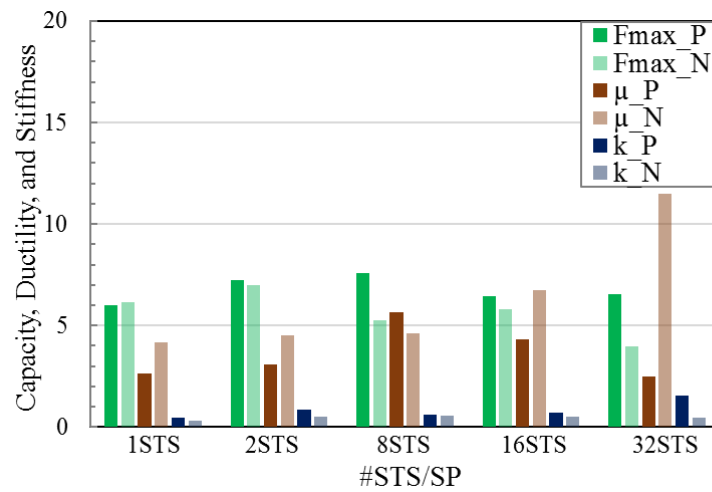
Figure 4.41: Comparison between quasi-static monotonic and cyclic loading: a) Spline_Shear; b) Lap_Shear; c) Butt_Shear; d) Lap-Withdr; e) Butt-Withdr; and f) Lap_Shear&Withdr



a)



b)



c)

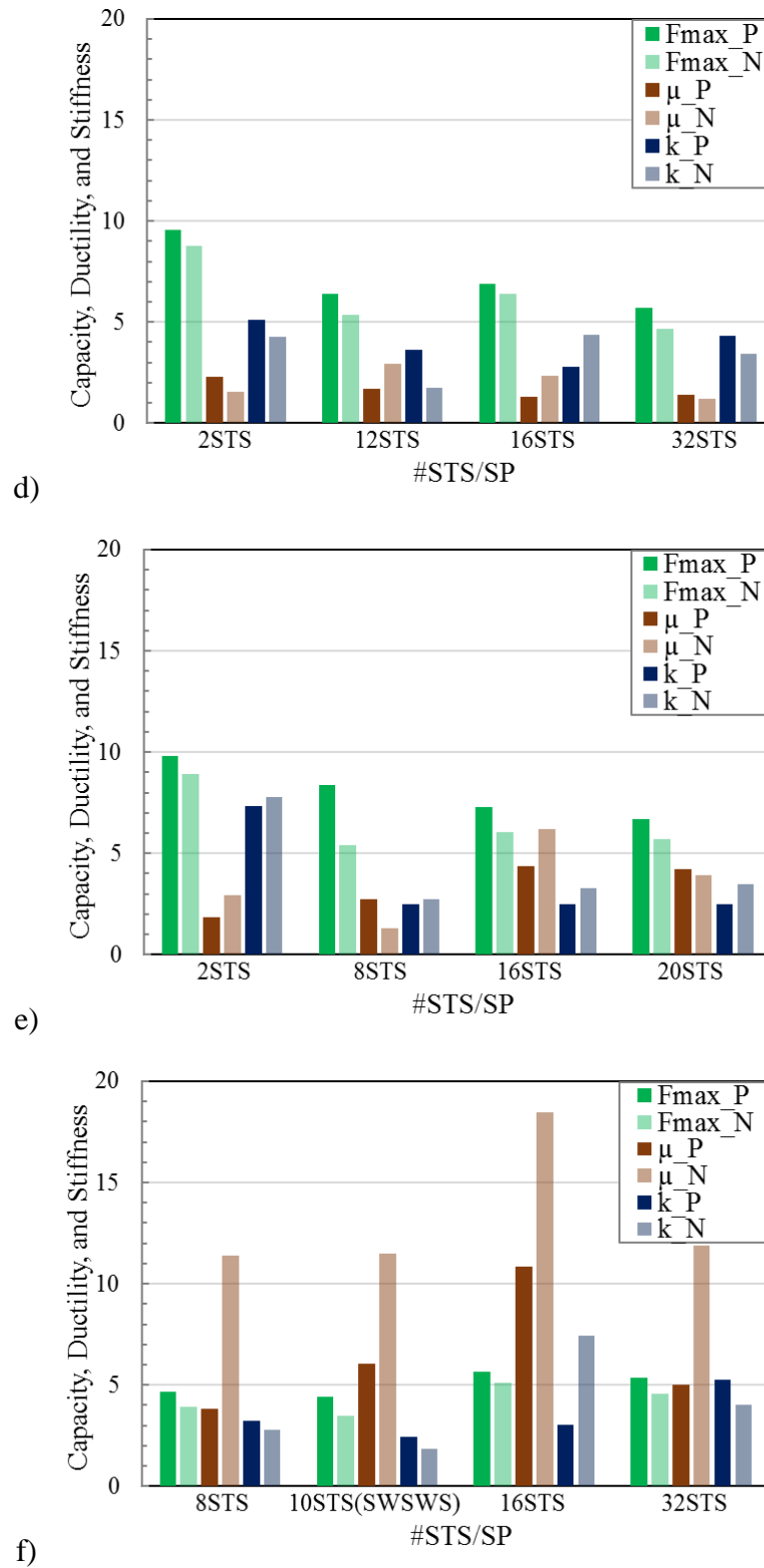


Figure 4.42: Comparison between positive and negative envelopes in cyclic loading: a) Spline_Shear; b) Lap_Shear; c) Butt_Shear; d) Lap-Withdr; e) Butt-Withdr; and f) Lap_Shear&Withdr

The comparison in Figure 4.42 showed that assemblies consistently reached on average 17% higher capacity in their positive envelopes (where loading was initiated) compared to their negative envelopes (this increase varied from 21% for Butt_Shear to 13% for Lap_Withdr). A possible explanation is that the down strokes partially withdrew half of the screws, and thus weakened them before they were needed to carry a compression load in the upstrokes. And this caused reduced capacity in the negative envelope in each following cycle. No specific trend was found for ductility and stiffness.

4.4.10 Impact of friction

The impact of friction was evaluated in small sized specimen with one shear plane using 8 STS per shear plane with and without plastic membrane in five different joints: Spline_Shear, Lap_Shear, Lap_Withdr, Butt_Withdr, and Lap_Shear&Withdr. Specimen with plastic membrane was denoted as no friction (NF) in the graphs. From the results illustrated in the graphs of Figure 4.43, it can be seen that there is not much effect of friction in all the joints except lap joint in shear where joints with no friction showed 1.1 times higher capacity with comparable stiffness and ductility. For the connections (i.e. Lap_Withdr. and Butt_Withdr.) with pairs of crossed STS loaded in a axial-lateral combination, their in-plane resistance, is the sum of a tension-shear component and a compression-shear component. For the cross screws, the friction components get canceled out which might be a reason for not having any effect in any of those joints with crossed screws. Similarly, the in-plane load-carrying capacity of laterally loaded single screws i.e. Lap_Shear and Spline_Shear joint might be affected by the friction effect due to not having that friction component cancelling out. However, Lap-Shear and Spline_Shear both should have some friction effect according to this assumption. Only Lap_Shear joint was found to be having effect of friction. More tests need to be done in order to verify this.

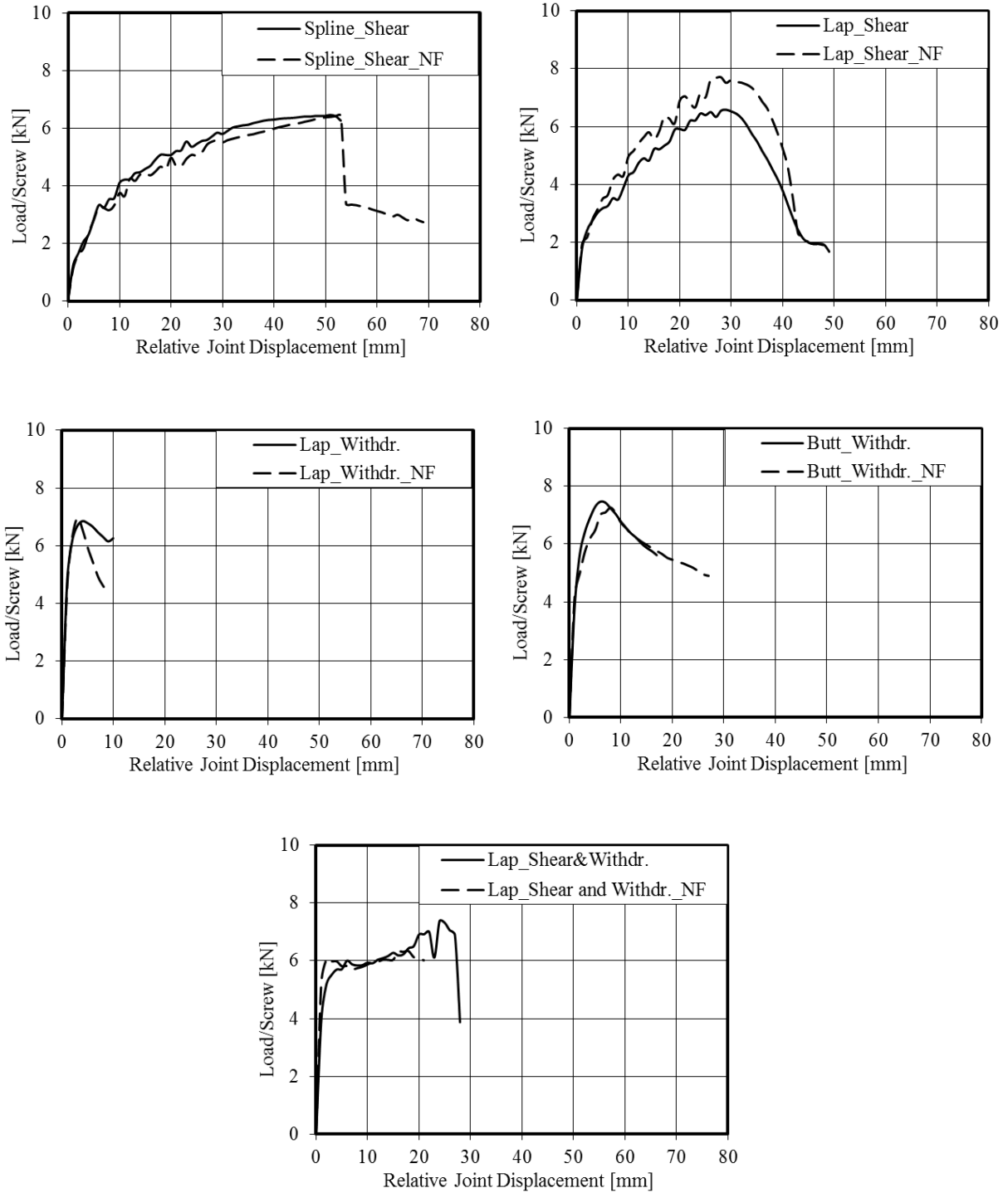


Figure 4.43: Test series that included friction and non-friction (3-ply_1SP): a) Spline_Shear, b) Lap_Shear, c) Lap_Withdr., d) Butt_Withdr., and e) Lap_Shear&Withdr

4.4.11 Group effect

The average values for load-carrying capacity and stiffness per screw as a function of the number of screws as well as the ductility values of the CLT assemblies summarized in Table 4.13 to Table 4.19 and illustrated in the graphs of Figure 4.44. In these graphs, load values are reported per individual screw and the displacements are the averages of the two measurements from the back and the front of the specimen at each shear plane.

Investigating the results from the quasi-static monotonic tests, no group effect was observed for the joints where the screws acted in shear; however, for the joints where the screws acted in withdrawal, a reduction in capacity was observed which can be best described by the expression $n_{\text{eff}} = 0.9 \cdot n$. The reduction in capacity observed from the reversed cyclic tests showed a more pronounced group-effect which, independently from the type of screw action (shear and withdrawal) can be expressed as $n_{\text{eff}} = n^{0.9}$.

When evaluating the joint stiffness under quasi-static monotonic loading, no clear trend as a function of screws acting either in shear or in withdrawal was observed. Conservatively, the group effect could be described by the expression $n_{\text{eff}} = n^{0.8}$. However, a more severe reduction in stiffness (up to 70%) was observed for spline joints with the screws acting in shear. Even less consistent results were obtained from the reversed cyclic tests. While the group effect for the Lap joints can be expressed as $n_{\text{eff}} = n^{0.8}$, the butt joints with screws acting in withdrawal and the spline joints exhibited a much larger reduction and conversely the butt joints with screws acting in shear exhibited almost no reduction in stiffness as a function of the number of screws.

Joint ductility ranged between brittle (lap joints with STS acting in withdrawal), moderately ductile (butt joints with STS acting in shear or withdrawal) and ductile (lap and spline joints with STS

acting in shear). The group-effect on ductility for all the joints can be reasonably expressed with the equation $n_{\text{eff}} = n^{0.9}$ for the quasi-static as well as for the reversed cyclic loading case.

The test results confirmed the established findings that CLT shear connections with STS exhibit high stiffness and low ductility when the screws are primarily loaded in withdrawal. Ductile joints with low stiffness, however, were achieved when the screws were loaded primarily in shear. A relatively low CoV for capacities (7% on average and no larger than 15%) was obtained, with a clear trend towards reduced variability between test specimens with a larger number of screws. This phenomenon can be easily explained by the averaging effect of having multiple fasteners in one connection and it also justifies the lower number of replicates used for the test series with a larger number of screws.

The comparison between the experimentally obtained group effect $n_{\text{eff}} = 0.9 \cdot n$ and the existing design guidance for lag-screws in CSA-O86 (Figure 1) clearly demonstrates that the CSA-O86 provisions are far too conservative for connections with STS screws in CLT. Moreover, the standard only provides group effect factors for a maximum of 12 screws in one row, while the proposed reduction relationship is experimentally validated for up to 32 STS in one row. Furthermore, it is hypothesized that the observed relationships are valid for any number of fasteners; this hypothesis should be experimentally tested in future research.

Another noteworthy finding is that the capacity of CLT shear connections under reversed cyclic loading was on average 10-20% lower than the capacity under monotonic loading, independently for joint type, with small differences depending on the number of screws. Furthermore, the group effect for capacity was more pronounced under reversed cyclic loading. Since most manufactures

only provide information on the monotonic performance of their screws, these findings should be considered for seismic design.

Previous research discussed in Section 2.4.5 showed that the established design models for stiffness are not fully adequate, the results point towards the existence of a significant group effect for stiffness of STS connections in CLT. The obtained values showed a relatively high scatter with an average CoV of 27% for all test series. Therefore, the proposed expression $n_{\text{eff}} = n^{0.8}$ to describe the group effect on stiffness should be further evaluated and confirmed by both experimental and analytical investigations.

Comparing the shear connection stiffness as a function of loading protocol, a clear dependency on the screw action was observed: on average 19% larger values were obtained under reversed cyclic loading for the joints where the STS were loaded in shear, while a 9% reduction was observed for those joint types where the STS acted in withdrawal. Although the relatively high variation within and between test series does give reason to caution, it seems safe to state that there is no group effect for stiffness for STS joints under cyclic loading loaded in shear, but stiffness reduction was observed for the STS joints loaded in withdrawal.

The effect of the number of STS on joint ductility can be expressed by the equation $n_{\text{eff}} = n^{0.9}$ for both monotonic and reversed cyclic loading. As observed in previous testing [14], the ductility decreased under cyclic loading, herein on average by 15%. This reduction was found to be a function of the screw action: the reduction in case of ductile joints was only 10% on average, while the ductility of the brittle joints was reduced by an average of 25%. The observed variability within test series, however, was relatively high (29%); therefore, similar to the conclusions for the stiffness, these test results will require further experimental validation.

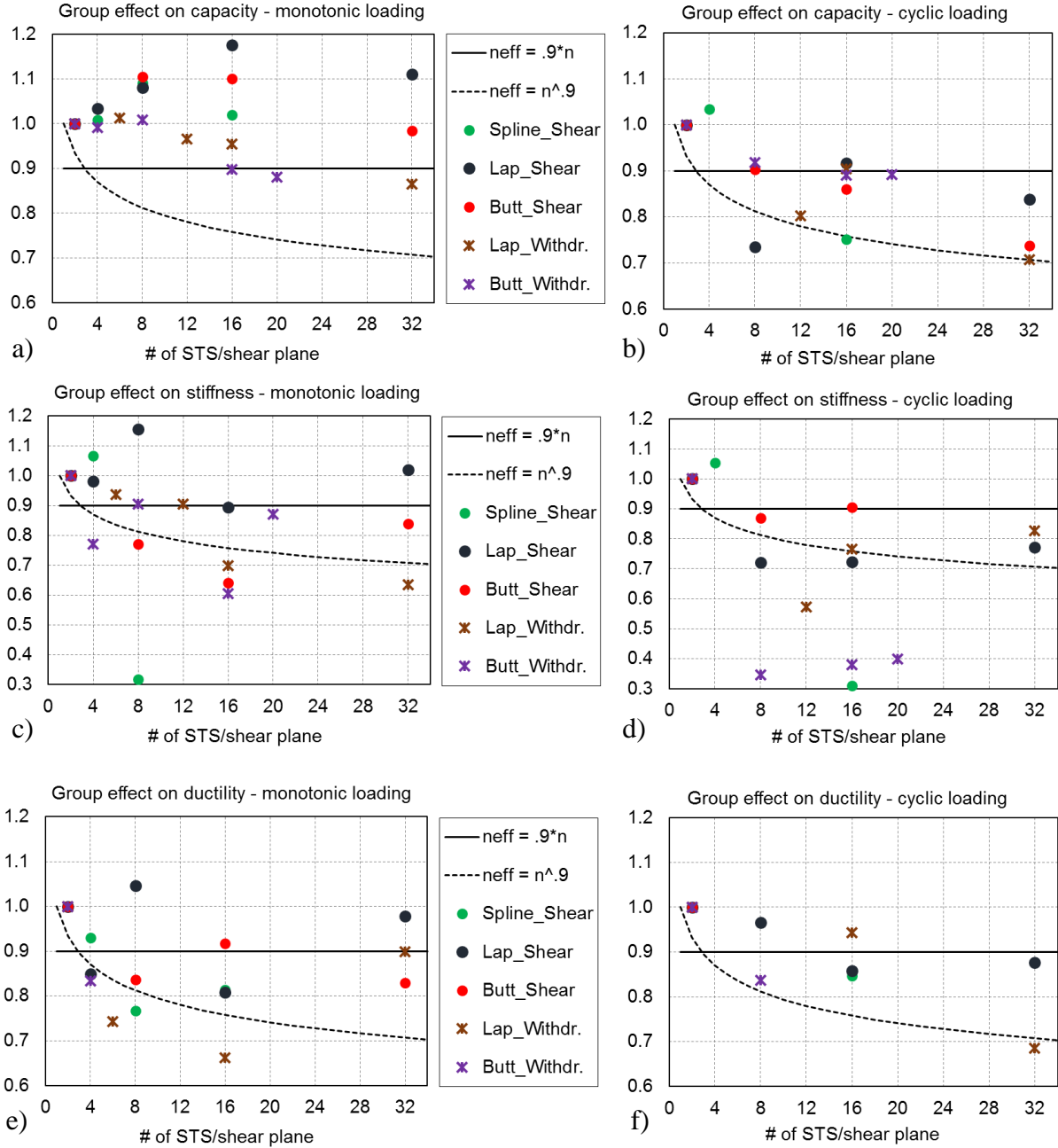


Figure 4.44: Group-effect on: capacity a) monotonic, and b) cyclic loading; stiffness c) monotonic, and d) cyclic loading; ductility e) monotonic, and f) cyclic loading

Chapter 5: Conclusion

5.1 Summary

In the first part of this research, withdrawal tests of Self-tapping screws (STS) in Canadian softwood Cross-laminated Timber (CLT) were conducted since the Canadian product approval for these screws (CCMC 13677-R, 2012) is limited to visually graded lumber, glued-laminated timber and structural composite lumber produced from Canadian wood species. A total of 180 withdrawal tests on STS installed in CLT was performed varying three different parameters: screw diameter, penetration depth, and angle of screw axis to CLT grain. The results showed that the CCMC 13677-R (2012) equation to predict the withdrawal resistance of STS can be safely applied to CLT made of Canadian softwood lumber.

In the second and main part of this research, the performance of shear joints in 3-ply and 5-ply CLT panel assemblies connected with STS was investigated. Different traditional joint types (surface spline with STS in shear and half-lap joints with STS in either shear or withdrawal) along with two innovative solutions were evaluated. The first novel assembly used STS with double inclination of fasteners (butt joints) and the second a combination of STS acting in withdrawal with STS acting in shear.

A total of 60 quasi-static monotonic and 48 reversed cyclic mini sized test, 60 small sized specimen with 2 shear planes under quasi-static monotonic, 141 small sized specimen with one shear plane under quasi-static monotonic, and 21 under reversed cyclic, 5 medium sized specimen under quasi-static monotonic and 15 under reversed cyclic, and 10 full sized specimen under quasi-static monotonic and 12 under reversed cyclic loading were conducted.

The data obtained from this study can be used by engineers to specify connection assemblies for lateral load resisting systems, specifically shear walls and floor diaphragms of CLT structures. The findings will be shared with designers and code officials in an effort to introduce design values for STS in the next edition of the Canadian Standard for Engineering Design in Wood.

5.2 Withdrawal tests

The main result from the withdrawal tests is that the CCMC 13677-R (2012) equation can safely be applied to predict the withdrawal resistance of STS in CLT made of Canadian softwood lumber. The ratios between the test results and the design values indicate that design values obtained using the approval are conservative in CLT. Further results were:

1. Failure in all tests was brittle with ductility ratios of smaller than 2 for all series. The variability of resistance within the individual test series was on average 13.5%.
2. Resistance was proportional to screw embedment l_{ef} with $12d$ embedment leading to approx. 50% larger resistance than $8d$ and therefore almost exactly the expected increase.
3. Resistance was proportional to screw diameter d with 10 mm screws leading to approx. 46% larger resistance than 8mm screws. The expected difference, however, was only 15%. Based on the small number of replicates n , no explanation can be offered.
4. No conclusive relation between screw angle and resistance was found. On average, an inclination of 45^0 to the top CLT layer did not decrease resistance when compared to an inclination of 90^0 to the top CLT layer. Further research is required to validate this finding.

5.3 CLT-STs shear connections

5.3.1 Overview

Several key findings were obtained from these tests:

1. The test set-up using specimens with one shear plane proved to be superior in determining the structural performance of the connections in quasi-static monotonic tests. Test specimens exhibiting two shear planes were influenced by out of plane bending of the assemblies. Both capacity and ductility obtained from tests on specimens with one shear plane were higher.
2. In the reversed cyclic tests, however, the inclined set-up with one shear plane created a tension component perpendicular to the shear plane which affected the results, specifically lower capacity and ductility in the negative envelopes. Future research needs to address this issue.
3. The novel layout combining STS loaded in shear with STS loaded in withdrawal combines high capacity and high stiffness with high ductility.
4. The tests series investigating the effect of friction demonstrated that the friction activated between the CLT panels does not affect the structural performance of connection.
5. The reversed cyclic tests confirmed the differences in terms of stiffness and ductility depending on the screw layout as determined in the quasi-static monotonic tests.
6. The performance of STS shear connections reversed cyclic loading is comparable to that of these connections under quasi-static loading; however, all performance values, are reduced by between 11% (load-carrying capacity) and 40% (stiffness). This finding demonstrates the

necessity to provide designers and engineers with data of connection performance under cyclic loading for reliable seismic performance.

5.3.2 Different screw layouts

1. Using STS in shear leads to ductile connections ($\mu > 4$) that can reach large displacements (> 30 mm) before failing. Assemblies with STS loaded in shear are appropriate for application where connection ductility and deformation capacity are required, e.g. for the energy dissipative connections of CLT structures.
2. Using STS in withdrawal leads to significantly stiffer joints (on average four-fold increase) compared to using STS in shear. These joints, however, are brittle and fail at very small displacements (< 2 mm) and are not suited as energy-dissipative connection for seismic applications.
3. The combination of STS in withdrawal and shear allows for joints that exhibit both high stiffness and high ductility. In fact, stiffness of such joints was very similar to the stiffness of joints using STS in withdrawal only, and ductility of these joints was similar to that of joints using STS only in shear.

5.3.3 Group effect

Based on the tests, the following conclusions can be drawn:

1. The expression $n_{\text{eff}} = 0.9 \cdot n$ is sufficient to describe the reduction in capacity for all joints under quasi-static monotonic loading with STS acting in shear or withdrawal. This approach is significantly less conservative than the existing Canadian design guidance for lag-screws.

2. The capacity (strength) obtained under reversed cyclic loading was on average 11% lower than that obtained from monotonic loading. The expression $n_{\text{eff}} = n^{0.9}$ can be used to account for the group effect of STS joints under cyclic loading.
3. The effect of number of screws on the joint stiffness can conservatively be described by the expression $n_{\text{eff}} = n^{0.8}$. High variation within test series and large differences between test series require further investigation.
4. Stiffness under reversed cyclic loading was on average 9% lower than under monotonic loading for joints with STS acting in withdrawal, while it was not reduced for STS in shear.
5. The group-effect on ductility for all the joints can be expressed with the equation $n_{\text{eff}} = n^{0.9}$ for both, monotonic and reversed cyclic loading cases.

These findings will be presented to the Technical Committee of CSA O86 for potential inclusion into the next edition of the Canadian Standard for Engineering Design in Wood.

5.4 Future research

5.4.1 Experimental testing

In this research, only 3-ply and 5-ply CLT from one manufacturer using homogeneous layups of Canadian softwood lumber was tested. There are multiple manufacturers in North America and also layups with combinations of species/grades to optimize the properties and achieve economic efficiency. Future testing should validate the findings presented on other CLT products and layups with particular interest in thicker panels such as 7-ply or even 9-ply for higher shear demands.

In this research, only 8mm STS from one manufacturer were used. Future testing should validate the findings using other diameter of screws, particularly in the common range from 6mm to 10 mm, and for the findings on the group effect of screws.

This research focused on panel-to panel connections with both panels in the same plane. Future work should be extended toward testing panels connected in different planes such as those used in wall-to-floor connections.

5.4.2 Numerical modelling

This research was predominantly of experimental nature and provided valuable input data for design. Commercial finite element software package could be used to develop micro-scale component models of the CLT STS shear connections. The connections between the panels can be modelled using multiple linear and/or non-linear spring elements. These models can be calibrated using the experimental results and be used for parametric studies to optimize the screw layout for certain target performances in terms of strength, stiffness and/or ductility.

Such models would allow calibrating non-linear spring elements for macro-scale building models. Numerical models for both the component level and building system would be beneficial to understand the overall impact of connection properties on the performance of CLT shear walls and diaphragms, and ultimately on the performance of CLT buildings.

5.4.3 Extension to structural system level

This research focused on the performance of CLT panel-to-panel connections under quasi-static monotonic and reversed cyclic loading. The goal of these experiments was to determine the connections' strength, stiffness, and ductility. The provided data is an essential component for the safe

and reliable design of a structures lateral load resisting systems (LLRS), i.e. shear walls and diaphragms.

Future work should extend the scope of testing towards applying the shear connections in both experimental testing and numerical modelling of LLRS, and ultimately complete buildings. The currently available guidance for CLT buildings in Canada is limited to platform-type construction with very limits in CLT panel aspect ratios. Research is required on large-scale CLT panels to be used in balloon-type construction to fully take advantage of the large dimensions in which CLT can be manufactured. Such work can contribute towards providing more economic seismic force reduction factor, R_d , which accounts for the energy dissipation of the LLRS.

Finally, cost analyses needs to be completed with the connection specifications from fabrication to installation for CLT panel-to-panel shear connections after the design of the building.

Bibliography

- Kevarinmäki, A. (2002). Joints with Inclined Screws. In *Proceedings of CIB-W18 Timber Structures, Meeting 35* (Paper 35–7–3). September 16-19, 2002, Kyoto, Japan.
- Abukari, H. A., Cote, M., Rogers, C., Salenikovich, A. (2012). Withdrawal Resistance of Structural Screws in Canadian Glued Laminated Timber. In *Proceedings of World Conference on Timber Engineering, WCTE 2012*. July 15-19, 2012, Auckland, Newzealand.
- AFPA. (1997). National Design Specification for Wood Construction. Washington, D.C., USA
- Alter, L. (2015). World's Largest Cross-Laminated Timber Apartment Complex being built in Montreal. Green Architecture, Treehugger.
- ArchDaily. (2013). Earth Sciences Building / Perkins + Will.
- ArchDaily. (2015a). Fort McMurray International Airport / Office of Mcfarlane Biggar Architects + Designers Inc.
- ArchDaily. (2015b). Wood Innovation Design Centre / Michael Green Architecture.
- ASCE. (2016). Minimum Design Loads for Buildings and Other Structures. Reston, VA, USA.
- BCBC. (2009). Use of Wood in Mid-Rise Construction-Changes to Ontario Building Code. The Beck Group. Forest Products Planning & Consulting, Portland, OR, USA.
- BECK. (2018). Mass Timber Market Analysis, completed for: Council of Western State Foresters. The Beck Group. Forest Products Planning & Consulting, Portland, OR, USA.
- Bejtka, I. (2005). Verstärkung von Bauteilen aus Holz mit Vollgewindeschrauben. *Ph.D. Thesis*. Universität Karlsruhe, Germany.
- Bejtka, I., Blass, H. J. (2002). Joints with Inclined Screws. In *Proceedings of CIB-W18 Timber Structures, Meeting 35* (Paper 35–7–5). September 16-19, 2002, Kyoto, Japan.

- Bejtka, I., Blass, H. J. (2006). Self-Tapping-Screws as Reinforcement in Beam Supports. In *Proceedings of CIB-W18 Timber Structures, Meeting 39* (Paper 39–7–2). August 28-31, 2006, Florence, Italy.
- Bill 9 -2009: Wood First Act. 2009 Legislative Session: 1st Session, 39th Parliament. First Reading.
- Blass, H. J., Bejtka, I. (2004). Selbstbohrende Holzschrauben und ihre Anwendungsmöglichkeiten. In *ISBN 3-87104-136-X, Holzbau Kalender* (pp. 516-541). Bruderverlag Karlsruhe.
- Blass, H. J., Bejtka, I. (2001). Screws With Continuous Threads in Timber Connections. In *Joints in Timber Structures. Proceedings of the International RILEM Symposium* (pp. 193–202). Stuttgart, Germany.
- Blass, H. J., Fellmoser, P. (2004). Design of Solid Wood Panels with Cross Layers. In *Proceedings of the 8th World Conference on Timber Engineering, WCTE 2004* (pp. 543–548). June 14-17, 2004. Lahti, Finland.
- Brandner, R. (2016). Group Action of Axially-Loaded Screws in the Narrow Face of Cross Laminated Timber. In *Proceedings of World Conference on Timber Engineering, WCTE 2016*. August 22-25, 2016, Wien, Austria.
- Brandner, R., Bogensperger, T., Schickhofer, G. (2013). In plane Shear Strength of Cross Laminated Timber (CLT): Test Configuration, Quantification, and Influencing Parameters. In *Proceedings of CIB-W18 Timber Structures, Meeting 46* (Paper 46–12–2). August 26-29, 2013, Vancouver, Canada.
- Brandner, R., Flatscher, G., Ringhofer, A., Schickhofer, G., Thiel, A. (2016). Cross Laminated Timber (CLT): Overview and Development. *European Journal of Wood Products*, 74(3), 331–351.

- CCE. (2017). 12-storey wood condo, project Origine, in Quebec celebrates capping. *Canadian Consulting Engineer*.
- CCMC. (2018). *CCMC 13677-R SWG ASSY® VG Plus and SWG ASSY® 3.0 Self-Tapping Wood Screws*.
- Cramer, C. O. (1968). Load Distribution in Multiple-bolt Tension Joints. *Journal of the Structural Division, ASCE*, 94 (ST5, Proc. Paper 5939), 1101–1117.
- Crespell, P., Gagnon, S. (2010). Cross Laminated Timber: A Primer. *FPIInnovations*. Vancouver, BC, Canada.
- CSA O86. (1984). Engineering Design in Wood. Mississauga, Canada.
- CSA O86. (1989). Engineering Design in Wood. Mississauga, Canada.
- CSA O86. (2009). Engineering Design in Wood. Mississauga, Canada.
- CSA O86. (2014). Engineering Design in Wood. Mississauga, Canada.
- CSA O86. (2016) Supplement. Engineering Design in Wood. Mississauga, Canada.
- D1761. (2012). Standard Test Methods for Mechanical Fasteners in Wood. *ASTM International*. West Conshohocken, PA, USA.
- D198-13. (2012). Standard Test Methods of Static Tests of Lumber in Structural Sizes. *ASTM International*. West Conshohocken, PA, USA.
- Danzig, I., Closen, M., Tannert, T. (2014). High Performance Cross-laminated-timber Shear Connection with Self-tapping-screw Assemblies. In *Proceedings of World Conference on Timber Engineering, WCTE 2014*. August 10-14, 2014. Québec City, QC, Canada.

- DIBt. (2011). Deutsches Institut für Bautechnik, Z-9.1-472, Allgemeine Bauaufsichtliche Zulassung, SFS Befestiger WT-S-6,5; WT-T-6,5; WT-T-8,2; WR-T-9.0 und WR-T-13 als Holzverbindungsmittel. Berlin, Germany.
- Dietsch, P., Brandner, R. (2015). Self-tapping Screws and Threaded Rods as Reinforcement for Structural Timber Elements – A state-of-the-art report. *Construction and Building Materials*, 97, 78–89.
- DIN 1052. (2009). Design of Timber Structures - General Rules and Rules for Buildings, *Edition: 2008-12. DIN Standards Committee Timber and Furniture*. Berlin, Germany.
- Doyle, D. V. (1964). Performance of Joints with Eight Bolts in Laminated Douglas fir. *U.S. Forest Service*. Research Paper, FPL 10. Madison, WI, USA.
- E2126–11. (2014). Standard Test Methods for Cyclic (Reversed) Load Test for Shear Resistance of Vertical Elements of the Lateral Force Resisting Systems for Buildings. *ASTM International*. West Conshohocken, PA, USA.
- Editors. (2019). Explore these Maps of North America’s Blooming Timber Industry. *The Architect’s Newspaper*.
- Ehlbeck, J., Larsen, H. (1993). Eurocode 5 – Design of Timber Structures: Joints. *Forest Product Society* (pp 9-23). Madison, WI, USA.
- EN-26891. (1991). Timber Structures, Joints Made with Mechanical Fasteners, General Principles for the Determination of Strength and Deformation Characteristics. *European Committee for Standardization (CEN)*. Brussels, Belgium.
- EN 1995-1-1. (1994). Eurocode 5: Design of Timber Structures. European Committee for Standardization. *European Committee for Standardization (CEN)*. Brussels, Belgium.

- EN 1995-1-1. (2004). Eurocode 5: Design of Timber Structures. European Committee for Standardization. *European Committee for Standardization (CEN)*. Brussels, Belgium.
- EN 1995-1-1. (2008). Eurocode 5: Design of Timber Structures – Part 1-1: General – Common Rules and Rules for Buildings. *European Committee for Standardization (CEN)*. Brussels, Belgium.
- EN 408. (2010). Timber Structures – Structural Timber and Glued Laminated Timber – Determination of some Physical and Mechanical Properties. *European Committee for Standardization (CEN)*. Brussels, Belgium
- EN 12512. (2001). Timber Structures—Test Methods—Cyclic Testing of Joints made with Mechanical Fasteners. *European Committee for Standardization (CEN)*. Brussels, Belgium.
- ETA-11/0190 (2013). Würth Self-tapping Screws for use in Timber Constructions. *European Technical Approval*. Berlin, Germany. 2013
- ETA-11/0190 (2018). Würth Self-tapping Screws for use in Timber Constructions. *European Technical Approval*. Berlin, Germany. 2013
- ETA-11/0030 (2017). Rotho Blaas Self-tapping Screws for use in Timber Structures. *European Technical Approval, 2017–2022*. Berlin, Germany.
- Epp, L. (2015). T3 Minneapolis – 7 storey Mass Timber Office. *StructureCraft*. Vancouver, BC, Canada.
- ESR-3178. (2018). ICC-ES Evaluationa Report: Division:06 00 00-Wood, Plastic, and Composites, Section: 06 05 23-Wood, Plastic, and Composite Fastenings. *Simpson Strong-Tie Company Inc*. Pleasanton, CA, USA.
- Evans, L. (2015). Cross Laminated Timber: Taking Wood Buildings to the next Level. Sponsored by *reThink Wood, American Wood Council, and FPInnovations*.

- Fahlbusch, H. (1949). *Ein Beitrag zur Frage der Tragfähigkeit von Bolzen in Holz bei statischer Belastung*. Ber. Nr. 49-09 des Inst. für Maschinenkonstruktion u. Leichtbau d. Techn. Hochsch., Braunschweig.
- Follesa, M., Brunetti, M., Cornacchini, R., Grasso, S. (2010). Mechanical In-Plane Joints Between Cross Laminated Timber Panels. In *Proceedings of World Conference on Timber Engineering, WCTE 2010*. June 20-24, 2010, Riva del Garda, Trentino, Italy.
- Frangi, A., Fontana, M., Hugi, E., Jübstl, R. (2009). Experimental Analysis of Cross-Laminated Timber Panels in Fire. *Fire Safety Journal*, 44(8), 1078–1087.
- Frese, M., Blass, H. J. (2009). Models for the Calculation of the Withdrawal Capacity of Self-tapping Screws. In *Proceedings of CIB-W18 Timber Structures, Meeting 42* (Paper 42–7–3). August 24-27, 2009, Dübendorf, Switzerland.
- Gagnoon, S., Pirvu, C. (2011). CLT Handbook (Canadian Edition). *FPIInnovations*, Québec City, QC, Canada.
- Gavric, I. (2013). Seismic Behaviour of Cross-Laminated Timber Buildings. *Ph.D. Thesis*. University of Trieste, Italy.
- Gavric, I., Ceccotti, A., Fragiaco, M. (2011). Experimental Cyclic Tests on Cross-laminated timber Panels and Typical Connections. In *Proceedings of the 14th ANIDIS Conference*. September 18-22, 2011, Bari, Italy.
- Gavric, I., Fragiaco, M., Ceccotti, A. (2015a). Cyclic Behavior of CLT Wall Systems: Experimental Tests and Analytical Prediction Models. *Journal of Structural Engineering*, (5), 1–14.
- Gavric, I., Fragiaco, M., Ceccotti, A. (2015b). Cyclic Behavior of Typical Screwed Connections for Cross-laminated (CLT) Structures. *European Journal of Wood and Wood Products*, 73(2), 179–191.

- Gavric, I., Fragiaco, M., Popovski, M., Ceccotti, A. (2014). Behaviour of Cross-Laminated Timber Panels under Cyclic Loads. *Materials and Joints in Timber Structures*, 9, 689–702.
- Gehri, E. (1996). Design of Joints and Frame Corners using Dowel Type Fasteners. In *Proceedings of CIB-W18 Timber Structures, Meeting 29* (Paper 29–7–6). August 26-29, 1996, Bordeaux, France.
- Hansen, K. F. (2002). Mechanical Properties of Self-tapping Screws and Nails in Wood. *Canadian Journal of Civil Engineering*, 29(5), 725–733.
- Hossain, A., Danzig, I., Tannert, T. (2016). Cross-Laminated Timber Shear Connections with Double-Angled Self-Tapping Screw Assemblies. *Journal of Structural Engineering*, 142(11).
- Hossain, A., Popovski, M., Tannert, T. (2016). Shear Connections with Self-tapping-screws for Cross-laminated-timber Panels. In *Proceedings of World Conference on Timber Engineering, WCTE 2016*. August 22-25, 2016, Wien, Austria.
- IBC. (2015). International Building Code. *International Code Council*.
- Jockwer, R., Steiger, R., Frangi, A. (2014). Fully Threaded Self-tapping Screws Subjected to Combined Axial and Lateral Loading with Different Load to Grain Angles. *Materials and Joints in Timber Structures*, 9, 265–272.
- Jockwer, R., Steiger, R., Frangi, A. (2014). Design Model for Inclined Screws under Varying Load to Grain Angles. In *1st meeting of the International Network on Timber Engineering Research, (INTER 2014)* (pp 11). September 1-4, Bath, United Kingdom.
- Joebstl, R., Bogensperger, T., Schickhofer, G. (2008). *In-Plane Shear Strength of Cross Laminated Timber*. In *Proceedings of CIB-W18 Timber Structures, Meeting 41* (Paper 41–12–3). August 24-28, 2008, St. Andrews, NB, Canada.

- Johansen, K. (1949). Theory of timber connections. *International Association of Bridge and Structural Engineering (IABSE)*, 9, 249–262.
- Jorissen, A. (1998). *Double Shear Timber Connections with Dowel Type Fasteners. Ph.D. Thesis.* Technical University of Delft, The Netherlands.
- Joyce, T., Ballerini, M., Smith, I. (2011). Mechanical Behaviour of In-plane Shear Connections between CLT Wall Panels. In *Proceedings of CIB-W18 Timber Structures, Meeting 44*. August 29-September 1, 2011, Alghero, Italy.
- Karacabeyli, E., Douglas, B. (2013). CLT Handbook (U.S. Edition). *FPInnovations*, Pointe-Claire, QC, Canada.
- Karacabeyli, E., Lum, C. (2014). Technical Guide for the Design and Construction of Tall Wood Buildings in Canada. *FPInnovations Special Publication SP-55E*. Vancouver, BC, Canada;.
- Krenn, H., Schickhofer, G. (2009). Joints with Inclined Screws and Steel Plates as Outer Members. In *Proceedings of CIB-W18 Timber Structures, Meeting 42* (Paper 42–7–2). August 24-27, 2009, Dübendorf, Switzerland.
- Kunesh, R. H., Johnson, J. W. (1968). Strength of Multiple-bolt Joints; Influence of Spacing and Other Variables. *Forestry Research Laboratory*, Report T-24. School of Forestry, Oregon State University, Corvallis, OR, USA.
- Lam, F. (2011). Cross Laminated Timber (CLT) Connection Tests for UBC Bioenergy Research & Demonstration Project Nexterra Building. Report prepared for *CST Innovation Ltd.*
- Lantos, G. (1969). Load Distribution in a Row of Fasteners Subjected to Lateral Load. *Wood Science*, 1(3), 129–130.
- Lau, W. (2016). The University of British Columbia’s Brock Commons Takes the Title of Tallest Wood Tower. *The Journal of the American Institute of Architects*.

- Madsen, B. (1992). *Structural Behaviour of Timber*. Timber Engineering Ltd. North Vancouver, BC, Canada.
- Masse, D. I., Salinas, J. J., Turnbull, J. (1989). Lateral Strength and Stiffness of Single and Multiple Bolts in Glued-laminated Timber Loaded Parallel to Grain. *Engineering and Statistical Research Centre, Research Branch, Agriculture Canada*. Contribution No. C-029, Ottawa, ON, Canada.
- Moudgil, M., Tannert, T. (2017). Structural Design, Approval and Monitoring of UBC Tall Wood Building. In *Proceedings of the ASCE Structures Congress*. April 6-8, 2017, Denver, CO, USA.
- MyTiCon. (2014). ASSY® Structural Wood Screws: The Basics. Surrey, BC, Canada.
- NBCC. (2015). National Building Code of Canada. *National Research Council*. Ottawa, ON, Canada.
- NDS. (1973). National Design Specification for Wood Construction. *American Wood Council*. Leesburg, VA, USA.
- NDS. (1986). National Design Specification for Wood Construction. *American Wood Council*. Leesburg, VA, USA.
- NDS. (2015). National Design Specification for Wood Construction. *American Wood Council*. Leesburg, VA, USA.
- NDS. (2018). National Design Specification for Wood Construction. *American Wood Council*. Leesburg, VA, USA.
- NRCan. (2017). Natural Resources Canada-Overview of Canada's forest industry. *Natural Resources Canada*.

- OBC. (2014). CodeNews Issue 232 - Amendments to Ontario's Building Code Allowing Mid-Rise Wood Frame Buildings. *Ministry of the Solicitor General*.
- Oh, J.-K., Kim, K.-M., Lee, J.-J., Lee, H.-J., Lee, S.-J., Hong, J.-P., Kim, G.-C. (2018). End Distance of Single-Shear Screw Connection in Cross Laminated Timber. In *Proceedings of World Conference on Timber Engineering, WCTE 2018*. August 20-23, 2018, Seoul, South Korea.
- Pei, S., Rammer, D., Popovski, M., Williamson, T., Line, P., van de Lind JW. (2016). An Overview of CLT Research and Implementation in North America. In *Proceedings of World Conference on Timber Engineering, WCTE 2016*. August 22-25, 2016, Wien, Austria.
- Popovski, M., Schneider, J., Schweinsteiger, M. (2010). Lateral Load Resistance of Cross-Laminated Wood Panels. In *Proceedings of World Conference on Timber Engineering, WCTE 2010*. June 20-24, 2010, Riva del Garda, Trentino, Italy.
- Prat-Vincent, F., Rogers, C., Salenikovich, A. (2010). Evaluation of the Performance of Joist-to-Header Self-tapping Screw Connections. In *Proceedings of World Conference on Timber Engineering, WCTE 2010*. June 20-24, 2010, Riva del Garda, Trentino, Italy.
- PRG-320. (2018). ANSI/APA Standard for Performance-Rated Cross-Laminated Timber. *ANSI APA - The Engineered Wood Association*. Tacoma, WA, USA.
- Prinbacher, G., Brandner, R., Schickhofer, G. (2009). Base Parameters of Self-tapping Screws. In *Proceedings of CIB-W18 Timber Structures, Meeting 42* (Paper 42-7-3). August 24-27, 2009, Dübendorf, Switzerland.
- Richardson, B. L. (2015). *Examination of the Lateral Resistance of Cross-laminated Timber Panel-to-panel Connection. Master's Thesis*. Virginia Polytechnic Institute and State University, Blacksburg, Virginia.

- Ringhofer, A., Brandner, R., Schickhofer, G. (2015). Withdrawal Resistance of Self-tapping Screws in Unidirectional and Orthogonal Layered Timber Products. *Materials and Structures*, 48(5), 1435–1447.
- Sadeghi, M., Smith, I. (2014). Edge Connections for CLT Plates: In-Plane Shear Tests on Half-Lapped and Single-Spline Joints. In *Proceedings of World Conference on Timber Engineering, WCTE 2014*. August 10-14, 2014. Québec City, QC, Canada.
- Sandhass, C., Kuilen, J. van de, Boukes, J., Ceccotti, A. (2009). Analysis of X-lam Panel-to-panel Connections under Monotonic and Cyclic Loading. In *Proceedings of CIB-W18 Timber Structures, Meeting 42* (Paper 42–12–2). August 24-27, 2009, Dübendorf, Switzerland.
- Smith, I., Asiz, A., Snow, M., Chui, Y. H. (2006). Possible Canadian / ISO Approach to Deriving Design Values From Test Data. In *Proceedings of CIB-W18 Timber Structures, Meeting 39* (Paper 39–17–1). August 28-31, 2006, Florence, Italy.
- Smith, I., Frangi, A. (2014). Use of Timber in Tall Multi-storey Buildings. In *ISBN 978-3-85748-133-8, Structural Engineering Documents 13. IABSE, ETH Zürich*.
- Structurlam. (2011). *Cross Laminated Timber Design Guide*. Penticton, BC, Canada.
- Sullivan, K., Miller, T. H., Rakesh, G. (2018). Behavior of Cross-laminated Timber Diaphragm Connections with Self-tapping Screws. *Engineering Structures*, 168, 505–524.
- Tannert, T., Lam, F. (2009). Progress in Structural Engineering and Materials: Timber Construction Self-tapping Screws as Reinforcement for Rounded Dovetail Connections. *Structural Control and Health Monitoring*, 16(3), 374–384.
- Tomasi, R., Crosatti, A., Piazza, M. (2010). Theoretical and Experimental Analysis of Timber-to-Timber Joints Connected with Inclined Screws. *Construction and Building Materials*, 24(9), 1560–1571.

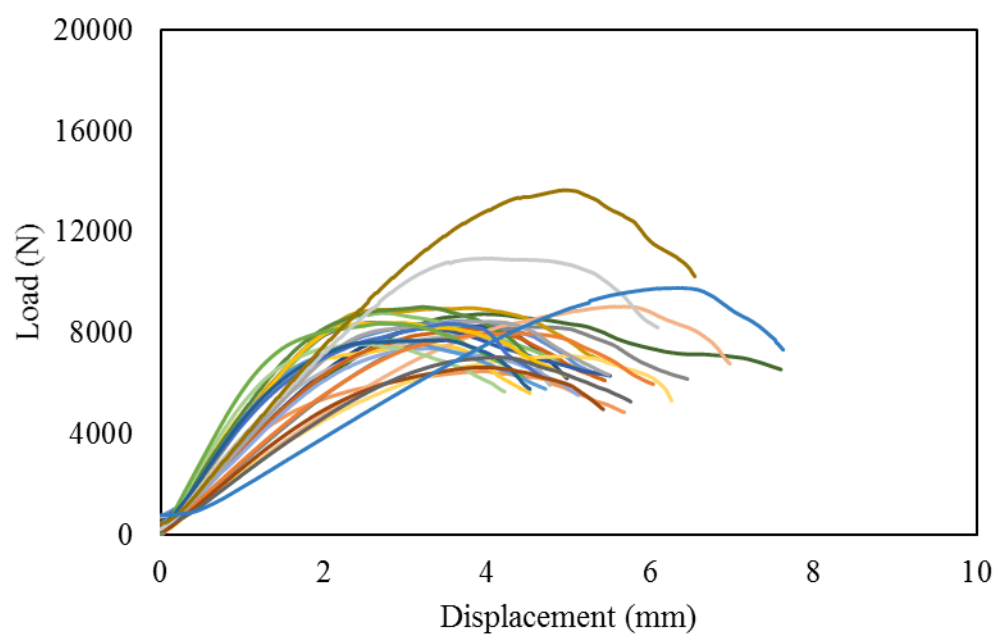
- Tomasi, R., Piazza, M., Angeli, A., Mores, M. (2006). A New Ductile Approach Design of Joints Assembled with Screw Connectors. *Unpublished technical report*.
- Uibel, T., Blass, H. J. (2010). Determining Suitable Spacings and Distances for Self-tapping Screws by Experimental and Numerical Studies. In *Proceedings of World Conference on Timber Engineering, WCTE 2010*. June 20-24, 2010, Riva del Garda, Trentino, Italy.
- Vessby, J., Enquist, B., Petersson, H., Alsmarker, T. (2009). Experimental Study of Cross-Laminated Timber Wall Panels. *European Journal of Wood and Wood Products*, 67(2), 211–218.
- Wardell, C. (2015). Use of Cross-Laminated Timber on the Rise. *ProSales Magazine*.
- Wilkinson, T. L. (1980). Assessment of Modification Factors for a Row of Bolts or Timber Connectors. *U.S. Forest Service*. Research Paper, FPL-RP-376. Madison, WI, USA.
- Wilkinson, T. L., Laatsch, T. R. (1970). Lateral and Withdrawal Resistance of Tapping Screws in Three Densities of Wood. *Forest Products Journal*, 20(7), 34–41.
- Yasumura, M., Murota, T., Nakai, H. (1987). Ultimate Properties of Bolted Joints in Glued-Laminated Timber. In *Proceedings of CIB-W18 Timber Structures, Meeting 20* (Paper 20–7–3). August 31–September 3, 1987, Dublin, Ireland.
- Yeh, M.-C., Lin, Y.-L., Huang, G.-P. (2013). Investigation of the structural performance of glulam beam connections using self-tapping screws. *Journal of Wood Science*, 60(1), 39–48. h
- Yeh, M.-C., Lin, Y.-L., Sung, Y.-W. (2018). Evaluation of the Performance of the Vertical Withdrawal Resistance of Structural Self-tapping Screws in Wood. *Taiwan Journal of Forest Science*, 33(2), 109–123.
- Yeh, M.-C., Wang, B., Wu, K.-C. (2007). Tensile Strength of Bolt Joints for Structural Glulam Members Made of Japanese Cedar. *Taiwan Journal of Forest Science*, 22(2), 101–111.

- Yeh, M.-C., Wu, K.-C., Lin, Y.-L. (2008). Moment-resisting Capacity of Bolt Connections in Japanese Cedar Structural Glulam Members. *Taiwan Journal of Forest Science*, 23(4), 365–375.
- Zahn, J. J. (1991). Design Equation for Multiple-fastener Wood Connections. *Journal of Structural Engineering*, 117(11), 3477–3486.
- Zhang, X., Fairhurst, M., Tannert, T. (2015). Seismic Reliability Analyses of Timber-steel-hybrid System. In *The 12th International Conference on Applications of Statistics and Probability in Civil Engineering (ICASPI2)*. July 12-15, 2015, Vancouver, BC, Canada.
- Zhang, X., Fairhurst, M., Tannert, T. (2016). Ductility Estimation for a Novel Timber-steel-hybrid System. *Journal of Structural Engineering*, 142(4).

Appendix A Detailed test results of withdrawal testing

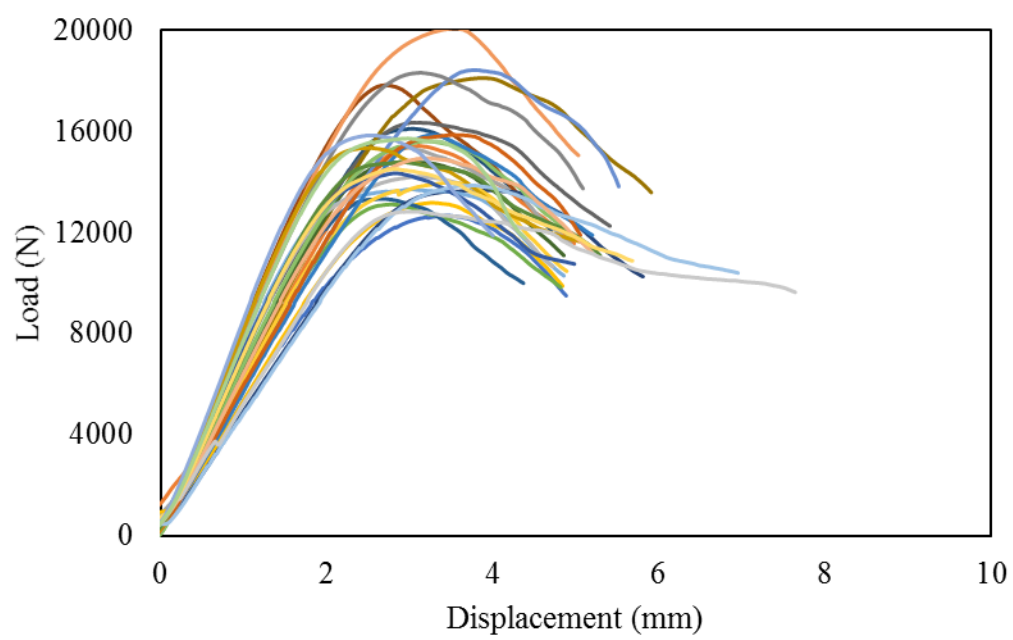
A.1 Series 1 (8mm_8d_90°)

Spec	F _{max} [N]	F _Y [N]	d _{Fmax} [mm]	d _{FY} [mm]	μ (-)	k [N/mm]	k _{90%} [N/mm]
1	8289.3	7435.7	3.8	2.2	1.7	3315.7	3223.6
2	8762.2	7845.1	4.0	2.2	1.8	3504.9	3066.8
3	6501.7	5854.3	4.0	1.6	2.6	3715.2	3250.8
4	7929.4	6596.9	3.7	1.7	2.2	3964.7	3469.1
5	7502.5	6425.9	3.1	1.2	2.5	5001.7	4774.3
6	8497.6	8414.9	3.7	2.3	1.6	3776.7	3717.7
7	8797.8	8249.5	2.7	1.8	1.5	4398.9	4398.9
8	8573.8	5825.8	9.1	4.7	1.9	1224.8	1132.4
9	8177.2	8118.4	3.8	2.4	1.6	3270.9	3180.0
10	8254.1	7642.6	4.5	2.7	1.7	2751.4	2751.4
11	8999.2	8416.6	3.8	1.8	2.1	4499.6	4199.6
12	8424.9	7892.2	2.6	1.8	1.4	4212.4	4536.5
13	9042.1	7462.1	3.2	1.5	2.2	5166.9	4521.1
14	13662.4	12432.1	5.0	3.3	1.5	3903.5	3678.3
15	9053.2	8163.9	5.7	3.3	1.7	2414.2	2263.3
16	10965.9	10254.0	4.0	2.7	1.5	3655.3	3489.1
17	7095.5	6423.2	5.0	2.6	1.9	2365.2	2159.5
18	7400.3	6880.4	3.3	2.1	1.6	3289.0	3237.6
19	7578.7	6108.2	2.5	1.1	2.2	5052.5	5305.1
20	7727.3	6776.1	3.0	1.5	2.0	4415.6	4507.6
21	7982.3	7418.5	4.4	2.5	1.7	2902.6	2793.8
22	8472.0	8426.3	3.8	2.4	1.6	3388.8	3488.5
23	8408.8	7809.6	2.9	1.8	1.6	4204.4	4527.8
24	8372.4	6894.6	3.6	1.5	2.4	4784.2	3907.1
25	8387.4	7071.1	2.7	1.2	2.2	5591.6	5871.2
26	7723.4	6578.2	3.5	1.5	2.4	4413.4	4505.3
27	6651.7	6361.7	4.0	2.4	1.7	2660.7	2586.8
28	7051.1	6446.7	4.1	2.7	1.5	2350.4	2350.4
29	9792.3	8867.5	6.3	4.6	1.4	1958.5	1904.1
30	10459.6	10700.0	3.9	3.1	1.2	3486.5	3486.5
Avg.	8484.5	7659.7	4.0	2.3	1.8	3654.7	3542.8



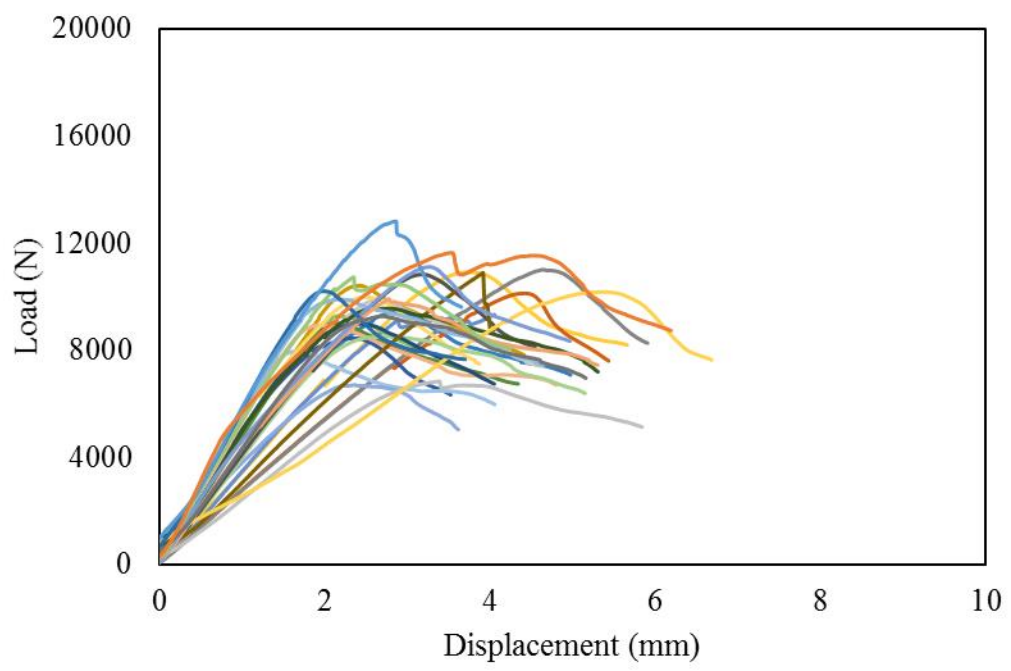
A.2 Series 2 (8mm_12d_90°)

Spec	F _{max} [N]	F _Y [N]	d _{Fmax} [mm]	d _{FY} [mm]	μ (-)	k [N/mm]	k _{90%} [N/mm]
1	15421.5	13053.4	3.1	2.1	1.5	6168.6	5997.3
2	15354.4	12723.0	3.0	2.0	1.5	6141.8	6322.4
3	13169.1	10463.3	3.3	2.0	1.7	5267.6	5422.6
4	12661.1	10299.7	3.5	1.9	1.8	5064.4	4923.8
5	13106.9	10722.9	2.8	1.8	1.6	5825.3	6116.6
6	13318.4	8108.7	2.7	1.2	2.2	6659.2	6659.2
7	17819.2	12791.1	2.7	1.6	1.7	7919.6	8315.6
8	16330.4	14849.6	3.1	2.0	1.5	7258.0	6724.3
9	18099.5	17026.8	3.9	2.7	1.4	6581.6	6334.8
10	13666.7	12959.7	3.9	2.6	1.5	4969.7	4783.3
11	14786.2	12445.6	3.0	1.9	1.6	6571.6	6468.9
12	13695.4	11821.9	3.0	1.6	1.9	7825.9	7374.5
13	20050.4	16674.9	3.6	2.1	1.7	8020.2	7797.4
14	14196.8	11491.7	3.1	1.7	1.9	7098.4	7098.4
15	13953.7	11778.4	3.4	2.0	1.7	6201.7	6104.8
16	18414.3	16459.2	3.8	2.8	1.3	5665.9	5859.1
17	15603.3	13253.2	3.2	1.9	1.7	6934.8	6826.4
18	15859.7	14082.5	3.3	2.5	1.3	5767.2	5550.9
19	15851.0	13411.9	3.5	2.2	1.6	5764.0	5839.9
20	18302.3	15343.0	3.1	2.0	1.6	8134.4	7536.3
21	15334.2	14228.1	2.5	1.7	1.5	7667.1	8256.9
22	14331.1	12709.4	2.8	1.7	1.7	7165.5	7165.5
23	14779.1	13238.0	2.9	1.9	1.6	7389.5	6896.9
24	13853.5	12861.0	3.8	2.7	1.4	4617.8	4848.7
25	14933.2	13237.4	3.2	2.1	1.5	6637.0	6533.3
26	12820.6	12001.2	3.0	2.4	1.3	5128.2	5279.1
27	14503.4	14043.9	2.8	1.9	1.4	7251.7	7251.7
28	15829.5	7503.8	2.5	0.9	2.8	9045.5	8523.6
29	15709.9	9677.0	3.0	1.3	2.4	7854.9	7854.9
30	16092.7	12621.5	3.0	1.9	1.6	6437.1	6626.4
Avg.	15261.6	12729.4	3.2	2.0	1.7	6634.5	6576.4



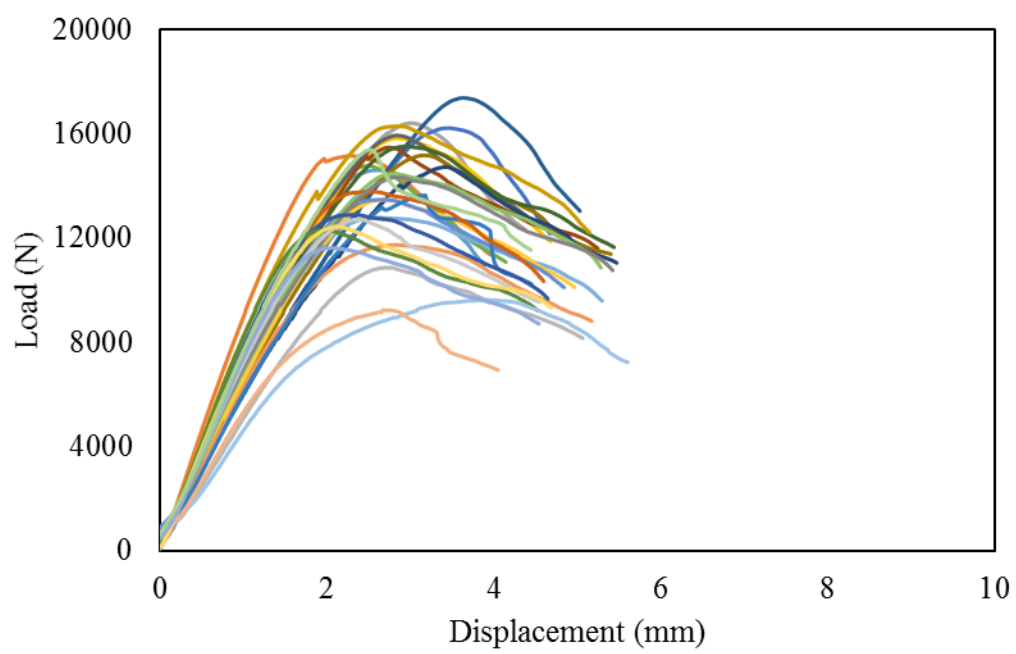
A.3 Series 3 (8mm_8d_45°)

Spec	F _{max} [N]	F _Y [N]	d _{Fmax} [mm]	d _{FY} [mm]	μ (-)	k [N/mm]	k _{90%} [N/mm]
1	11100.2	10118.7	3.7	3.0	1.2	3356.0	3319.5
2	10854.5	9339.4	6.9	2.7	2.6	3339.8	3303.5
3	9263.0	4073.3	2.2	0.8	2.6	4631.5	4631.5
4	9424.8	8180.2	2.9	1.9	1.5	4188.8	4123.3
5	10120.0	9438.1	4.4	3.4	1.3	2698.7	2623.7
6	10982.8	10034.2	4.7	3.7	1.3	2745.7	2651.0
7	10406.3	7003.1	2.4	1.5	1.6	4625.0	4856.3
8	8437.2	4388.4	2.4	0.9	2.8	4821.3	4921.7
9	8983.4	5751.4	2.1	1.2	1.7	4491.7	4837.2
10	7953.9	2232.1	1.7	0.4	4.0	5302.6	5567.7
11	8929.0	9555.3	1.9	1.9	1.0	5102.3	5208.6
12	9868.2	6314.2	2.7	1.5	1.8	4385.9	4317.3
13	9978.3	6426.3	2.5	1.2	2.1	5701.9	4989.1
14	6671.1	3984.7	2.3	1.0	2.4	3812.1	3592.1
15	8506.5	7826.6	2.8	1.9	1.5	3780.7	3969.7
16	8979.6	6449.5	2.4	1.3	1.8	5131.2	4835.2
17	12767.6	6998.4	2.8	1.2	2.3	5674.5	5257.3
18	10822.8	8480.7	3.2	2.1	1.5	3935.6	3788.0
19	10854.5	9356.0	3.9	3.0	1.3	3101.3	2922.4
20	11625.8	10145.5	3.5	1.6	2.2	5812.9	4521.1
21	9578.5	8889.6	2.6	1.9	1.4	4789.3	4789.3
22	9896.4	8422.2	2.2	1.5	1.5	5655.1	5772.9
23	9801.6	8754.1	2.8	2.0	1.4	4356.3	4036.0
24	6799.4	6237.8	3.3	2.6	1.3	2472.5	2379.8
25	10172.2	10104.9	5.4	4.6	1.2	2260.5	2225.2
26	11093.4	9435.8	3.3	2.0	1.6	4437.4	4087.0
27	10621.3	6431.4	2.3	1.2	2.0	5310.6	5310.6
28	10204.8	6326.6	2.0	1.1	1.8	5831.3	5952.8
29	7048.3	5928.0	2.6	1.8	1.4	3132.6	3083.6
30	9268.3	8569.2	2.7	2.0	1.4	4119.2	4325.2
Avg.	9700.5	7506.5	3.0	1.9	1.8	4300.1	4206.6



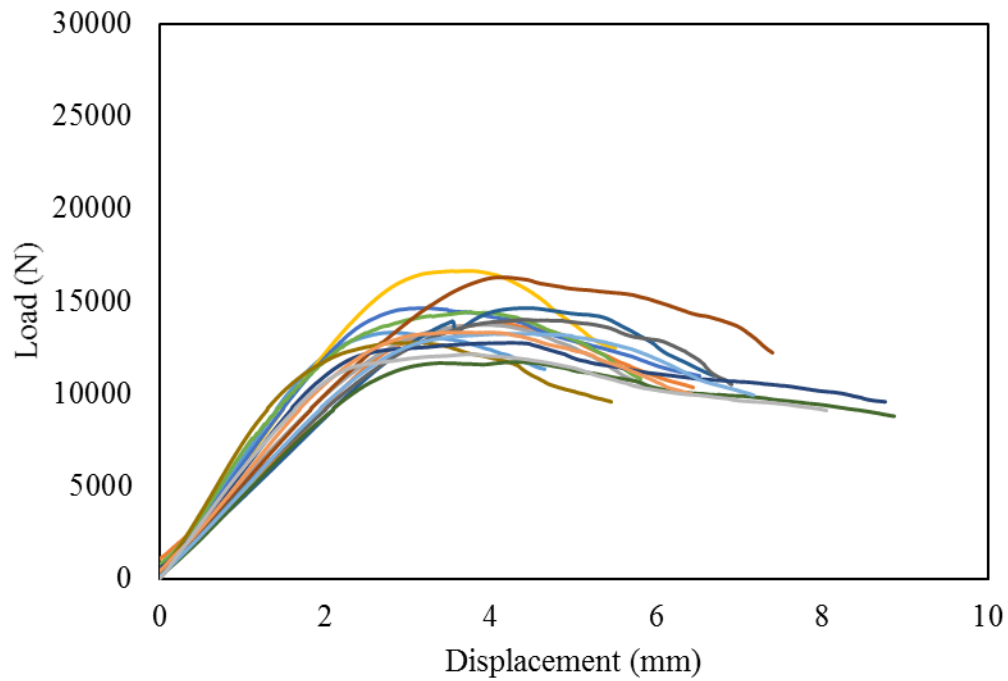
A.4 Series 4 (8mm_12d_45°)

Spec	F _{max} [N]	F _Y [N]	d _{Fmax} [mm]	d _{FY} [mm]	μ (-)	k [N/mm]	k _{90%} [N/mm]
1	14607.1	9368.7	2.6	1.3	2.0	7303.6	7303.6
2	15150.0	10144.7	2.3	1.1	2.1	8657.1	8837.5
3	16412.8	10604.1	3.0	1.4	2.1	7294.6	6758.2
4	15813.0	12672.6	2.8	1.6	1.8	7906.5	6918.2
5	16212.5	9583.0	3.5	1.6	2.2	5895.5	5674.4
6	14767.7	10681.4	2.5	1.5	1.7	7383.8	6891.6
7	17368.0	15068.6	3.6	2.5	1.4	5789.3	5526.2
8	15459.4	14887.7	2.7	2.3	1.2	6870.9	6365.6
9	15926.1	13569.0	2.8	1.7	1.6	7963.0	6967.7
10	15169.2	14857.3	3.2	2.2	1.5	6741.9	5899.1
11	14720.8	13496.1	3.4	2.2	1.6	6542.6	5423.4
12	15510.2	14581.8	3.0	2.0	1.5	6893.4	6785.7
13	12783.5	11552.4	2.6	1.6	1.6	7304.9	6391.8
14	11731.5	10773.9	2.8	1.7	1.7	6703.7	5865.8
15	10863.5	9639.1	2.7	1.9	1.4	4828.2	5069.6
16	13469.5	11803.3	2.7	1.7	1.6	6734.8	6285.8
17	13465.7	11503.2	2.6	1.6	1.7	6732.8	6732.8
18	14473.6	12960.7	2.8	1.9	1.5	7236.8	6754.3
19	13607.7	10665.9	3.1	1.7	1.8	6047.8	5603.2
20	13774.5	11120.0	2.5	1.4	1.8	7871.2	7417.0
21	14333.6	13009.2	2.9	1.7	1.7	7166.8	6270.9
22	16282.3	14250.1	2.8	1.7	1.7	8141.1	7598.4
23	12889.3	10776.1	2.3	1.4	1.7	7365.3	7518.8
24	12287.1	8176.4	2.0	1.0	2.0	8191.4	7819.0
25	9629.7	8863.4	3.9	1.9	2.0	4814.9	4493.9
26	9227.8	6607.1	2.7	1.2	2.2	5273.1	4968.8
27	12705.2	7920.3	2.4	1.1	2.3	7260.1	6841.3
28	12435.8	10173.8	2.1	1.3	1.6	8290.5	7254.2
29	11612.9	9475.7	2.1	1.3	1.7	7742.0	7390.0
30	15377.0	11359.4	2.5	1.5	1.7	7688.5	7175.9
Avg.	13935.6	11338.2	2.8	1.6	1.7	7021.2	6560.1



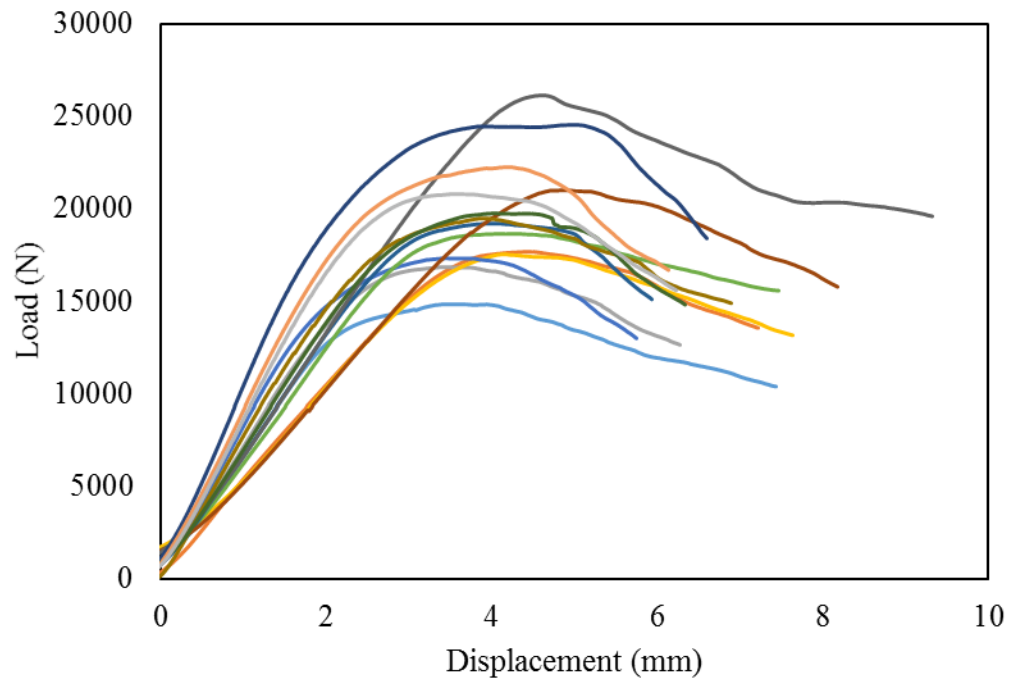
A.5 Series 5 (10mm_8d_90°)

Spec	F _{max} [N]	F _Y [N]	d _{Fmax} [mm]	d _{FY} [mm]	μ (-)	k [N/mm]	k _{90%} [N/mm]
1	13340.5	8038.9	2.8	1.2	2.2	6670.2	6670.2
2	13826.1	12960.7	4.1	2.7	1.5	4608.7	4608.7
3	13700.5	12646.6	3.9	2.4	1.6	5480.2	5047.6
4	16604.4	16460.0	3.7	2.8	1.3	6038.0	6117.4
5	14635.7	13545.1	3.2	2.2	1.5	6504.8	6026.5
6	14375.2	13201.9	3.7	1.9	1.9	7187.6	6289.2
7	14643.3	13828.4	4.4	3.2	1.4	4505.6	4456.7
8	16277.1	14957.7	4.1	3.0	1.4	5008.3	4953.9
9	13978.0	12919.1	4.4	2.7	1.6	4659.3	4447.5
10	12764.8	12632.1	2.8	1.7	1.6	7294.2	6873.4
11	12701.5	11661.0	4.4	2.4	1.8	4618.7	5230.0
12	11689.4	10764.2	4.3	2.4	1.8	4250.7	4306.6
13	13213.9	12513.6	4.3	2.6	1.6	4805.0	4624.8
14	13325.5	-49893.0	3.5	-9.0	-0.4	5330.2	5487.0
15	12158.6	11200.3	3.8	1.9	2.0	6079.3	5674.0
Avg.	13815.6	8495.8	3.8	1.6	1.5	5536.1	5387.6



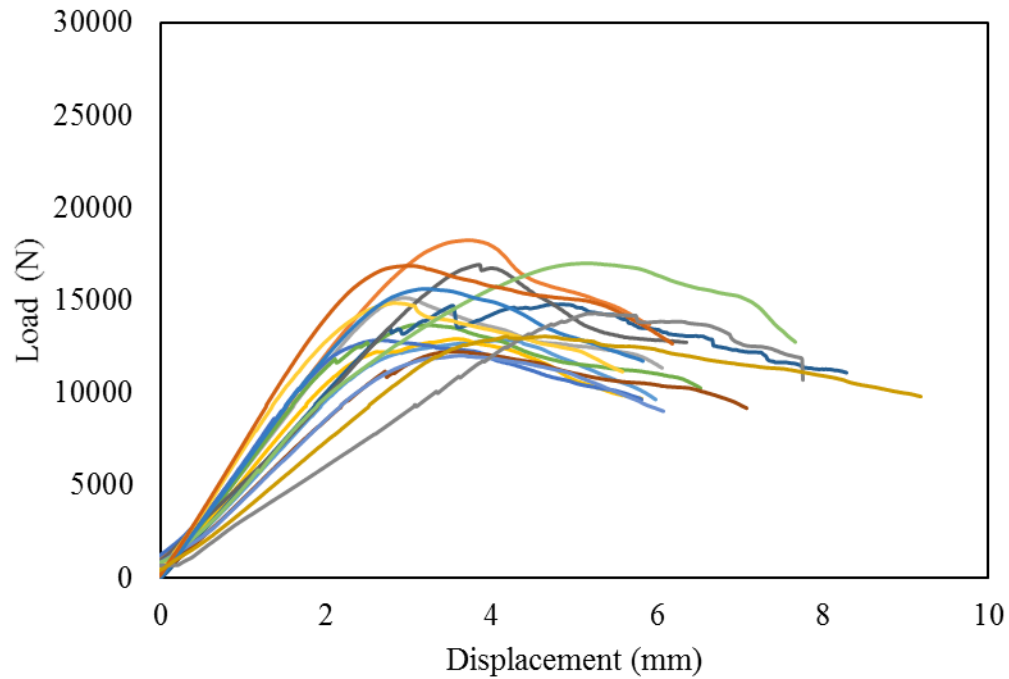
A.6 Series 6 (10mm_12d_90°)

Spec	F _{max} [N]	F _Y [N]	d _{Fmax} [mm]	d _{FY} [mm]	μ (-)	k [N/mm]	k _{90%} [N/mm]
1	14861.5	13827.1	3.5	2.1	1.7	6605.1	6501.9
2	17700.9	16447.6	4.4	3.1	1.4	5446.4	5162.8
3	16817.6	15813.8	3.5	2.2	1.6	6727.1	6924.9
4	17527.4	16521.3	4.2	3.3	1.3	5007.8	5112.2
5	17291.7	16242.7	3.7	2.0	1.8	8645.9	8069.5
6	18618.8	17234.2	4.3	2.8	1.6	6206.3	6206.3
7	19225.3	18367.1	4.0	2.8	1.4	6408.4	6408.4
8	20997.9	19646.8	4.9	3.9	1.3	4940.7	5068.5
9	26079.1	24175.4	4.6	3.7	1.2	6519.8	6519.8
10	19488.9	17983.4	3.9	2.3	1.7	7795.5	7579.0
11	24526.9	23065.4	5.0	2.3	2.2	9810.8	9538.2
12	19760.0	18693.7	4.0	2.7	1.5	7185.4	6916.0
13	19994.8	18621.9	4.3	2.8	1.5	6664.9	6664.9
14	22222.5	20845.0	4.2	2.3	1.8	8889.0	8642.1
15	20770.9	19569.2	3.6	2.3	1.6	8308.4	8552.7
Avg.	19725.6	18470.3	4.1	2.7	1.6	7010.8	6924.5



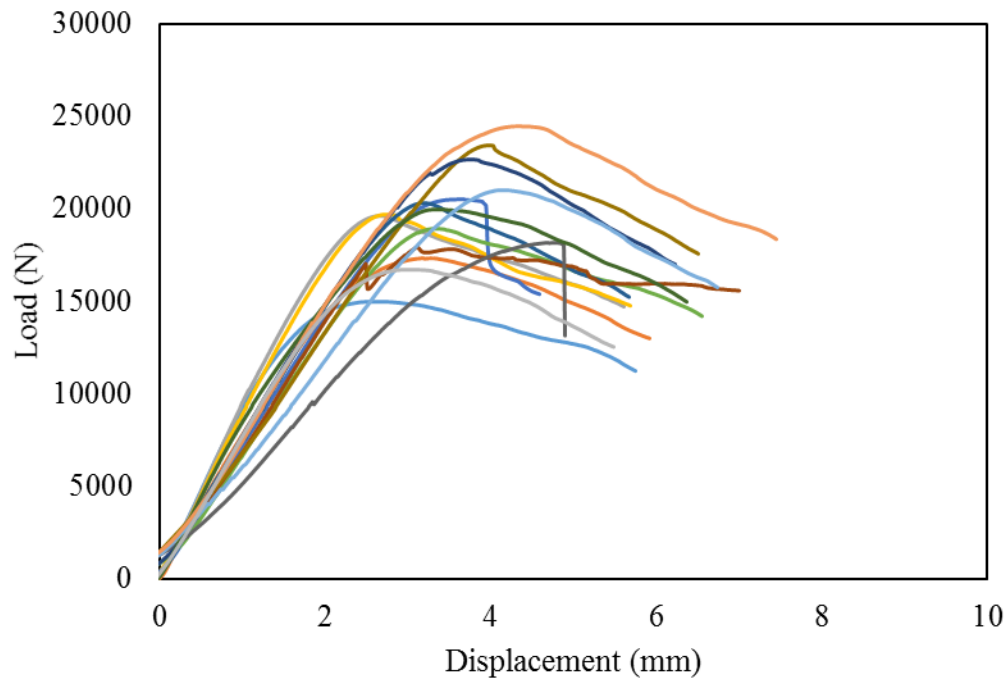
A.7 Series 7 (10mm_8d_45°)

Spec	F _{max} [N]	F _Y [N]	d _{Fmax} [mm]	d _{FY} [mm]	μ (-)	k [N/mm]	k _{90%} [N/mm]
1	12874.6	12040.9	4.2	2.5	1.7	4681.7	4743.3
2	18280.9	16838.9	3.7	2.8	1.3	6093.6	6093.6
3	15149.9	13589.5	3.0	2.3	1.3	6060.0	5891.6
4	12887.1	12151.4	3.6	2.3	1.5	5154.8	5306.4
5	12862.2	12093.3	2.6	2.0	1.3	6431.1	6002.3
6	13674.8	12393.0	3.2	2.2	1.5	6077.7	5982.7
7	14746.9	13619.3	4.8	2.7	1.8	4915.6	4915.6
9	16888.2	15859.7	3.8	3.2	1.2	4825.2	4925.7
10	14858.2	13677.2	2.8	2.0	1.4	6603.6	6933.8
11	12020.2	11298.0	3.6	2.6	1.4	4371.0	4207.1
12	16971.9	15944.4	5.2	3.5	1.5	4849.1	4569.4
13	15654.5	14473.5	3.2	2.4	1.3	6261.8	6087.8
14	16843.5	15531.6	3.0	2.1	1.4	7486.0	7369.0
15	14242.2	13209.6	5.2	4.4	1.2	2998.3	3021.1
16	13025.3	12065.4	4.2	3.3	1.3	3721.5	3647.1
Avg.	14732.0	13652.4	3.7	2.7	1.4	5368.7	5313.1



A.8 Series 8 (10mm_12d_45°)

Spec	F _{max} [N]	F _Y [N]	d _{Fmax} [mm]	d _{FY} [mm]	μ (-)	k [N/mm]	k _{90%} [N/mm]
1	14956.0	13760.9	2.5	1.5	1.7	9970.7	8724.3
2	17282.7	15756.7	3.2	2.0	1.6	7681.2	7561.2
3	19603.4	17643.2	2.7	1.9	1.4	9801.7	9148.3
4	19690.6	17814.7	2.8	2.0	1.4	8751.4	8614.6
5	20535.9	9424.8	3.6	1.3	2.7	7467.6	7187.6
6	18901.9	17240.9	3.3	2.6	1.3	6873.4	6615.7
7	20282.0	18498.6	3.2	2.5	1.3	7375.3	7472.3
8	17909.9	15981.5	3.1	2.4	1.3	6512.7	6965.0
9	18155.2	15703.8	6.9	7.7	0.9	2017.2	2704.0
10	23446.6	21654.4	4.0	3.3	1.2	6699.0	6565.1
11	22625.2	20643.2	3.8	2.7	1.4	7541.7	7198.9
12	19955.1	17986.9	3.4	2.1	1.6	8868.9	7351.9
13	21028.5	19761.4	4.2	3.4	1.2	6008.2	5888.0
14	24449.1	22596.2	4.3	3.1	1.4	7522.8	7131.0
15	16735.9	16135.9	3.0	2.1	1.4	7438.2	7810.1
Avg.	19703.9	17373.5	3.6	2.7	1.5	7368.7	7129.2



Appendix B Spacing of CLT-STs test series

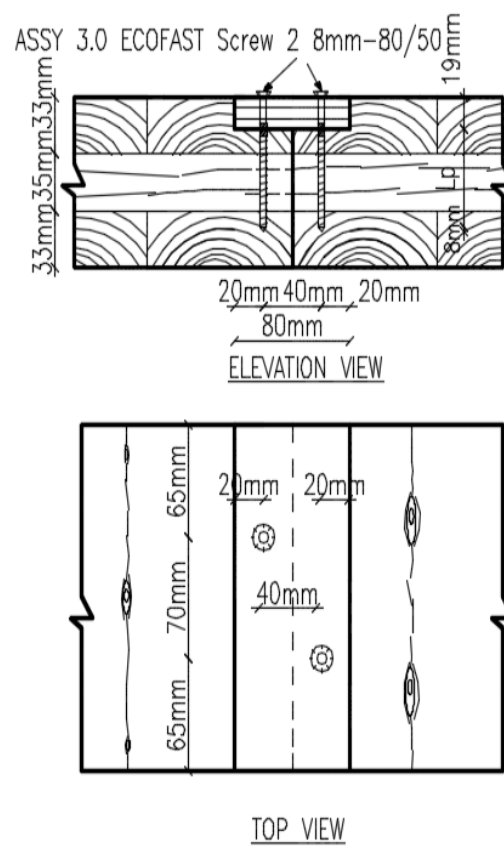
Series Name	Screw Type	a ₁₋₉₀ or S _p	a _{1-45/33} or S _p	a _{1T} or a _L	a _{1C} or a _L	a ₂ or S _Q	a _{2T} or a _{2C} or e
SS-2-m-3ply-2SP	PT	70	-	65	65	40	20
SS-2-c-3ply-2SP	PT	70	-	65	65	40	20
SS-4-m-3ply-2SP	PT	68	-	49	49	40	20
SS-4-c-3ply-2SP	PT	68	-	49	49	40	20
SS-8-m-3ply-1SP	PT	120	-	90	90	40	20
SS-8-m-5ply-1SP	PT	120	-	90	90	40	20
SS-10-m-3ply-2SP	PT	64	-	56	56	33	55
SS-10-m-5ply-2SP	PT	64	-	56	56	33	55
SS-16-m-3ply-1SP	PT	64	-	60	60	40	20
SS-16-m-3ply-1SP*	PT	64	-	60	60	40	20
SS-16-c-3ply-1SP	PT	64	-	160	160	40	20
SS-16-m-5ply-1SP	PT	64	-	60	60	40	20
SS-20-m-3ply-2SP	PT	64	-	56	56	40 (56)	20
SS-20-m-5ply-2SP	PT	64	-	56	56	40 (56)	20
SS-32-m-3ply-2SP	PT	40	-	50	50	40 (56)	20
SS-32-m-5ply-2SP	PT	40	-	50	50	40 (56)	20
LS-1-m-3ply-2SP	PT	-	-	100	100	-	20
LS-1-c-3ply-2SP	PT	-	-	100	100	-	20
LS-2-m-3ply-2SP	PT	70	-	65	65	-	20
LS-2-c-3ply-2SP	PT	70	-	65	65	-	20
LS-4-m-3ply-1SP	PT	120	-	120	120	-	-
LS-4-m-5ply-1SP	PT	120	-	120	120	-	-
LS-5-m-3ply-2SP	PT	64	-	72	72	-	40
LS-5-m-5ply-2SP	PT	64	-	72	72	-	40
LS-8-m-3ply-1SP	PT	64	-	76	76	-	-
LS-8-m-3ply-1SP*	PT	64	-	76	76	-	-
LS-8-c-3ply-1SP	PT	64	-	176	176	-	40
LS-8-m-3ply-2SP	PT	40	-	60	60	-	40
LS-8-m-5ply-1SP	PT	64	-	76	76	-	-
LS-8-m-5ply-2SP	PT	40	-	60	60	-	40
LS-16-m-3ply-2SP	PT	120	-	180	180	30	25
LS-16-c-3ply-2SP	PT	120	-	180	180	30	25
LS-32-m-3ply-2SP	PT	120	-	300	300	40	20
LS-32-c-3ply-2SP	PT	120	-	300	300	40	20
LW-1-m-3ply-2SP	FT	-	-	50	150	-	20
LW-2-m-3ply-2SP	FT	-	100	50	50	30	25
LW-2-c-3ply-2SP	FT	-	100	50	50	30	25
LW-4-m-5ply-1SP	FT	-	100	175	175	30	25
LW-6-m-3ply-1SP	FT	-	120	144	144	30	25
LW-6-m-5ply-2SP	FT	-	80	60	60	30	25
LW-8-m-3ply-2SP	FT	-	80	60	60	30	25
LW-10-m-5ply-1SP	FT	-	50	188	188	30	25
LW-12-m-3ply-1SP	FT	-	80	80	80	30	25
LW-12-m-3ply-1SP*	FT	-	80	80	80	30	25
LW-12-c-3ply-1SP	FT	-	80	180	180	30	25
LW-16-m-3ply-2SP	FT	-	120	150	150	-	-
LW-16-c-3ply-2SP	FT	-	120	150	150	-	-
LW-32-m-3ply-2SP	FT	-	120	270	270	-	-

Series Name	Screw Type	a ₁₋₉₀ or S _p	a _{1-45/33} or S _p	a _{1T} or a _L	a _{1C} or a _L	a ₂ or S _Q	a _{2T} or a _{2C} or e
LW-32-c-3ply-2SP	FT	-	120	270	270	-	-
LC-WSSW-8-m-3ply-1SP	PT+FT	120	120	90	90	30	25
LC-WSSW-8-m-3ply-1SP*	PT+FT	120	120	90	90	30	25
LC-WSSW-8-c-3ply-1SP	PT+FT	120	120	190	190	30	25
LC-WSSW-8-m-5ply-1SP	PT+FT	170	90	80	80	30	25
LC-SWWS-8-m-3ply-1SP	PT+FT	120	120	90	90	30	25
LC-SWWS-8-m-5ply-1SP	PT+FT	80	160	80	80	30	25
LC-SWSWS-10-m-3ply-1SP	PT+FT	80	120	80	80	30	25
LC-SWSWS-10-c-3ply-1SP	PT+FT	80	120	180	180	30	25
LC-SWSWS-10-m-5ply-1SP	PT+FT	60	160	65	65	30	25
LC-WSSW-16-m-3ply-2SP	PT+FT	120	120	150	150	30	25
LC-WSSW-16-c-3ply-2SP	PT+FT	120	120	150	150	30	25
LC-WSSW-32-m-3ply-2SP	PT+FT	120	120	270	270	30	25
LC-WSSW-32-c-3ply-2SP	PT+FT	120	120	270	270	30	25
BS-1-m-3ply-2SP	PT	-	-	100	100	-	50
BS-1-c-3ply-2SP	PT	-	-	100	100	-	50
BS-2-m-3ply-2SP	PT	-	70	65	65	-	50
BS-2-c-3ply-2SP	PT	-	70	65	65	-	50
BS-8-m-3ply-1SP	PT		128	76	76	-	50
BS-8-c-3ply-1SP	PT		128	176	176	-	50
BS-16-m-3ply-2SP	PT		120	150	150	-	50
BS-16-c-3ply-2SP	PT		120	150	150	-	50
BS-32-m-3ply-2SP	PT		120	300	300	-	50
BS-32-c-3ply-2SP	PT		120	300	300	-	50
BW-1-m-3ply-2SP	FT	-	-	50	150	-	53
BW-2-m-3ply-2SP	FT	-	-	30	170	-	53
BW-2-c-3ply-2SP	FT	-	-	30	170	-	53
BW-4-m-3ply-1SP	FT	-	-	110	200	-	53
BW-8-m-3ply-1SP	FT	-	80	60	110	-	53
BW-8-m-3ply-1SP*	FT	-	80	60	110	-	53
BW-8-c-3ply-1SP	FT	-	80	160	110	-	53
BW-8-m-3ply-2SP	FT	See Appendix D.1		35	35	-	53
BW-16-m-3ply-2SP	FT	-	90	90	135	-	53
BW-16-c-3ply-2SP	FT	-	90	90	135	-	53
BW-20-m-3ply-2SP	FT	-	90	90	90	-	53
BW-20-c-3ply-2SP	FT	-	90	90	90	-	53
Minimum Requirement (ETA)	PT & FT	5d = 40	5d = 40	6d = 48 15d=	6d = 48 15d=	2.5d= 20	2.5d = 20
Laterally Loaded (CCMC)	PT	12d=96	-	120	120	5d=40	5d=40
Laterally Loaded (CCMC)	FT	5d=40	-	12d=96	-	3d=24	3d=24
Axially Loaded (CCMC)	FT	-	5d=40	5d=40	-	2.5d=20	-

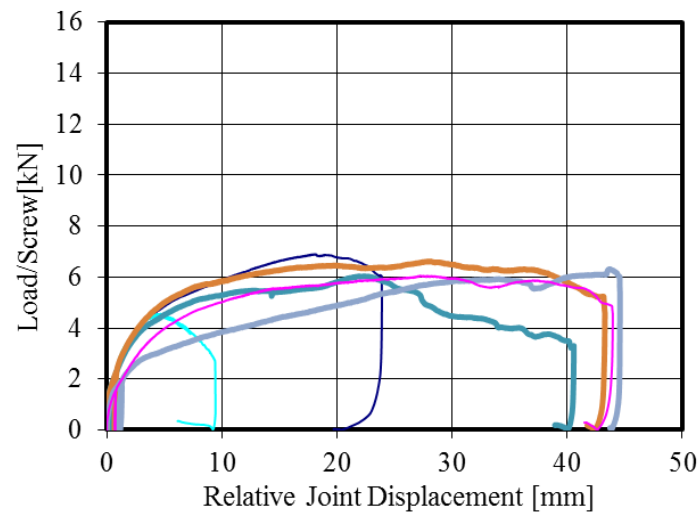
* All dimensions are in mm

Appendix C Detailed test results of mini-sized specimens with 1 and 2 planes (Mi-1 & Mi-2)

C.1 Mi-1: Spline joints



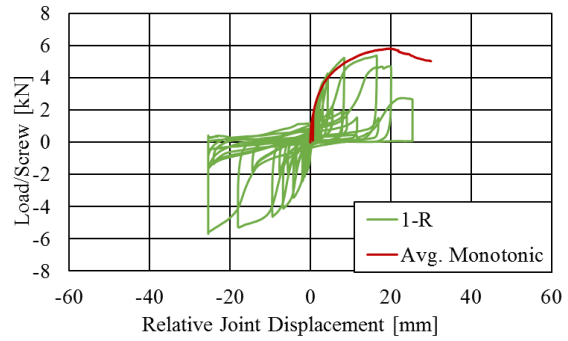
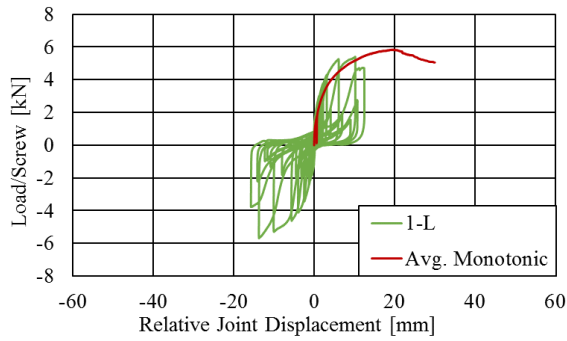
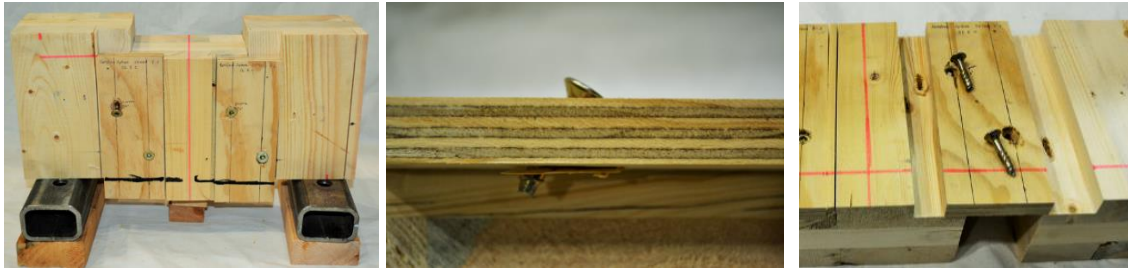
SS-2-m-3ply-2SP



Spec.	F_{max} [kN]	F_Y [kN]	d_{Fmax} [mm]	$d_{F,Y}$ [mm]	μ (-)	k [kN/mm]
1	6.9	6.0	18.0	2.4	7.6	2.3
2	6.0	5.2	22.0	1.9	11.4	1.8
3	6.6	5.8	28.0	2.1	13.2	1.9
4	6.3	4.7	44.0	4.3	10.2	0.8
5	6.0	5.2	27.0	4.0	6.7	1.0
Avg.	6.4	5.4	27.8	3.0	9.8	1.6

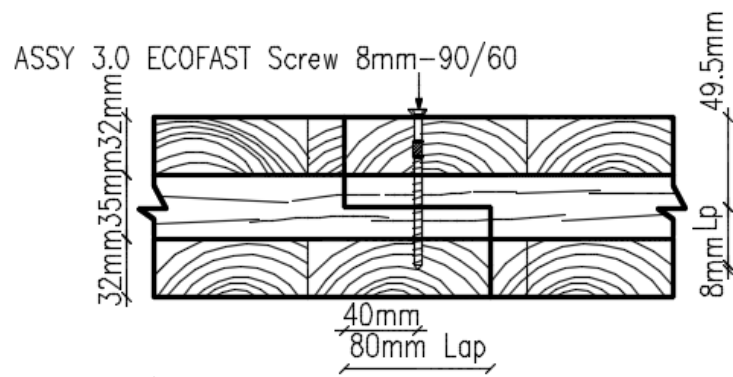
Note: All values are per screw

SS-2-c-3ply-2SP

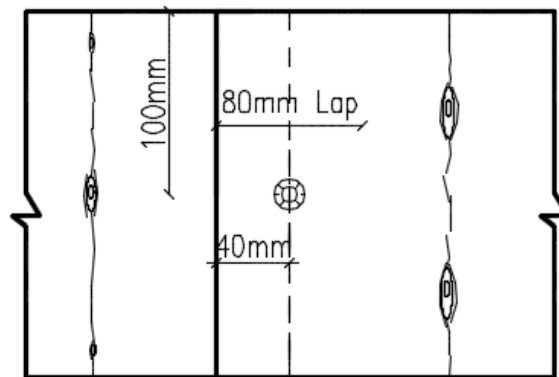


Spec.	F_{\max} [kN]	F_Y [kN]	$d_{F\max}$ [mm]	$d_{F,Y}$ [mm]	μ (-)	k [kN/mm]
1-L	5.4 (5.6)	4.4 (4.3)	10.0 (13.0)	1.2 (2.3)	8.6 (5.6)	2.8 (1.7)
1-R	5.4 (5.6)	4.3 (4.9)	16.0 (25.0)	2.8 (4.3)	5.7 (5.8)	1.5 (1.1)
1	5.4 (5.6)	4.4 (4.6)	13.0 (19.0)	2.0 (3.3)	7.1 (5.7)	2.2 (1.4)
2-L	6.8 (5.4)	5.5 (4.1)	13.0 (14.0)	3.1 (2.0)	4.2 (7.0)	2.0 (1.5)
2-R	6.8 (5.5)	5.0 (4.3)	18.0 (10.0)	2.8 (0.7)	6.3 (13.4)	1.6 (8.2)
2	6.8 (5.4)	5.3 (4.2)	15.5 (12.0)	3.0 (1.4)	5.2 (10.2)	1.8 (4.8)
3-L	5.9 (4.7)	4.5 (3.8)	16.0 (12.0)	2.4 (2.6)	6.7 (4.7)	1.8 (1.4)
3-R	5.9 (4.7)	4.6 (4.1)	14.0 (6.8)	2.3 (2.0)	6.0 (3.4)	1.8 (2.0)
3	5.9 (4.7)	4.6 (4.0)	15.0 (9.4)	2.4 (2.3)	6.4 (4.0)	1.8 (1.7)
4-L	6.8 (5.6)	5.2 (5.3)	13.0 (17.0)	3.4 (2.7)	3.8 (6.4)	1.4 (1.7)
4-R	6.8 (5.8)	5.3 (4.3)	14.0 (18.0)	2.8 (2.2)	4.9 (8.2)	1.7 (1.9)
4	6.8 (5.7)	5.2 (4.8)	13.5 (17.5)	3.1 (2.4)	4.4 (7.3)	1.5 (1.8)
5-R	5.9 (4.7)	4.7 (3.9)	9.2 (7.7)	1.9 (1.4)	4.7 (5.4)	2.2 (2.8)
5	5.9 (4.7)	4.7 (3.9)	9.2 (7.7)	1.9 (1.4)	4.7 (5.4)	2.2 (2.8)
6-L	7.0 (5.7)	5.2 (4.5)	13.0 (16.0)	1.8 (2.5)	7.4 (6.3)	2.6 (1.4)
6-R	7.2 (6.0)	5.4 (4.5)	14.0 (17.0)	1.9 (2.4)	7.4 (7.0)	2.4 (1.5)
6	7.1 (5.8)	5.3 (4.5)	13.5 (16.5)	1.8 (2.5)	7.4 (6.7)	2.5 (1.5)
Avg.	6.3 (5.3)	4.9 (4.3)	13.3 (13.7)	2.4 (2.2)	5.9 (6.5)	2.0 (1.8)

C.2 Mi-1: Lap joints with STS in shear

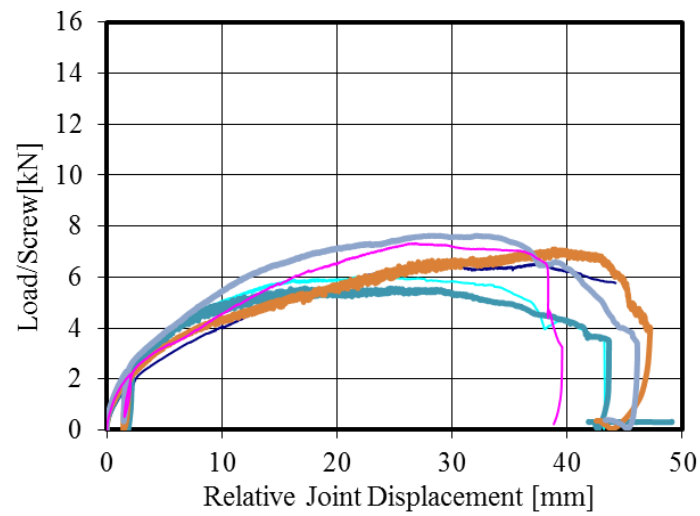


ELEVATION VIEW



TOP VIEW

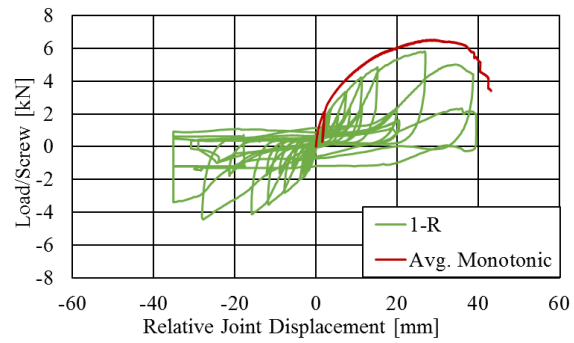
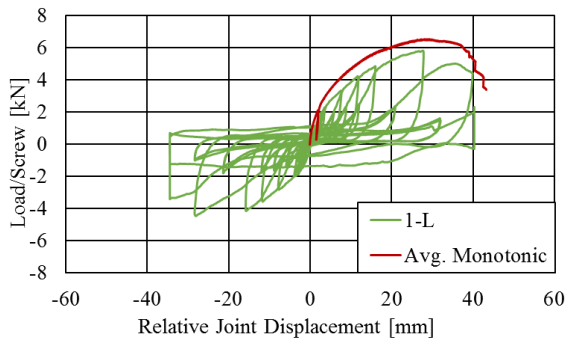
LS-1-m-3ply-2SP



Spec.	F_{\max} [kN]	F_Y [kN]	$d_{F_{\max}}$ [mm]	$d_{F,Y}$ [mm]	μ (-)	k [kN/mm]
1	6.5	5.2	37.0	7.7	4.8	0.5
2	6.0	5.3	23.0	4.9	4.7	0.9
3	5.5	4.9	19.0	4.8	4.0	0.8
4	6.9	4.8	39.0	7.4	5.3	0.5
5	7.6	6.3	29.0	6.2	4.7	0.8
6	7.3	5.9	27.0	7.5	3.6	0.6
Avg.	6.6	5.4	29.0	6.4	4.5	0.7

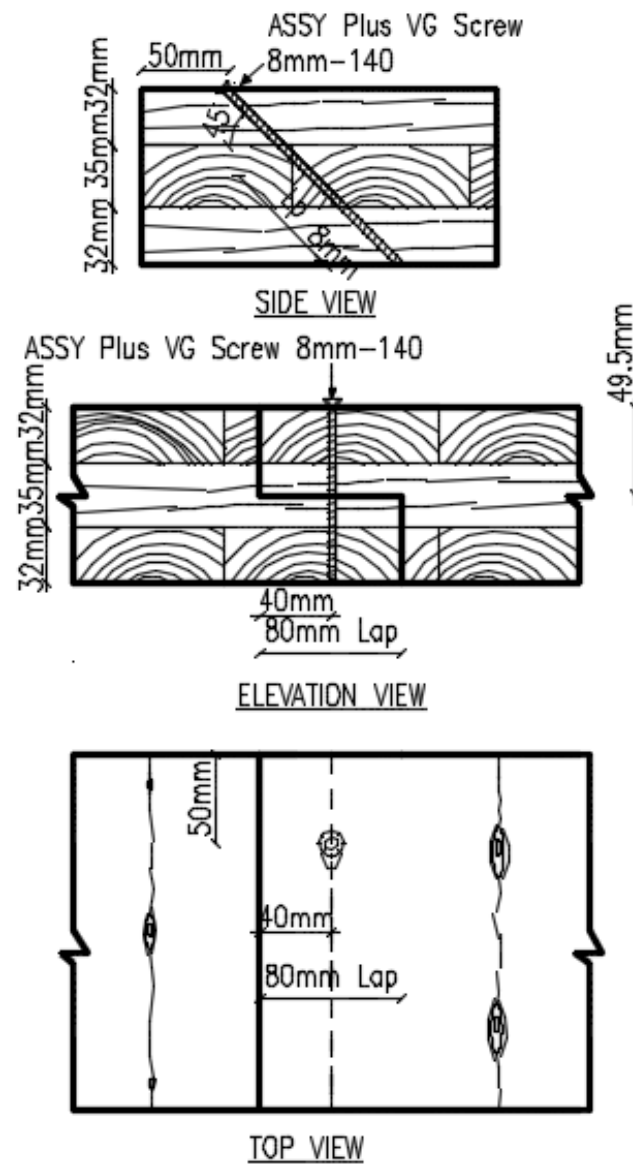
Note: All values are per screw

LS-1-c-3ply-2SP

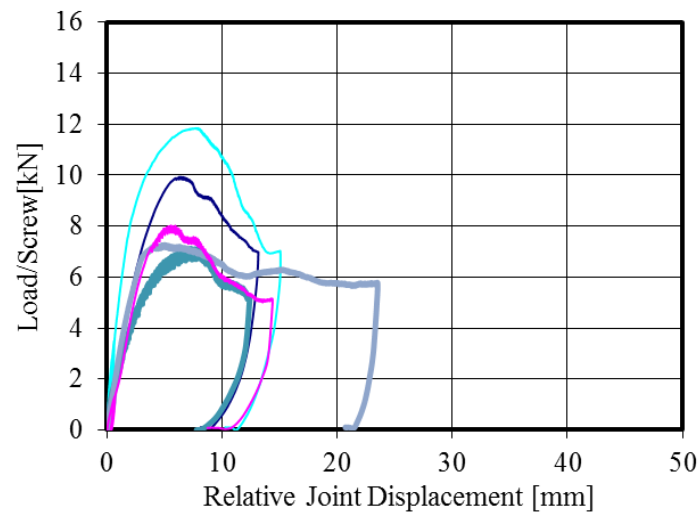


Spec.	F_{max} [kN]	F_Y [kN]	d_{Fmax} [mm]	$d_{F,Y}$ [mm]	μ (-)	k [kN/mm]
1-L	5.8 (4.3)	3.7 (2.8)	26.0 (28.0)	5.8 (4.5)	4.5 (6.2)	0.6 (0.6)
1-R	5.8 (4.3)	3.6 (2.8)	26.0 (28.0)	5.6 (4.4)	4.7 (6.4)	0.6 (0.6)
1	5.8 (4.3)	3.7 (2.8)	26.0 (28.0)	5.7 (4.4)	4.6 (6.3)	0.6 (0.6)
2-L	5.3 (4.0)	3.6 (2.8)	25.0 (27.0)	4.5 (5.3)	5.5 (5.1)	1.2 (0.7)
2-R	5.2 (3.9)	3.5 (2.7)	25.0 (22.0)	5.1 (5.5)	4.9 (4.0)	1.0 (0.6)
2	5.2 (4.0)	3.6 (2.7)	25.0 (24.5)	4.8 (5.4)	5.2 (4.5)	1.1 (0.7)
3-L	5.0 (4.5)	3.3 (2.9)	25.0 (27.0)	5.2 (3.9)	4.8 (7.0)	0.7 (0.8)
3-R	5.0 (4.4)	3.3 (2.9)	25.0 (21.0)	5.7 (3.1)	4.4 (6.7)	0.6 (0.8)
3	5.0 (4.4)	3.3 (2.9)	25.0 (24.0)	5.4 (3.5)	4.6 (6.8)	0.6 (0.8)
4-L	6.3 (10.3)	4.5 (8.2)	13.0 (8.1)	2.2 (3.0)	6.0 (2.7)	2.1 (2.8)
4-R	6.3 (10.3)	4.5 (9.1)	13.0 (3.8)	2.2 (1.6)	6.0 (2.3)	2.1 (5.1)
4	6.3 (10.3)	4.5 (8.6)	13.0 (6.0)	2.2 (2.3)	6.0 (2.5)	2.1 (4.0)
5-L	5.6 (6.4)	3.5 (4.3)	25.0 (14.0)	3.4 (2.3)	7.3 (6.2)	1.4 (1.9)
5-R	5.5 (6.4)	3.7 (4.3)	25.0 (14.0)	3.7 (2.3)	6.8 (6.1)	1.5 (1.7)
4	5.6 (6.4)	3.6 (4.3)	25.0 (14.0)	3.6 (2.3)	7.0 (6.2)	1.5 (1.8)
6-L	6.2 (5.9)	3.9 (3.9)	26.0 (27.0)	6.0 (4.3)	4.3 (6.3)	0.6 (0.8)
6-R	6.2 (5.9)	3.9 (3.9)	26.0 (27.0)	6.1 (4.4)	4.3 (6.2)	0.6 (0.8)
6	6.2 (5.9)	3.9 (3.9)	26.0 (27.0)	6.1 (4.3)	4.3 (6.2)	0.6 (0.8)
Avg.	5.7 (5.9)	3.8 (4.2)	23.3 (20.6)	4.6 (3.7)	5.3 (5.4)	1.1 (1.4)

C.3 Mi-1: Lap joints with STS in withdrawal



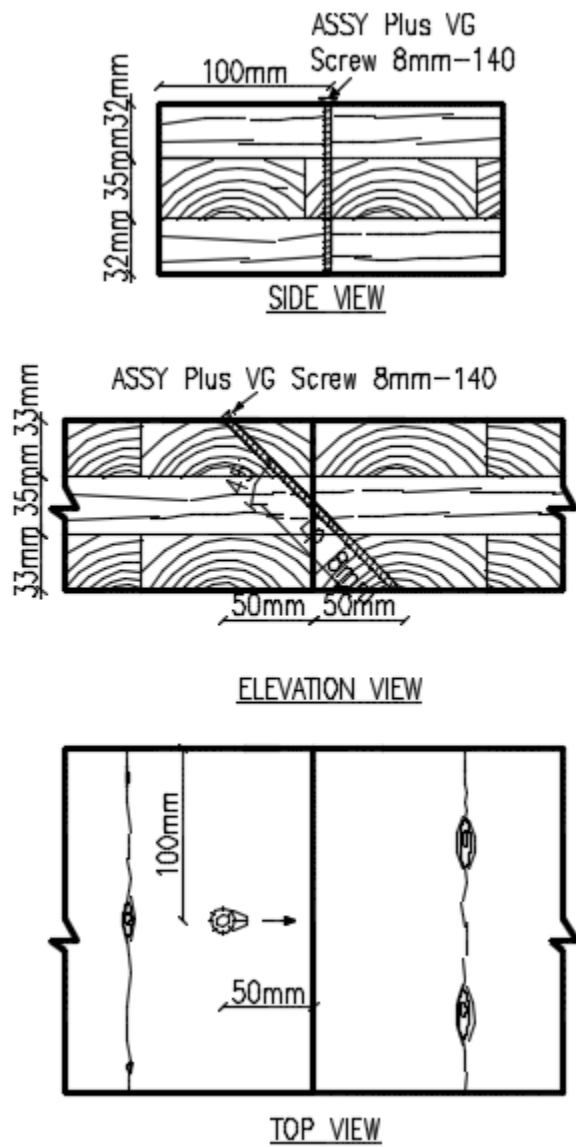
LW-1-m-3ply-2SP



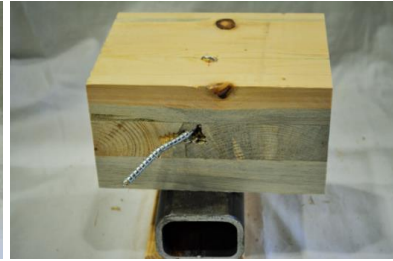
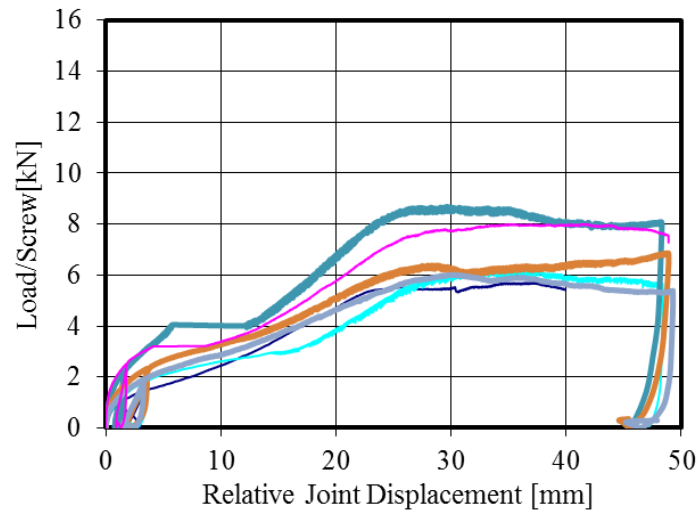
Spec.	F_{max} [kN]	F_Y [kN]	d_{Fmax} [mm]	$d_{F,Y}$ [mm]	μ (-)	k [kN/mm]
1	9.9	8.5	6.4	3.3	2.0	2.5
2	11.8	10.0	7.8	2.0	3.9	5.9
3	7.1	5.9	7.9	2.6	3.1	2.1
4	7.3	6.5	4.9	2.3	2.1	3.1
5	8.0	7.1	5.6	3.5	1.6	1.8
Avg.	8.8	7.6	6.5	2.7	2.5	3.1

Note: All values are per screw

C.4 Mi-1: Butt joints with STS in shear



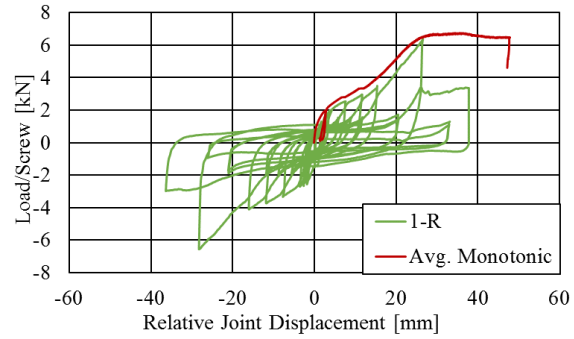
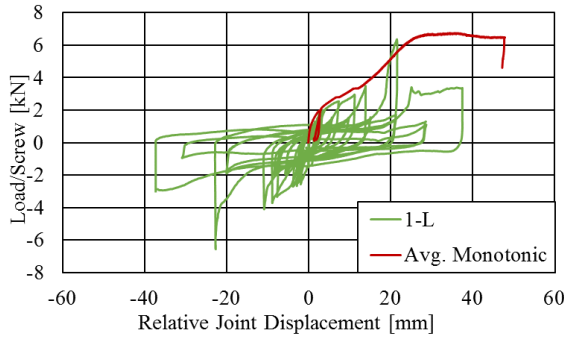
BS-1-m-3ply-2SP



Spec.	F_{max} [kN]	F_Y [kN]	d_{Fmax} [mm]	$d_{F, Y}$ [mm]	μ (-)	k [kN/mm]
1	5.7	4.8	37.0	19.1	1.9	0.2
2	6.2	4.3	33.0	14.3	2.3	0.2
3	8.6	5.7	31.0	7.6	4.1	0.9
4	6.8	4.8	48.0	7.5	6.4	0.4
5	6.0	4.6	30.0	11.5	2.6	0.3
6	8.0	4.5	41.0	7.5	5.5	0.5
Avg.	6.9	4.8	36.7	11.2	3.8	0.4

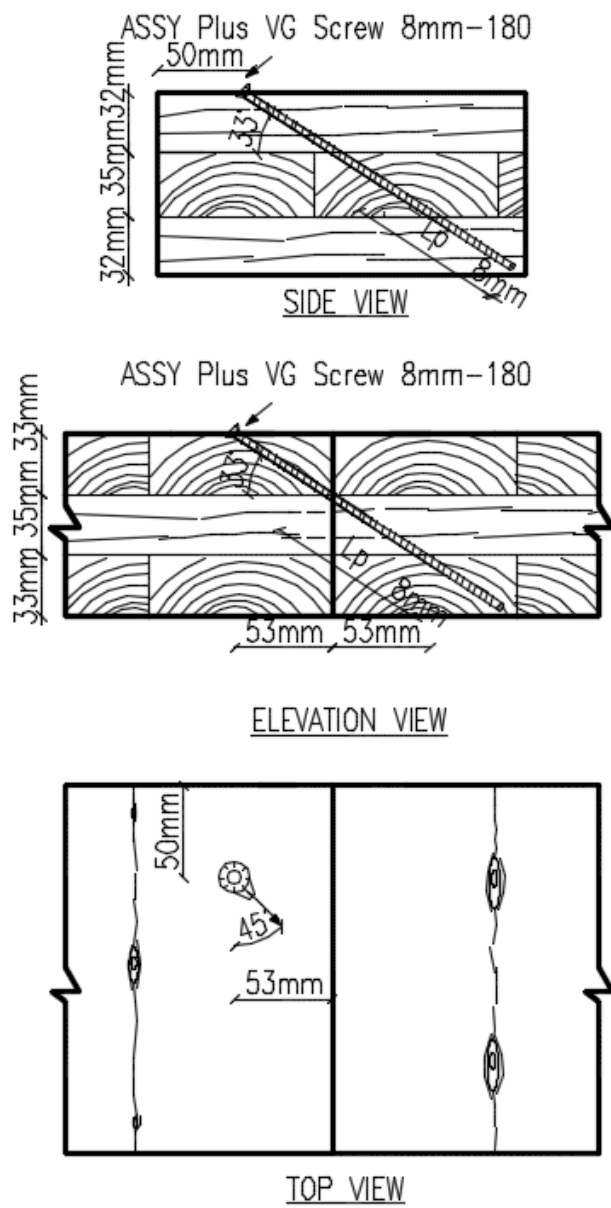
Note: All values are per screw

BS-1-c-3ply-2SP

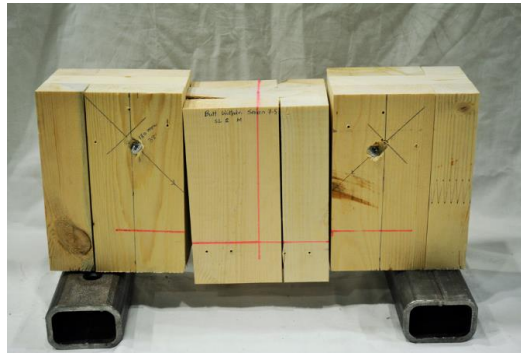
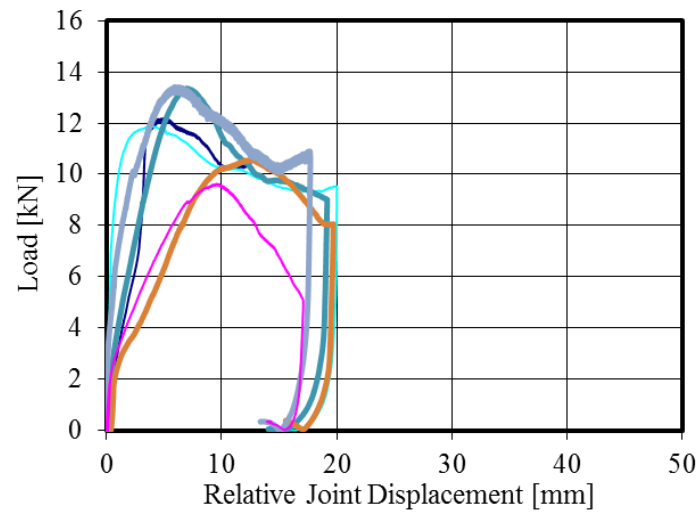


Spec.	F_{\max} [kN]	F_Y [kN]	$d_{F\max}$ [mm]	$d_{F,Y}$ [mm]	μ (-)	k [kN/mm]
1-L	6.5 (6.7)	4.2 (4.1)	21.0 (22.0)	12.1 (5.6)	1.7 (3.9)	0.3 (0.7)
1-R	6.5 (6.7)	4.1 (4.1)	26.0 (28.0)	11.7 (5.3)	2.2 (5.3)	0.3 (0.7)
1	6.5 (6.7)	4.1 (4.1)	23.5 (25.0)	11.9 (5.5)	2.0 (4.6)	0.3 (0.7)
2-L	5.3 (7.3)	3.2 (4.5)	29.0 (30.0)	8.4 (12.2)	3.4 (2.5)	0.3 (0.3)
2-R	5.2 (7.2)	4.5 (4.5)	37.0 (27.0)	11.8 (11.7)	3.1 (2.3)	0.3 (0.3)
2	5.2 (7.3)	3.8 (4.5)	33.0 (28.5)	10.1 (12.0)	3.3 (2.4)	0.3 (0.3)
3-L	5.6 (5.2)	3.6 (3.0)	18.0 (36.0)	6.7 (9.1)	2.7 (4.0)	0.5 (0.3)
3-R	5.6 (5.2)	3.5 (3.1)	25.0 (36.0)	6.8 (9.4)	3.7 (3.8)	0.5 (0.3)
3	5.6 (5.2)	3.5 (3.1)	21.5 (36.0)	6.8 (9.2)	3.2 (3.9)	0.5 (0.3)
4-L	5.9 (6.2)	3.6 (4.6)	34.0 (32.0)	10.3 (10.4)	3.3 (3.1)	0.3 (0.4)
4-R	5.6 (6.2)	3.7 (3.9)	36.0 (37.0)	10.4 (8.4)	3.5 (4.4)	0.3 (0.4)
4	5.7 (6.2)	3.7 (4.3)	35.0 (34.5)	10.4 (9.4)	3.4 (3.7)	0.3 (0.4)
5-L	6.5 (-)	4.1 (-)	35.0 (-)	13.5 (-)	2.6 (-)	0.2 (-)
5-R	6.7 (5.2)	4.1 (3.1)	30.0 (27.0)	13.2 (3.7)	2.3 (7.3)	0.2 (0.5)
5	6.6 (5.2)	4.1 (3.1)	32.5 (27.0)	13.3 (3.7)	2.4 (7.3)	0.2 (0.5)
6-L	6.4 (6.2)	4.1 (3.9)	18.0 (26.0)	12.8 (8.1)	1.4 (3.2)	0.3 (0.4)
6-R	6.5 (6.4)	4.1 (4.0)	27.0 (27.0)	14.6 (8.6)	1.9 (3.1)	0.2 (0.4)
6	6.4 (6.3)	4.1 (3.9)	22.5 (26.5)	13.7 (8.3)	1.6 (3.2)	0.2 (0.4)
Avg.	6.0 (6.2)	3.9 (3.8)	28.0 (29.6)	11.0 (8.0)	2.6 (4.2)	0.3 (0.4)

C.5 Mi-1: Butt joints with STS in withdrawal



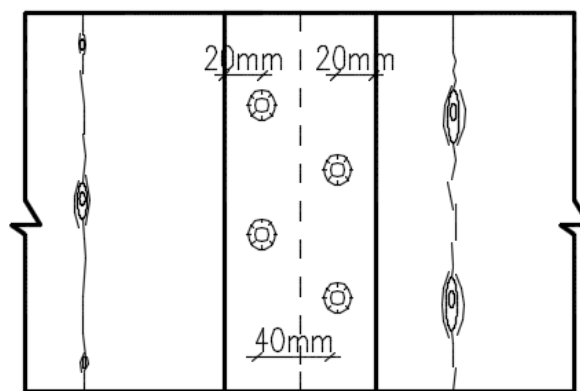
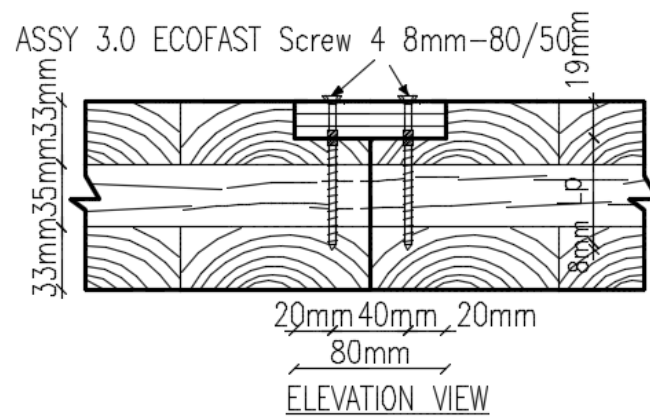
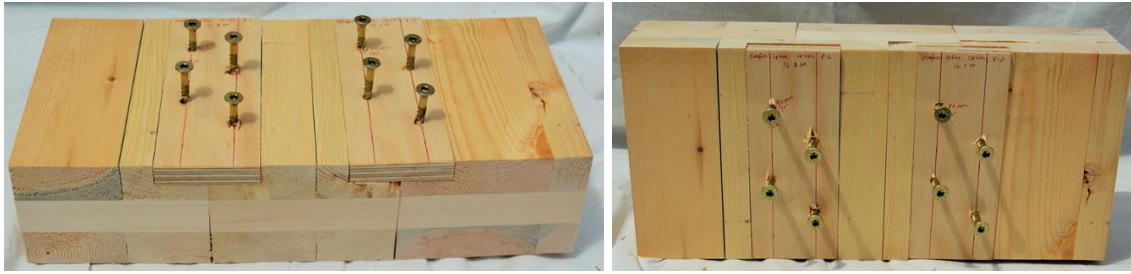
BW-1-m-3ply-2SP



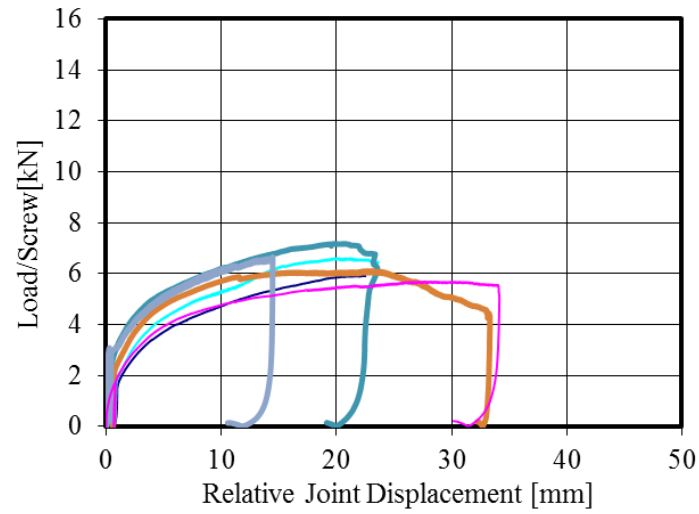
Spec.	F_{\max} [kN]	F_Y [kN]	$d_{F\max}$ [mm]	$d_{F,Y}$ [mm]	μ (-)	k [kN/mm]
1	12.1	11.3	4.8	4.3	1.1	2.6
2	11.9	11.0	3.8	1.0	3.7	14.9
3	13.4	10.9	7.0	3.1	2.3	3.3
4	10.6	7.3	12.5	5.1	2.5	1.3
5	13.4	11.5	6.2	1.2	5.0	7.2
6	9.6	7.3	9.7	3.0	3.2	2.0
Avg.	11.8	9.9	7.3	3.0	3.0	5.2

Note: All values are per screw

C.6 Mi-2: Spline joints



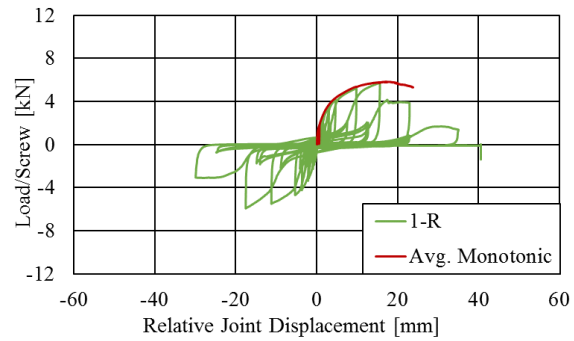
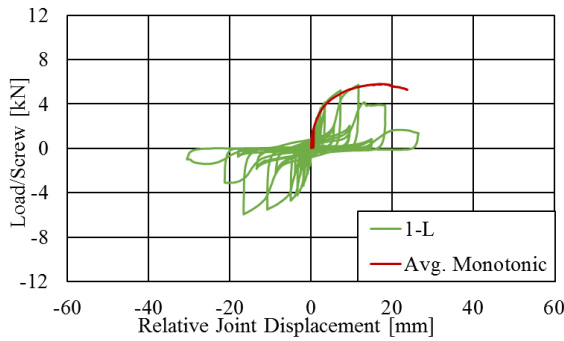
SS-4-m-3ply-2SP



Spec.	F_{max} [kN]	F_Y [kN]	d_{Fmax} [mm]	$d_{F,Y}$ [mm]	μ (-)	k [kN/mm]
1	6.0	5.2	27.0	4.1	6.5	1.0
2	6.6	5.9	20.0	4.1	4.9	1.1
3	7.2	6.2	20.0	1.4	13.8	3.1
4	6.1	5.5	23.0	2.0	11.7	1.8
5	5.7	5.1	28.0	3.2	8.8	1.3
Avg.	6.3	5.6	23.6	3.0	9.1	1.7

Note: All values are per screw

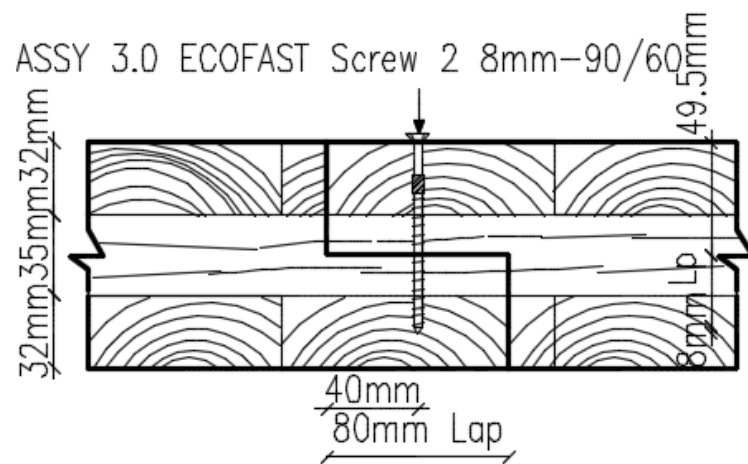
SS-4-c-3ply-2SP



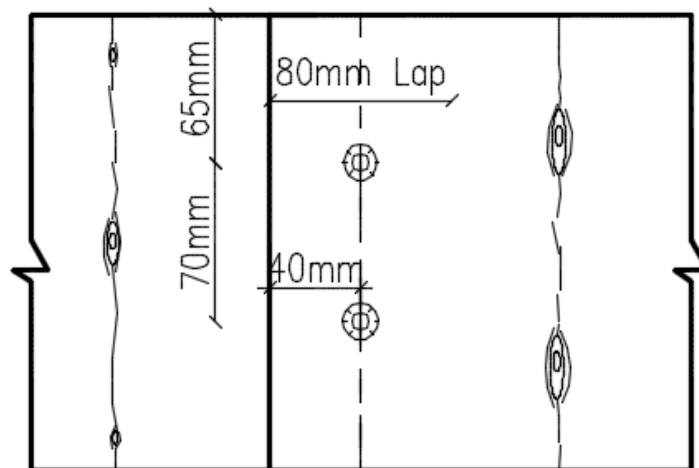
Spec.	F_{\max} [kN]	F_Y [kN]	$d_{F\max}$ [mm]	$d_{F,Y}$ [mm]	μ (-)	k [kN/mm]
1-L	5.8 (6.5)	4.4 (4.8)	11.0 (15.0)	2.2 (2.2)	5.0 (6.7)	1.6 (1.8)
1-R	5.7 (5.8)	4.1 (4.5)	15.0 (17.0)	2.3 (2.5)	6.5 (6.9)	1.4 (1.6)
1	5.7 (6.2)	4.2 (4.6)	13.0 (16.0)	2.3 (2.4)	5.8 (6.8)	1.5 (1.7)
2-L	5.7 (6.0)	4.4 (4.6)	11.0 (14.0)	2.5 (2.0)	4.4 (6.9)	1.6 (2.0)
2-R	5.7 (5.8)	4.4 (4.5)	11.0 (12.0)	2.3 (2.0)	4.8 (6.1)	1.6 (2.2)
2	5.7 (5.9)	4.4 (4.5)	11.0 (13.0)	2.4 (2.0)	4.6 (6.5)	1.6 (2.1)
3-L	6.3 (6.5)	4.5 (5.5)	16.0 (14.0)	5.4 (0.4)	3.0 (34.6)	0.9 (13.1)
3-R	6.3 (6.6)	4.9 (5.2)	11.0 (15.0)	1.2 (0.6)	8.9 (23.8)	4.7 (8.9)
3	6.3 (6.5)	4.7 (5.3)	13.5 (14.5)	3.3 (0.5)	5.9 (29.2)	2.8 (11.0)
4-L	5.6 (6.0)	4.4 (4.8)	17.0 (22.0)	2.0 (2.0)	8.6 (10.8)	2.1 (2.6)
4-R	5.9 (5.8)	4.4 (5.1)	9.0 (3.3)	1.7 (0.7)	5.4 (4.9)	2.5 (7.9)
4	5.8 (5.9)	4.4 (5.0)	13.0 (12.7)	1.8 (1.4)	7.0 (7.9)	2.3 (5.3)
5-L	6.4 (6.0)	4.7 (4.9)	11.0 (13.0)	1.8 (1.8)	6.3 (7.2)	2.1 (2.6)
5-R	6.3 (5.8)	4.4 (4.7)	14.0 (9.5)	3.1 (2.1)	4.5 (4.6)	1.4 (2.2)
5	6.3 (5.9)	4.5 (4.8)	12.5 (11.3)	2.4 (1.9)	5.4 (5.9)	1.7 (2.4)
Avg.	6.0 (6.1)	4.5 (4.9)	12.6 (13.5)	2.4 (1.6)	5.7 (11.3)	2.0 (4.5)

Note: All values are per screw, L=left side, R=right side of the connection, negative envelope values within parenthesis

C.7 Mi-2: Lap joints with STS in shear

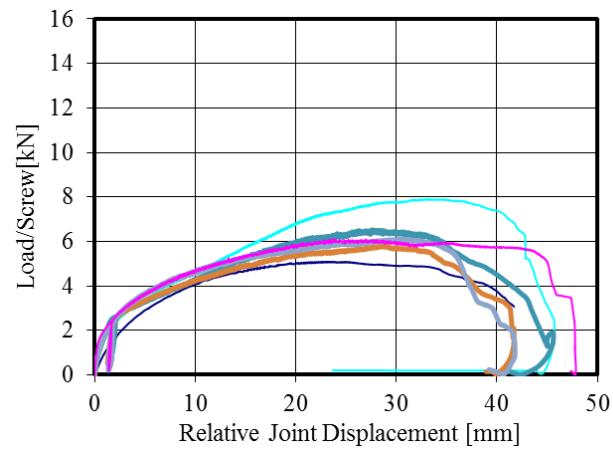


ELEVATION VIEW



TOP VIEW

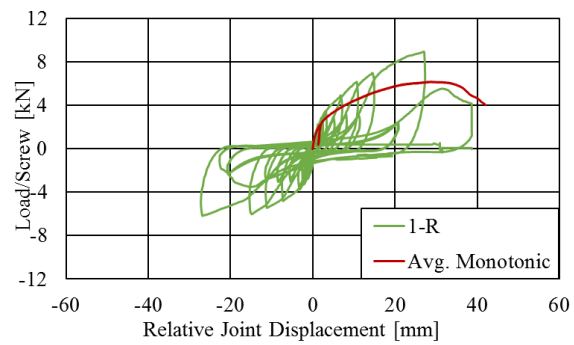
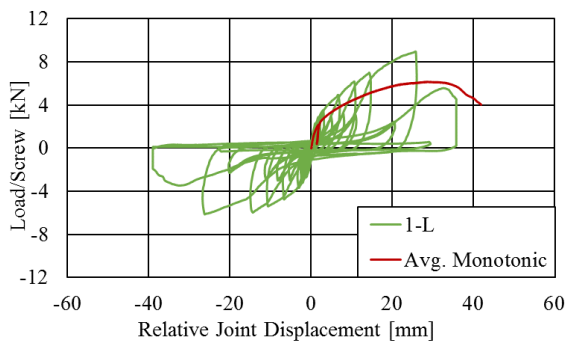
LS-2-m-3ply-2SP



Spec.	F_{\max} [kN]	F_Y [kN]	$d_{F\max}$ [mm]	$d_{F,Y}$ [mm]	μ (-)	k [kN/mm]
1	5.1	4.4	23.0	6.0	3.8	0.6
2	7.9	6.2	34.0	7.8	4.3	0.7
3	6.5	5.1	28.0	4.3	6.5	0.9
4	5.8	4.7	29.0	3.7	7.8	1.0
5	6.1	5.0	31.0	4.1	7.6	1.0
6	6.0	5.1	27.0	3.6	7.6	1.1
Avg.	6.2	5.1	28.7	4.9	6.3	0.9

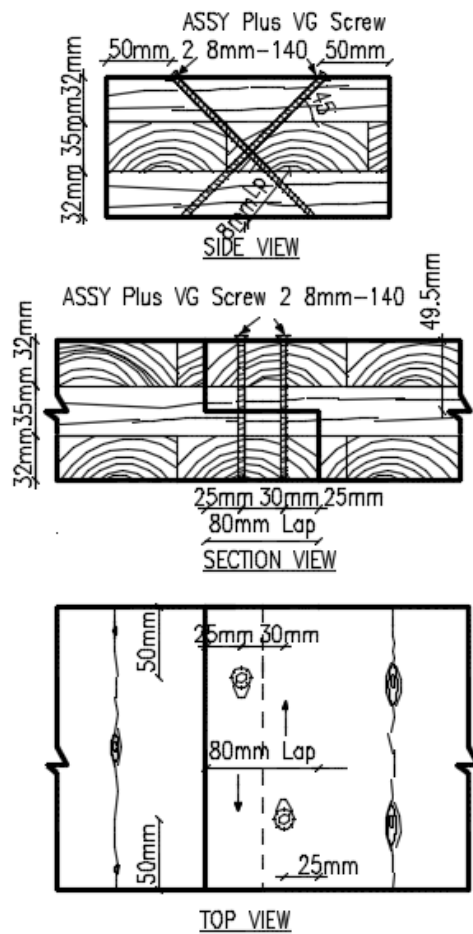
Note: All values are per screw

LS-2-c-3ply-2SP

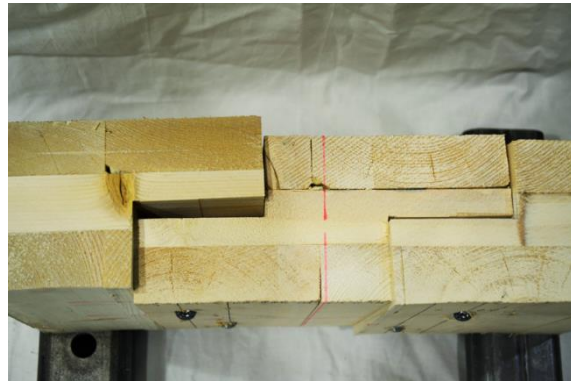
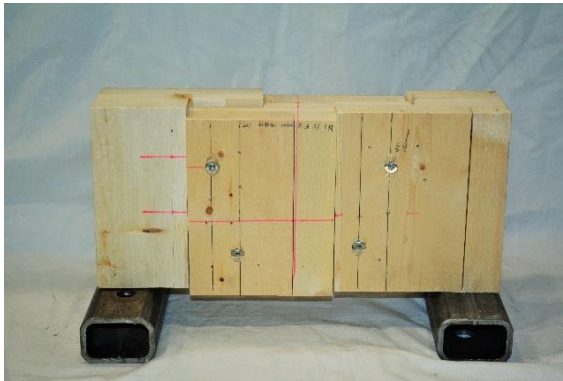
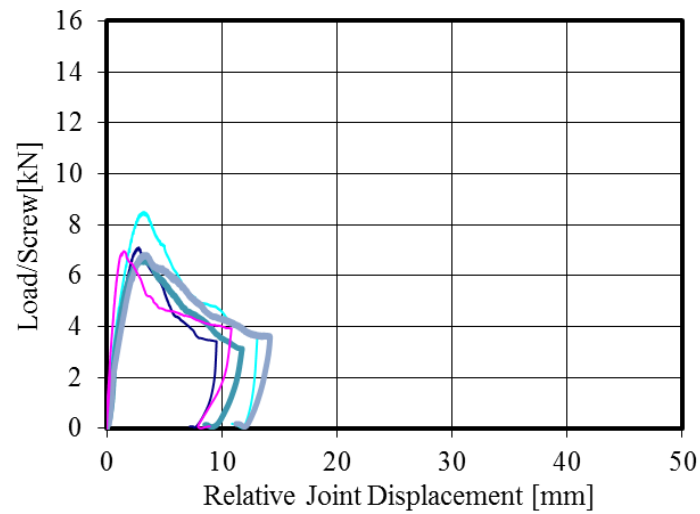


Spec.	F_{\max} [kN]	F_Y [kN]	$d_{F\max}$ [mm]	$d_{F,Y}$ [mm]	μ (-)	k [kN/mm]
1-L	9.1 (6.2)	5.8 (4.3)	25.0 (26.0)	5.4 (6.5)	4.6 (4.0)	1.0 (0.7)
1-R	9.2 (6.4)	5.8 (4.2)	26.0 (26.0)	5.8 (6.8)	4.5 (3.8)	1.0 (0.1)
1	9.2 (6.3)	5.8 (4.2)	25.5 (26.0)	5.6 (6.7)	4.6 (3.9)	1.0 (0.4)
2-L	6.3 (7.0)	4.3 (4.8)	26.0 (24.0)	4.5 (3.1)	5.8 (7.8)	0.9 (1.6)
2-R	6.2 (6.4)	4.1 (4.7)	26.0 (24.0)	3.7 (2.7)	7.0 (8.7)	1.1 (1.7)
2	6.3 (6.7)	4.2 (4.8)	26.0 (24.0)	4.1 (2.9)	6.4 (8.3)	1.0 (1.7)
3-L	7.3 (6.9)	4.8 (6.1)	26.0 (28.0)	4.3 (2.5)	6.0 (11.2)	1.0 (1.6)
3-R	7.2 (6.9)	4.8 (6.2)	24.0 (20.0)	3.1 (4.0)	7.6 (5.0)	1.4 (3.5)
3	7.3 (6.9)	4.8 (6.2)	25.0 (24.0)	3.7 (3.3)	6.8 (8.1)	1.2 (2.5)
4-L	5.9 (5.5)	3.7 (3.7)	24.0 (25.0)	6.4 (6.2)	3.8 (4.1)	0.5 (0.6)
4-R	5.9 (5.6)	3.9 (3.6)	36.0 (26.0)	6.9 (6.6)	5.2 (4.0)	0.5 (0.5)
4	5.9 (5.6)	3.8 (3.6)	30.0 (25.5)	6.7 (6.4)	4.5 (4.0)	0.5 (0.6)
5-L	8.1 (6.9)	5.2 (4.6)	23.0 (26.0)	6.5 (4.8)	3.6 (5.4)	0.8 (0.9)
5-R	8.1 (6.7)	4.9 (4.9)	24.0 (25.0)	7.2 (3.8)	3.3 (6.6)	0.7 (1.3)
5	8.1 (6.8)	5.0 (4.7)	23.5 (25.5)	6.8 (4.3)	3.5 (6.0)	0.7 (1.1)
6-L	6.4 (7.0)	4.3 (4.7)	23.0 (25.0)	4.5 (2.3)	5.2 (10.8)	0.9 (1.5)
6-R	6.4 (7.0)	4.2 (4.7)	24.0 (26.0)	4.8 (3.5)	5.0 (7.3)	0.9 (1.3)
6	6.4 (7.0)	4.3 (4.7)	23.5 (25.5)	4.6 (2.9)	5.1 (9.1)	0.9 (1.4)
Avg.	7.2 (6.6)	4.6 (4.7)	25.6 (25.1)	5.3 (4.4)	5.1 (6.6)	0.9 (1.3)

C.8 Mi-2: Lap joints with STS in withdrawal



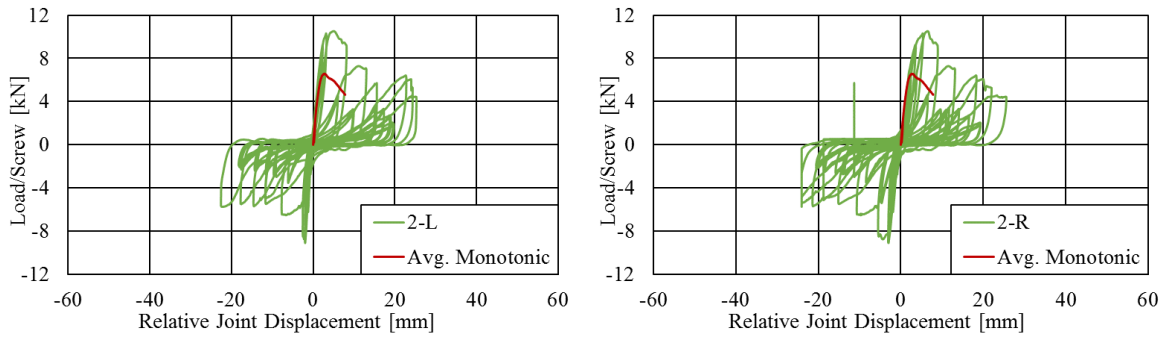
LW-2-m-3ply-2SP



Spec.	F_{\max} [kN]	F_Y [kN]	$d_{F\max}$ [mm]	$d_{F,Y}$ [mm]	μ (-)	k [kN/mm]
1	7.1	6.3	2.7	1.6	1.7	4.2
2	8.5	7.5	3.2	1.4	2.3	4.1
3	6.6	6.0	3.4	1.5	2.2	3.3
4	6.1	5.5	3.0	1.4	2.1	4.6
5	6.8	6.1	3.2	1.8	1.8	2.9
6	6.9	6.2	1.5	0.7	2.3	7.7
Avg.	7.0	6.2	2.8	1.4	2.1	4.5

Note: All values are per screw

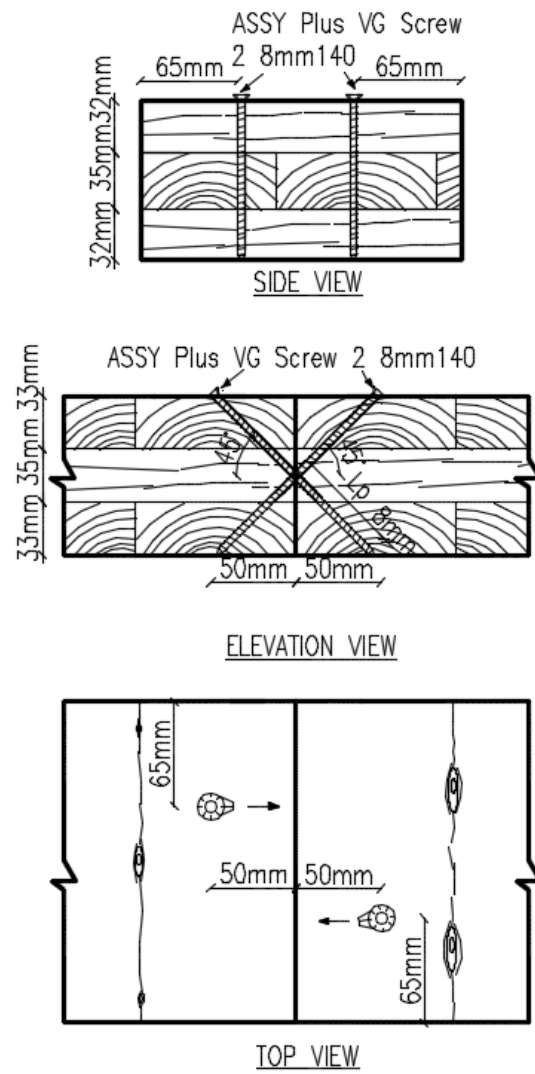
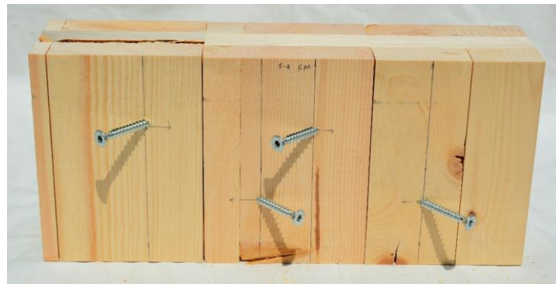
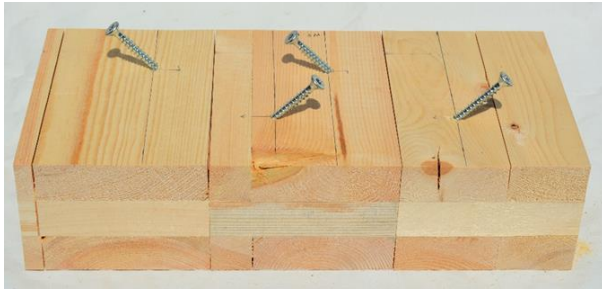
LW-2-c-3ply-2SP



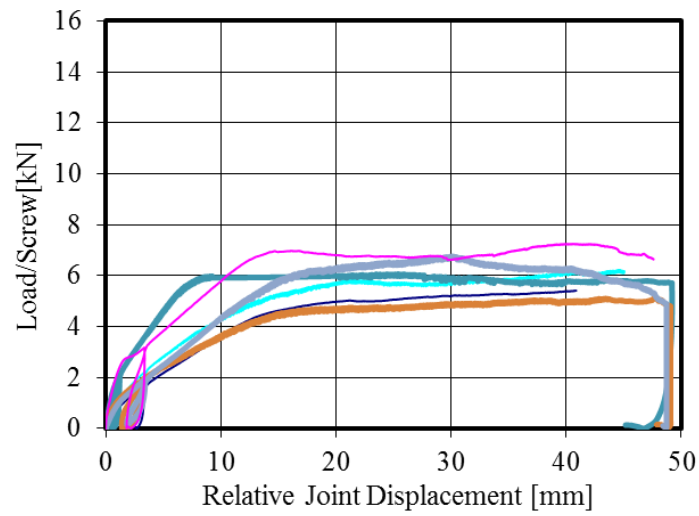
Spec.	F_{max} [kN]	F_Y [kN]	d_{Fmax} [mm]	$d_{F,Y}$ [mm]	μ (-)	k [kN/mm]
1-R	8.0 (10.1)	6.9 (9.3)	3.5 (3.3)	1.3 (1.9)	2.7 (1.7)	4.8 (6.1)
1	8.0 (10.1)	6.9 (9.3)	3.5 (3.3)	1.3 (1.9)	2.7 (1.7)	4.8 (6.1)
2-L	10.3 (9.1)	9.5 (8.4)	11.0 (1.9)	1.8 (2.0)	6.0 (1.0)	2.4 (5.5)
2-R	10.3 (9.1)	9.2 (8.2)	5.4 (2.9)	3.0 (2.6)	1.8 (1.1)	2.8 (3.4)
2	10.3 (9.1)	9.3 (8.3)	8.2 (2.4)	2.4 (2.3)	3.9 (1.1)	2.6 (4.4)
3-L	9.3 (7.7)	8.2 (7.1)	3.5 (2.0)	2.0 (2.5)	1.8 (0.8)	3.1 (3.3)
3-R	9.3 (7.5)	8.0 (6.9)	3.0 (1.5)	1.4 (1.6)	2.1 (0.9)	3.8 (4.5)
3	9.3 (7.6)	8.1 (7.0)	3.3 (1.8)	1.7 (2.0)	1.9 (0.9)	3.5 (3.9)
4-L	10.0 (9.3)	9.3 (8.5)	4.5 (1.6)	2.7 (1.0)	1.7 (1.6)	3.3 (8.4)
4-R	9.8 (9.3)	9.7 (8.6)	2.7 (2.3)	2.7 (1.6)	1.0 (1.4)	3.7 (4.6)
4	9.9 (9.3)	9.5 (8.5)	3.6 (2.0)	2.7 (1.3)	1.3 (1.5)	3.5 (6.5)
5-L	10.2 (7.8)	9.0 (6.7)	2.3 (3.0)	1.8 (1.2)	1.3 (2.5)	6.1 (4.7)
5-R	10.1 (-)	9.0 (-)	2.1 (-)	1.1 (-)	1.9 (-)	7.6 (-)
5	10.1 (7.8)	9.0 (6.7)	2.2 (3.0)	1.5 (1.2)	1.6 (2.5)	6.8 (4.7)
Avg.	9.5 (8.8)	8.6 (8.0)	4.2 (2.5)	1.9 (1.7)	2.3 (1.5)	4.3 (5.1)

Note: All values are per screw, L=left side, R=right side of the connection, negative envelope values within parenthesis

C.9 Mi-2: Butt joints with STS in shear



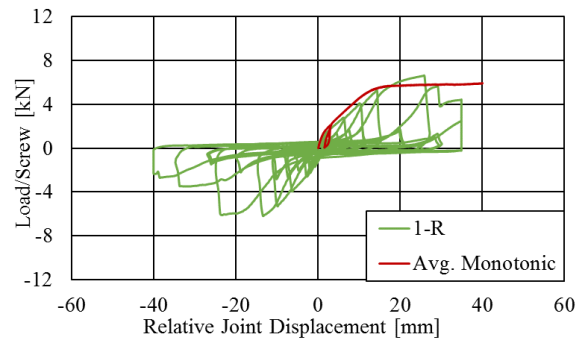
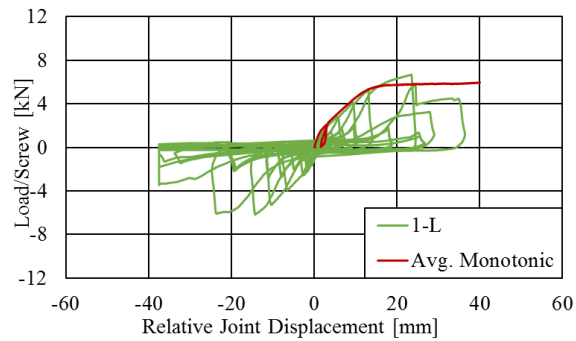
BS-2-m-3ply-2SP



Spec.	F_{max} [kN]	F_Y [kN]	d_{Fmax} [mm]	$d_{F,Y}$ [mm]	μ (-)	k [kN/mm]
1	5.5	4.6	43.0	9.3	4.6	0.4
2	6.2	5.3	44.0	8.3	5.3	0.5
3	6.0	5.4	26.0	3.6	7.2	1.3
4	5.1	3.4	48.0	5.4	8.9	0.4
5	6.7	5.8	30.0	12.2	2.5	0.4
6	7.2	6.2	40.0	5.5	7.3	0.9
Avg.	6.1	5.1	38.5	7.4	6.0	0.7

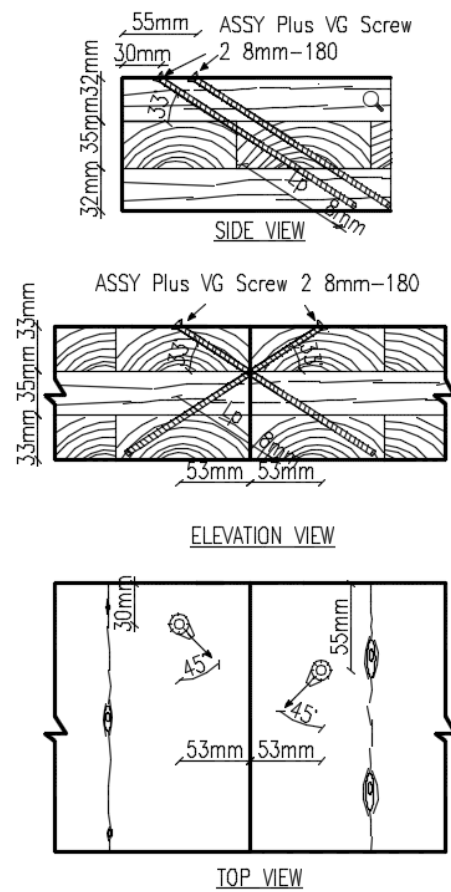
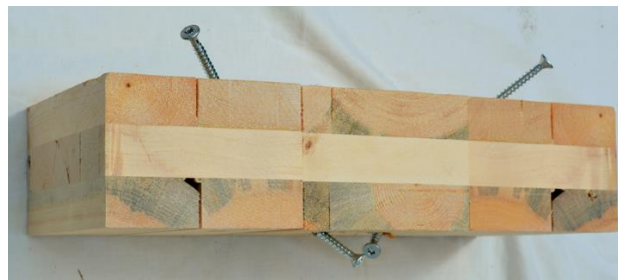
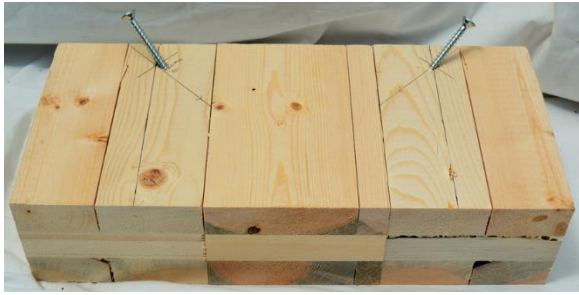
Note: All values are per screw

BS-2-c-3ply-2SP

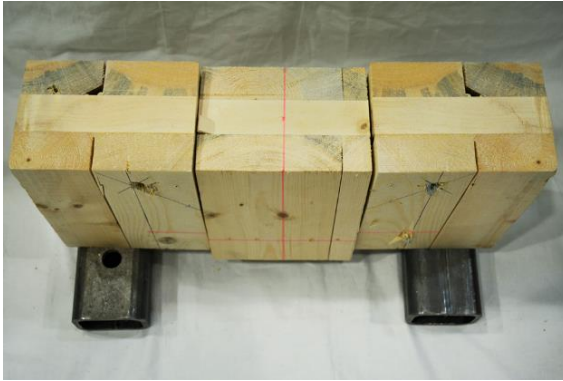
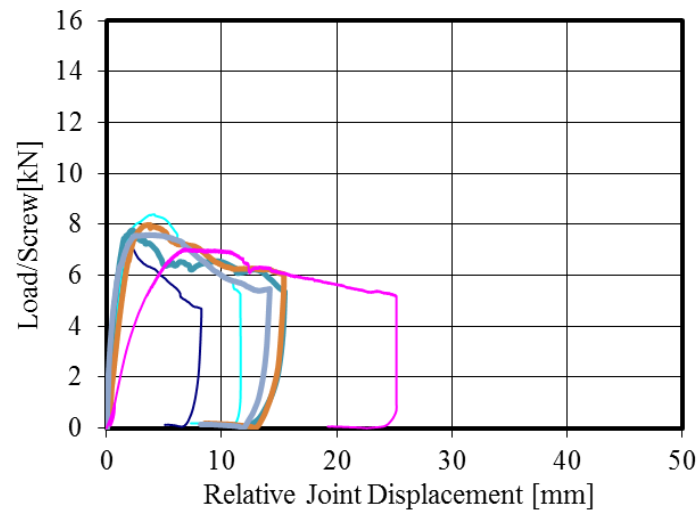


Spec.	F_{\max} [kN]	F_Y [kN]	$d_{F\max}$ [mm]	$d_{F,Y}$ [mm]	μ (-)	k [kN/mm]
1-L	7.1 (6.1)	5.0 (4.0)	26.0 (26.0)	10.0 (3.2)	2.6 (8.2)	0.4 (1.3)
1-R	6.7 (6.4)	4.1 (5.5)	26.0 (14.0)	8.7 (4.4)	3.0 (3.2)	0.4 (1.1)
1	6.9 (6.2)	4.5 (4.8)	26.0 (20.0)	9.4 (3.8)	2.8 (5.7)	0.4 (1.2)
2-L	6.9 (6.9)	6.0 (4.6)	36.0 (26.0)	10.8 (3.6)	3.3 (7.2)	0.5 (1.1)
2-R	6.9 (6.9)	5.9 (4.4)	36.0 (25.0)	10.6 (3.3)	3.4 (7.7)	0.4 (1.3)
2	6.9 (6.9)	5.9 (4.5)	36.0 (25.5)	10.7 (3.4)	3.4 (7.4)	0.5 (1.2)
3-L	7.0 (7.3)	4.3 (4.8)	26.0 (15.0)	7.4 (5.8)	3.5 (2.6)	0.5 (0.8)
3-R	7.1 (7.4)	4.3 (5.0)	26.0 (11.0)	8.2 (5.0)	3.2 (2.2)	0.5 (0.9)
3	7.0 (7.3)	4.3 (4.9)	26.0 (13.0)	7.8 (5.4)	3.3 (2.4)	0.5 (0.8)
4-L	7.4 (6.8)	4.3 (4.3)	23.0 (13.0)	8.1 (11.1)	2.8 (1.2)	0.5 (0.4)
4-R	7.4 (6.8)	4.3 (3.9)	23.0 (24.0)	8.4 (9.1)	2.7 (2.6)	0.5 (0.4)
4	7.4 (6.8)	4.3 (4.1)	23.0 (18.5)	8.3 (10.1)	2.8 (1.9)	0.5 (0.4)
5-L	7.3 (7.0)	6.5 (4.6)	34.0 (38.0)	14.5 (4.7)	2.3 (8.1)	0.4 (0.8)
5-R	7.3 (6.7)	7.8 (6.1)	37.0 (37.0)	11.9 (8.7)	3.1 (4.2)	0.4 (0.6)
5	7.3 (6.9)	7.2 (5.4)	35.5 (37.5)	13.2 (6.7)	2.7 (6.2)	0.4 (0.7)
6-L	7.9 (7.9)	5.0 (4.9)	21.0 (25.0)	6.1 (7.4)	3.4 (3.4)	0.8 (0.6)
6-R	7.9 (7.8)	4.9 (4.9)	21.0 (25.0)	6.5 (6.4)	3.2 (3.9)	0.7 (0.7)
6	7.9 (7.8)	5.0 (4.9)	21.0 (25.0)	6.3 (6.9)	3.3 (3.6)	0.7 (0.7)
Avg.	7.2 (7.0)	5.2 (4.7)	27.9 (23.3)	9.3 (6.1)	3.1 (4.5)	0.5 (0.8)

C.10 Mi-2: Butt joints with STS in withdrawal



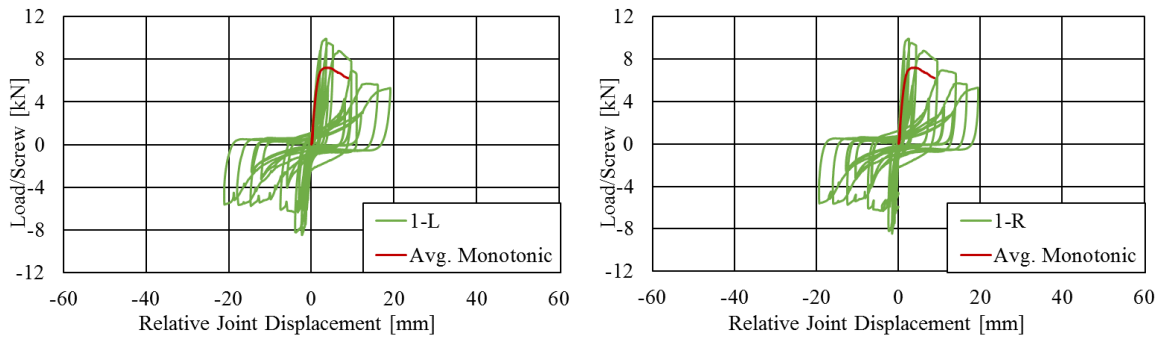
BW-2-m-3ply-2SP



Spec.	F_{\max} [kN]	F_Y [kN]	$d_{F\max}$ [mm]	$d_{F,Y}$ [mm]	μ (-)	k [kN/mm]
1	7.4	6.4	1.9	1.1	1.7	5.5
2	8.4	7.6	4.0	1.4	2.9	6.3
3	7.8	6.6	2.3	0.8	3.0	7.1
4	8.0	7.3	3.6	1.9	1.9	4.8
5	7.6	6.9	3.5	0.4	8.5	9.5
6	7.0	5.9	6.7	3.3	2.0	2.1
Avg.	7.7	6.8	3.7	1.5	3.3	5.9

Note: All values are per screw

BW-2-c-3ply-2SP



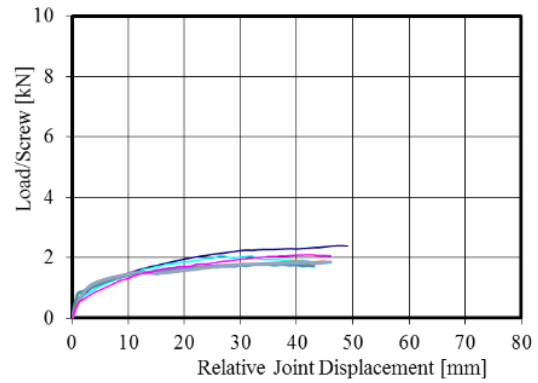
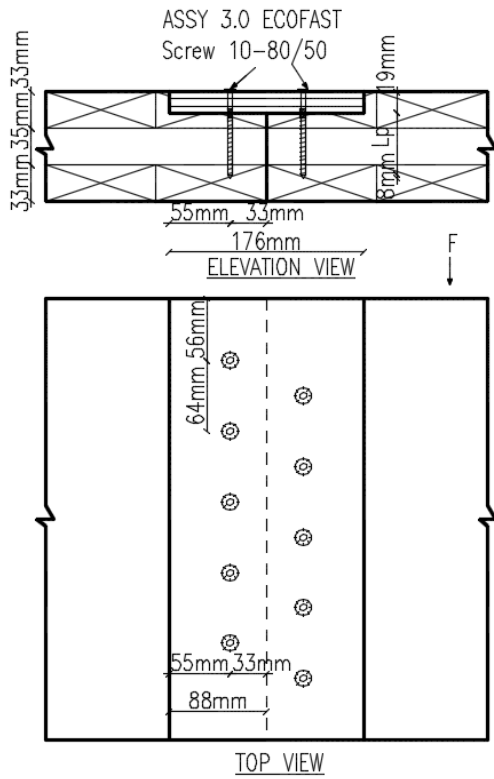
Spec.	F_{max} [kN]	F_Y [kN]	d_{Fmax} [mm]	$d_{F,Y}$ [mm]	μ (-)	k [kN/mm]
1-L	9.9 (8.4)	8.8 (7.5)	3.5 (2.0)	1.8 (1.0)	2.0 (2.0)	5.0 (8.4)
1-R	9.9 (8.4)	8.9 (7.6)	2.4 (1.4)	1.2 (1.1)	2.0 (1.3)	9.9 (12.5)
1	9.9 (8.4)	8.8 (7.6)	3.0 (1.7)	1.5 (1.1)	2.0 (1.6)	7.4 (10.4)
2-L	10.0 (7.8)	9.2 (7.0)	3.2 (1.7)	1.7 (0.6)	1.9 (2.7)	6.0 (8.3)
2-R	10.2 (7.8)	9.1 (7.1)	3.2 (2.0)	1.1 (0.1)	3.0 (15.8)	10.2 (46.7)
2	10.1 (7.8)	9.1 (7.1)	3.2 (1.9)	1.4 (0.4)	2.4 (9.2)	8.1 (27.5)
3-L	9.0 (8.2)	8.0 (7.4)	2.3 (1.6)	1.3 (0.8)	1.7 (1.9)	6.7 (7.3)
3-R	9.3 (8.7)	8.5 (8.3)	1.5 (0.5)	1.4 (1.0)	1.1 (0.5)	9.3 (32.7)
3	9.1 (8.5)	8.2 (7.8)	1.9 (1.1)	1.4 (0.9)	1.4 (1.2)	8.0 (20.0)
4-L	9.9 (10.2)	9.0 (9.4)	1.8 (0.7)	1.6 (1.4)	1.1 (0.5)	5.9 (27.8)
4-R	9.9 (10.2)	9.1 (9.0)	2.0 (1.3)	1.9 (1.3)	1.0 (1.0)	5.0 (7.7)
4	9.9 (10.2)	9.0 (9.2)	1.9 (1.0)	1.8 (1.4)	1.1 (0.7)	5.5 (17.8)
5-L	9.9 (9.8)	8.7 (8.7)	2.2 (2.4)	0.9 (1.4)	2.4 (1.8)	9.9 (7.3)
5	9.9 (9.8)	8.7 (8.7)	2.2 (2.4)	0.9 (1.4)	2.4 (1.8)	9.9 (7.3)
Avg.	9.8 (8.9)	8.8 (8.1)	2.4 (1.6)	1.4 (1.0)	1.9 (2.9)	7.8 (16.6)

Note: All values are per screw, L=left side, R=right side of the connection, negative envelope values within parenthesis

Appendix D Detailed test results of small sized specimens (S-2SP, and S-1SP)

D.1 S-2SP: Spline joints - Monotonic

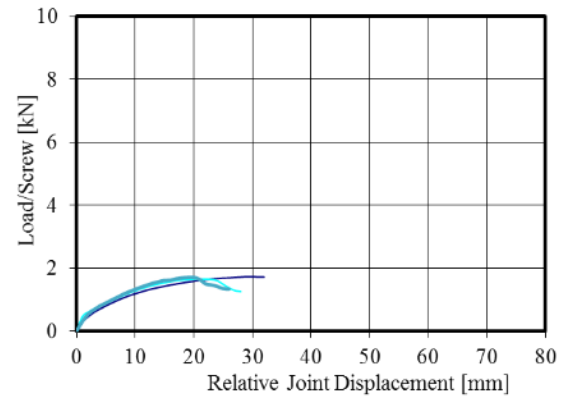
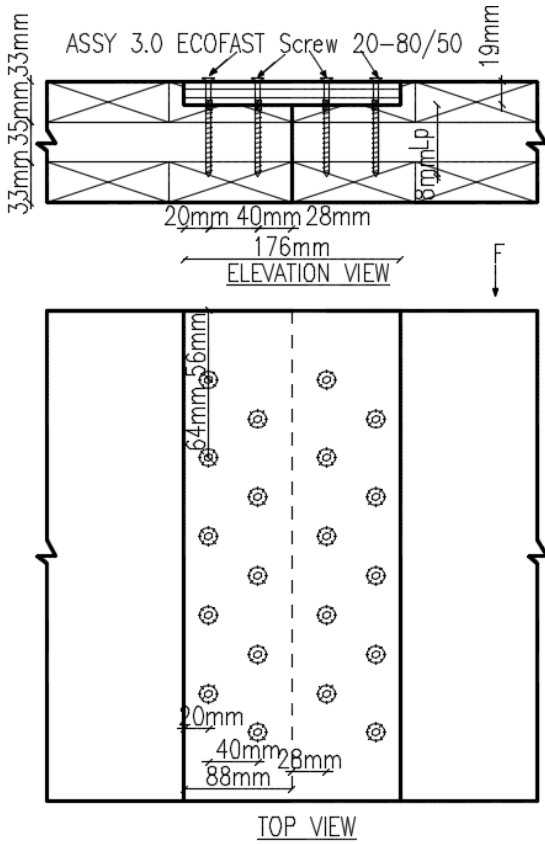
SS-10-m-3ply-2SP



	F_{\max}	F_Y	$d_{F\max}$	$d_{F,Y}$	μ	k
SS-10-m-3ply-2SP	[kN]	[kN]	[mm]	[mm]	(-)	[kN/mm]
1	4.8	3.1	48.0	5.4	8.9	0.5
2	4.1	2.8	32.0	5.0	6.4	0.5
3	3.6	2.3	35.0	4.0	8.8	1.8
4	3.7	2.6	45.0	2.9	15.4	0.8
5	3.7	2.6	49.0	3.1	15.9	1.0
6	4.2	3.6	42.0	7.7	5.5	0.4
Avg.	4.0	2.8	41.8	4.7	10.1	0.8

Note: All values are per screw

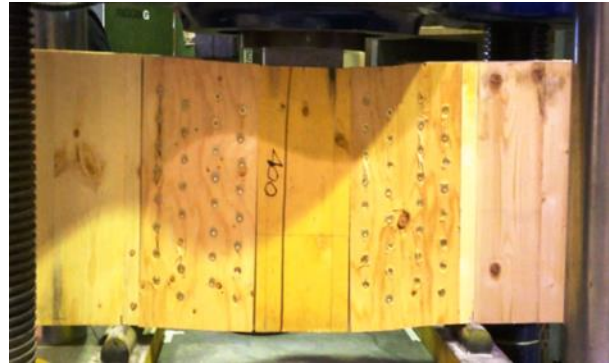
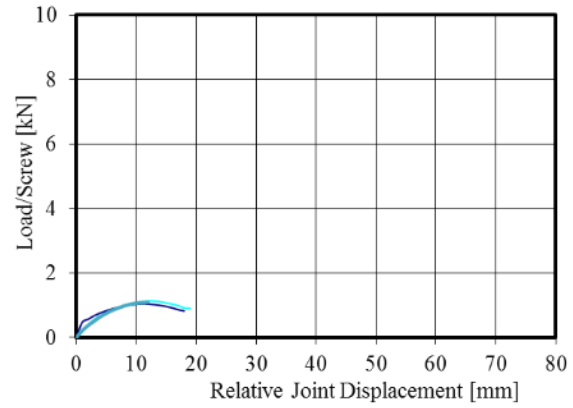
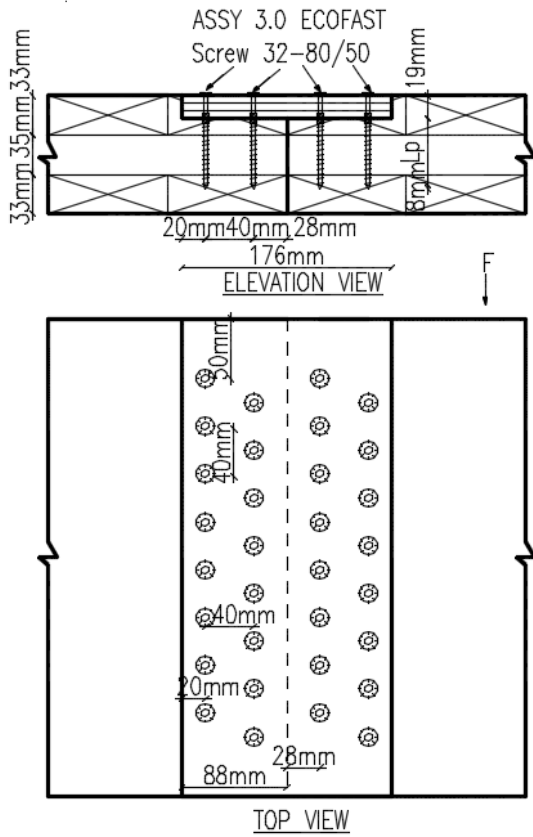
SS-20-m-3ply-2SP



	F_{\max}	F_Y	$d_{F\max}$	$d_{F,Y}$	μ	k
SS-20-m-3ply-2SP	[kN]	[kN]	[mm]	[mm]	(-)	[kN/mm]
1	3.5	2.3	29.0	6.3	4.6	0.3
2	3.3	2.2	20.0	4.1	4.9	0.5
3	3.4	2.3	20.0	5.1	3.9	0.4
Avg.	3.4	2.3	23.0	5.2	4.5	0.4

Note: All values are per screw

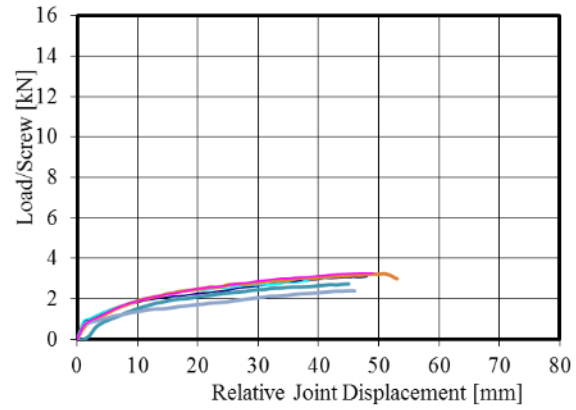
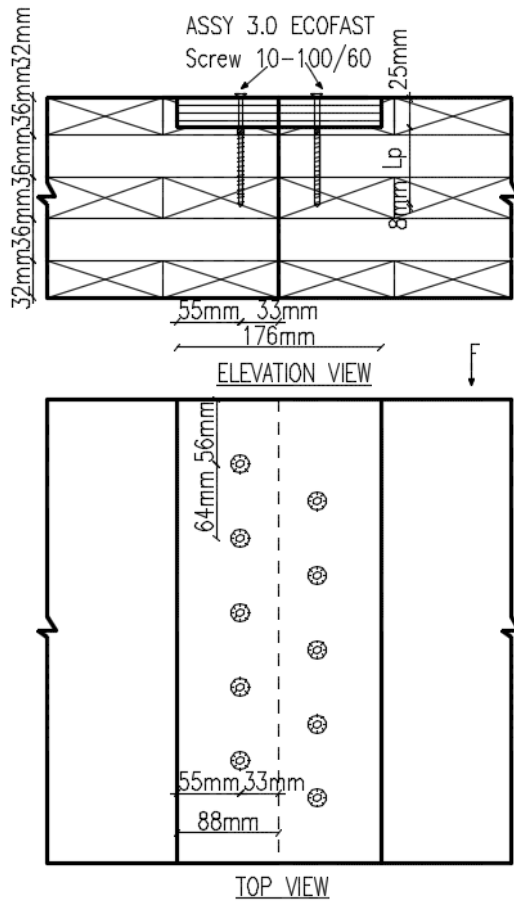
SS-32-m-3ply-2SP



	F_{\max}	F_Y	$d_{F\max}$	$d_{F,Y}$	μ	k
SS-32-m-3ply-2SP	[kN]	[kN]	[mm]	[mm]	(-)	[kN/mm]
1	2.1	1.6	11.0	4.0	2.8	1.0
2	2.3	1.7	12.0	4.3	2.8	0.4
3	2.2	1.9	12.0	5.2	2.3	0.3
Avg.	2.2	1.7	11.7	4.5	2.6	0.6

Note: All values are per screw

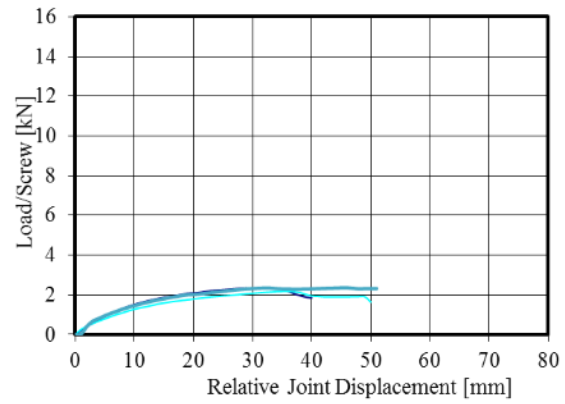
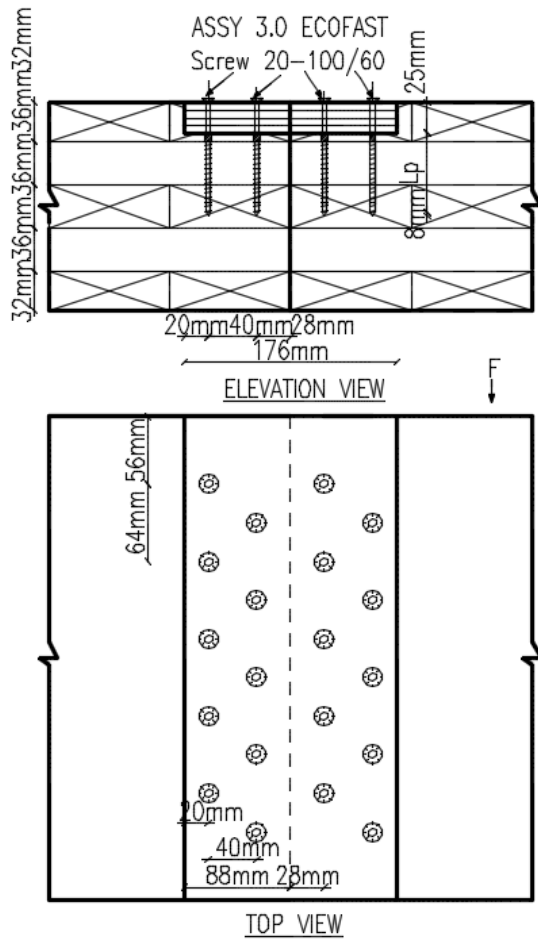
SS-10-m-5-ply-2SP



	F_{\max}	F_Y	$d_{F\max}$	$d_{F,Y}$	μ	k
SS-10-m-5ply-2SP	[kN]	[kN]	[mm]	[mm]	(-)	[kN/mm]
1	6.3	5.3	51.0	8.0	6.4	0.5
2	7.0	4.4	52.0	7.4	7.0	0.4
3	5.5	3.2	45.0	8.3	5.4	0.4
4	6.5	4.1	51.0	7.9	6.5	0.4
5	5.3	3.4	55.0	8.3	6.6	0.3
6	6.6	4.1	50.0	8.0	6.2	0.4
Avg.	6.2	4.1	50.7	8.0	6.4	0.4

Note: All values are per screw

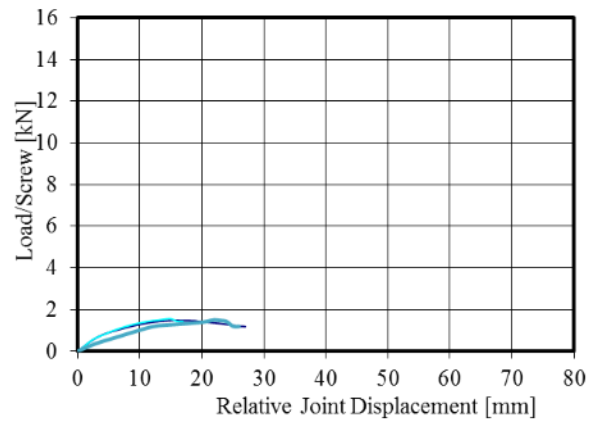
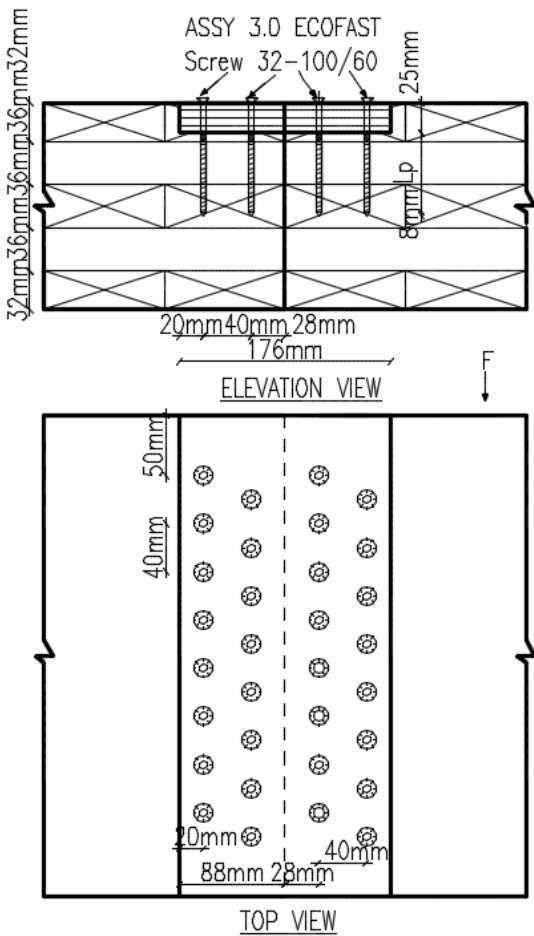
SS-20-m-5ply-2SP



	F_{max}	F_Y	d_{Fmax}	$d_{F,Y}$	μ	k
SS-20-m-5ply-2SP	[kN]	[kN]	[mm]	[mm]	(-)	[kN/mm]
1	4.7	2.9	32.0	8.1	3.9	0.3
2	4.4	2.7	36.0	10.5	3.4	0.3
3	4.7	2.9	46.0	8.3	5.6	0.4
Avg.	4.6	2.9	38.0	9.0	4.3	0.3

Note: All values are per screw

SS-32-m-5ply-2SP

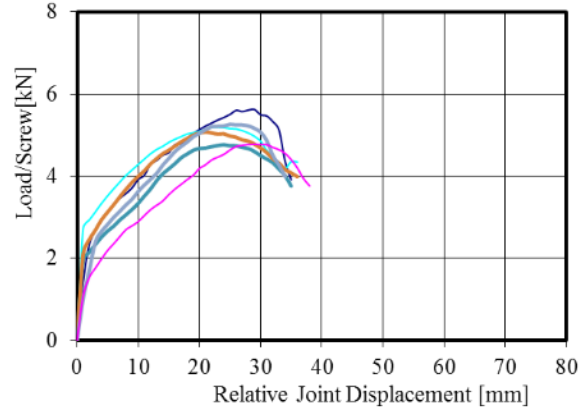
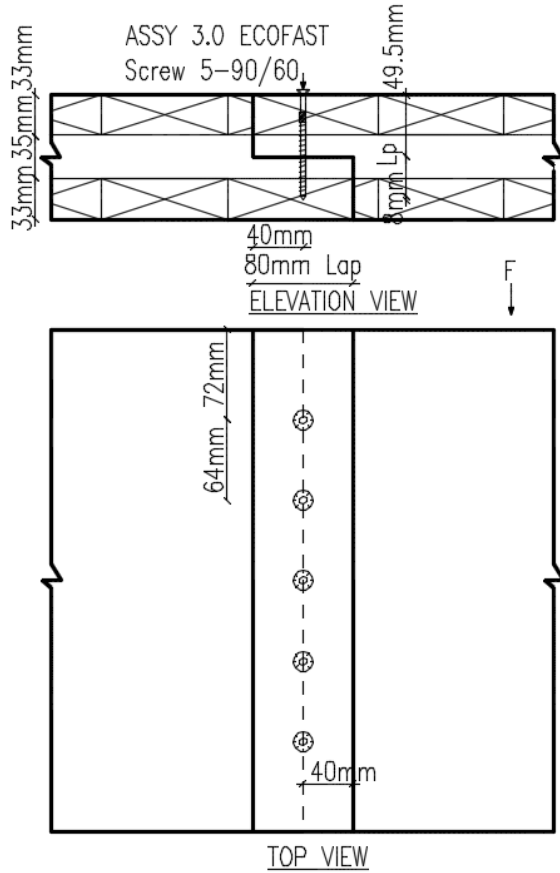


	F_{max}	F_Y	d_{Fmax}	$d_{F,Y}$	μ	k
SS-32-m-5ply-2SP	[kN]	[kN]	[mm]	[mm]	(-)	[kN/mm]
1	3.0	2.1	16.0	4.8	3.3	0.4
2	3.1	2.1	15.0	4.7	3.2	0.4
3	3.0	1.9	22.0	8.6	2.5	0.2
Avg.	3.0	2.0	17.7	6.0	3.0	0.4

Note: All values are per screw

D.2 S-2SP: Lap joints shear - Monotonic

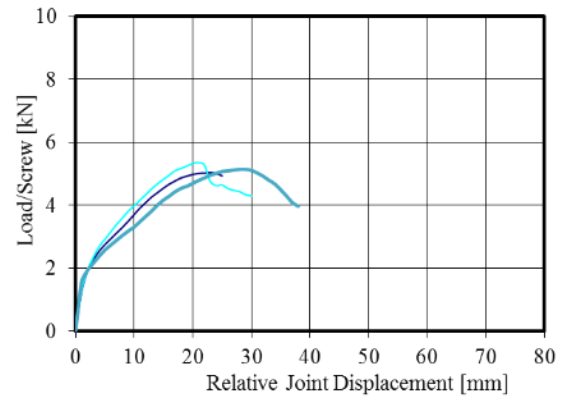
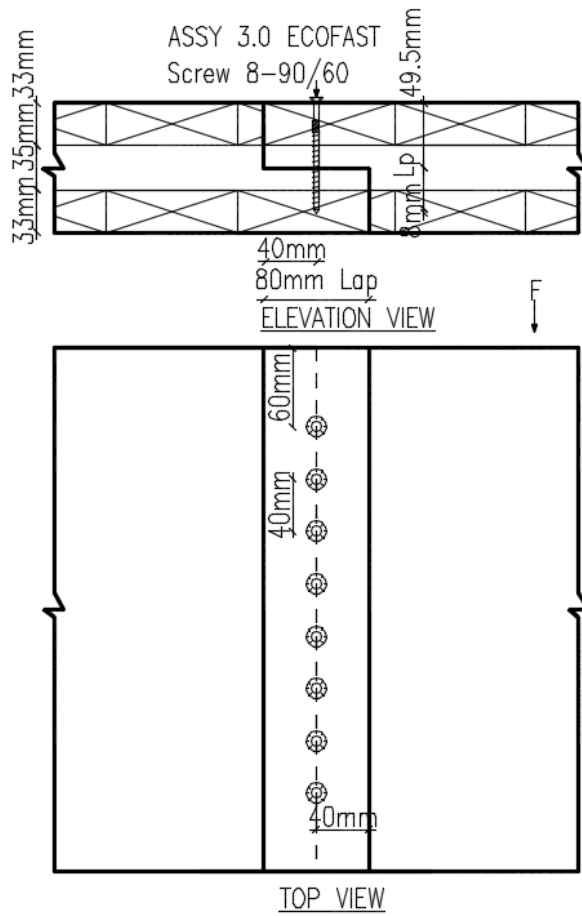
LS-5-m-3ply-2SP



	F_{\max}	F_Y	$d_{F_{\max}}$	$d_{F,Y}$	μ	k
LS-5-m-3ply-2SP	[kN]	[kN]	[mm]	[mm]	(-)	[kN/mm]
1	5.6	3.8	29.0	3.3	8.9	1.0
2	5.2	3.5	23.0	1.7	13.9	15.4
3	4.8	3.2	24.0	1.5	16.4	1.8
4	5.1	3.5	21.0	1.3	15.9	2.2
5	5.3	3.5	25.0	4.4	5.6	0.7
6	4.8	3.1	29.0	5.7	5.1	0.4
Avg.	5.1	3.4	25.2	3.0	11.0	1.2

Note: All values are per screw

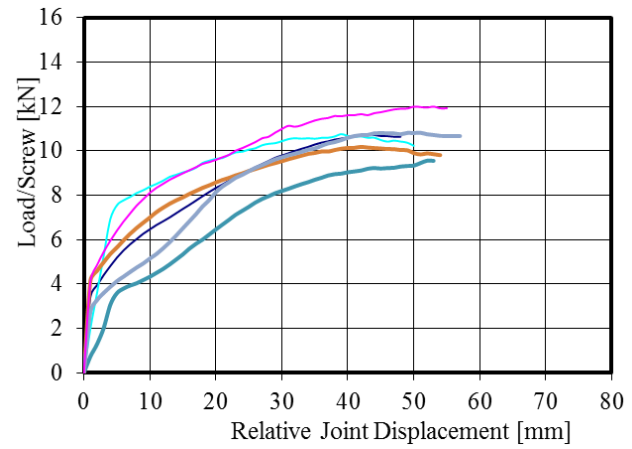
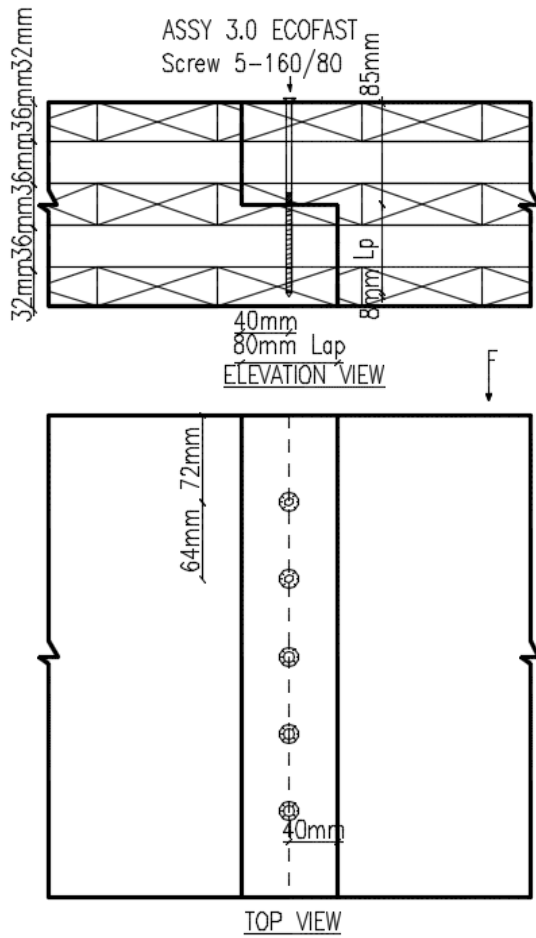
LS-8-m-3ply-2SP



	F_{\max}	F_Y	$d_{F\max}$	$d_{F,Y}$	μ	k
LS-8-m-3ply-2SP	[kN]	[kN]	[mm]	[mm]	(-)	[kN/mm]
1	5.0	3.4	23.0	3.8	6.0	0.8
2	5.4	3.6	21.0	4.1	5.1	0.7
3	5.1	3.4	28.0	4.1	6.8	0.7
Avg.	5.2	3.5	24.0	4.0	6.0	0.7

Note: All values are per screw

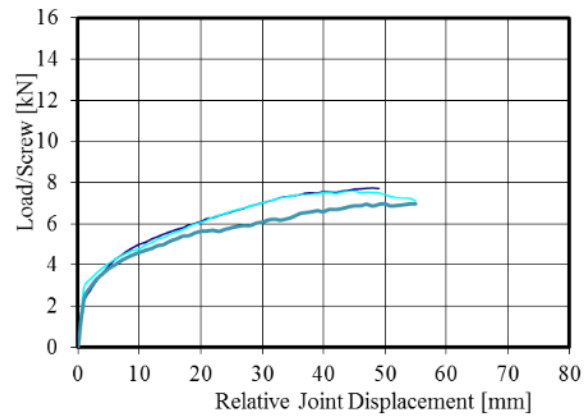
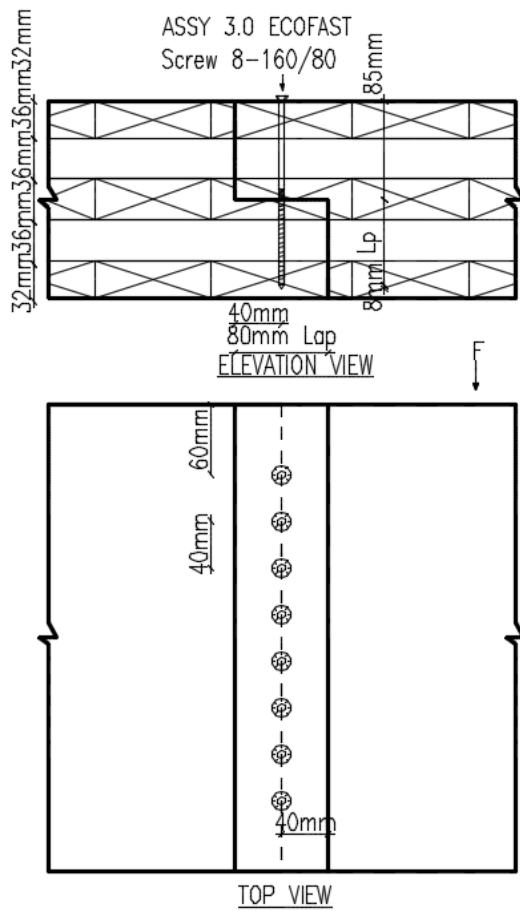
LS-5-m-5ply-2SP



	F_{max}	F_Y	d_{Fmax}	$d_{F,Y}$	μ	k
LS-5-m-5ply-2SP	[kN]	[kN]	[mm]	[mm]	(-)	[kN/mm]
1	10.7	7.0	44.0	4.6	9.6	1.2
2	10.8	8.0	39.0	4.5	8.7	1.5
3	9.6	5.9	52.0	8.3	6.3	0.6
4	10.2	6.9	42.0	4.2	10.0	3.4
5	10.8	6.5	51.0	8.7	5.8	0.6
6	12.0	7.9	50.0	3.0	16.4	1.9
Avg.	10.7	7.0	46.3	5.6	9.5	1.5

Note: All values are per screw

LS-8-m-5ply-2SP

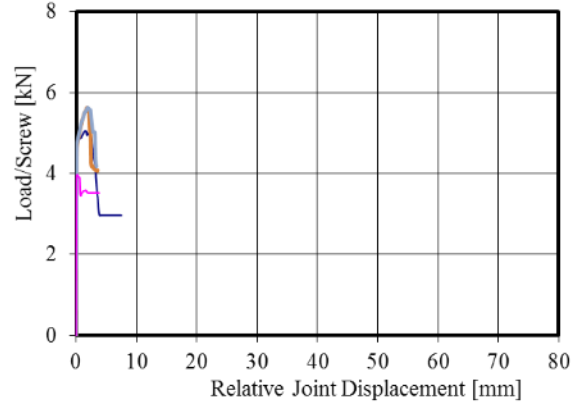
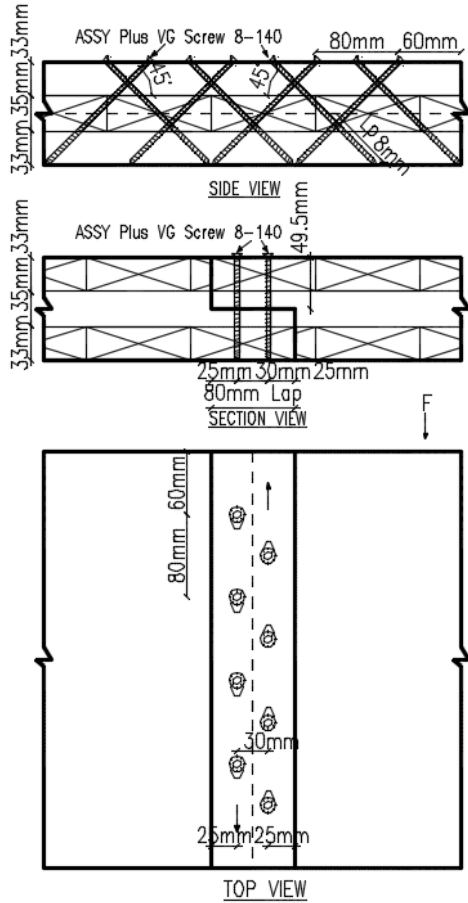


	F_{\max}	F_Y	$d_{F\max}$	$d_{F,Y}$	μ	k
LS-8-m-5ply-2SP	[kN]	[kN]	[mm]	[mm]	(-)	[kN/mm]
1	7.7	5.2	48.0	4.4	10.8	0.9
2	7.6	5.1	45.0	4.0	11.2	1.8
3	7.0	4.5	55.0	4.0	13.9	1.3
Avg.	7.4	4.9	49.3	4.1	12.0	1.3

Note: All values are per screw

D.3 S-2SP: Lap joints withdrawal - Monotonic

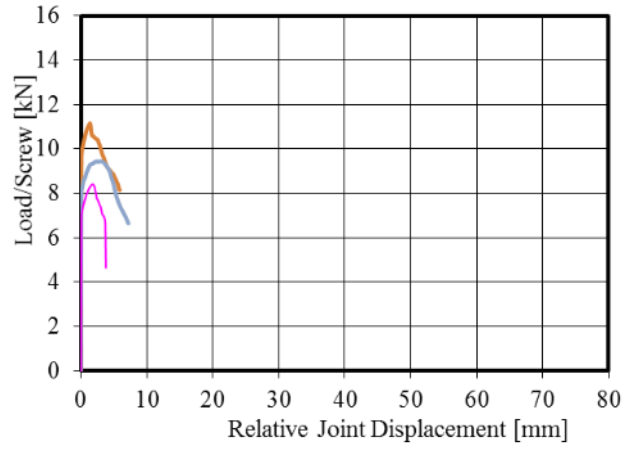
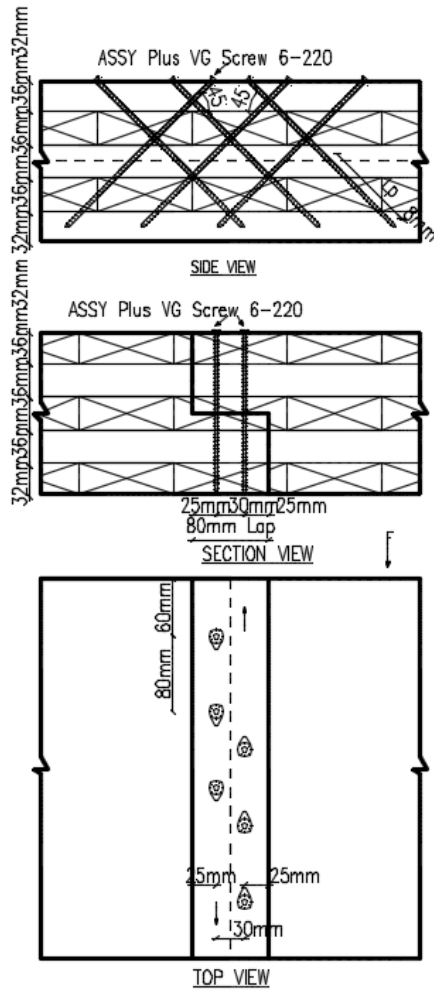
LW-8-m-3ply-2SP



	F_{\max}	F_Y	$d_{F_{\max}}$	$d_{F,Y}$	μ	k
LW-8-m-3ply-2SP	[kN]	[kN]	[mm]	[mm]	(-)	[kN/mm]
1	5.0	4.9	1.4	0.5	2.8	151.3
2	5.0	4.6	3.1	1.2	2.6	3.8
3	5.6	4.4	6.0	1.0	6.0	167.8
4	5.6	5.3	1.8	0.6	3.0	168.8
5	5.6	5.2	1.0	0.6	1.7	168.7
6	5.2	4.9	0.2	0.1	2.2	154.7
Avg.	5.3	4.9	2.3	0.7	3.0	135.9

Note: All values are per screw

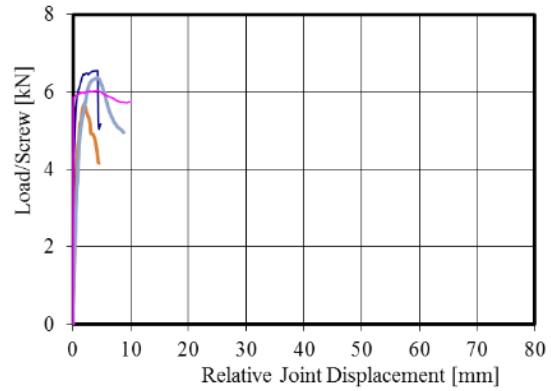
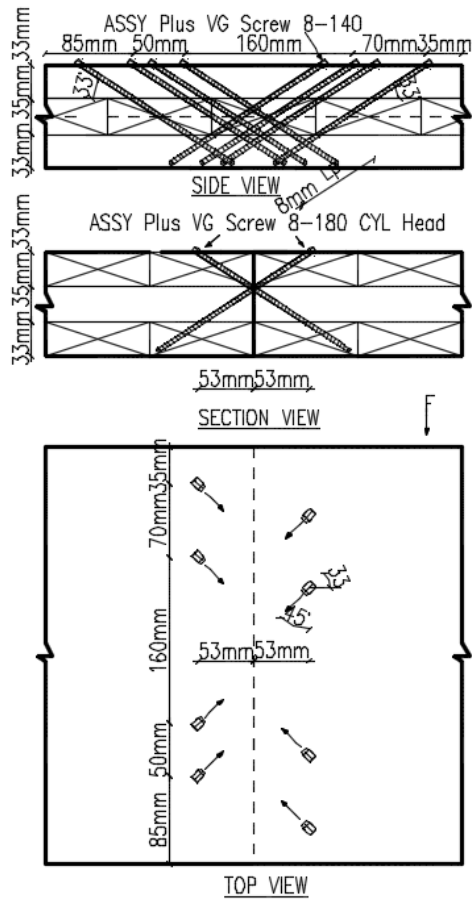
LW-6-m-5ply-2SP



	F_{\max}	F_Y	$d_{F\max}$	$d_{F,Y}$	μ	k
LW-6-m-5ply-2SP	[kN]	[kN]	[mm]	[mm]	(-)	[kN/mm]
1	10.7	10.1	1.9	1.0	1.9	319.8
2	11.2	10.6	1.4	0.8	1.8	334.6
3	9.4	9.0	2.9	1.5	1.9	283.4
4	10.1	9.3	1.8	1.0	1.8	303.0
Avg.	10.3	9.7	2.0	1.1	1.8	310.2

Note: All values are per screw

BW-8-m-3ply-2SP

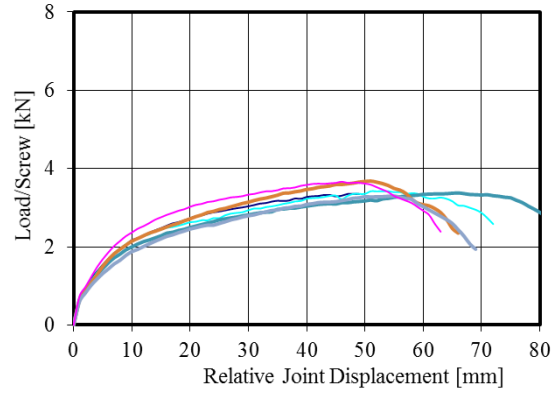
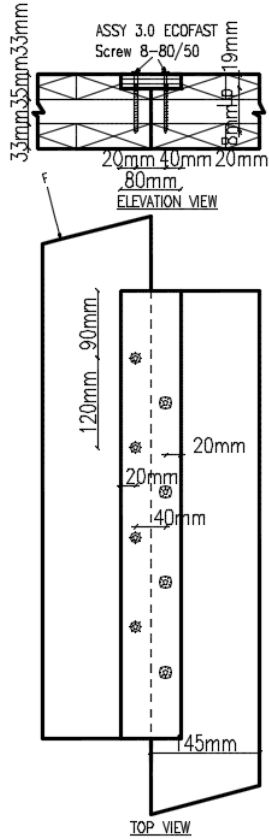


	F_{max}	F_Y	d_{Fmax}	$d_{F,Y}$	μ	k
BW-8-m-3ply-2SP	[kN]	[kN]	[mm]	[mm]	(-)	[kN/mm]
1	6.6	6.1	4.0	0.9	4.4	65.5
2	6.1	6.0	0.1	0.0	2.7	183.8
3	5.7	5.2	0.7	0.2	3.5	172.3
4	5.7	5.3	1.9	0.8	2.4	4.9
5	6.4	5.7	4.2	0.9	4.9	4.8
6	6.0	5.9	4.2	1.0	4.2	180.9
Avg.	6.1	5.7	2.5	0.6	3.7	102.0

Note: All values are per screw

D.4 S-1SP: Spline joints - Monotonic

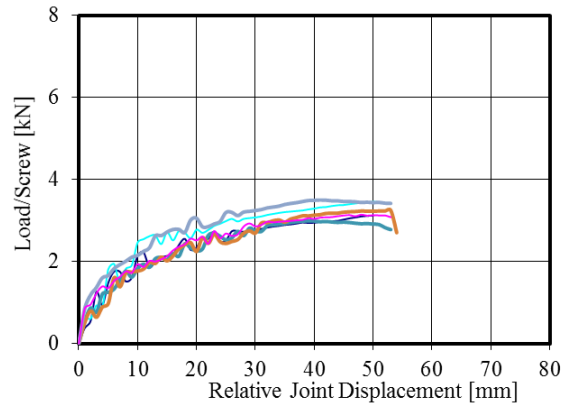
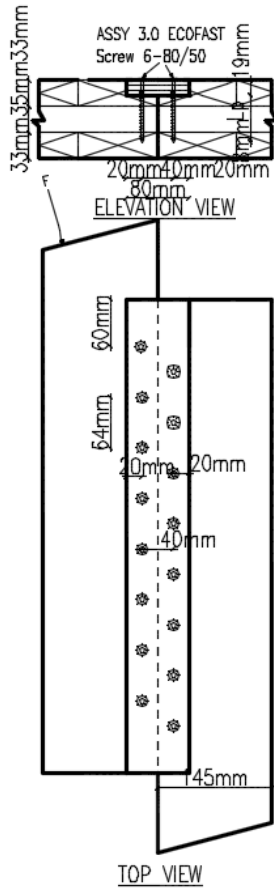
SS-8-m-3ply-1SP



	F_{\max}	F_Y	$d_{F\max}$	$d_{F,Y}$	μ	k
SS-8-m-3ply-1SP	[kN]	[kN]	[mm]	[mm]	(-)	[kN/mm]
1	6.7	4.4	48.0	6.3	7.6	0.5
2	6.8	4.4	51.0	6.7	7.6	0.5
3	6.8	4.3	66.0	7.7	8.5	0.5
4	7.4	4.6	51.0	7.5	6.8	0.5
5	6.6	4.6	55.0	7.5	7.3	0.4
6	7.3	4.8	46.0	6.3	7.3	0.6
Avg.	6.9	4.5	52.8	7.0	7.5	0.5

Note: All values are per screw

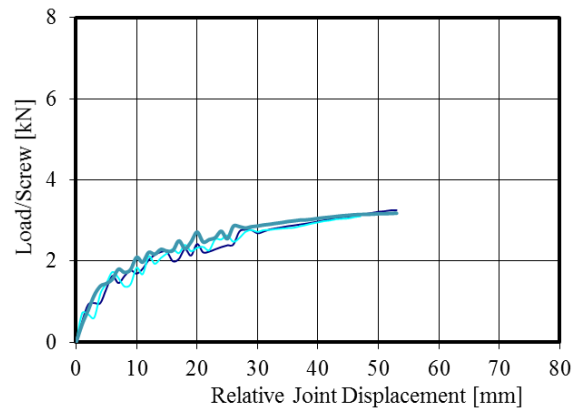
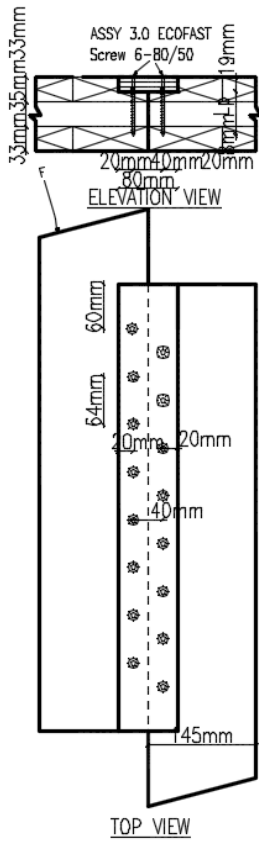
SS-16-m-3ply-1SP



	F_{\max}	F_Y	$d_{F\max}$	$d_{F,Y}$	μ	k
SS-16-m-3ply-1SP	[kN]	[kN]	[mm]	[mm]	(-)	[kN/mm]
1	6.2	3.8	50.0	4.5	11.2	0.4
2	6.9	4.8	50.0	7.2	7.0	0.4
3	6.0	3.6	39.0	5.5	7.1	0.4
4	6.5	4.2	53.0	6.7	7.9	0.5
5	7.0	4.8	41.0	5.9	6.9	0.6
6	6.3	4.2	48.0	6.1	7.9	0.5
Avg.	6.5	4.2	46.8	6.0	8.0	0.5

Note: All values are per screw

SS-16-m-3ply-1SP*

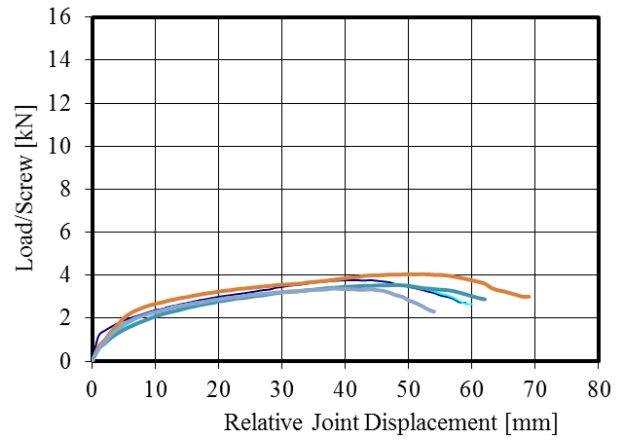
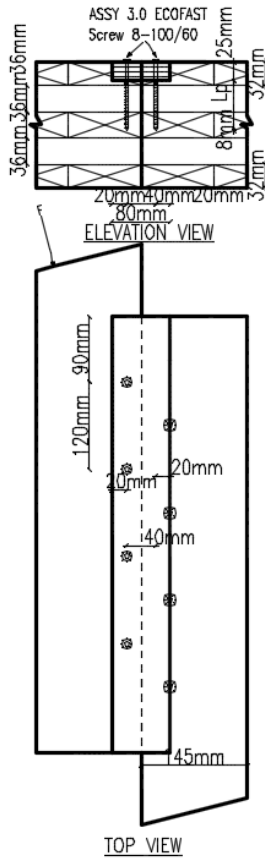


	F_{\max}	F_Y	$d_{F\max}$	$d_{F,Y}$	μ	k
SS-16-m-3ply-1SP*	[kN]	[kN]	[mm]	[mm]	(-)	[kN/mm]
1	6.5	4.2	53.0	7.6	7.0	0.5
2	6.3	4.1	52.0	6.8	7.7	0.5
3	6.4	4.2	53.0	6.6	8.1	0.6
Avg.	6.4	4.2	52.7	7.0	7.6	0.5

Note: All values are per screw

*indicates specimen with friction-eliminating membrane

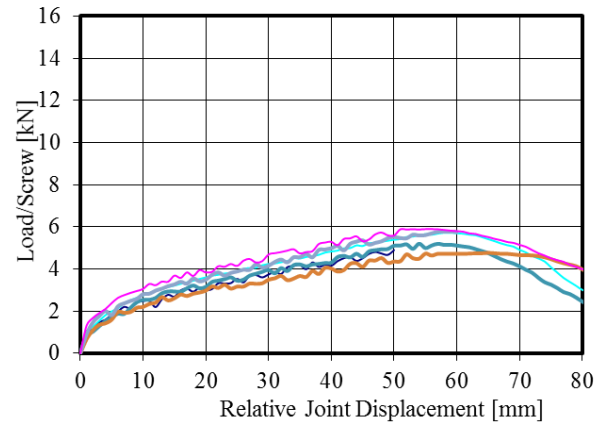
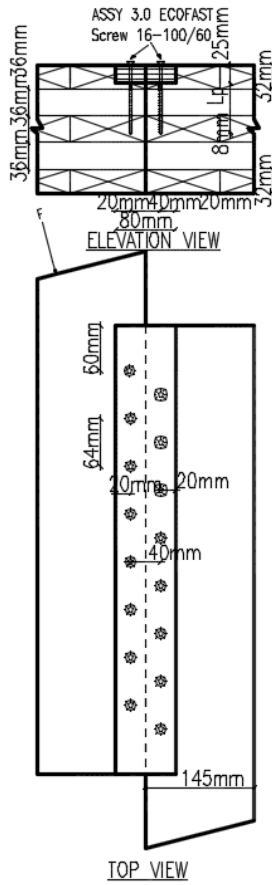
SS-8-m-5ply-1SP



	F_{max}	F_Y	d_{Fmax}	$d_{F,Y}$	μ	k
SS-8-m-5ply-1SP	[kN]	[kN]	[mm]	[mm]	(-)	[kN/mm]
1	7.6	5.0	44.0	4.7	9.3	0.9
2	7.1	4.7	48.0	7.2	6.7	0.6
3	7.1	4.4	48.0	7.3	6.6	0.5
4	8.1	5.4	52.0	5.3	9.8	0.7
5	6.8	4.6	38.0	5.8	6.6	9.2
Avg.	7.3	4.8	46.0	6.1	7.8	2.4

Note: All values are per screw

SS-16-m-5ply-1SP

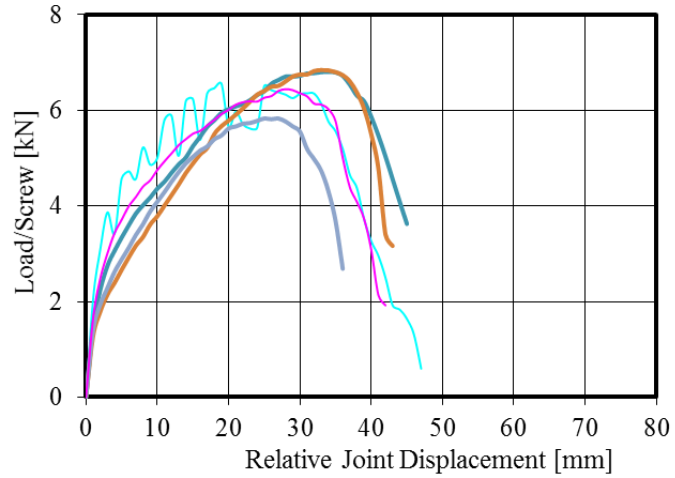
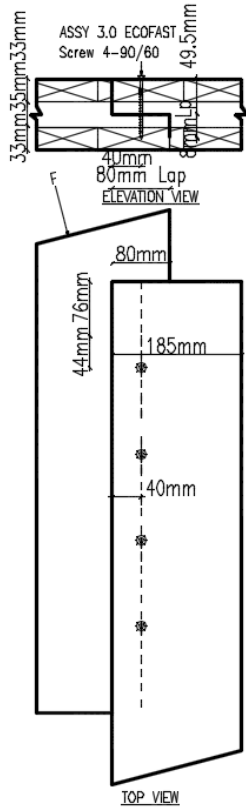


	F_{\max}	F_Y	$d_{F\max}$	$d_{F,Y}$	μ	k
SS-16-m-5ply-1SP	[kN]	[kN]	[mm]	[mm]	(-)	[kN/mm]
1	10.0	6.2	53.0	8.5	6.2	0.5
2	11.4	6.7	59.0	8.8	6.7	0.6
3	10.4	6.8	54.0	14.8	3.7	0.4
4	9.5	5.8	65.0	7.3	8.9	0.4
5	11.6	10.4	59.0	10.0	5.9	0.5
6	11.8	7.4	55.0	7.3	7.6	0.8
Avg.	10.8	7.2	57.5	9.4	6.5	0.5

Note: All values are per screw

D.5 S-1SP: Lap joints Shear - Monotonic

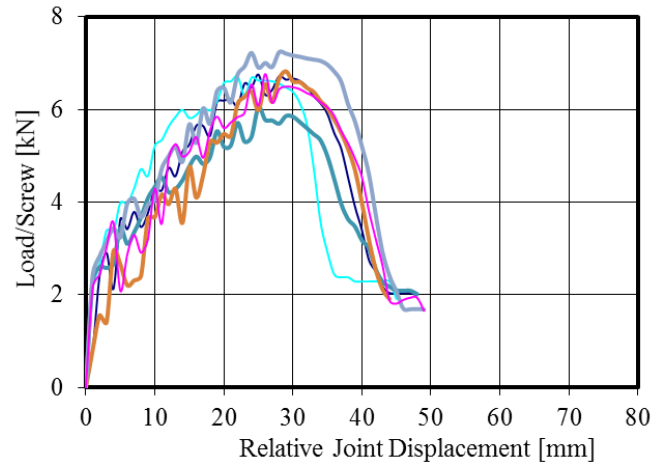
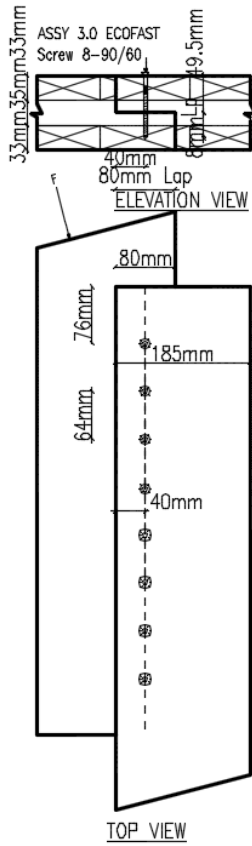
LS-4-m-3ply-1SP



LS-4-m-3ply-1SP	F_{max} [kN]	F_Y [kN]	d_{Fmax} [mm]	$d_{F,Y}$ [mm]	μ (-)	k [kN/mm]
1	6.1	3.6	9.8	2.3	4.2	1.3
2	6.6	4.9	19.0	4.2	4.5	1.2
3	6.8	4.5	34.0	5.1	6.7	0.8
4	6.8	4.6	33.0	6.3	5.2	0.4
5	5.8	3.9	25.0	6.2	4.0	0.6
6	6.4	4.5	28.0	3.8	7.3	0.9
Avg.	6.4	4.3	24.8	4.7	5.3	0.9

Note: All values are per screw

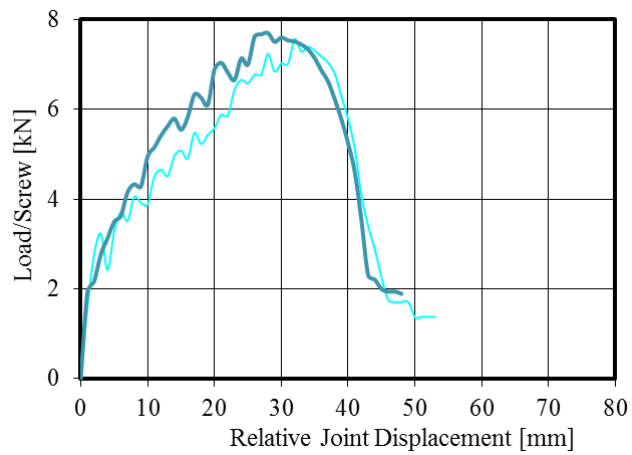
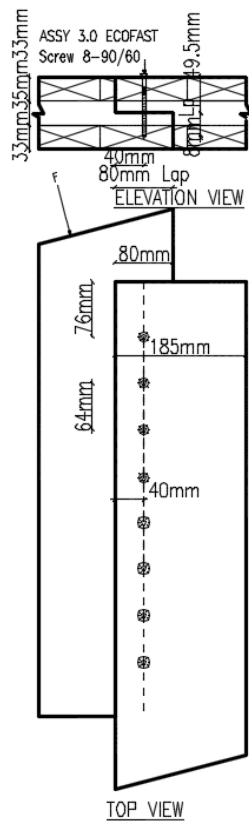
LS-8-m-3ply-1SP



	F_{\max}	F_Y	$d_{F\max}$	$d_{F,Y}$	μ	k
LS-8-m-3ply-1SP	[kN]	[kN]	[mm]	[mm]	(-)	[kN/mm]
1	6.8	4.7	25.0	5.9	4.2	1.0
2	6.7	4.3	22.0	2.8	7.9	0.9
3	6.0	3.9	25.0	2.6	9.7	1.2
4	6.8	4.0	29.0	6.4	4.5	0.8
5	7.2	4.8	28.0	3.7	7.5	1.1
6	6.8	3.9	26.0	4.7	5.5	1.1
Avg.	6.7	4.3	25.8	4.4	6.6	1.0

Note: All values are per screw

LS-8-m-3ply-1SP*

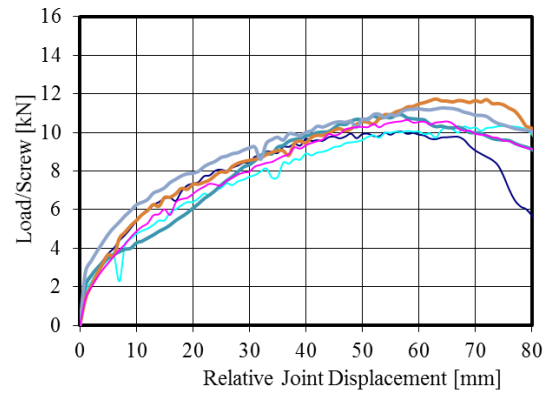
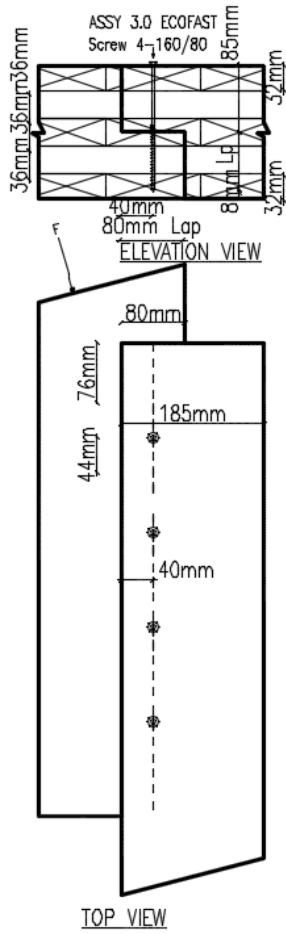


	F_{\max}	F_Y	$d_{F\max}$	$d_{F,Y}$	μ	k
LS-8-m-3ply-1SP*	[kN]	[kN]	[mm]	[mm]	(-)	[kN/mm]
1	7.6	4.9	32.0	7.1	4.5	1.1
2	7.7	5.1	28.0	7.0	4.0	0.7
Avg.	7.6	5.0	30.0	7.0	4.3	0.9

Note: All values are per screw

*indicates specimen with friction-eliminating membrane

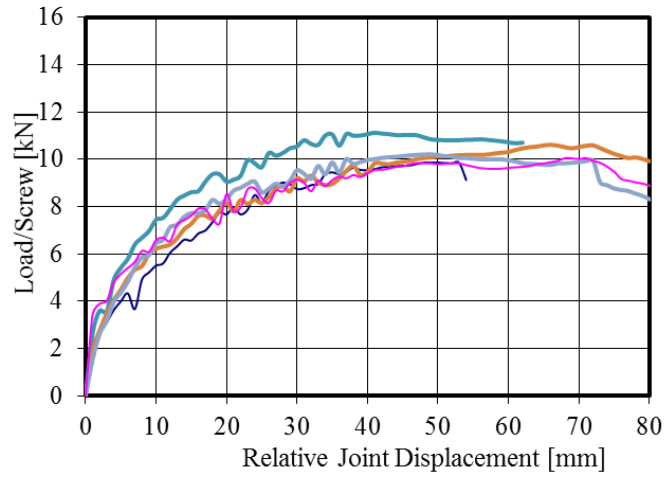
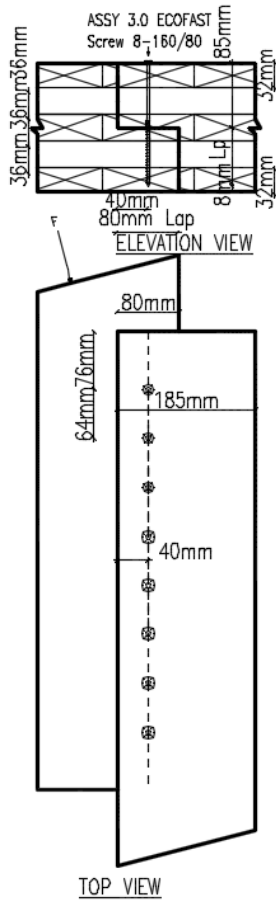
LS-4-m-5ply-1SP



	F_{\max}	F_Y	$d_{F\max}$	$d_{F,Y}$	μ	k
LS-4-m-5ply-1SP	[kN]	[kN]	[mm]	[mm]	(-)	[kN/mm]
1	10.0	8.2	57.0	11.7	4.9	0.5
2	10.3	6.1	75.0	12.8	5.9	0.4
3	10.9	6.6	57.0	17.3	3.3	0.3
4	11.7	6.4	63.0	14.1	4.5	0.5
5	11.3	7.1	64.0	7.0	9.2	0.8
6	10.7	6.5	58.0	19.8	2.9	0.8
Avg.	10.8	6.8	62.3	13.8	5.1	0.6

Note: All values are per screw

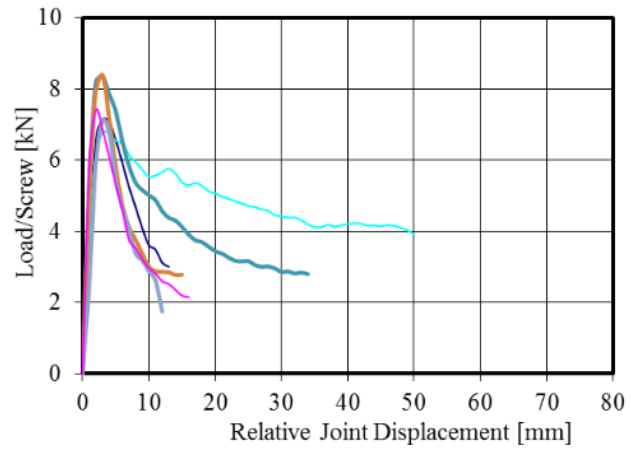
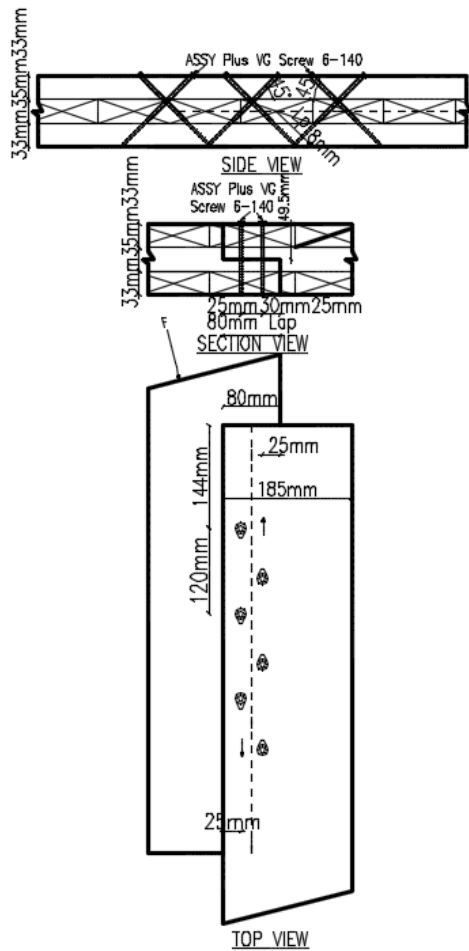
LS-8-m-5ply-1SP



	F_{max}	F_Y	d_{Fmax}	$d_{F,Y}$	μ	k
LS-8-m-5ply-1SP	[kN]	[kN]	[mm]	[mm]	(-)	[kN/mm]
1	9.9	5.8	49.0	4.6	10.6	0.7
2	13.7	7.8	84.0	3.6	23.1	0.7
3	11.5	7.6	70.0	5.8	12.0	1.0
4	10.6	6.9	66.0	7.6	8.7	0.7
5	10.2	6.5	49.0	7.0	7.0	0.8
6	10.1	6.6	68.0	4.8	14.0	1.0
Avg.	11.0	6.9	64.3	5.6	12.6	0.8

Note: All values are per screw

LW-6-m-3ply-1SP

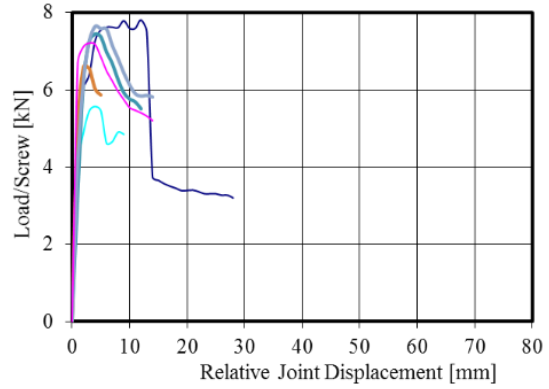
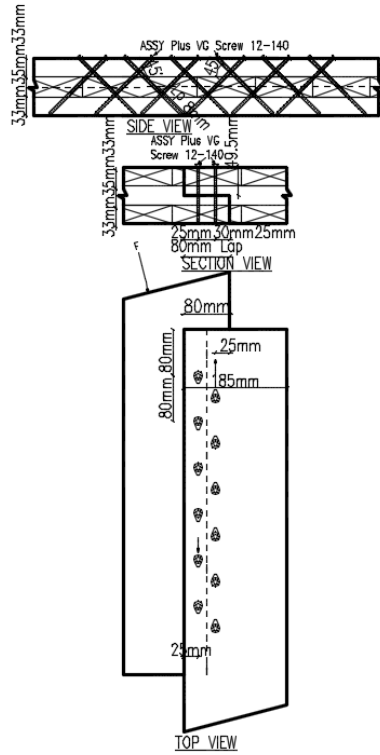


LW-6-m-3ply-1SP	F_{\max} [kN]	F_Y [kN]	$d_{F\max}$ [mm]	$d_{F,Y}$ [mm]	μ (-)	k [kN/mm]
1	7.2	6.7	3.1	1.9	1.6	3.6
2	6.8	6.2	3.3	1.8	1.8	3.4
3	8.4	8.0	2.7	1.7	1.6	5.1
4	8.5	7.8	2.6	1.5	1.7	5.1
5	7.2	7.3	2.9	2.9	1.0	2.4
6	7.4	6.9	1.8	1.2	1.5	5.6
Avg.	7.6	7.1	2.7	1.8	1.5	4.2

Note: All values are per screw

D.6 S-1SP: Lap joints Withdrawal - Monotonic

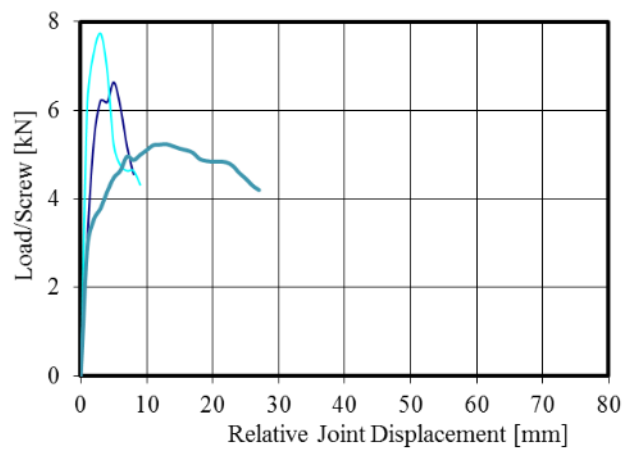
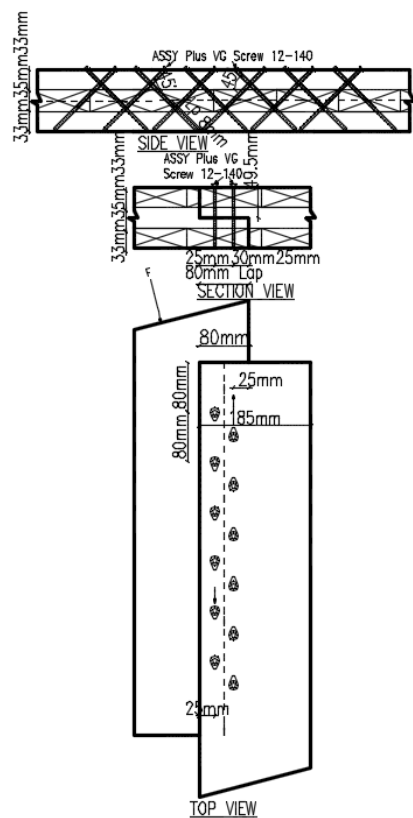
LW-12-m-3ply-1SP



	F_{max}	F_Y	d_{Fmax}	$d_{F,Y}$	μ	k
LW-12-m-3ply-1SP	[kN]	[kN]	[mm]	[mm]	(-)	[kN/mm]
1	7.8	6.2	13.4	3.0	4.5	234.5
2	5.8	5.2	4.4	0.9	4.9	3.6
3	7.6	7.0	4.2	2.1	2.0	4.6
4	7.0	5.9	2.6	1.0	2.7	5.2
5	7.8	7.0	5.1	2.5	2.0	5.9
6	7.4	6.3	3.2	2.2	1.4	221.7
Avg.	7.2	6.3	5.5	2.0	2.9	4.8

Note: All values are per screw

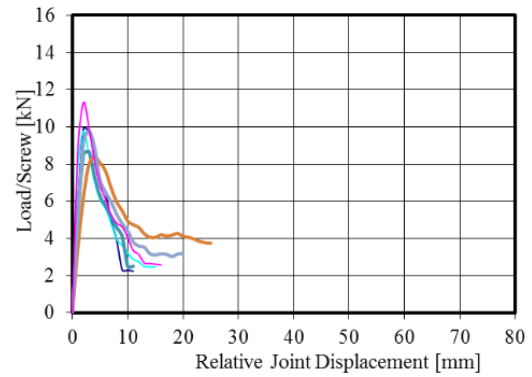
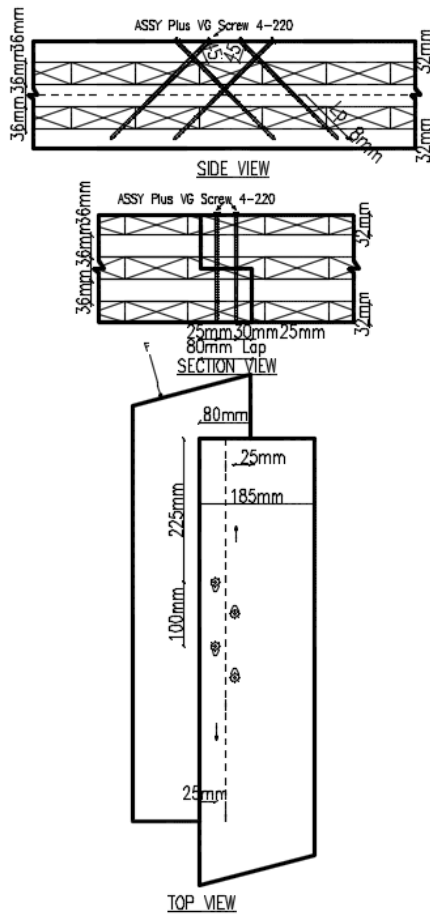
LW-12-m-3ply-1SP*



	F_{max}	F_Y	d_{Fmax}	$d_{F,Y}$	μ	k
LW-12-m-3ply-1SP*	[kN]	[kN]	[mm]	[mm]	(-)	[kN/mm]
1	6.7	5.6	4.8	1.9	2.6	2.9
2	7.8	7.2	3.1	0.9	3.3	8.3
3	5.4	3.5	11.4	0.5	23.0	5.4
Avg.	6.6	5.5	6.4	1.1	9.6	5.5

Note: All values are per screw
*indicates specimen with friction-eliminating membrane

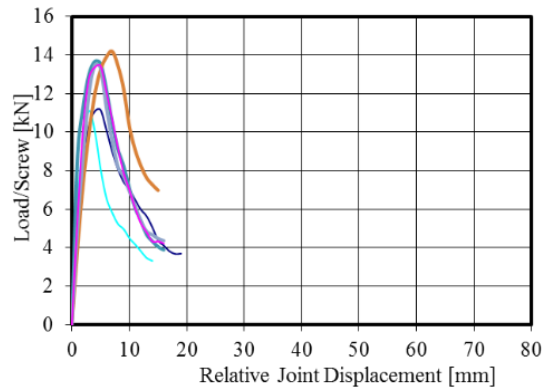
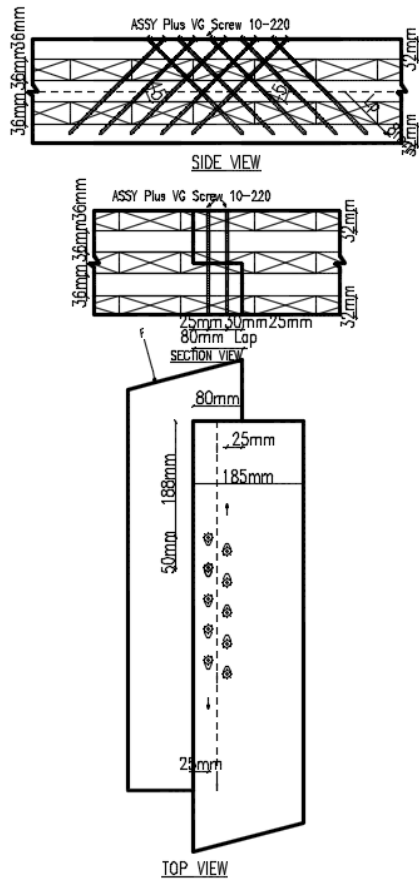
LW-4-m-5ply-1SP



	F_{max}	F_Y	d_{Fmax}	$d_{F,Y}$	μ	k
LW-4-m-5ply-1SP	[kN]	[kN]	[mm]	[mm]	(-)	[kN/mm]
1	10.1	9.6	2.4	1.8	1.3	5.1
2	9.8	9.0	1.9	1.0	1.9	7.3
3	8.9	8.3	2.6	1.6	1.6	5.4
4	8.4	7.5	3.8	2.0	1.9	2.5
5	9.9	9.4	2.8	2.1	1.4	4.9
6	11.3	10.1	2.1	1.0	2.1	8.5
Avg.	9.7	9.0	2.6	1.6	1.7	5.6

Note: All values are per screw

LW-10-m-5ply-1SP

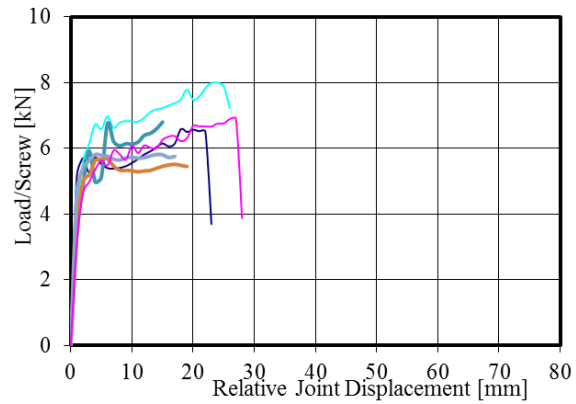
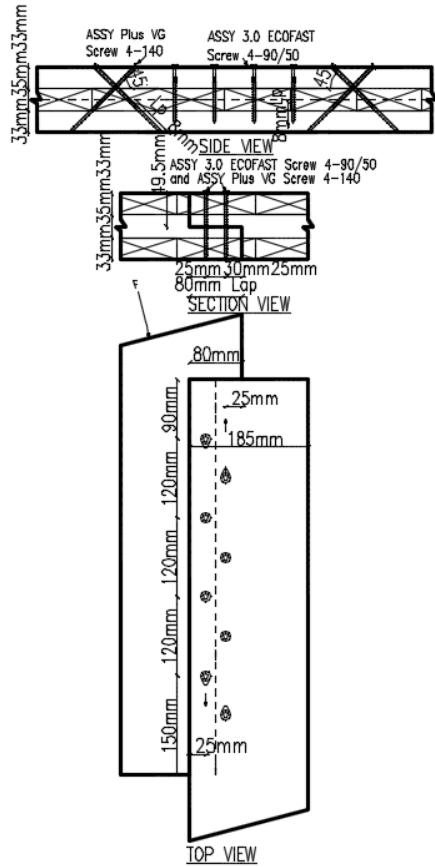


	F_{\max}	F_Y	$d_{F\max}$	$d_{F,Y}$	μ	k
LW-10-m-5ply-1SP	[kN]	[kN]	[mm]	[mm]	(-)	[kN/mm]
1	11.3	9.9	4.8	1.3	3.8	6.8
2	11.3	9.8	3.2	1.3	2.4	5.6
3	13.9	11.8	4.2	1.0	4.2	20.9
4	14.2	12.0	6.6	3.1	2.1	3.9
5	13.6	11.8	4.7	2.4	2.0	4.5
6	13.7	12.6	4.5	2.2	2.0	5.1
Avg.	13.0	11.3	4.7	1.9	2.8	5.2

Note: All values are per screw

D.7 S-1SP: Lap joints Combined - Monotonic

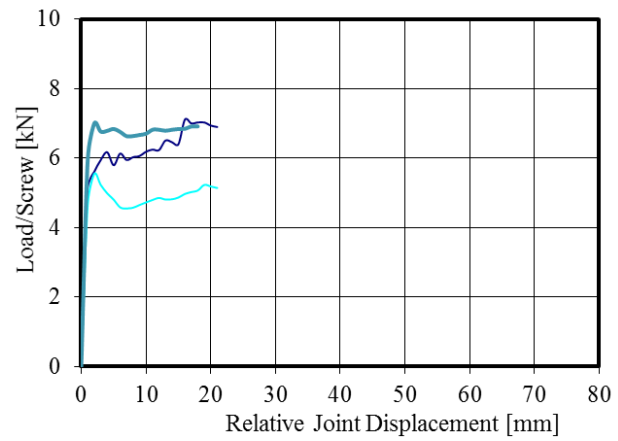
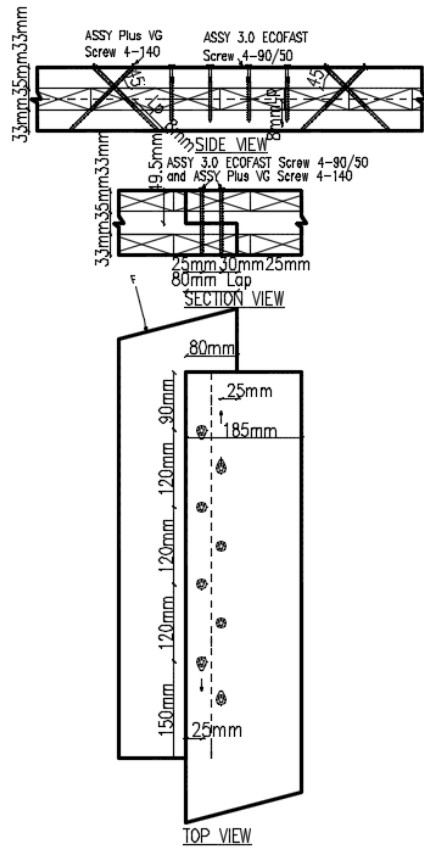
LC-WSSW-8-m-3ply-1SP



	F_{\max}	F_Y	$d_{F\max}$	$d_{F,Y}$	μ	k
LC-WSSW-8-m-3ply-1SP	[kN]	[kN]	[mm]	[mm]	(-)	[kN/mm]
1	6.6	5.4	17.2	0.5	34.4	24.7
2	8.0	4.1	21.6	0.8	25.5	3.9
3	6.8	5.2	14.1	1.3	11.0	3.4
4	5.8	4.1	5.5	1.0	5.5	3.5
5	6.1	5.8	4.2	1.4	3.0	5.7
6	7.0	6.2	25.8	1.0	25.8	52.2
Avg.	6.7	5.1	14.7	1.0	17.5	4.1

Note: All values are per screw

LC-WSSW-8-m-3ply-1SP*

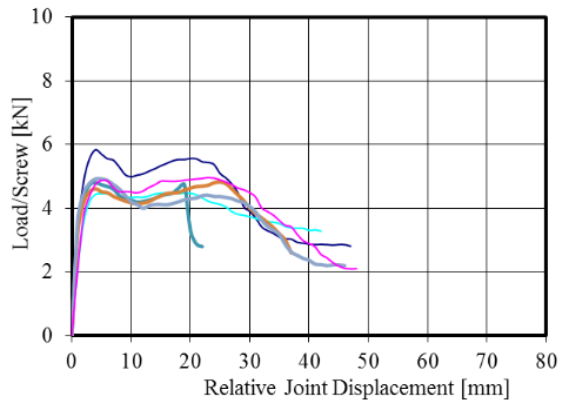
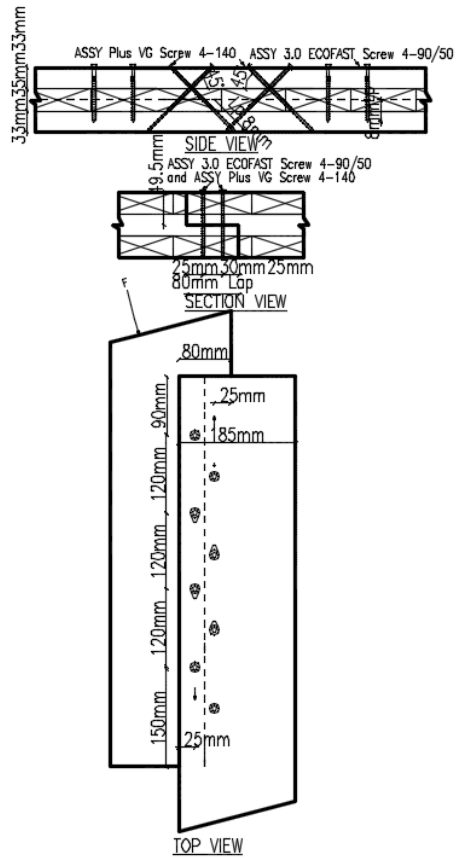


	F_{\max}	F_Y	$d_{F\max}$	$d_{F,Y}$	μ	k
LC-WSSW-8-m-3ply-1SP*	[kN]	[kN]	[mm]	[mm]	(-)	[kN/mm]
1	7.1	5.9	17.5	0.9	18.6	6.1
2	5.7	5.4	5.7	1.0	5.7	18.9
3	7.3	5.3	2.9	0.9	3.2	8.1
Avg.	6.7	5.6	8.7	0.9	9.2	7.1

Note: All values are per screw

*indicates specimen with friction-eliminating membrane

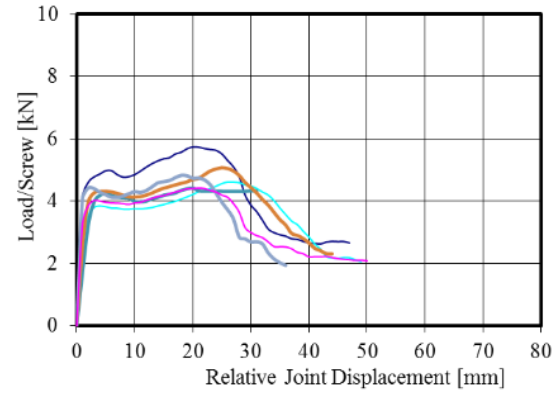
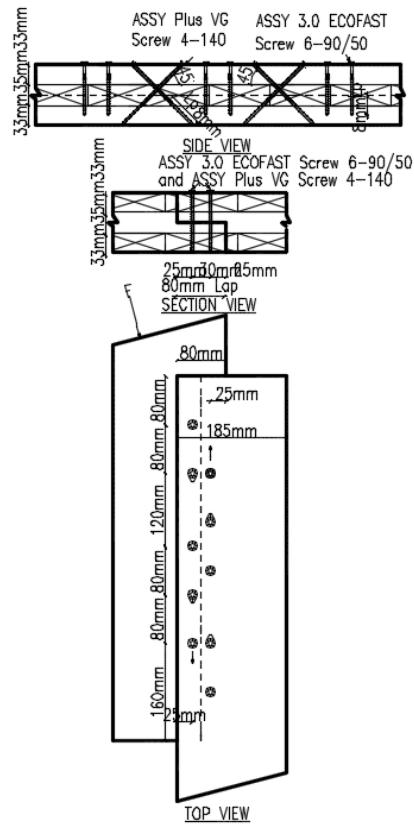
LC-SWWS-8-m-3ply-1SP



	F_{\max}	F_Y	$d_{F\max}$	$d_{F,Y}$	μ	k
LC-SWWS-8-m-3ply-1SP	[kN]	[kN]	[mm]	[mm]	(-)	[kN/mm]
1	5.8	5.3	4.1	1.5	2.8	3.5
2	4.5	4.2	15.6	1.9	8.2	1.9
3	4.8	4.3	3.7	0.8	4.9	5.2
4	4.8	4.2	24.5	1.0	25.0	3.5
5	4.9	4.4	4.7	1.0	4.7	7.8
6	5.0	4.3	22.8	2.5	9.0	2.1
Avg.	5.0	4.5	12.6	1.4	9.1	4.0

Note: All values are per screw

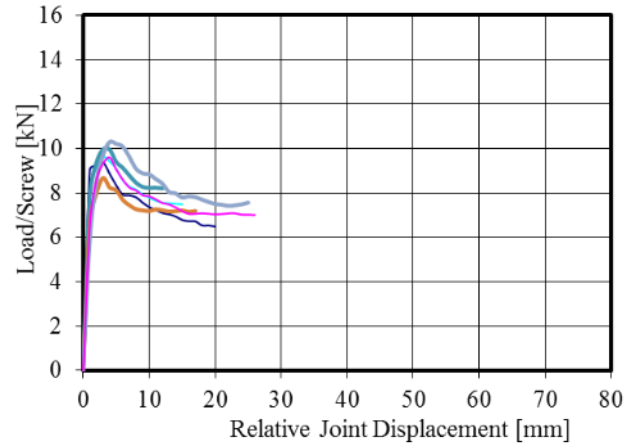
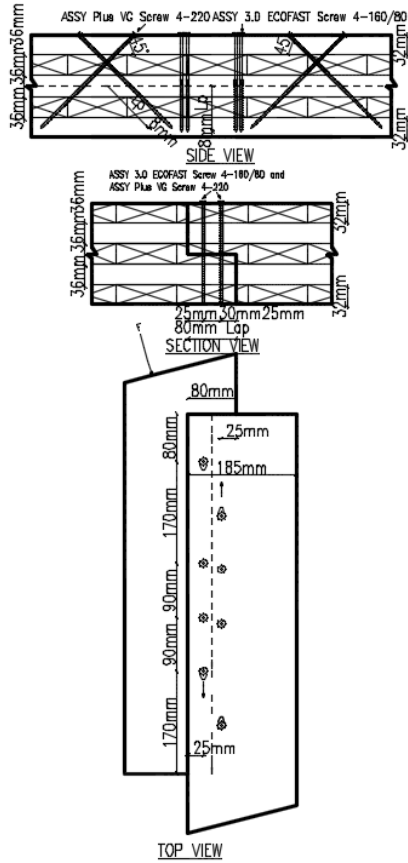
LC-SWSWS-10-m-3ply-1SP



LC-SWSWS-10-m-3ply-1SP	F_{max} [kN]	F_Y [kN]	d_{Fmax} [mm]	$d_{F,Y}$ [mm]	μ (-)	k [kN/mm]
1	5.8	4.8	20.7	1.0	20.7	17.3
2	4.6	4.1	26.3	1.7	15.1	2.8
3	4.8	4.6	38.0	4.6	8.2	1.6
4	5.1	4.5	25.2	1.7	15.1	2.5
5	4.8	4.2	18.1	1.0	18.1	72.7
6	4.4	3.9	20.8	1.0	20.8	4.7
Avg.	4.9	4.3	24.9	1.8	16.3	2.9

Note: All values are per screw

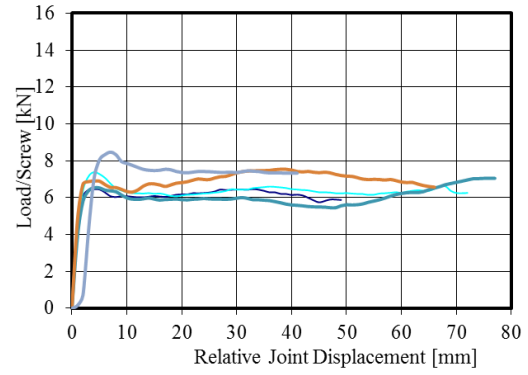
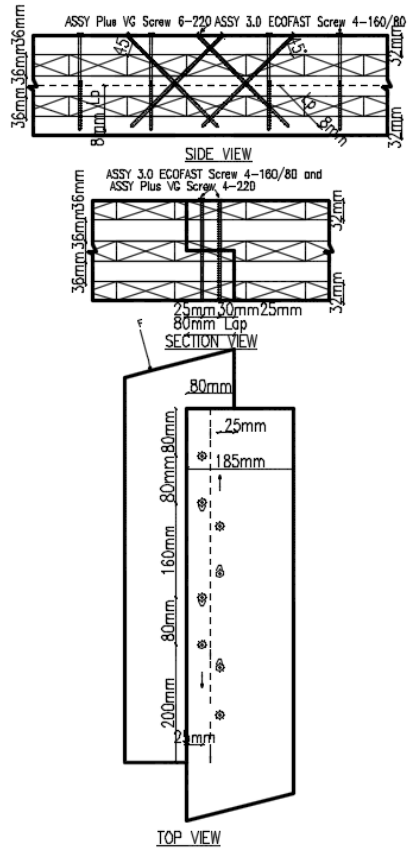
LC-WSSW-8-m-5ply-1SP



	F_{max}	F_Y	d_{Fmax}	$d_{F,Y}$	μ	k
LC-WSSW-8-m-5ply-1SP	[kN]	[kN]	[mm]	[mm]	(-)	[kN/mm]
1	10.0	4.4	1.8	0.2	8.2	149.8
2	9.6	8.7	3.8	0.6	6.0	12.6
3	10.1	9.0	3.5	0.8	4.2	9.5
4	8.8	7.7	3.1	0.7	4.5	7.1
5	10.5	9.3	4.6	1.4	3.4	5.0
6	9.7	8.5	3.4	0.3	11.0	9.7
Avg.	9.8	7.9	3.4	0.7	6.2	7.8

Note: All values are per screw

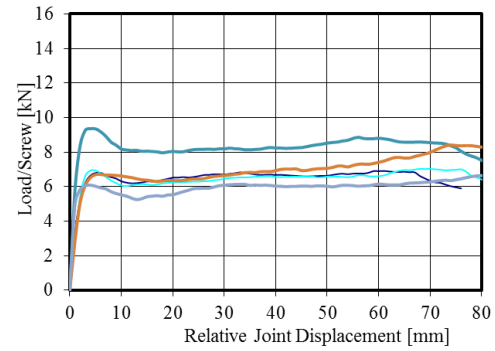
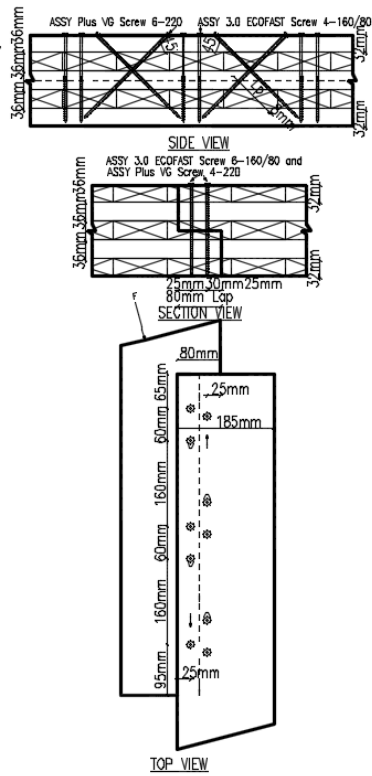
LC-SWWS-8-m-5ply-1SP



	F_{max}	F_Y	d_{Fmax}	$d_{F,Y}$	μ	k
LC-SWWS-8-m-5ply-1SP	[kN]	[kN]	[mm]	[mm]	(-)	[kN/mm]
1	6.5	6.1	3.6	0.7	5.1	6.3
2	7.4	6.7	4.1	1.6	2.6	3.7
3	6.5	6.2	4.3	1.1	3.9	3.9
4	7.5	6.8	37.9	1.4	27.9	5.7
5	8.5	7.8	7.2	1.2	6.0	3.6
Avg.	7.3	6.7	11.4	1.2	9.1	4.6

Note: All values are per screw

LC-SWSWS-10-m-5ply-1SP

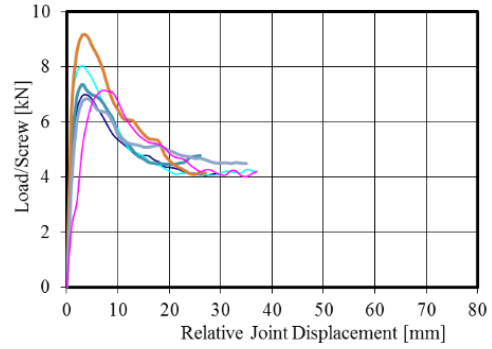
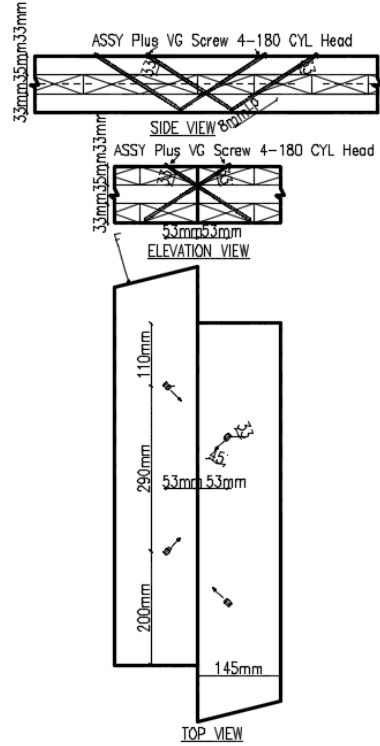


LC-SWSWS-10-m-5ply-1SP	F _{max}	F _Y	d _{Fmax}	d _{F,Y}	μ	k
	[kN]	[kN]	[mm]	[mm]	(-)	[kN/mm]
1	6.8	6.1	33.1	1.7	19.2	3.4
2	7.0	6.4	4.4	2.0	2.2	3.0
3	9.4	8.4	3.7	0.5	16.8	5.1
4	7.1	6.5	48.4	1.0	48.4	2.6
5	6.2	5.5	33.4	0.7	46.3	9.2
Avg.	7.3	6.6	24.6	1.2	26.6	4.7

Note: All values are per screw

D.8 S-1SP: Butt joints Withdrawal - Monotonic

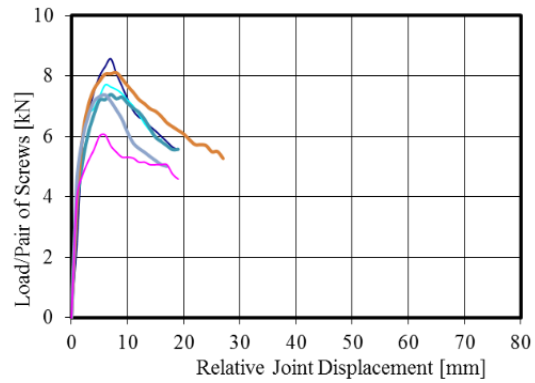
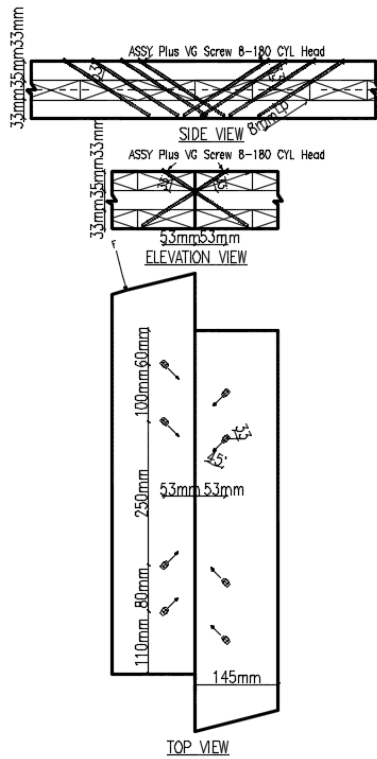
BW-4-m-3ply-1SP



	F_{\max}	F_Y	$d_{F\max}$	$d_{F,Y}$	μ	k
BW-4-m-3ply-1SP	[kN]	[kN]	[mm]	[mm]	(-)	[kN/mm]
1	7.0	6.3	3.4	1.0	3.4	5.1
2	8.1	7.5	2.9	1.0	2.9	7.8
3	7.4	6.4	2.9	0.9	3.1	4.9
4	9.2	8.4	2.4	0.8	2.9	92.0
5	6.9	6.3	4.0	1.6	2.6	3.4
6	7.2	6.3	7.4	4.2	1.7	1.3
Avg.	7.6	6.9	3.8	1.6	2.8	4.5

Note: All values are per screw

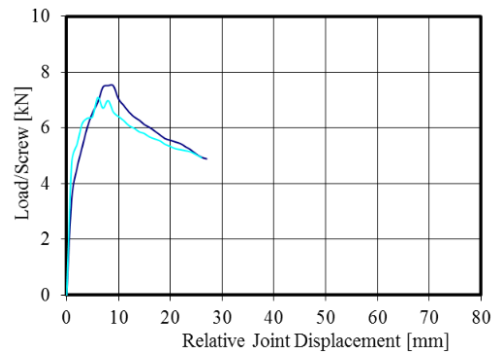
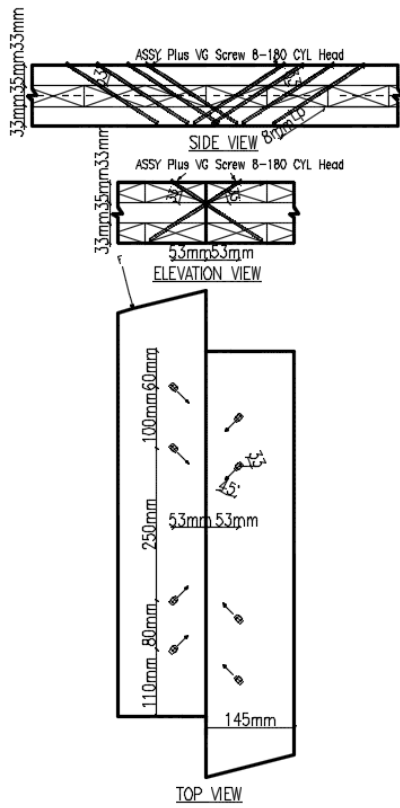
BW-8-m-3ply-1SP



	F_{max}	F_Y	d_{Fmax}	$d_{F,Y}$	μ	k
BW-8-m-3ply-1SP	[kN]	[kN]	[mm]	[mm]	(-)	[kN/mm]
1	8.6	7.3	7.0	2.0	3.5	4.3
2	7.9	6.4	7.1	1.0	7.1	4.5
3	7.7	6.3	7.6	1.4	5.6	3.7
4	8.5	7.6	6.9	1.1	6.6	6.4
5	7.8	6.7	4.6	1.0	4.5	7.8
6	6.1	5.2	5.6	1.1	5.2	61.3
Avg.	7.8	6.6	6.5	1.2	5.4	5.3

Note: All values are per screw

BW-8-m-3ply-1SP*



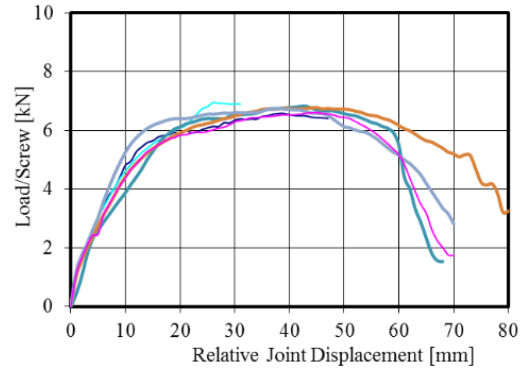
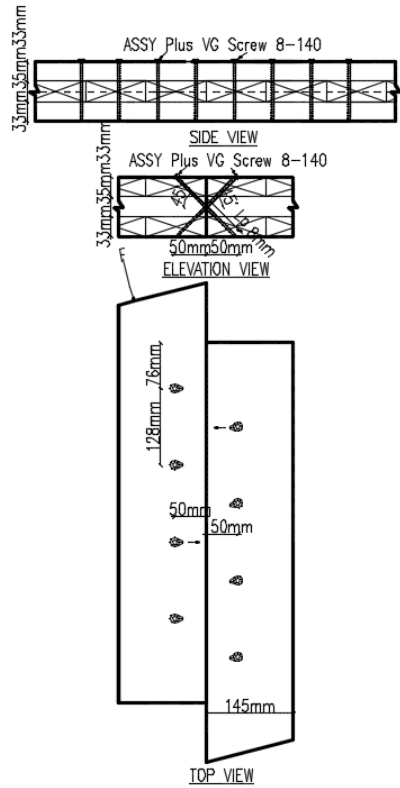
	F_{max}	F_Y	d_{Fmax}	$d_{F,Y}$	μ	k
BW-8-m-3ply-1SP*	[kN]	[kN]	[mm]	[mm]	(-)	[kN/mm]
1	7.5	6.3	8.4	2.0	4.2	4.3
2	7.1	6.3	6.5	1.1	6.0	4.3
Avg	7.3	6.3	7.4	1.5	5.1	4.3

Note: All values are per screw

*indicates specimen with friction-eliminating membrane

D.9 S-1SP: Butt joints Shear - Monotonic

BS-8-m-3ply-1SP

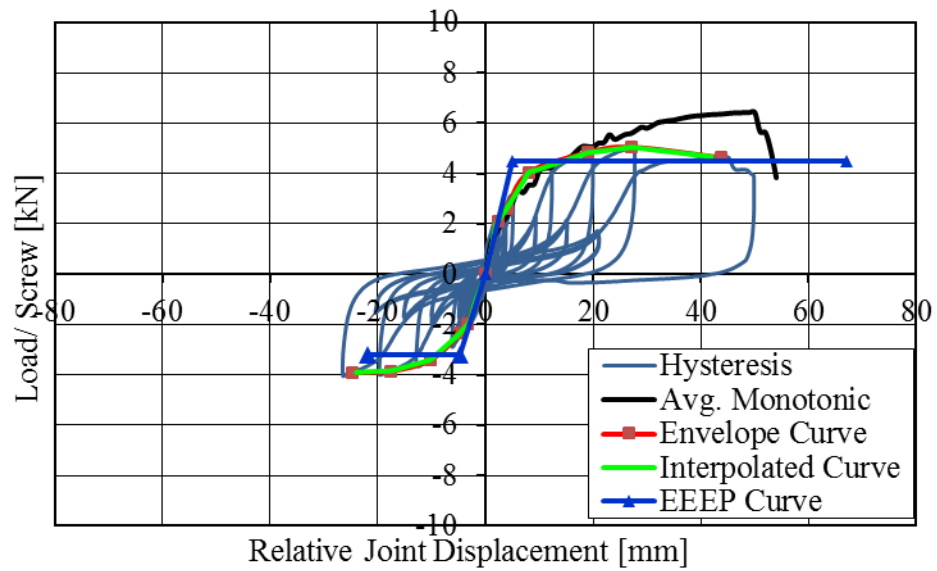
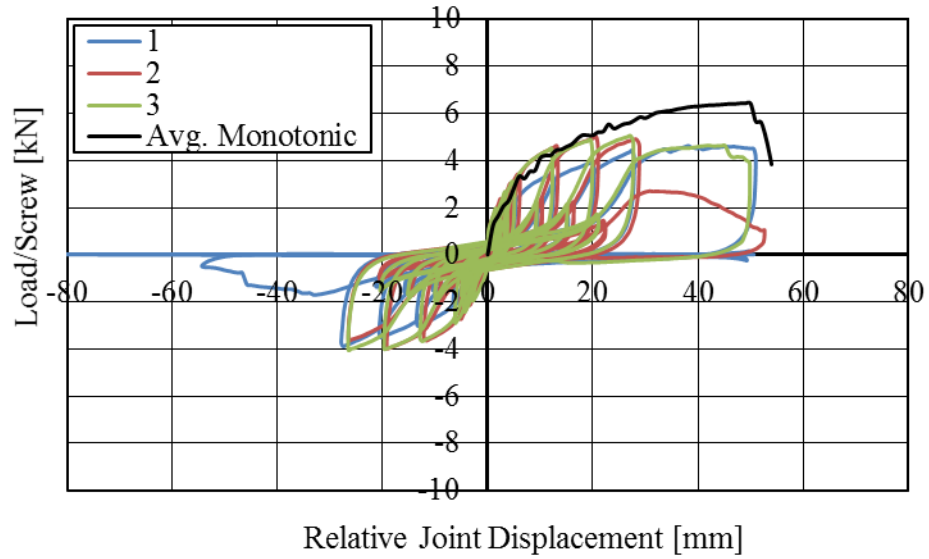


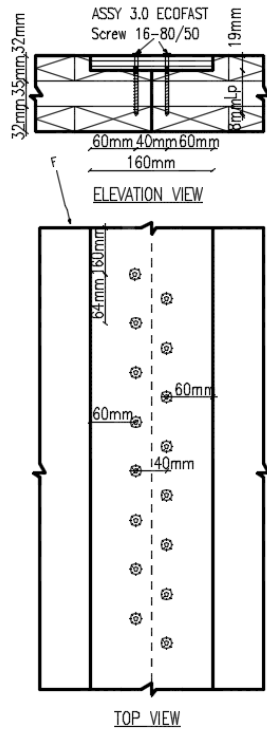
	F_{\max}	F_Y	$d_{F\max}$	$d_{F,Y}$	μ	k
BS-8-m-3ply-1SP	[kN]	[kN]	[mm]	[mm]	(-)	[kN/mm]
1	6.6	4.1	38.0	8.0	4.8	0.6
2	7.0	4.5	26.0	7.8	3.3	0.5
3	6.8	4.2	43.0	8.0	5.4	0.5
4	6.8	4.2	45.0	7.4	6.0	0.5
5	6.8	4.5	38.0	7.7	4.9	0.5
6	6.6	4.2	45.0	8.3	5.4	0.4
Avg.	6.8	4.3	39.2	7.9	5.0	0.5

Note: All values are per screw

D.10 S-1SP: Spline joints - Cyclic

SS-16-c-3ply-1SP



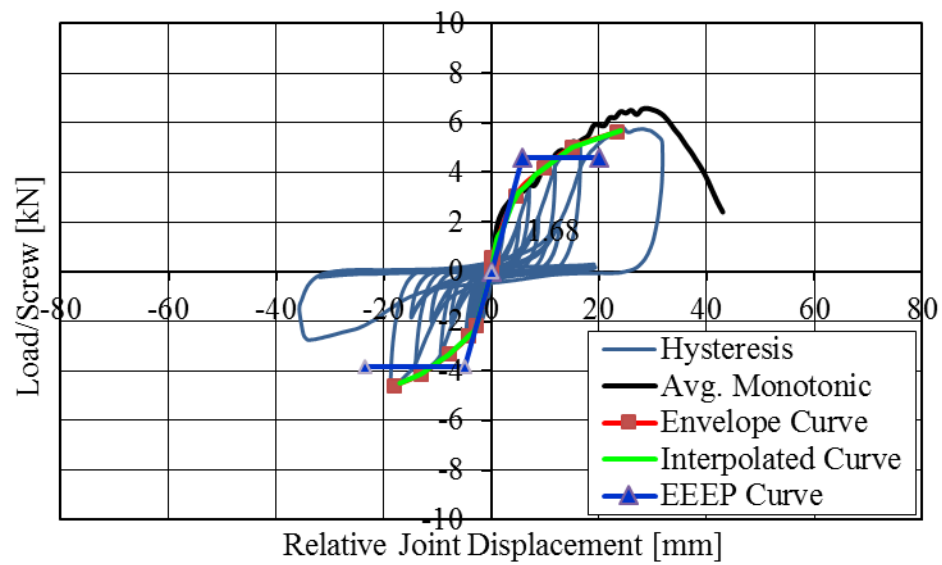
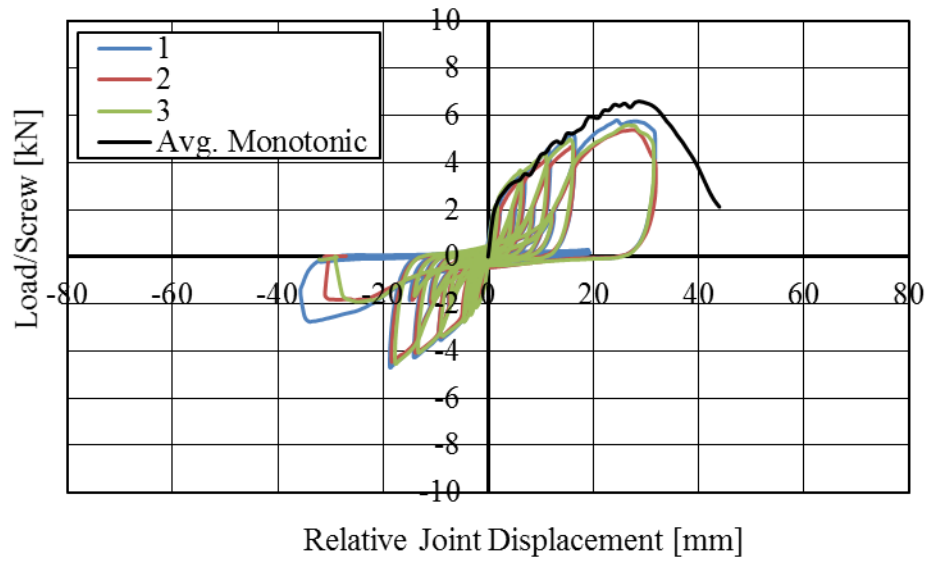


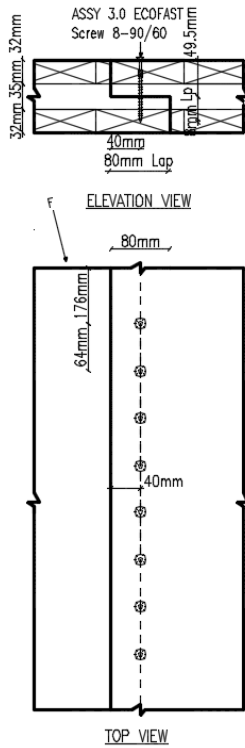
Spec.	F_{max} [kN]	F_Y [kN]	d_{Fmax} [mm]	$d_{F,Y}$ [mm]	μ (-)	k [kN/mm]
1	4.5 (3.9)	2.6 (2.4)	40.0 (27.0)	9.7 (6.3)	4.1 (4.3)	0.2 (0.4)
2	5.0 (3.9)	3.5 (2.7)	28.0 (18.0)	4.5 (4.0)	6.2 (4.5)	0.7 (0.7)
3	5.0 (4.0)	3.5 (2.7)	27.0 (25.0)	3.8 (4.7)	7.1 (5.4)	0.9 (0.5)
Avg.	4.8 (3.9)	3.2 (2.6)	31.7 (23.3)	6.0 (5.0)	5.8 (4.7)	0.6 (0.5)

Note: All values are per screw, negative envelope values within parenthesis

D.11 S-1SP: Lap joints Shear - Cyclic

LS-8-c-3ply-1SP



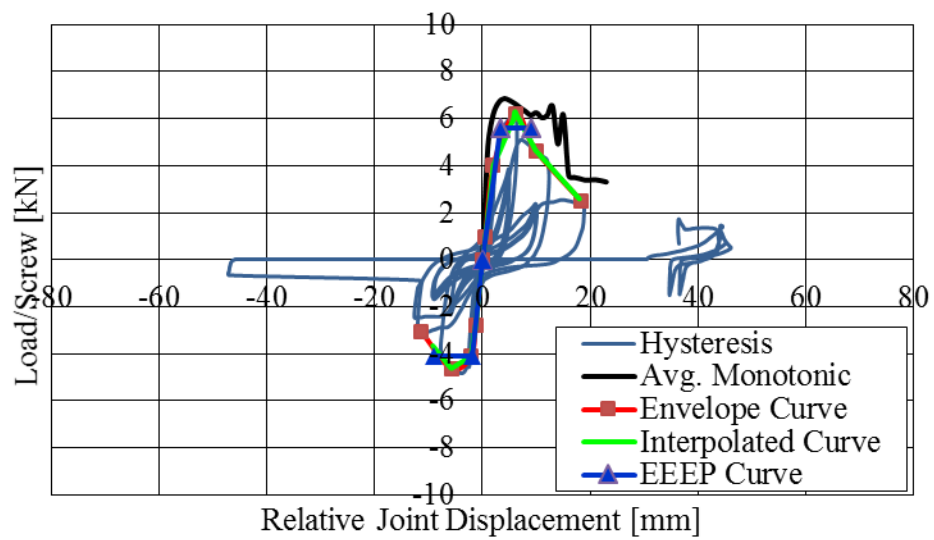
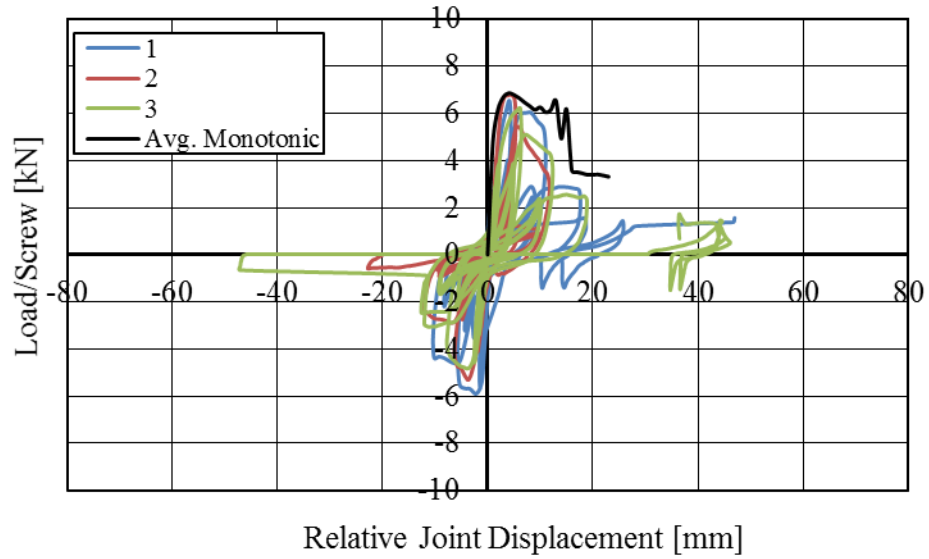


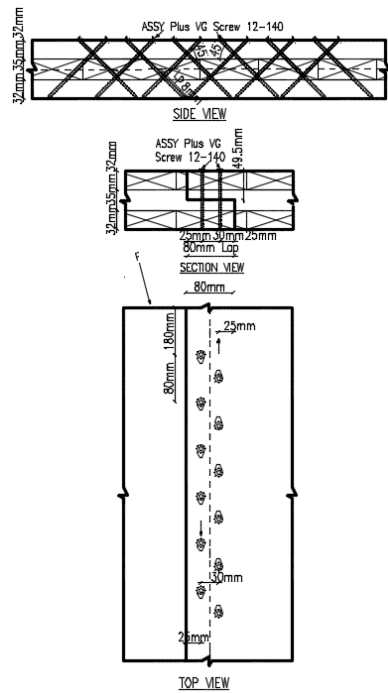
Spec.	F_{max} [kN]	F_Y [kN]	d_{Fmax} [mm]	$d_{F,Y}$ [mm]	μ (-)	k [kN/mm]
1	5.6 (4.6)	3.8 (3.2)	27.0 (18.0)	3.4 (4.1)	7.9 (4.4)	1.0 (0.8)
2	5.6 (4.3)	3.7 (3.0)	27.0 (18.0)	5.1 (4.4)	5.3 (4.1)	0.6 (0.7)
3	5.6 (4.5)	3.9 (3.1)	27.0 (17.0)	3.5 (3.8)	7.7 (4.5)	0.9 (0.8)
Avg.	5.6 (4.5)	3.8 (3.1)	27.0 (17.7)	4.0 (4.1)	7.0 (4.3)	0.8 (0.7)

Note: All values are per screw, negative envelope values within parenthesis

D.12 S-1SP: Lap joints Withdrawal - Cyclic

LW-12-c-3ply-1SP



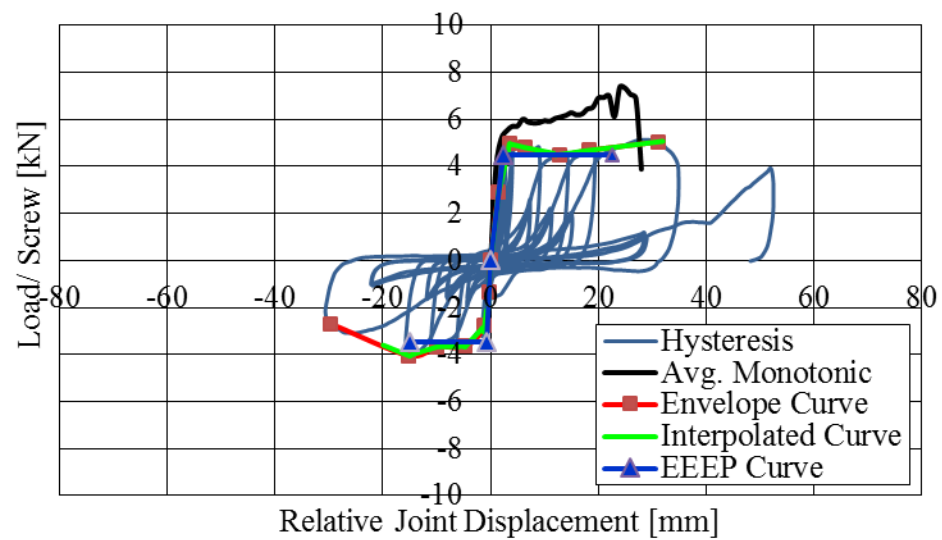
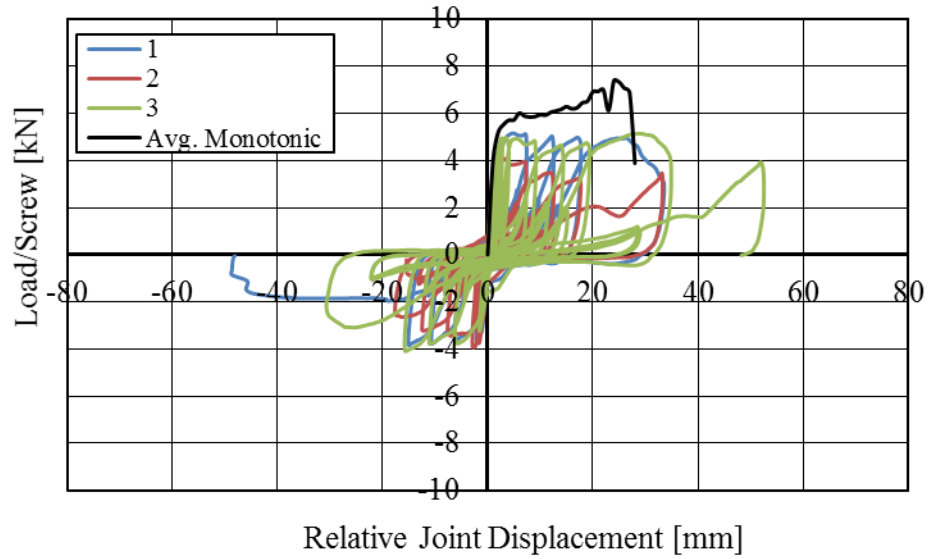


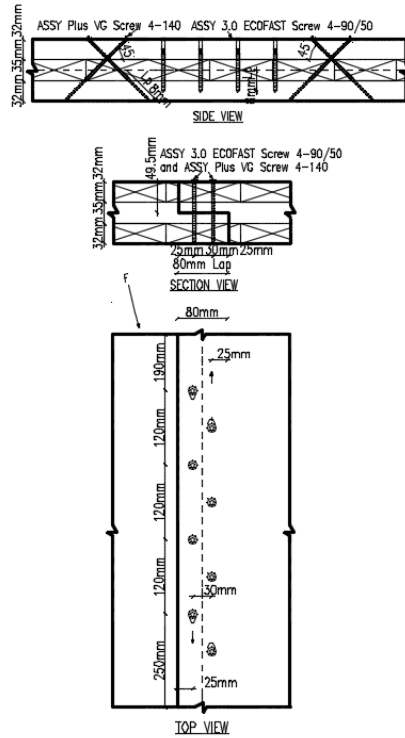
Spec.	F_{max} [kN]	F_Y [kN]	d_{Fmax} [mm]	$d_{F,Y}$ [mm]	μ (-)	k [kN/mm]
1	6.5 (5.7)	5.8 (5.1)	4.0 (3.3)	2.4 (1.1)	1.6 (2.9)	2.0 (4.3)
2	6.5 (5.7)	5.8 (5.1)	4.0 (3.3)	2.4 (1.1)	1.6 (2.9)	2.0 (4.3)
3	6.3 (4.6)	4.8 (4.1)	6.1 (5.8)	3.5 (1.9)	1.7 (3.1)	1.3 (2.3)
Avg.	6.4 (5.3)	5.5 (4.8)	4.7 (4.1)	2.8 (1.4)	1.7 (3.0)	1.7 (3.6)

Note: All values are per screw, negative envelope values within parenthesis

D.13 S-1SP: Lap joints Combined - Cyclic

LC-WSSW-8-c-3ply-1SP

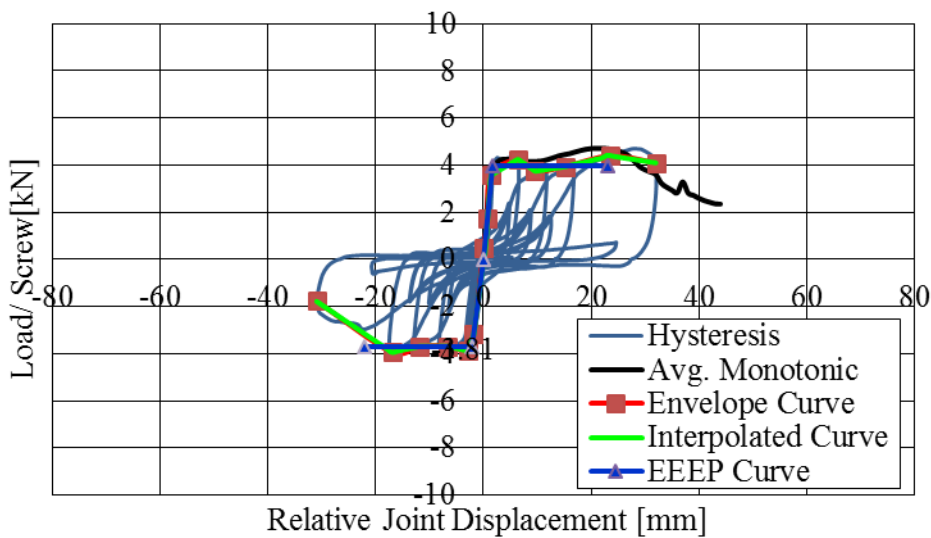
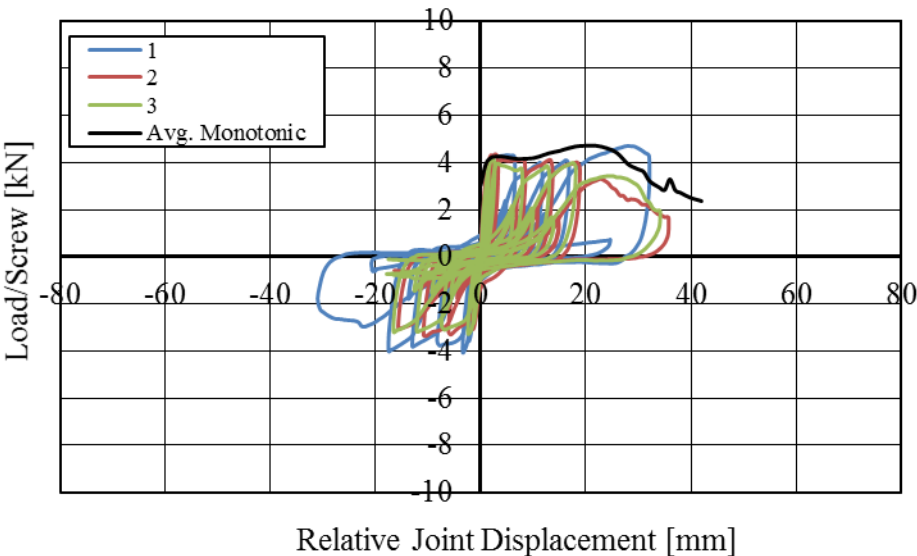


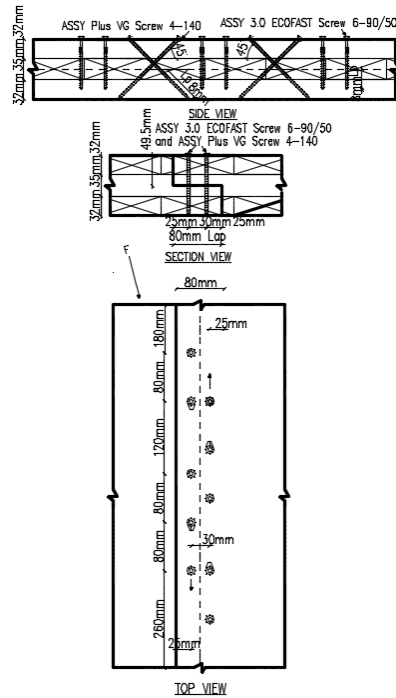


Spec.	F_{max} [kN]	F_Y [kN]	d_{Fmax} [mm]	$d_{F,Y}$ [mm]	μ (-)	k [kN/mm]
1	5.2 (3.8)	4.6 (3.5)	4.7 (14.0)	1.7 (1.1)	2.7 (12.8)	2.6 (3.8)
2	3.8 (3.9)	3.4 (3.4)	4.6 (2.3)	0.6 (1.3)	7.2 (1.7)	3.7 (2.9)
3	5.0 (4.1)	4.4 (3.4)	3.5 (15.0)	2.3 (0.8)	1.5 (19.6)	2.1 (3.0)
Avg.	4.6 (3.9)	4.1 (3.4)	4.3 (10.4)	1.6 (1.1)	3.8 (11.4)	2.8 (3.2)

Note: All values are per screw, negative envelope values within parenthesis

LC-SWSWS-10-c-3ply-1SP



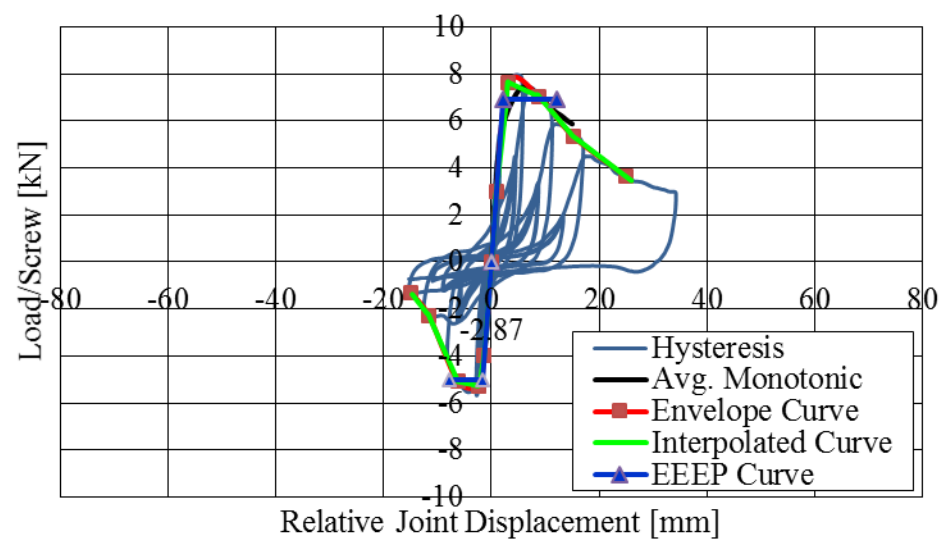
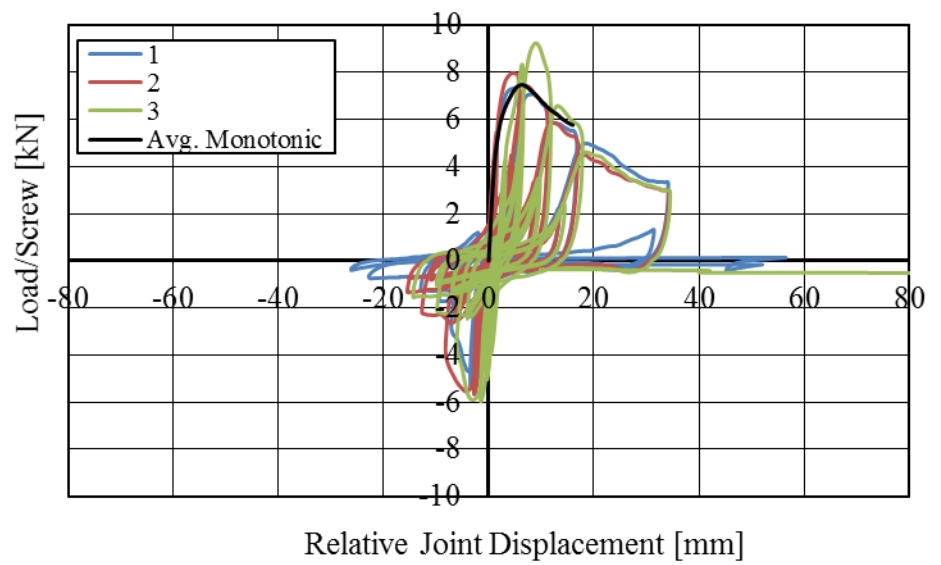


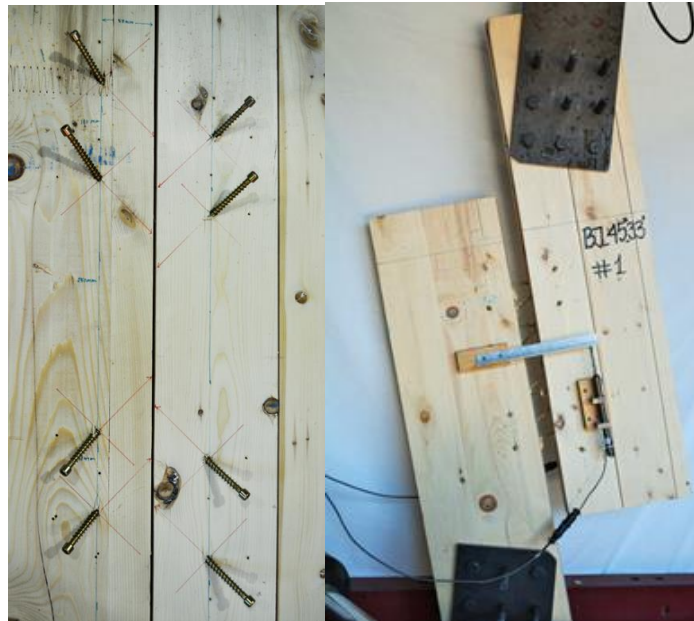
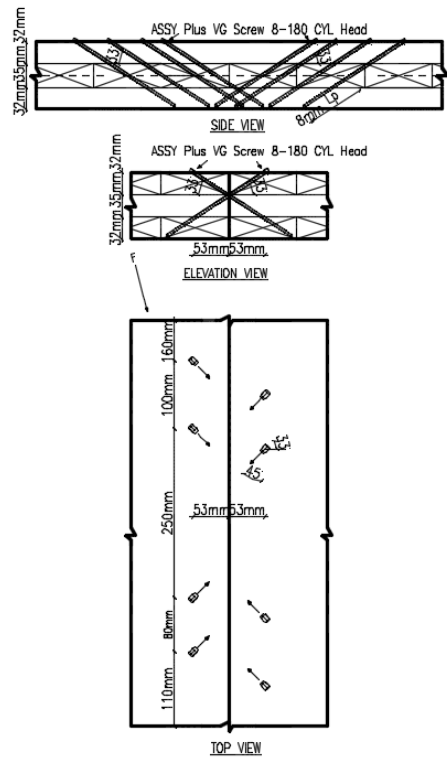
Spec.	F_{max} [kN]	F_Y [kN]	d_{Fmax} [mm]	$d_{F,Y}$ [mm]	μ (-)	k [kN/mm]
1	4.7 (3.9)	3.9 (3.5)	27.0 (17.0)	1.7 (2.0)	16.0 (8.6)	2.3 (1.7)
2	4.4 (3.3)	3.9 (2.9)	2.8 (9.7)	2.6 (0.8)	1.1 (12.2)	1.5 (3.2)
3	4.2 (3.2)	3.7 (2.9)	2.2 (16.0)	2.0 (1.2)	1.1 (13.8)	1.8 (2.4)
Avg.	4.4 (3.5)	3.8 (3.1)	10.7 (14.2)	2.1 (1.3)	6.1 (11.5)	1.9 (2.4)

Note: All values are per screw, negative envelope values within parenthesis

D.14 S-1SP: Butt joints Withdrawal - Cyclic

BW-8-c-3ply-1SP





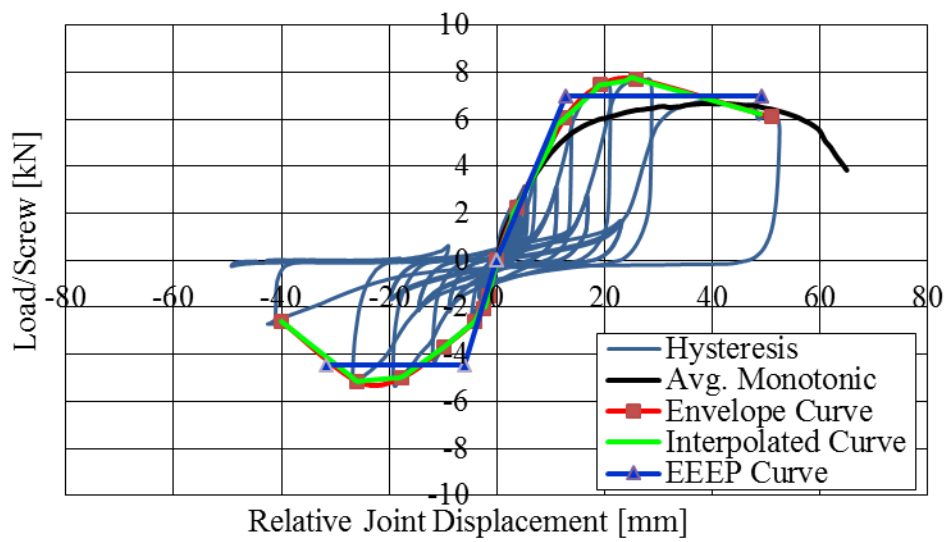
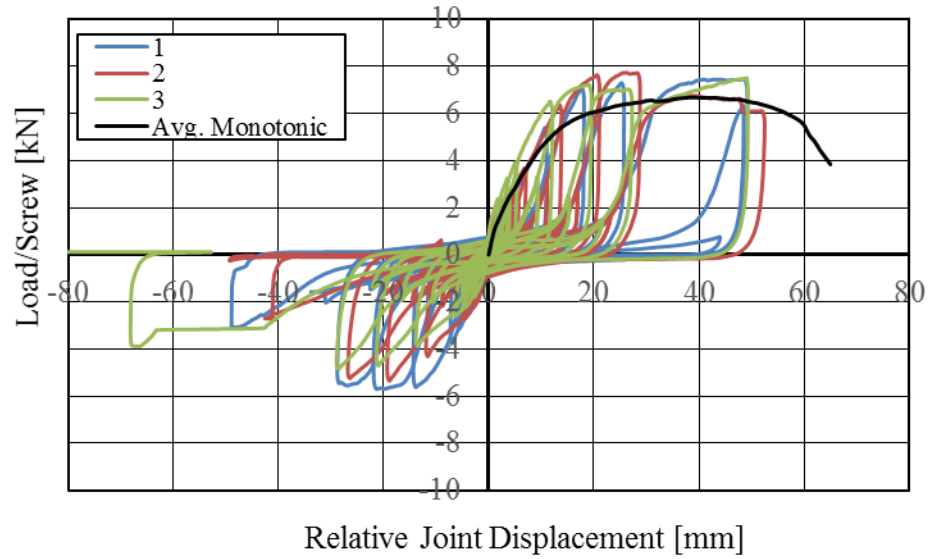
Positive envelope

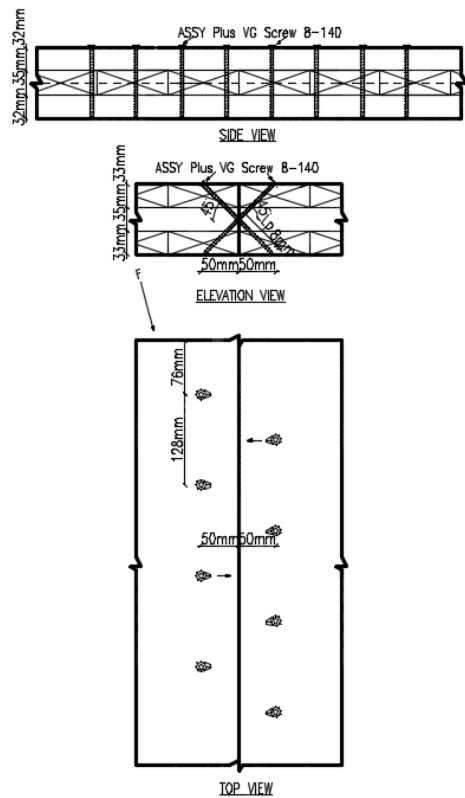
Spec.	F_{max} [kN]	F_Y [kN]	d_{Fmax} [mm]	$d_{F,Y}$ [mm]	μ (-)	k [kN/mm]
1	7.0 (5.2)	6.4 (4.7)	8.8 (2.9)	2.3 (2.0)	3.9 (1.5)	2.6 (2.2)
2	7.6 (5.3)	6.8 (4.9)	3.1 (2.3)	2.1 (1.7)	1.5 (1.4)	3.3 (3.2)
3	10.4 (5.7)	7.7 (5.3)	8.7 (2.3)	3.1 (2.2)	2.8 (1.0)	2.2 (2.1)
Avg.	8.3 (5.4)	7.0 (5.0)	6.9 (2.5)	2.5 (2.0)	2.7 (1.3)	2.7 (2.5)

Note: All values are per screw, negative envelope values within parenthesis

D.15 S-1SP: Butt joints Shear - Cyclic

BS-8-c-3ply-1SP





Positive envelope

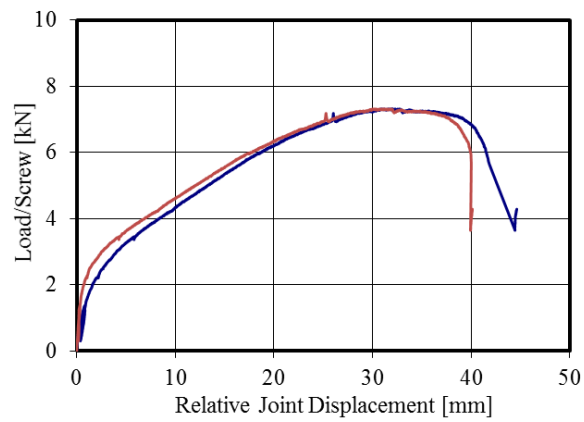
Spec.	F_{\max} [kN]	F_Y [kN]	$d_{F\max}$ [mm]	$d_{F,Y}$ [mm]	μ (-)	k [kN/mm]
1	7.5 (5.7)	4.3 (3.7)	49.0 (19.0)	8.6 (6.7)	5.7 (2.8)	0.4 (0.6)
2	7.8 (5.3)	4.5 (3.5)	25.0 (25.0)	7.0 (4.2)	3.6 (6.0)	0.5 (0.8)
3	7.5 (4.8)	4.7 (3.0)	48.0 (28.0)	6.2 (5.6)	7.7 (5.0)	0.7 (0.5)
Avg.	7.6 (5.3)	4.5 (3.4)	40.7 (24.0)	7.3 (5.5)	5.7 (4.6)	0.5 (0.6)

Note: All values are per screw, negative envelope values within parenthesis

Appendix E Detailed test results of medium sized specimens (M-2SP)

E.1 M-2SP: Lap joints Shear

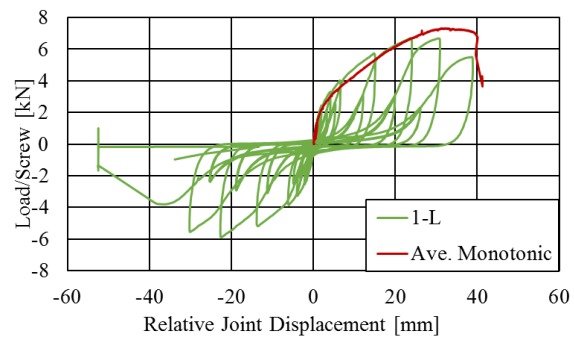
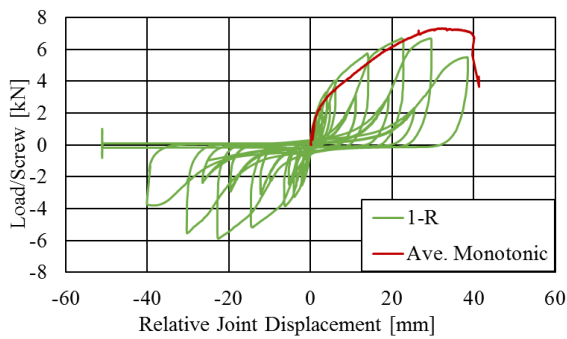
LS-16-m-3ply-2SP



Spec.	F_{\max} [kN]	F_Y [kN]	$d_{F\max}$ [mm]	$d_{F,Y}$ [mm]	μ (-)	k [kN/mm]
R	7.3	6.1	31.0	8.3	3.7	0.6
L	7.3	6.0	31.0	4.8	6.4	1.0
Avg.	7.3	6.0	31.0	6.6	5.1	0.8

Note: All values are per screw, R=right side, L=left side of the connection

LS-16-c-3ply-2SP

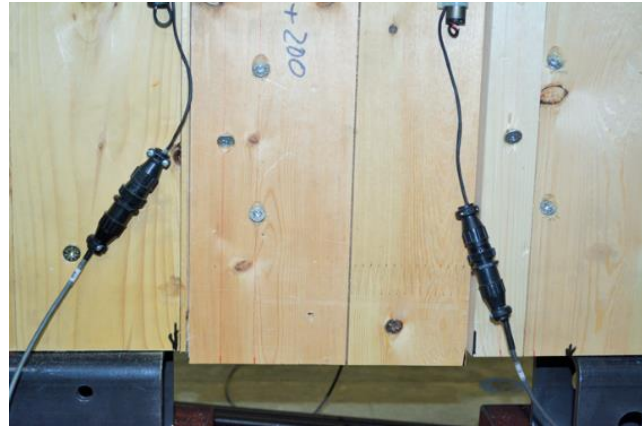
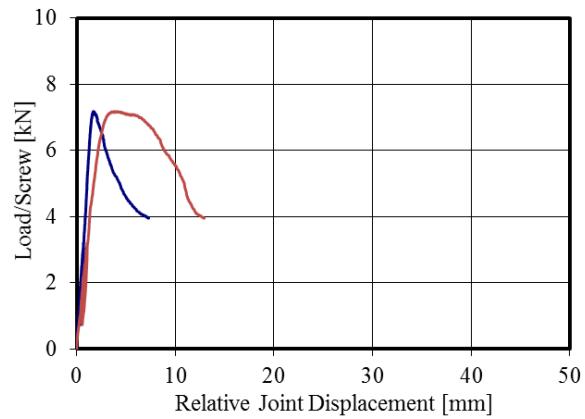


Spec.	F_{max} [kN]	F_Y [kN]	d_{Fmax} [mm]	$d_{F,Y}$ [mm]	μ (-)	k [kN/mm]
1-R	6.7 (5.9)	5.6 (5.1)	27.0 (22.0)	7.7 (4.4)	3.5 (5.0)	0.6 (0.9)
1-L	6.9 (5.9)	6.0 (5.1)	27.0 (22.0)	8.0 (4.9)	3.4 (4.5)	0.6 (0.9)
1	6.8 (5.9)	5.8 (5.1)	27.0 (22.0)	7.9 (4.7)	3.4 (4.7)	0.6 (0.9)
2-L	6.3 (6.4)	5.4 (5.7)	27.0 (29.0)	8.0 (4.1)	3.4 (7.1)	0.4 (1.0)
2	6.3 (6.4)	5.4 (5.7)	27.0 (29.0)	8.0 (4.1)	3.4 (7.1)	0.4 (1.0)
3-R	6.4 (6.1)	5.3 (5.2)	31.0 (29.0)	7.5 (5.0)	4.1 (5.8)	0.6 (0.9)
3-L	6.4 (5.9)	5.2 (5.2)	33.0 (30.0)	7.4 (3.5)	4.5 (8.6)	0.4 (1.8)
3	6.4 (6.0)	5.3 (5.2)	32.0 (29.5)	7.5 (4.2)	4.3 (7.2)	0.5 (1.3)
Avg.	6.5 (6.1)	5.5 (5.3)	28.7 (26.8)	7.8 (4.3)	3.7 (6.3)	0.5 (1.1)

Note: All values are per screw, R=right side, L=left side of the connection, negative envelope values within parenthesis, replicate 2 right transducer did not work properly

E.2 M-2SP: Lap joints Withdrawal

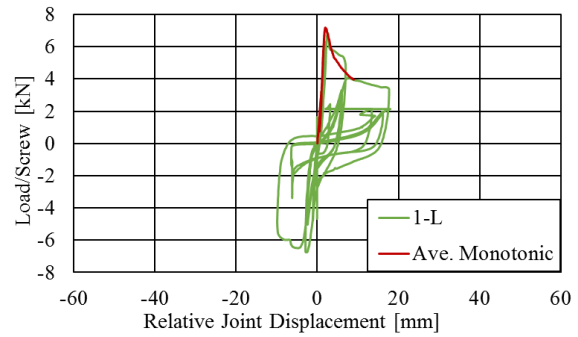
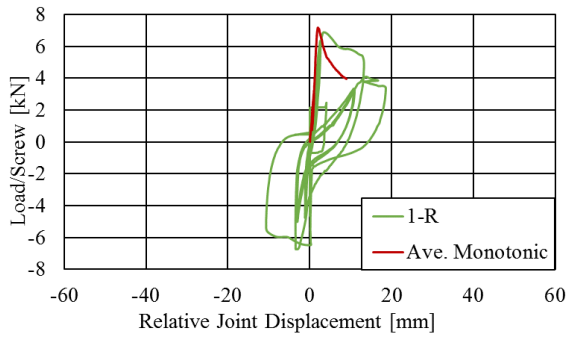
LW-16-m-3ply-2SP



Spec.	F_{\max} [kN]	F_Y [kN]	$d_{F\max}$ [mm]	$d_{F,Y}$ [mm]	μ (-)	k [kN/mm]
R	7.1	6.5	1.7	1.4	1.2	3.6
L	7.2	6.8	3.9	2.5	1.5	2.7
Avg.	7.2	6.6	2.8	2.0	1.4	3.1

Note: All values are per screw, R=right side, L=left side of the connection

LW-16-c-3ply-2SP

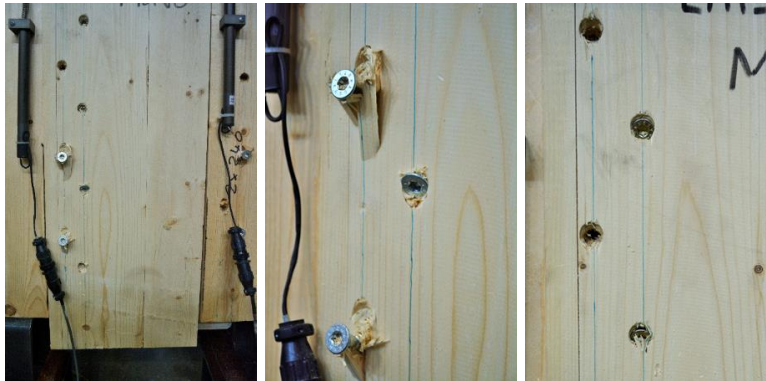
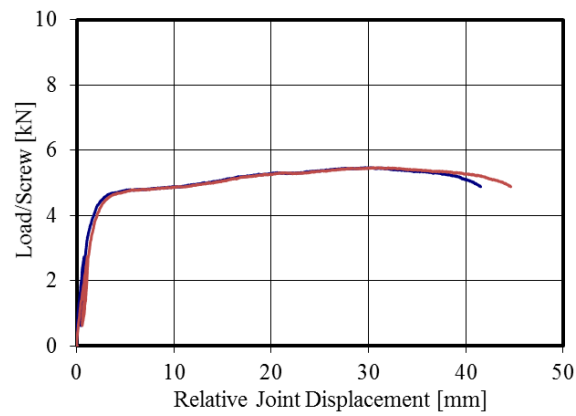
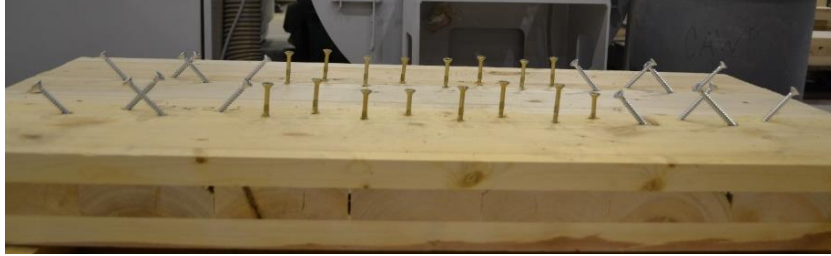


Spec.	F_{\max} [kN]	F_Y [kN]	$d_{F_{\max}}$ [mm]	$d_{F,Y}$ [mm]	μ (-)	k [kN/mm]
1-R	6.7 (6.7)	5.9 (4.2)	2.4 (2.4)	1.7 (1.1)	1.4 (2.2)	4.0 (2.8)
1-L	6.7 (6.7)	6.1 (4.3)	2.9 (2.8)	2.5 (1.2)	1.2 (2.3)	2.5 (2.9)
1	6.7 (6.7)	6.0 (4.3)	2.7 (2.6)	2.1 (1.2)	1.3 (2.2)	3.3 (2.8)
2-R	6.9 (5.9)	6.3 (5.7)	3.3 (3.4)	2.2 (2.3)	1.5 (1.5)	3.4 (3.6)
2-L	6.9 (5.8)	5.0 (5.0)	1.0 (7.0)	0.7 (1.1)	1.4 (6.4)	10.3 (1.9)
2	6.9 (5.9)	5.6 (5.3)	2.2 (5.2)	1.4 (1.7)	1.5 (3.9)	6.9 (2.7)
3-L	7.1 (6.6)	6.8 (3.5)	2.2 (1.6)	2.1 (2.0)	1.1 (0.8)	3.0 (2.8)
3	7.1 (6.6)	6.8 (3.5)	2.2 (1.6)	2.1 (2.0)	1.1 (0.8)	3.0 (2.8)
Avg.	6.9 (6.4)	6.1 (4.4)	2.3 (3.1)	1.9 (1.6)	1.3 (2.3)	4.4 (2.8)

Note: All values are per screw, R=right side, L=left side of the connection, negative envelope values within parenthesis, replicate 3 right transducer did not work properly

E.3 M-2SP: Lap joints Combined

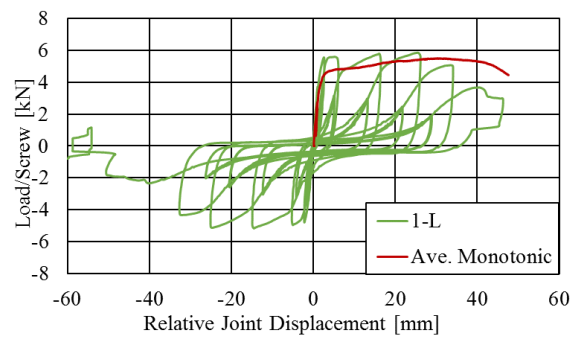
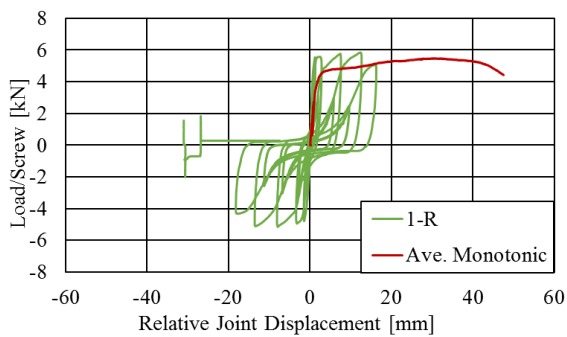
LC-WSSW-16-m-3ply-2SP



Spec.	F_{\max} [kN]	F_Y [kN]	$d_{F\max}$ [mm]	$d_{F,Y}$ [mm]	μ (-)	k [kN/mm]
R	5.5	5.0	30.0	0.5	55.2	2.7
L	5.5	5.0	32.0	2.4	13.6	1.8
Avg.	5.5	5.0	31.0	1.4	34.4	2.3

Note: All values are per screw, R=right side, L=left side of the connection

LC-WSSW-16-c-3ply-2SP

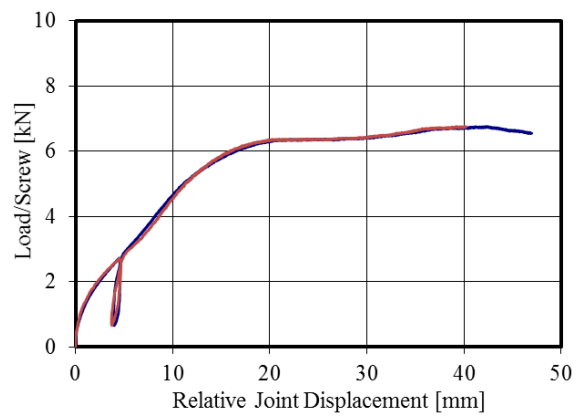


Spec.	F_{\max} [kN]	F_Y [kN]	$d_{F\max}$ [mm]	$d_{F,Y}$ [mm]	μ (-)	k [kN/mm]
1-R	5.8 (5.2)	5.4 (5.0)	12.0 (13.0)	0.9 (0.4)	13.2 (32.5)	8.7 (3.9)
1-L	5.7 (5.1)	5.4 (4.4)	14.0 (25.0)	2.4 (1.3)	5.7 (18.7)	8.5 (3.0)
1	5.7 (5.1)	5.4 (4.7)	13.0 (19.0)	1.7 (0.9)	9.5 (25.6)	8.6 (3.5)
2-R	5.8 (5.1)	5.3 (5.0)	12.0 (13.0)	0.4 (0.4)	33.3 (31.7)	8.7 (3.1)
2-L	5.7 (5.1)	4.8 (4.5)	15.0 (25.0)	1.7 (1.4)	8.8 (17.6)	2.4 (3.1)
2	5.7 (5.1)	5.0 (4.7)	13.5 (19.0)	1.0 (0.9)	21.1 (24.7)	5.6 (3.1)
3-R	5.4 (5.1)	5.2 (3.6)	5.0 (4.0)	2.5 (0.8)	2.0 (5.1)	8.2 (2.5)
3	5.4 (5.1)	5.2 (3.6)	5.0 (4.0)	2.5 (0.8)	2.0 (5.1)	8.2 (2.5)
Avg.	5.6 (5.1)	5.2 (4.3)	10.5 (14.0)	1.7 (0.9)	10.8 (18.4)	7.4 (3.0)

Note: All values are per screw, R=right side, L=left side of the connection, negative envelope values within parenthesis, replicate 3 right transducer did not work properly

E.4 M-2SP: Butt joints Shear

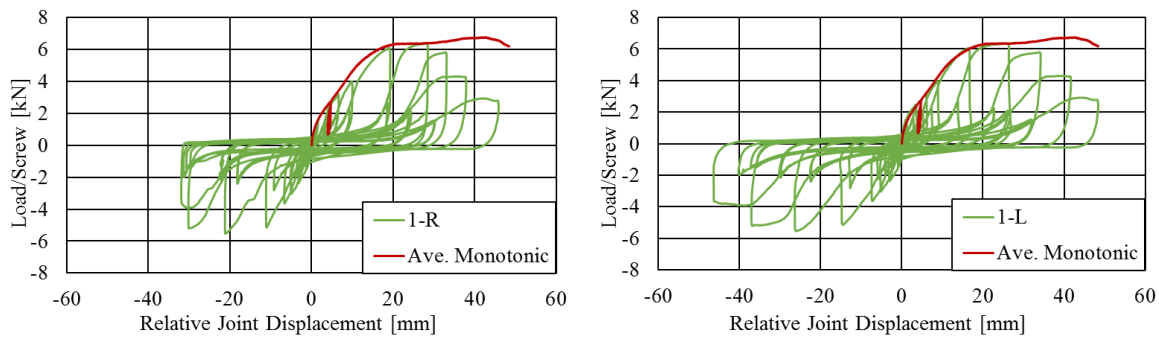
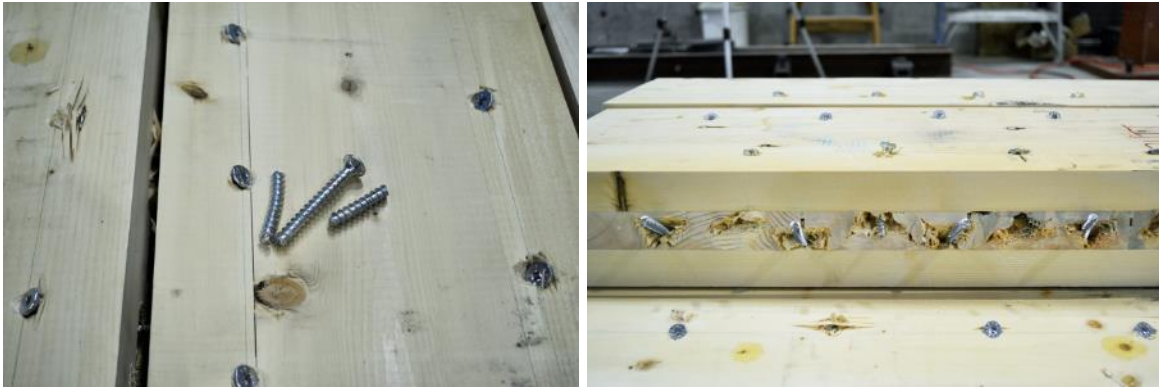
BS-16-m-3ply-2SP & BS-16-c-3ply-2SP



	F_{\max}	F_Y	$d_{F\max}$	$d_{F,Y}$	μ	k
Spec.	[kN]	[kN]	[mm]	[mm]	(-)	[kN/mm]
R	6.7	5.0	43.0	9.1	4.7	0.4
L	6.7	4.3	41.0	6.6	6.2	0.4
Avg.	6.7	4.7	42.0	7.9	5.5	0.4

Note: All values are per screw, R=right side, L=left side of the connection

BS-16-c-3ply-2SP

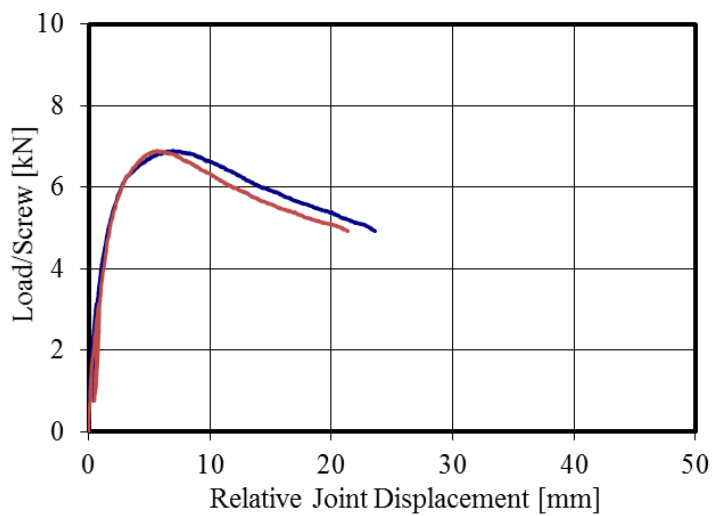


Spec.	F_{max} [kN]	F_Y [kN]	d_{Fmax} [mm]	$d_{F,Y}$ [mm]	μ (-)	k [kN/mm]
1-R	6.3 (5.5)	5.7 (4.9)	28.0 (21.0)	5.7 (3.5)	4.9 (5.9)	0.4 (0.6)
1-L	6.2 (5.5)	5.3 (4.8)	26.0 (26.0)	5.3 (3.2)	4.9 (8.2)	0.5 (1.0)
1	6.2 (5.5)	5.5 (4.9)	27.0 (23.5)	5.5 (3.4)	4.9 (7.1)	0.5 (0.8)
2-R	6.9 (6.4)	6.0 (5.7)	22.0 (26.0)	6.0 (7.3)	3.7 (3.6)	0.6 (0.7)
2-L	6.9 (6.4)	6.0 (5.4)	24.0 (23.0)	6.0 (3.3)	4.0 (7.0)	0.5 (0.7)
2	6.9 (6.4)	6.0 (5.5)	23.0 (24.5)	6.0 (5.3)	3.8 (5.3)	0.5 (0.7)
3-R	6.3 (5.4)	5.6 (4.5)	22.0 (26.0)	5.6 (3.1)	3.9 (8.3)	0.5 (0.6)
3-L	6.2 (5.5)	5.4 (4.6)	24.0 (23.0)	5.4 (3.1)	4.4 (7.5)	0.6 (0.6)
3	6.2 (5.4)	5.5 (4.6)	23.0 (24.5)	5.5 (3.1)	4.2 (7.9)	0.6 (0.6)
Avg.	6.5 (5.8)	5.7 (5.0)	24.3 (24.2)	5.7 (3.9)	4.3 (6.8)	0.5 (0.7)

Note: All values are per screw, R=right side, L=left side of the connection, negative envelope values within parenthesis

E.5 M-2SP: Butt joints Withdrawal

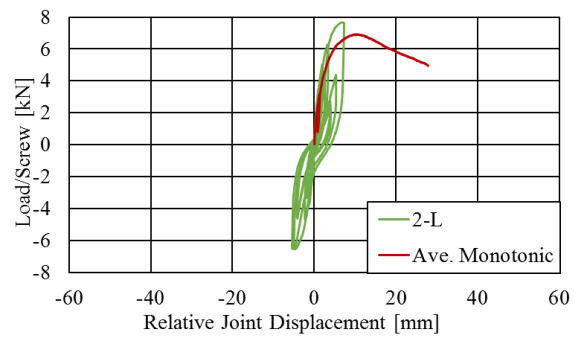
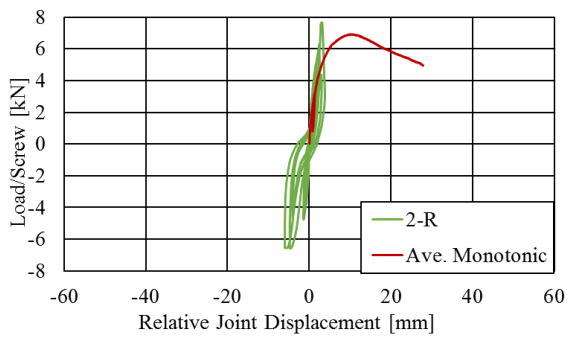
BW-16-m-3ply-2SP



	F_{\max}	F_Y	$d_{F_{\max}}$	$d_{F,Y}$	μ	k
BW-16-m-3ply-2SP	[kN]	[kN]	[mm]	[mm]	(-)	[kN/mm]
R	6.9	6.1	7.0	0.8	9.3	4.1
L	6.9	6.1	6.0	1.8	3.4	3.0
Avg.	6.9	6.1	6.5	1.3	6.4	3.6

Note: All values are per screw, R=right side, L=left side of the connection

BW-16-c-3ply-2SP



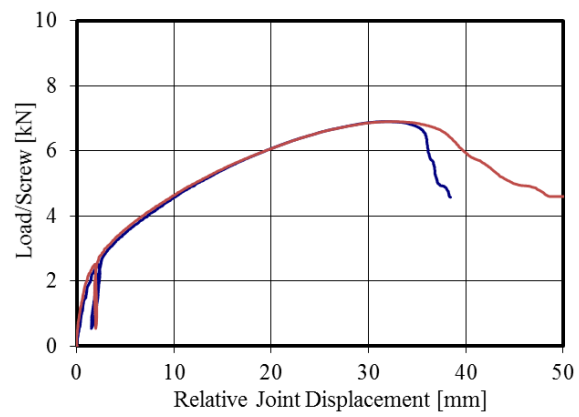
Spec.	F_{\max} [kN]	F_Y [kN]	$d_{F\max}$ [mm]	$d_{F,Y}$ [mm]	μ (-)	k [kN/mm]
1-R	6.8 (5.5)	5.5 (5.2)	7.0 (6.0)	1.2 (1.0)	5.9 (6.0)	3.1 (2.1)
1	6.8 (5.5)	5.5 (5.2)	7.0 (6.0)	1.2 (1.0)	5.9 (6.0)	3.1 (2.1)
2-R	7.8 (6.5)	5.4 (5.3)	2.7 (5.7)	1.1 (1.0)	2.6 (5.7)	3.9 (3.9)
2-L	7.6 (6.6)	5.3 (5.6)	7.0 (5.7)	1.4 (1.0)	4.9 (5.7)	3.8 (3.3)
2	7.7 (6.6)	5.3 (5.4)	4.9 (5.7)	1.2 (1.0)	3.7 (5.7)	3.9 (3.6)
3-R	7.3 (6.1)	6.3 (5.8)	8.0 (6.0)	2.3 (1.0)	3.5 (6.0)	2.4 (2.0)
3-L	7.4 (6.0)	6.5 (5.6)	8.0 (7.9)	2.3 (1.0)	3.5 (7.9)	3.2 (1.4)
3	7.3 (6.0)	6.4 (5.7)	8.0 (7.0)	2.3 (1.0)	3.5 (7.0)	2.8 (1.7)
Avg.	7.3 (6.0)	5.7 (5.4)	6.6 (6.2)	1.6 (1.0)	4.4 (6.2)	3.3 (2.5)

Note: All values are per screw, R=right side, L=left side of the connection, negative envelope values within parenthesis, replicate 1 left transducer did not work properly

Appendix F Detailed test results of large sized specimens (L-2SP)

F.1 L-2SP: Lap joints Shear

LS-32-m-3ply-2SP

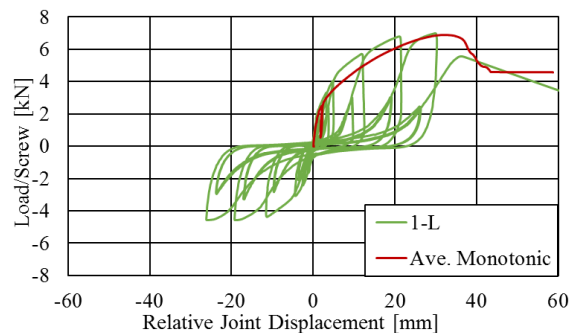
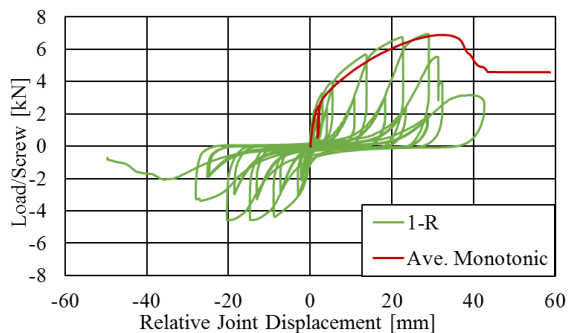


Spec.	F_{max}	F_Y	d_{Fmax}	$d_{F,Y}$	μ	k
	[kN]	[kN]	[mm]	[mm]	(-)	[kN/mm]
R	6.9	5.7	32.0	5.5	5.8	0.9
L	6.9	5.8	33.0	5.1	6.4	0.9

Avg.	6.9	5.7	32.5	5.3	6.1	0.9
-------------	------------	------------	-------------	------------	------------	------------

Note: All values are per screw, R=right side, L=left side of the connection

LS-32-c-3ply-2SP

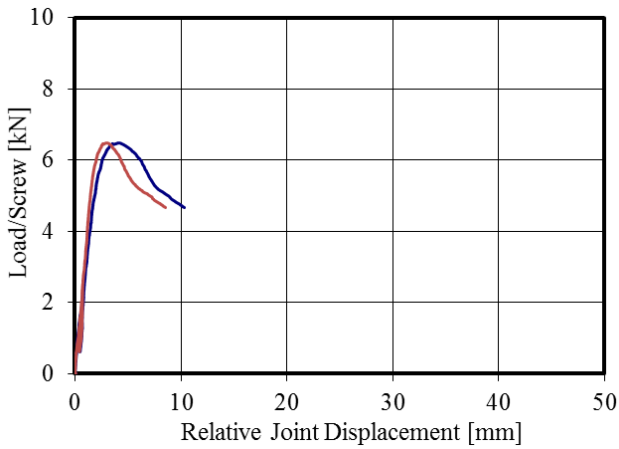


Spec.	F_{max} [kN]	F_Y [kN]	d_{Fmax} [mm]	$d_{F,Y}$ [mm]	μ (-)	k [kN/mm]
1-R	6.9 (4.6)	5.0 (4.2)	27.0 (14.0)	7.4 (1.4)	3.6 (9.8)	0.5 (1.5)
1-L	7.0 (4.6)	5.3 (2.4)	27.0 (14.0)	7.4 (4.1)	3.7 (3.4)	0.5 (0.8)
Avg.	7.0 (4.6)	5.1 (3.3)	27.0 (14.0)	7.4 (2.7)	3.6 (6.6)	0.5 (1.1)

Note: All values are per screw, R=right side, L=left side of the connection, negative envelope values within parenthesis, only 1 specimen was tested

F.2 L-2SP: Lap joints Withdrawal

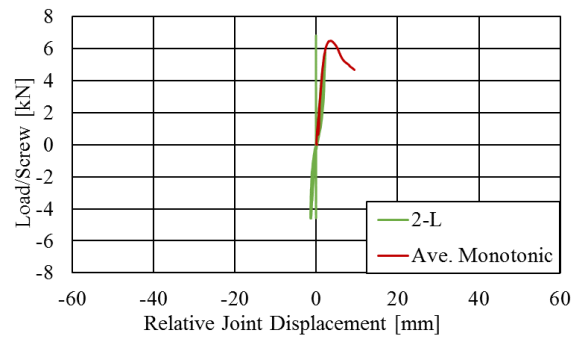
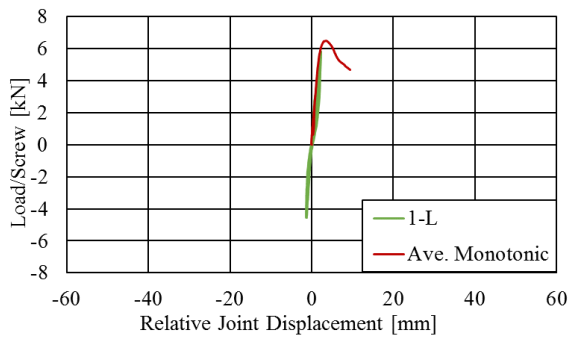
LW-32-m-3ply-2SP



Spec.	F_{\max} [kN]	F_Y [kN]	$d_{F\max}$ [mm]	$d_{F,Y}$ [mm]	μ (-)	k [kN/mm]
R	6.5	6.1	4.1	2.1	1.9	2.4
L	6.5	6.0	3.0	1.7	1.8	3.2
Avg.	6.5	6.0	3.6	1.9	1.9	2.8

Note: All values are per screw, R=right side, L=left side of the connection

LW-32-c-3ply-2SP

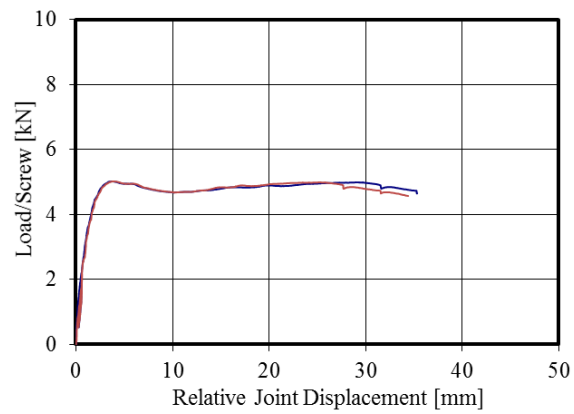


Spec.	F_{max} [kN]	F_Y [kN]	d_{Fmax} [mm]	$d_{F,Y}$ [mm]	μ (-)	k [kN/mm]
1-L	5.7 (4.6)	5.5 (4.1)	2.5 (1.2)	1.7 (1.0)	1.4 (1.2)	3.4 (4.0)
2-L	5.7 (4.7)	5.5 (4.4)	2.5 (1.2)	1.8 (1.0)	1.4 (1.2)	3.4 (4.7)
Avg.	5.7 (4.7)	5.5 (4.2)	2.5 (1.2)	1.8 (1.0)	1.4 (1.2)	3.4 (4.3)

Note: All values are per screw, R=right side, L=left side of the connection, negative envelope values within parenthesis, right transducer was not working properly for both of the specimens

F.3 L-2SP: Lap joints Combined

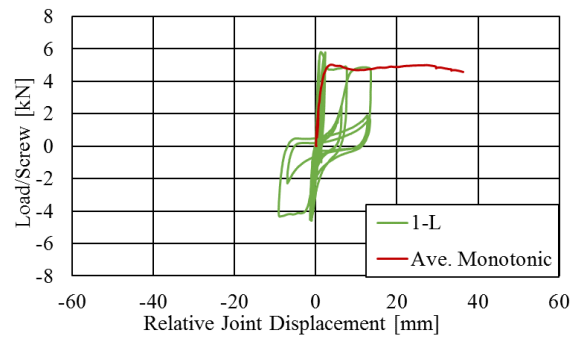
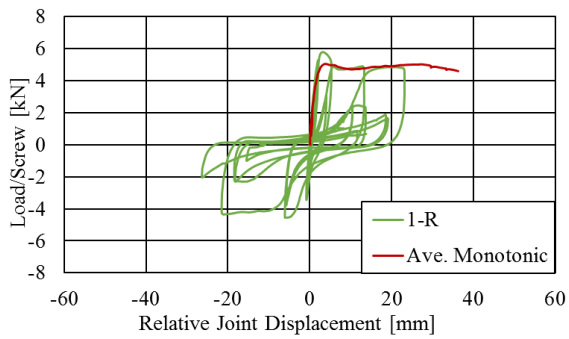
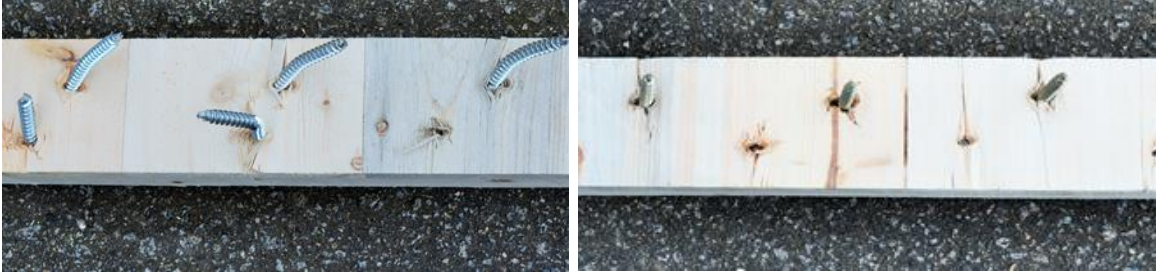
LC-WSSW-32-m-3ply-2SP



Spec.	F_{max} [kN]	F_Y [kN]	d_{Fmax} [mm]	$d_{F,Y}$ [mm]	μ (-)	k [kN/mm]
R	5.0	5.0	15.0	1.2	12.2	3.8
L	5.0	5.1	15.0	1.7	8.9	3.0
Avg.	5.0	5.1	15.0	1.5	10.5	3.4

Note: All values are per screw, R=right side, L=left side of the connection

LC-WSSW-32-c-3ply-2SP



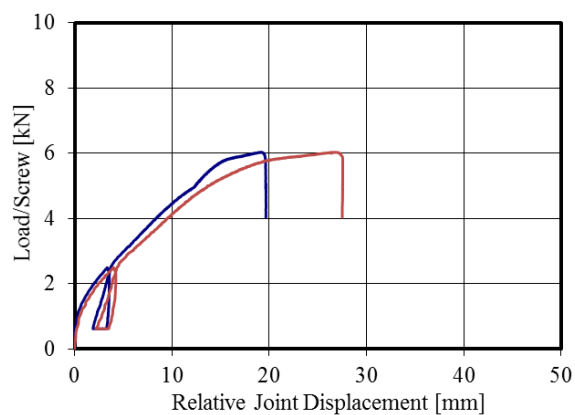
Spec.	F_{max} [kN]	F_Y [kN]	d_{Fmax} [mm]	$d_{F,Y}$ [mm]	μ (-)	k [kN/mm]
1-R	5.8 (4.5)	4.4 (3.5)	3.0 (5.0)	1.6 (0.8)	1.9 (6.3)	4.4 (6.8)
1-L	5.8 (4.7)	5.3 (4.1)	3.0 (3.0)	1.7 (0.6)	1.8 (4.9)	4.3 (3.1)
1	5.8 (4.6)	4.9 (3.8)	3.0 (4.0)	1.6 (0.7)	1.8 (5.6)	4.3 (4.9)
2-R	4.9 (4.5)	4.4 (3.4)	3.0 (8.0)	1.6 (0.3)	1.9 (25.8)	3.6 (4.5)
2-L	5.0 (4.5)	4.9 (2.0)	23.0 (7.0)	1.6 (0.7)	14.5 (10.6)	3.8 (6.8)
2	4.9 (4.5)	4.6 (2.7)	13.0 (7.5)	1.6 (0.5)	8.2 (18.2)	3.7 (5.6)

Avg.	5.4 (4.5)	4.7 (3.3)	8.0 (5.8)	1.6 (0.6)	5.0 (11.9)	4.0 (5.3)
-------------	------------------	------------------	------------------	------------------	-------------------	------------------

Note: All values are per screw, R=right side, L=left side of the connection, negative envelope values within parenthesis

F.4 L-2SP: Butt joints Shear

BS-32-m-3ply-2SP

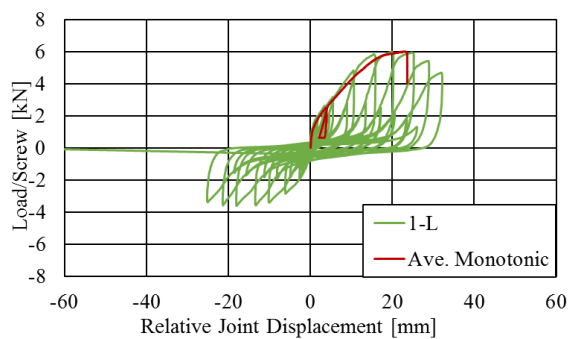
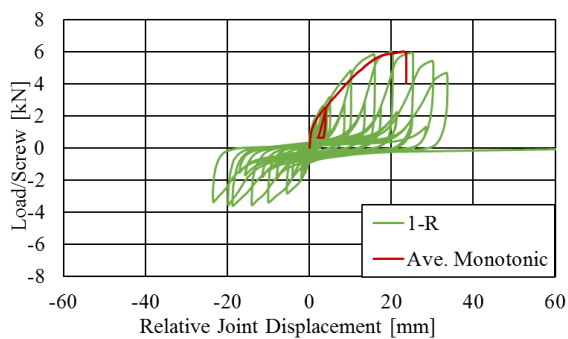


	F_{\max}	F_Y	$d_{F\max}$	$d_{F,Y}$	μ	k
Spec.	[kN]	[kN]	[mm]	[mm]	(-)	[kN/mm]
R	6.0	4.1	19.0	4.4	4.3	0.6

L	6.0	4.1	27.0	5.5	4.9	0.5
Avg.	6.0	4.1	23.0	5.0	4.6	0.5

Note: All values are per screw, R=right side, L=left side of the connection

BS-32-c-3ply-2SP



Spec.	F_{max} [kN]	F_Y [kN]	d_{Fmax} [mm]	$d_{F,Y}$ [mm]	μ (-)	k [kN/mm]
1-R	5.9 (3.3)	2.4 (3.0)	18.0 (13.0)	4.2 (0.9)	4.2 (14.8)	0.5 (3.3)
1-L	5.9 (3.4)	4.4 (2.2)	18.0 (17.0)	8.9 (1.5)	2.0 (11.1)	0.4 (1.5)
1	5.9 (3.4)	3.4 (2.6)	18.0 (15.0)	6.6 (1.2)	3.1 (12.9)	0.4 (2.4)
2-R	7.1 (4.5)	6.4 (3.5)	15.0 (19.0)	7.0 (1.9)	2.1 (10.2)	0.6 (0.7)
2-L	7.2 (4.6)	6.8 (3.6)	15.0 (18.0)	10.0 (1.8)	1.5 (9.8)	0.5 (0.7)
2	7.2 (4.5)	6.6 (3.5)	15.0 (18.5)	8.5 (1.8)	1.8 (10.0)	0.5 (0.7)

Avg.	6.5 (4.0)	5.0 (3.1)	16.5 (16.8)	7.5 (1.5)	2.5 (11.5)	0.5
Note: All values are per screw, R=right side, L=left side of the connection, negative envelope values within parenthesis						